

000 001 002 003 004 005 006 007 008 009 010 011 012 013 014 015 016 017 018 019 020 021 022 023 024 025 026 027 028 029 030 031 032 033 034 035 036 037 038 039 040 041 042 043 044 045 046 047 048 049 050 051 052 053 FULL-GRAPH VS. MINI-BATCH TRAINING: COMPREHENSIVE ANALYSIS FROM A BATCH SIZE AND FAN-OUT SIZE PERSPECTIVE

Anonymous authors

Paper under double-blind review

ABSTRACT

Full-graph and mini-batch Graph Neural Network (GNN) training approaches have distinct system design demands, making it crucial to choose the appropriate approach to develop. A core challenge in comparing these two GNN training approaches lies in characterizing their model performance (i.e., convergence and generalization) and computational efficiency. While a batch size has been an effective lens in analyzing such behaviors in deep neural networks (DNNs), GNNs extend this lens by introducing a fan-out size, as full-graph training can be viewed as mini-batch training with the largest possible batch size and fan-out size. However, the impact of the batch and fan-out size for GNNs remains insufficiently explored. To this end, this paper systematically compares full-graph vs. mini-batch training of GNNs through empirical and theoretical analyses from the view points of the batch size and fan-out size. Our key contributions include: 1) We provide a novel generalization analysis using the Wasserstein distance to study the impact of the graph structure, especially the fan-out size. 2) We uncover the non-isotropic effects of the batch size and the fan-out size in GNN convergence and generalization, providing practical guidance for tuning these hyperparameters under resource constraints. Finally, full-graph training does not always yield better model performance or computational efficiency than well-tuned smaller mini-batch settings. The implementation can be found in the anonymous link: https://anonymous.4open.science/r/GNN_fullgraph_minibatch_training-8040/README.md.

1 INTRODUCTION

Graph neural networks (GNNs) have demonstrated exceptional performance across diverse machine learning tasks involving graph-structured data (Zhang & Chen, 2018; Xu et al., 2018; Gilmer et al., 2017). A defining characteristic of GNNs is their reliance on the graph structure to facilitate message-passing, enabling the learning of rich node representations from both structural and feature information (Gilmer et al., 2017). Consequently, the computational patterns of GNNs depend strongly on the underlying graph structure, leading to two prominent and distinct paradigms for training GNNs: *full-graph* and *mini-batch* training (Bajaj et al., 2024; Hamilton et al., 2017; Zheng et al., 2022).

Full-graph training and mini-batch training are distinct GNN training paradigms. In full-graph training, the entire graph is processed simultaneously, and each node aggregates information from its neighbors across multiple message-passing layers. In contrast, mini-batch training divides the graph into smaller subgraphs or batches, training the model iteratively on subsets of nodes and their (sampled) local neighborhoods. These paradigms exhibit fundamentally different computational patterns, each requiring distinct system designs, training pipelines, and optimization strategies. For example, full-graph training necessitates efficient communication mechanisms to synchronize aggregations over the entire graph (Md et al., 2021; Peng et al., 2022), whereas mini-batch training demands careful optimizations of CPU-GPU data loading to accommodate frequent batch processing (Chen et al., 2018; Zhu et al., 2019; Liu et al., 2023). *Understanding the differences between these two paradigms is essential for identifying suitable training methods in specific scenarios and guiding the design of optimised training systems.*

Existing Gaps. To systematically investigate the differences between full-graph and mini-batch training, the hyperparameters *batch size* (the number of sampled nodes) and *fan-out size* (the number of neighbors chosen per node at each hop (Hamilton et al., 2017)) offer critical lenses for analyzing

GNN performance and computational efficiency, as full-graph training can be viewed as a special case of mini-batch training with maximum batch and fan-out sizes. However, despite increasing attention in the literature, the impact of these hyperparameters remains insufficiently understood. Existing studies typically focus on individual parameters (e.g., batch size or fan-out size independently) (Hu et al., 2021; Yuan et al., 2023) or singular aspects of evaluation (e.g., convergence (Yang et al., 2023; Awasthi et al., 2021), accuracy (Tang & Liu, 2023; Verma & Zhang, 2019) , or system efficiency (Naman & Simmhan, 2024)), providing limited insights into the holistic trade-offs between the two paradigms (see Sec. 6 for further discussions). Although recent empirical studies, such as (Bajaj et al., 2024), have attempted comparisons between full-graph and mini-batch training, their results are largely observational and hardware- or environment-dependent, limiting their generalizability. Meanwhile, most of the existing GNN analyses typically rely on strong simplifications, such as infinite-width assumptions that average out per-neuron gradient noise (Yadati, 2022) or linear models with convex losses that remove local optima (Yang et al., 2023; Lin et al., 2023), which obscure the effects of batch sizes or fan-out sizes on training dynamics. Thus, *a critical open question remains: How do the batch size and fan-out size influence the optimization dynamics, generalization capabilities, and computational efficiency of GNN training, particularly when comparing full-graph and mini-batch training paradigms?*

Challenges. Comparing full-graph and mini-batch GNN training paradigms presents multiple intertwined challenges. First, while the batch size and fan-out size are useful for analyzing differences between these paradigms, their impacts on model performance and system efficiency inherently depend on the hardware environment used. Therefore, meaningful comparisons necessitate measurement frameworks that are hardware-agnostic and supported by rigorous theoretical analyses. Second, both the computational dynamics of GNNs and the statistical properties of graph data are intrinsically tied to the underlying graph structure, which is directly influenced by choices of batch size and fan-out size. Altering these hyperparameters thus introduces complex interactions, highlighting the need for flexible analytical frameworks that can accurately capture these dynamics. Finally, comprehensively understanding the trade-offs between full-graph and mini-batch training demands frameworks capable of jointly evaluating model efficiency and generalization, ultimately guiding the development of practically optimized systems.

Contribution. To address the aforementioned research gap, in this paper, we conduct a systematic study of full-graph and mini-batch GNN training under different batch sizes and fan-out sizes on transductive node classification tasks. The contributions are highlighted as follows.

▷ We characterize the role of the batch size and fan-out size in GNN optimization dynamic analysis (Theorem 1 and 2), extending the settings to irregular graphs and GNNs with non-linear activations, better aligning with the practice. We also provide a novel GNN generalization analysis (Theorem 3) using the Wasserstein distance to investigate the impact of graph structures, especially the fan-out size, where this distance can quantify graph structure differences between training and testing datasets.

▷ We theoretically uncover the non-isotropic impacts of the batch size and the fan-out size in GNN convergence and generalization, where the batch size has a greater impact on GNN optimization dynamics (Obs.1), while the fan-out size more strongly affects GNN generalization (Obs.2). These findings suggest that, under memory constraints, adjusting the batch size is preferable when generalization is the priority, given its more stable effect on generalization. In contrast, tuning the fan-out size is preferable when convergence is the concern, given its more consistent impact on convergence compared to batch size, while setting the fan-out size to moderate values balances convergence and computational efficiency as the magnitude of its impact on convergence decreases with larger values.

▷ We empirically use additional iteration-based convergence metrics for hardware-agnostic comparisons, rather than relying solely on time-based metrics. Experiments on four real-world datasets (Hamilton et al., 2017; Hu et al., 2020) and three GNN models (Zhang et al., 2019; Hamilton et al., 2017; Veličković et al., 2017) validate our theoretical findings. We recommend keeping batch size below half of the training nodes and the fan-out size under 15 for sparse graphs (Hamilton et al., 2017; Hu et al., 2020) to balance the model performance and computational efficiency.

Our theoretical and empirical findings support that full-graph training does not always yield superior model performance or computational efficiency compared to smaller mini-batch settings. Instead, carefully tuning the batch size and fan-out size in mini-batch settings often leads to better trade-offs,

108 such as faster convergence or improved generalization under resource constraints. These findings
 109 provide practical guidance for selecting training paradigms under specific task requirements.
 110

111 2 PRELIMINARIES

113 **Graph.** Given a homogeneous undirected graph with total n nodes and the maximal degree $d_{\max} \leq n$,
 114 set n_{train} nodes in the training set and n_{test} nodes in the testing set, with $n = n_{\text{train}} + n_{\text{test}}$. We allow
 115 arbitrary subsets of nodes to be selected as the training and testing sets. Let $b \leq n_{\text{train}}$ be the batch
 116 size and $\beta \leq d_{\max}$ be the fan-out size in mini-batch training, where uniform neighbor sampling is
 117 employed to select neighbors.

118 Each node is an instance (\mathbf{x}_i, y_i) with feature \mathbf{x}_i and label y_i . Let $\mathbf{X} \in \mathbb{R}^{n \times r}$ be the feature matrix,
 119 where \mathbf{x}_i is the i -th row of \mathbf{X} and r is the feature size. In the transductive learning setting, our task is
 120 to predict the labels of nodes $\{\mathbf{x}_i\}_{i=n_{\text{train}}+1}^n$ by the GNN model trained on $\{\mathbf{x}_i\}_{i=1}^n \cup \{y_i\}_{i=1}^{n_{\text{train}}}$. We
 121 assume that node features are fixed, and node labels are independently sampled from distributions
 122 conditioned on node features, which is widely adopted in the node classification task.

123 Let \mathbf{A} represent the adjacency matrix of graph. We define $\mathbf{A}_{\text{train}}^{\text{full}} \in \mathbb{R}^{n_{\text{train}} \times n}$ for full-graph training,
 124 $\mathbf{A}_{\text{train}}^{\text{mini}} \in \mathbb{R}^{b \times n}$ for mini-batch training, and $\mathbf{A}_{\text{test}} \in \mathbb{R}^{n_{\text{test}} \times n}$ for inference, where $\mathbf{A}_{\text{train}}^{\text{mini}}$ is a submatrix
 125 of $\mathbf{A}_{\text{train}}^{\text{full}}$. Let \mathbf{D}^{in} denote a diagonal in-degree matrix with $\mathbf{D}_{ii}^{\text{in}}$ representing the number of incoming
 126 edges to node i . We define $\mathbf{D}_{\text{train}}^{\text{in,full}} \in \mathbb{R}^{n_{\text{train}} \times n_{\text{train}}}$ for full-graph training, $\mathbf{D}_{\text{train}}^{\text{in,mini}} \in \mathbb{R}^{b \times b}$ for mini-
 127 batch training, and $\mathbf{D}_{\text{test}}^{\text{in}} \in \mathbb{R}^{n_{\text{test}} \times n_{\text{test}}}$ for testing. $\mathbf{D}^{\text{out}} \in \mathbb{R}^{n \times n}$ denotes the respective diagonal
 128 out-degree matrix. $\tilde{\mathbf{A}} = (\mathbf{D}^{\text{in}} + \mathbf{I})^{-\frac{1}{2}} (\mathbf{A} + \mathbf{I}) (\mathbf{D}^{\text{out}} + \mathbf{I})^{-\frac{1}{2}}$ is the respective normalized adjacency
 129 matrix with self-loops, where self-loops ensure that each node retains its own features during
 130 aggregation, improving the model’s learning ability. Here $\tilde{\mathbf{a}}_i$ denotes the i -th row of $\tilde{\mathbf{A}}$.

132 **GNN model.** Motivated by recent theoretical advances in understanding GNNs (Su & Wu, 2025;
 133 Awasthi et al., 2021), we analyze the training dynamics using a one-layer GNN model. This model
 134 serves as a powerful and well-established testbed for capturing phenomena arising from finite width
 135 and nonlinearity of GNNs. Its simplicity in model depth provides the analytical flexibility necessary to
 136 precisely characterize how batch size and fan-out size affect GNN training dynamics. In Appendix H,
 137 we further discuss how our analyses and results generalize to multi-layer settings. Concretely, let
 138 $\mathbf{W} \in \mathbb{R}^{h \times r}$ be the learnable model parameters of the GNN model and $\mathbf{W}^* \in \mathbb{R}^{h \times r}$ be the ground
 139 truth of \mathbf{W} , where \mathbf{w}_i is the i -th row of \mathbf{W} and h is the finite hidden dimension. We study a
 140 one-layer GNN with the ReLU activation, and define the output immediately after the first layer as
 141 $\mathbf{z}_i = \sigma(\tilde{\mathbf{a}}_{\text{train},i} \mathbf{X} \mathbf{W}^{\top})$, $\forall i \in$ training set, where $\sigma(x) = \max(x, 0)$ is the ReLU activation function,
 142 and the term $\tilde{\mathbf{a}}_{\text{train},i} \mathbf{X}$ represents the embedding aggregation on node i . This first-layer output may be
 143 followed by task-specific post-processing (e.g., a linear projection in binary classification). Similarly,
 144 during inference, the output of the first layer is given by $\mathbf{z}_i = \sigma(\tilde{\mathbf{a}}_{\text{test},i} \mathbf{X} \mathbf{W}^{\top})$, $\forall i \in$ testing set.

145 In this paper, we use $\|\cdot\|_2$, $\|\cdot\|$ and $\|\cdot\|_F$ to denote the 2-norm of vector, spectral norm of matrix
 146 and Frobenius norm of vector, respectively. For two sequences $\{p_n\}$ and $\{q_n\}$, we use $p_n = O(q_n)$
 147 to denote that $p_n \leq C_1 q_n$ for some absolute constant $C_1 > 0$. The notation table is in Appendix A.

148 3 OPTIMIZATION DYNAMIC

150 We present our theoretical studies on the GNN optimization dynamics. First, the optimization
 151 setup is introduced, representing how to handle interactions between batch size and fan-out size in
 152 optimization dynamics (Sec. 3.1). Next, we show the convergence results, answering our research
 153 question in GNN optimization dynamic. We then reveal an interesting observation, yielding actionable
 154 implications for accelerating convergence under memory constraints (Sec. 3.2).

155 3.1 OPTIMIZATION SETUP

156 **Optimization algorithms.** We aim to minimize the empirical risk $\hat{L}_{\text{train}}(\mathbf{W}, \tilde{\mathbf{A}}_{\text{train}}) =$
 157 $\frac{1}{n_{\text{train}}} \sum_{i \in \text{training set}} l(\mathbf{W}, \tilde{\mathbf{a}}_{\text{train},i})$, where $l(\cdot)$ denotes the loss function. In practice, Cross-Entropy
 158 (CE) and Mean Squared Error (MSE) are the most commonly used losses. Under *full-graph*
 159 training settings, the model parameters are updated via gradient descent (GD) as $\mathbf{W}_{t+1}^{\text{full}} =$
 160 $\mathbf{W}_t^{\text{full}} - \eta_t \nabla_{\mathbf{W}_t^{\text{full}}} \hat{L}_{\text{train}}(\mathbf{W}_t^{\text{full}}, \mathbf{A}_{\text{train}}^{\text{full}})$, where $\eta_t > 0$ is the learning rate at the t -th training iteration.
 161 Under *mini-batch* training settings, the model parameters are updated via stochastic gradient

162 descent (SGD) as $\mathbf{W}_{t+1}^{\text{mini}} = \mathbf{W}_t^{\text{mini}} - \eta_t \hat{\mathbf{G}}_t$, where $\hat{\mathbf{G}}_t = \frac{1}{b} \sum_{i \in \text{sampled nodes}} \nabla_{\mathbf{W}_{t+1}^{\text{mini}}} l(\mathbf{W}_t^{\text{mini}}, \hat{\mathbf{a}}_{\text{train},i}^{\text{mini}})$
 163 denotes the stochastic gradient at the t -th training iteration.
 164

165 **Handling interactions between batch size and fan-out size in optimization dynamic.** To handle
 166 these interactions, we isolate the impact of the graph structure in the loss and gradient expressions. A
 167 key challenge is that the nonlinear activation (e.g., ReLU) processes aggregated node features as input,
 168 making these expressions analytically intractable. To overcome this, we decouple the aggregated
 169 node features from the activation function. For instance, we extract the aggregation from the ReLU
 170 function by reformulating squared loss terms, or rewrite the ReLU function using a position-wise 0/1
 171 indicator matrix that can directly multiply the aggregated node features.
 172

3.2 CONVERGENCE RESULTS

173 Building on the aforementioned setup in Sec 3.1, we study GNN convergence results under suitable
 174 assumptions on the distribution of node features as well as the boundedness of the feature matrix
 175 norm, the ground truth parameter norm and the separation between aggregated node features with
 176 different labels in the training data (see Assumptions B.1.-B.2. in Appendix B and Assumption E.1. in
 177 Appendix E), with detailed proofs provided in Appendix B-E.
 178

179 **Theorem 1.** (Convergence of Mini-batch Training with MSE) Suppose \mathbf{W}^{mini} are generated by
 180 Gaussian initialization. Under Assumptions B.1. and B.2, if the fan-out size satisfies $C_1^{\text{mini}} \leq \beta \leq$
 181 $C_2^{\text{mini}} b^{\frac{3}{4}}$ for constants $C_1^{\text{mini}}, C_2^{\text{mini}} \in (0, 1)$ to ensure a sparser adjacency than a fully connected
 182 graph, then with high probability, $L_{\text{train}}(\mathbf{W}_T^{\text{mini}}, \mathbf{A}_{\text{train}}^{\text{mini}}) \leq \epsilon$ for any $\epsilon \in (0, 1)$, provided that the
 183 number of iterations $T = O\left(n_{\text{train}} h^2 b^{\frac{5}{2}} \beta^{-\frac{1}{2}} \epsilon^{-1} \log(h^2 \epsilon^{-1})\right)$ under the mini-batch training.
 184

185 **Theorem 2.** (Convergence of Mini-batch Training with CE) Suppose \mathbf{W}^{mini} are generated by
 186 Gaussian initialization. Under Assumptions B.1. and E.1, if the hidden dimension of a one-round
 187 GNN satisfies $h = \Omega(\log(n_{\text{train}}) \beta^{-1} (n_{\text{train}}^2 + \epsilon^{-1}))$ to ensure the finite width, then with high
 188 probability, $\hat{L}_{\text{train}}(\mathbf{W}_T^{\text{mini}}, \mathbf{A}_{\text{train}}^{\text{mini}}) \leq \epsilon$ for any $\epsilon \geq 0$, provided that the number of iterations $T =$
 189 $O\left(n_{\text{train}}^2 (\log(n_{\text{train}}))^{\frac{1}{2}} \alpha^{-2} b^{-1} \beta^{-\frac{5}{2}} (n_{\text{train}}^2 + \epsilon^{-1})\right)$ under the mini-batch training.
 190

191 When the fan-out size β reaches d_{max} and the batch size b reaches n_{train} , the upper bound on the
 192 number of iterations to convergence in mini-batch training matches that of full-graph training (see
 193 Theorem B.4. under MSE in Appendix B and Theorem D.2. under CE in Appendix D).
 194

195 *Remark 3.1.* Our theoretical results show that increasing the batch size b for a fixed fan-out size leads
 196 to more iterations to convergence under MSE (Theorem 1), but fewer iterations under CE (Theorem 2)
 197 in the mini-batch setting of one-round GNNs, different from DNN training. In contrast, increasing
 198 the fan-out size β under a fixed batch size consistently reduces the number of iterations required for
 199 convergence under both MSE (Theorem 1) and CE (Theorem 2).
 200

201 *Remark 3.2.* Our theoretical analysis reveals that the magnitude of the fan-out size's impact on
 202 GNN convergence jointly depends on the batch size b and the fan-out size β , diminishing as either
 203 b (under CE) or β (under MSE and CE) grows. The magnitude of this impact can be characterized
 204 by the absolute slope $|\partial T / \partial \beta|$ of the number of iterations T for convergence with respect to the
 205 fan-out size β , where a steeper slope indicates a stronger impact. Specifically, Theorem 1. gives
 206 $|\partial T / \partial \beta| = O(\beta^{-3/2} b^{5/2})$ under MSE and Theorem 2. gives $|\partial T / \partial \beta| = O(\beta^{-7/2} b^{-1})$ under CE .
 207

208 **Answering our research question:** Remark 3.1. and Remark 3.2. represent the impact and interplay
 209 of the batch size and the fan-out size in the GNN optimization dynamic. Therefore, we conclude
 210 that full-graph training does not always provide superior convergence speed than smaller mini-batch
 211 settings, especially under MSE.
 212

213 Furthermore, we present an interesting observation, providing insights into accelerating GNN conver-
 214 gence under memory constraints.
 215

216 **Obs.1: GNN convergence is more sensitive to batch size than to fan-out size.** Remark 3.1. high-
 217 lights a stronger dependence of GNN convergence on batch size b than on fan-out size β , as a larger
 218 batch size b leads to opposite convergence trends under MSE and CE, while increasing the fan-out size
 219 β exhibits a consistent trend. This observation cannot be fully interpreted by the popular explanation
 220 of DNNs, which posits that increasing the batch size reduces gradient variance, resulting in fewer
 221

iterations to converge (Cong et al., 2021a; Liu et al., 2024). We further consider the impact of message passing on the loss and gradient, providing the interpretation of Obs.1. in Appendix F.

Implication for accelerating convergence. Under memory constraints, Obs.1. suggests that adjusting the fan-out size β offers a more reliable way to accelerate GNN convergence, as the fan-out size β keeps the same convergence trends under both MSE and CE. To tune the fan-out size β , Remark 3.2. highlights that a moderate value of β provides a practical balance between convergence and computational efficiency, as the reduction in the number of iterations for convergence becomes smaller when increasing β beyond moderate values, particularly with large batches under CE.

4 GENERALIZATION OF MINI-BATCH TRAINING

We represent our theoretical study on GNN generalization. First, problem setup is introduced, representing how to isolate the impacts of batch size and fan-out size in generalization by employing Wasserstein distance (Sec. 4.1). Next, we show the generalization result, answering our research question in GNN generalization. We then present an interesting observation, yielding the actionable implication for improving generalization under memory constraints (Sec. 4.2).

4.1 PROBLEM SETUP

Basic setup. We aim to bound the generalization gap between the expected testing risk and the empirical training risk under the mini-batch training settings, where the expected testing risk is given by $L_{\text{test}}(\mathbf{W}^{\text{mini}}, \tilde{\mathbf{A}}_{\text{test}}^{\text{full}}) = \mathbb{E} \left[\frac{1}{n_{\text{test}}} \sum_{i \in \text{test set}} l(\mathbf{W}^{\text{mini}}, \tilde{\mathbf{a}}_{\text{test},i}^{\text{full}}) \right]$, and the empirical training risk is expressed as $\hat{L}_{\text{train}}(\mathbf{W}^{\text{mini}}, \tilde{\mathbf{A}}_{\text{train}}^{\text{mini}}) = \frac{1}{n_{\text{train}}} \sum_{i \in \text{training set}} l(\mathbf{W}^{\text{mini}}, \tilde{\mathbf{a}}_{\text{train},i}^{\text{mini}})$. Note that inference utilizes all testing neighbors across the entire graph, whereas mini-batch training relies on sampled neighbors within limited hops. We then employ the Wasserstein distance (Kantorovich, 1960) to quantify the difference in graph structures between training and testing datasets, as the Wasserstein distance effectively measures differences in non-i.i.d. data, particularly regarding geometric variations.

Definition 1. (Distance between Training Set and Testing Set). Define the distance from the training set to the testing set as the Wasserstein distance given by $\Delta(\beta, b) = \left\{ \inf_{\theta \in \Theta[\rho_{\text{train}}, \rho_{\text{test}}]} \sum_{i \in \text{train set}} \sum_{j \in \text{test set}} \theta_{i,j} \delta(y_i, y_j, \beta, b) \right\}$, where $\rho_{\text{train}}(y_i)$ and $\rho_{\text{test}}(y_i)$ denote the probability of y_i appearing in training and testing sets, respectively. $\Theta[\rho_{\text{train}}, \rho_{\text{test}}]$ is the joint probability of ρ_{train} and ρ_{test} . The infimum in the first equality is conditioned on $\sum_{j \in \text{test set}} \theta_{i,j} = \rho_{\text{train}}(y_i)$, $\sum_{i \in \text{training set}} \theta_{i,j} = \rho_{\text{test}}(y_j)$, $\theta_{i,j} \geq 0$. $\delta(y_i, y_j, \beta, b)$ is the distance function of any two points from training and testing sets, respectively.

We set $\delta(y_i, y_j, \beta, b) = \frac{C_\delta h^2}{n_{\text{min}}} (\delta_{i,j}^{\text{full}} + \delta_i^{\text{full-mini}})$ with a constant $C_\delta > 0$, $n_{\text{min}} = \min\{n_{\text{train}}, n_{\text{test}}\}$ and $\delta_i^{\text{full}} = \|\tilde{\mathbf{a}}_{\text{test},i}^{\text{full}} - \tilde{\mathbf{a}}_{\text{train},i}^{\text{full}}\|_F^2 + 2 \|\tilde{\mathbf{a}}_{\text{test},i}^{\text{full}}\|_F^2$, as a constant, mainly capturing the difference of distributions between the training and testing data in full-graph training. $\delta_i^{\text{full-mini}} = \|\tilde{\mathbf{a}}_{\text{train},i}^{\text{full}} - \tilde{\mathbf{a}}_{\text{train},i}^{\text{mini}}\|_F^2$ reflects the structural difference between full-graph and mini-batch graphs per node during training.

Isolating the impacts of batch size and fan-out size in generalization. To isolate these impacts, we focus on the discrepancy U between expected training and testing losses before training, which is the only term for non-i.i.d. graph data in our generalization analysis, with detailed proof in Appendix M. Since the training and testing datasets are split beforehand, U depends on the structural difference between training and testing graphs, which we quantify using the Wasserstein distance $\Delta(\beta, b)$. We show that greater similarity between training and testing graph structures leads to a smaller U .

4.2 GENERALIZATION RESULT

Building on the aforementioned setup in Sec 4.1, we use the Wasserstein distance to study the generalization result in PAC-Bayesian framework (McAllester, 2003) under mini-batch GNN training with MSE, given suitable assumptions on the boundedness of the Frobenius norm of the feature matrix and the parameter norm (see Assumptions G.1. and G.2. and the detailed proof in Appendix G).

Theorem 3. Suppose \mathbf{W}^{mini} are generated by Gaussian initialization. Under Assumptions G.1. and G.2. with high probability, for the posterior distribution \mathcal{Q} over hypothesis space in the mini-batch training settings with MSE, we have $L_{\text{test}}(\mathbf{W}^{\text{mini}}, \tilde{\mathbf{A}}_{\text{test}}^{\text{full}}; \mathcal{Q}) - \hat{L}_{\text{train}}(\mathbf{W}^{\text{mini}}, \tilde{\mathbf{A}}_{\text{train}}^{\text{mini}}; \mathcal{Q}) = O\left(\frac{1}{n_{\text{train}}} + \Delta(\beta, b)\right)$, where $\Delta(\beta, b_1) \leq \Delta(\beta, b_2)$ with $b_1 \geq b_2$,

270 $\Delta(\beta, b) \propto \sum_{i \in \text{training set}} \sum_{j \in \text{testing set}} \theta_{i,j} \delta_i^{\text{full-mini}}$, $\theta_{i,j} \in \Theta[\rho_{\text{train}}, \rho_{\text{test}}]$ and $\delta_i^{\text{full-mini}}$ has an overall
 271 non-increasing trend as the fan-out size β grows but small non-monotonic fluctuations exist. The
 272 posterior distribution Q represents the distribution of model parameters after training, and the
 273 hypothesis space denotes all possible models.

274 *Remark 4.1.* Theorem 3 reveals that increasing either the batch size b or the fan-out size β improves
 275 the GNN generalization. This is because the role of b and β in GNN generalization is captured by the
 276 Wasserstein distance $\Delta(\beta, b)$, where larger $\Delta(\beta, b)$ leads to poorer generalization performance. In
 277 Definition 1, the Wasserstein distance $\Delta(\beta, b)$ is proportional to the weighted sum of $\delta_i^{\text{full-mini}}$ (i.e.,
 278 the structural difference between full-graph and mini-batch graphs per node during training) over all
 279 training nodes, where $\delta_i^{\text{full-mini}}$ decreases with either the batch size b or the fan-out size β , though
 280 slightly non-monotonic fluctuations exist when varying β .

281 **Answering our research question:** Remark 4.1. represents how the batch size and the fan-out size
 282 characterize GNN generalization via the Wasserstein distance $\Delta(\beta, b)$. While full-graph training is
 283 expected to outperform smaller mini-batch settings, we remain cautious about the degradation in
 284 generalization performance at very large batch sizes or fan-out sizes, as similar issues have been
 285 observed in DNNs (You et al., 2019; 2017). We conduct an empirical study for further investigation.

286 In addition, we interpret an interesting observation, providing the implication for improving GNN
 287 generalization under memory constraints.

288 **Obs.2: GNN generalization is more sensitive to fan-out size than to batch size.** While increasing
 289 the fan-out size β and the batch size b both help align the mini-batch with the full graph during training,
 290 β has a greater impact on the generalization by directly controlling receptive field of each training
 291 node. Based on Remark 4.1, this can be interpreted using the Wasserstein distance $\Delta(\beta, b)$, which
 292 increases the weighted sum of $\delta_i^{\text{full-mini}}$ over all training nodes. A larger β can include unsampled
 293 but valid edges, turning zero terms $\tilde{a}_{\text{train},i}^{\text{mini}}$ into non-zero values in $\delta_i^{\text{full-mini}}$, potentially causing slight
 294 non-monotonic fluctuations. In contrast, increasing b does not introduce these edges, as all training
 295 nodes are included during summation of $\delta_i^{\text{full-mini}}$. With the more complex impact of β in $\Delta(\beta, b)$,
 296 we conclude that GNN generalization is more sensitive to fan-out size β than to batch size b (see
 297 Appendix M for the detailed proof).

298 **Implication for improving generalization.** Under memory constraints, Obs.2. suggests that adjusting
 299 the batch size b offers a more stable way to improve GNN generalization, as the batch size b introduces
 300 less non-monotonic fluctuations than the fan-out size β .

302 5 EMPIRICAL STUDY

303 We first explain the rationale for using the metrics (e.g., iteration-to-accuracy) in Sec. 5.1. We validate
 304 Remarks 3.1 - 3.2. and Obs.1. on GNN convergence (Sec. 5.2), and Remark 4.1. and Obs.2. on
 305 GNN generalization with the discussion about performance degradation (Sec. 5.3). We compare
 306 computational efficiency across varying batch sizes and fan-out sizes, answering our research question
 307 in computational efficiency (Sec. 5.4). Finally, we present an overall comparison of generalization
 308 performance between full-graph and mini-batch training after tuning batch size and fan-out size,
 309 yielding implications for tuning these two hyperparameters (Sec. 5.5).

310 **Results overview.** Non-isotropic impacts of batch size and fan-out size exist in model performance
 311 (i.e., generalization and convergence) and computational efficiency. Full-graph training does not
 312 always yield superior model performance or computational efficiency compared to well-tuned smaller
 313 mini-batch settings. Carefully tuning the batch size and the fan-out size in mini-batch settings often
 314 achieves more favorable trade-offs, such as faster convergence or better generalization.

315 **Datasets and models:** We conduct experiments on four real-world datasets: reddit (Hamilton et al.,
 316 2017), ogbn-arxiv (Hu et al., 2020), ogbn-products (Hu et al., 2020) and ogbn-papers100M (Hu
 317 et al., 2020). We train three representative GNN models: GCN (Zhang et al., 2019), GraphSAGE
 318 (Hamilton et al., 2017) with mean aggregation, and GAT (Veličković et al., 2017) with 2 heads for
 319 ogbn-papers100M and 4 heads for the other datasets. See more training settings in Appendix N.

321 5.1 METRIC: ITERATION-TO-ACCURACY

322 We evaluate convergence performance using three metrics: iteration-to-loss (i.e., the number of
 323 iterations to reach a target training loss), iteration-to-accuracy (i.e., the number of iterations to reach a
 target validation accuracy), and time-to-accuracy (i.e., the time to reach a target validation accuracy).

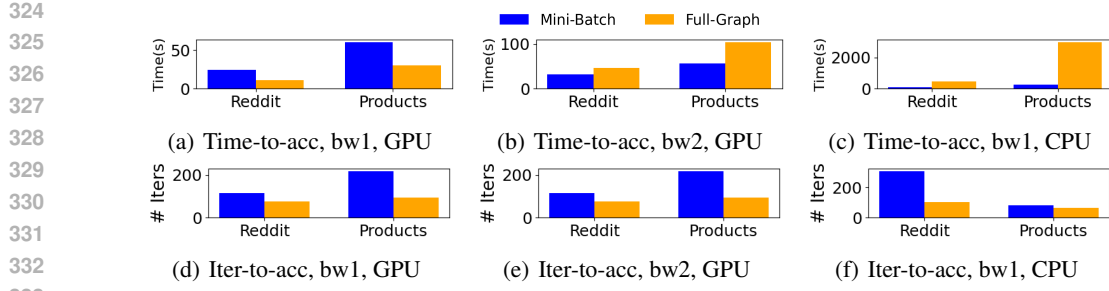


Figure 1: Time-to-acc and iteration-to-acc in mini-batch and full-graph training with varying bandwidths (i.e., two inter-GPU bandwidth values: $bw1=\infty > bw2=900GB/s$) and computational capacities (i.e., GPU with 40GB of memory and CPU with 512GB of host memory). **Figure representation updated.**

Since iteration-to-loss is from the theoretical analysis in Sec. 3 and time-to-accuracy is commonly used in empirical studies (Bajaj et al., 2024; Hu et al., 2020), we do not provide further explanation.

Rationale for using iteration-to-accuracy. However, time-to-accuracy is highly sensitive to hardware differences, entangling model performance improvement per iteration (e.g., accuracy) and computational efficiency (e.g., processed nodes per second). Thus, we additionally introduce *iteration-to-accuracy*, a hardware-agnostic metric, to capture this performance improvement during training.

To illustrate this rationale more clearly, we provide a simple, non-rigorous mathematical derivation, with details in Appendix N. Let b denote the batch size, β the fan-out size, and ν_l the iteration-to-accuracy. Suppose we compare two training setups under the same compute capacity but different bandwidths in distributed systems: a full-graph setting ($b = 1000$, $\beta = 50$, $\nu_l = 10$) and a mini-batch setting ($b = 10$, $\beta = 10$, $\nu_l = 10000$). At high bandwidths (1000 nodes/s), the full-graph setting converges faster, in 5.1×10^5 seconds, compared with 1.1×10^6 seconds for mini-batch training. In contrast, at low bandwidths (0.1 nodes/s), mini-batch training converges faster, requiring 2.1×10^6 seconds, whereas the full-graph setting requires 5.6×10^6 seconds.

Empirically, Figure 1 illustrates time-to-accuracy and iteration-to-accuracy with two training approaches under different inter-GPU bandwidth levels (i.e., $bw1=\infty$, simulated by a single GPU with no inter-device communication; $bw2=900GB/s$, two-GPU NVLink 4.0 setup) and computation capacities (i.e., GPU and CPU). Detailed settings are in Appendix N. For time-to-accuracy, mini-batch training underperforms full-graph training on a single GPU but outperforms it on two GPUs or a single CPU. In contrast, iteration-to-accuracy remains consistent across hardware environments, with a maximum variation of 41.28%, compared to 2787.05% for time-to-accuracy.

Therefore, both mathematical and empirical examples indicate that time-to-accuracy cannot reliably generalize convergence performance across hardware environments, while the iteration-to-accuracy is more reliable to guide early-stage configuration decisions. For example, in a new hardware setup, practitioners can use known iteration-to-accuracy trends to narrow the range of batch and fan-out size, and perform short runs to consider hardware-specific runtime, thereby reducing tuning overhead.

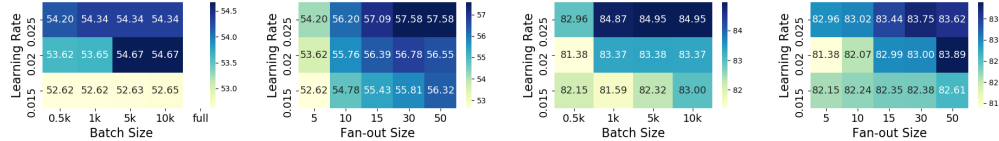
5.2 CONVERGENCE

Empirical Validation of Remarks 3.1, 3.2. and Obs.1. Remark 3.1. and Obs.1. are empirically validated by Figure 2 and Figures 7- 10 in Appendix N, which illustrate iteration-to-loss for three one-layer GNNs across four real-world datasets under varying fan-out sizes or batch sizes with different learning rates. In addition, Figure 4 in more general settings (e.g., multi-layer GraphSAGE) further confirms Remarks 3.1, 3.2. and Obs.1. using iteration-to-loss (see detailed settings in Appendix N). Due to more complex optimization dynamics in deeper GNNs, Figure 4 shows minor fluctuations across varying batch and fan-out sizes, where the batch size and fan-out size increase until mini-batch training transitions into full-graph training.

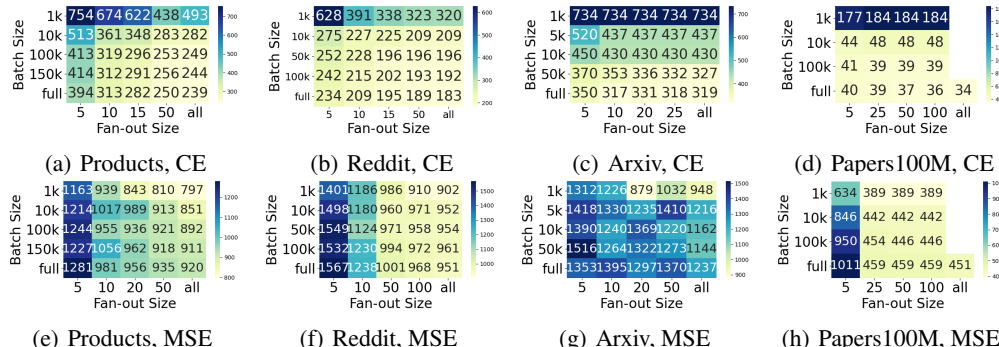
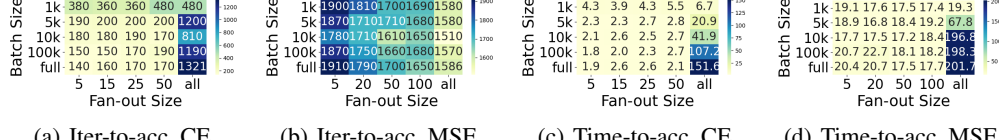
Extended experiments using iteration-to-accuracy and time-to-accuracy. To study model performance improvement during training, Figure 5 illustrates iteration-to-accuracy and time-to-accuracy across varying batch sizes and fan-out sizes for reddit (see more datasets in Appendix N), showing unstable convergence trends with varying batch sizes and very large fan-out sizes (explained further in Sec. 5.3). This is because these two metrics capture both convergence and generalization performance



(a) Batch size, CE (b) Fan-out size, CE (c) Batch size, b, MSE (d) Fan-out size, MSE

Figure 2: Iteration-to-loss of one-layer GraphSAGE under *CE* and *MSE* across varying learning rates and batch sizes or fan-out sizes for ogbn-products.

(a) Products, Batch size (b) Products, Fan-out size (c) Reddit, Batch size (d) Reddit, Fan-out size

Figure 3: Test accuracy of one-layer GraphSAGE under *MSE* across varying learning rates and batch sizes or fan-out sizes for ogbn-products and reddit.Figure 4: Iteration-to-loss of GraphSAGE under *CE* and *MSE* across varying batch and fan-out sizes.Figure 5: Iteration-to-accuracy and time-to-accuracy of GraphSAGE under *CE* and *MSE* across varying batch sizes and fan-out sizes for reddit.

due to the dependency on validation accuracy. Moderate fan-out sizes (e.g., around 15) are shown to balance convergence speed and computational efficiency (shown in time-to-accuracy), supporting the convergence acceleration implications in Sec 3.

5.3 GENERALIZATION

Empirical Validation of Remark 4.1. and Obs.2. Remark 4.1. and Obs.2. are empirically validated by Figure 3 and Figures 15-16 of one-layer GNNs in Appendix N, which illustrate test accuracies for three one-layer GNNs across four datasets under varying fan-out sizes or batch sizes with different learning rates. In addition, Figures 6(a)-(b) in more general settings for ogbn-products further confirm Obs.2. (see more datasets and details in Appendix N), as the variation of fan-out size induces more frequent and diverse shifts in test accuracies. Regarding Remark 4.1, Figure 6(b) under MSE generally aligns with our theoretical prediction, while Figure 6(a) under CE further shows that performance degradation occurs with very large fan-out sizes (typically more than 15 on these datasets) or batch sizes (exceeding half of the training nodes). This degradation is more severe with fan-out sizes than with batch sizes. We justify *our answer in Sec. 4 to the research question: full-graph training does not always outperform the smaller mini-batch settings in generalization due to degradation in generalization performance*.

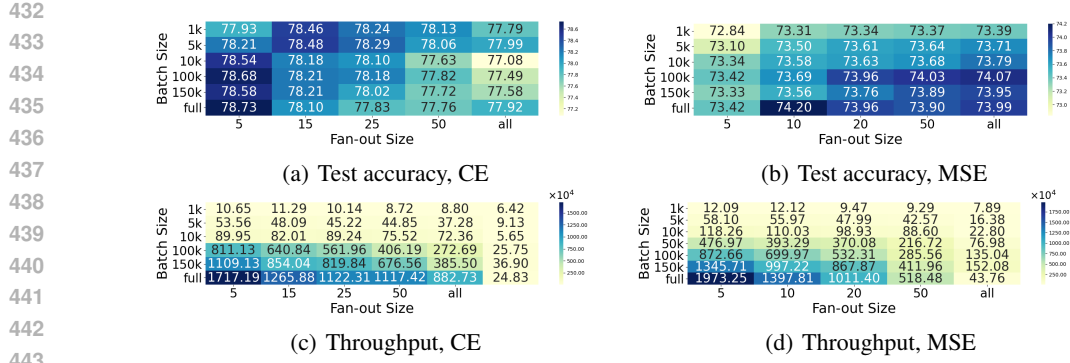


Figure 6: Test accuracies and training throughput (# nodes/s) of GraphSAGE under *CE* and *MSE* across varying batch sizes and fan-out sizes for ogbn-products.

Table 1: Best test accuracies of full-graph and mini-batch training of multi-layer GraphSAGE model without dropout layers after graph-based hyperparameter tuning.

Datasets	Reddit	Ogbn-arxiv	Ogbn-products	Ogbn-papers100M
Full-graph	96.13	70.96	77.92	59.54
Mini-batch	96.32	71.16	78.80	58.52

Understanding performance degradation. This degradation under *CE* arises as the models tend to converge to sharp minima under large batch sizes (Keskar et al., 2016). Since gradient variance decreases with larger batch and fan-out sizes, similar issues likely occur with large fan-out sizes. This degradation is more severe with fan-out sizes than batch sizes, as aggregating information from too many neighbors causes overfitting and weakens generalization. In contrast, such degradation is not obvious under *MSE*, which produces flatter minima due to weaker gradients near prediction boundaries (Bosman et al., 2020).

5.4 COMPUTATIONAL EFFICIENCY

Figures 6(c)-(d) show the training throughput as the number of target nodes processed per second on a single GPU for ogbn-products (see other datasets in Appendix N).

Answering our research question: Computational Efficiency improves with batch size as fixed computations (e.g., parameter updates) are distributed across more data, but becomes worse with larger fan-out sizes due to higher computational demands in message passing. Overall, mini-batch training achieves better computational efficiency than full-graph training.

Non-isotropic impacts of batch size and fan-out size in convergence, generalization, and computational efficiency. Based on the observations in Sec. 5.2 - 5.4, the batch size and the fan-out size exhibit distinct, non-uniform effects across different aspects of GNN training. These non-isotropic impacts highlight the need for careful tuning of both hyperparameters to balance computational efficiency, convergence, and generalization.

5.5 FULL-GRApH VS. MINI-BATCH TRAINING AFTER HYPERPARAMETER TUNING

Table 1 compares the generalization performance of full-graph and mini-batch training after tuning batch size and fan-out size via grid search. For the ogbn-papers100M dataset, two hidden layers with a hidden dimension of 128 are used due to resource constraints, limiting representation capacity. The best accuracy from mini-batch training is within 1.74% of full-graph training, suggesting that full-graph training does not consistently outperform well-tuned mini-batch settings.

Implications for tuning batch size b and fan-out size β . Based on both the theoretical and empirical observations above, we recommend keeping the batch size b below half of the training nodes and the fan-out size β under 15 for datasets with an average degree less than 50, to avoid generalization degradation and balance the trade-offs in computational efficiency and model performance.

6 RELATED WORK

The only existing comparison work (Bajaj et al., 2024) between full-graph and mini-batch GNN training empirically evaluates overall performance but does not investigate the impact of key hyperparameters (e.g., batch size and fan-out size) on model performance and computational efficiency,

486 thereby overlooking the trade-offs achieved by tuning these hyperparameters. Recent efforts (Yuan
 487 et al., 2023; Hu et al., 2021) focus on these hyperparameters but remain limited. For instance, Yuan
 488 et al. (Yuan et al., 2023) lack theoretical support, consider only limited batch sizes and fan-out
 489 values that are far smaller than those of full-graph training, and overlook the interplay of batch
 490 size and fan-out size. Hu et al. (Hu et al., 2021) rely on gradient variance to explain the role of
 491 batch size but do not consider fan-out size; thus their explanation conflicts with their empirical
 492 observations. Meanwhile, existing theoretical analyses of GNN training (Yang et al., 2023; Tang &
 493 Liu, 2023; Xu et al., 2021; Verma & Zhang, 2019; Yadati, 2022; Awasthi et al., 2021) overlook key
 494 graph-related factors (e.g., irregular graphs, the difference between training and testing graphs in
 495 mini-batch settings) and the impact of non-linear activation on gradients. Furthermore, due to GNN’s
 496 message-passing process, performance insights from DNNs (You et al., 2019; Smith, 2017; Golmant
 497 et al., 2018; Zou et al., 2020a; Bassily et al., 2018; Nabavinejad et al., 2021) cannot directly transfer
 498 to GNNs. We provide a more comprehensive related work discussion in Appendix O.

499 7 CONCLUSION

500 We provide a comprehensive empirical and theoretical study of full-graph vs. mini-batch GNN training
 501 from the view of batch size and fan-out size. We provide a novel theoretical GNN generalization
 502 analysis employing the Wasserstein distance, to study the impact of batch size and fan-out size. We
 503 empirically highlight the importance of iteration-based convergence metrics for hardware-independent
 504 evaluation. Our theoretical and empirical findings reveal the non-isotropic impact of batch size and
 505 fan-out size in GNN convergence and generalization. Finally, full-graph training does not consistently
 506 outperform well-tuned mini-batch settings in model performance or computational efficiency. These
 507 insights clarify the trade-offs between full-graph and mini-batch training. We further discuss the
 508 extension (e.g., link prediction tasks) and future work (e.g., different activations) in Appendix P.

509
 510
 511
 512
 513
 514
 515
 516
 517
 518
 519
 520
 521
 522
 523
 524
 525
 526
 527
 528
 529
 530
 531
 532
 533
 534
 535
 536
 537
 538
 539

540 REPRODUCIBILITY STATEMENT
541

542 For the theoretical results, all assumptions and complete proofs are provided in Appen-
543 dices A–E, G, and I–M, with additional important discussions in Appendices F, H, and P.
544 For the empirical study, the code is publicly available via an anonymous link provided in
545 the abstract: https://anonymous.4open.science/r/GNN_fullgraph_minibatch_training-8040/README.md. Detailed experimental configurations and additional experiment
546 results are represented in Appendix N, and all datasets are properly cited in the main text.
547

549 REFERENCES
550

551 Pranjal Awasthi, Abhimanyu Das, and Sreenivas Gollapudi. A convergence analysis of gradient
552 descent on graph neural networks. *Advances in Neural Information Processing Systems*, 34:
553 20385–20397, 2021.

554 Saurabh Bajaj, Hui Guan, and Marco Serafini. Graph neural network training systems: A performance
555 comparison of full-graph and mini-batch. *arXiv preprint arXiv:2406.00552*, 2024.

557 Raef Bassily, Mikhail Belkin, and Siyuan Ma. On exponential convergence of sgd in non-convex
558 over-parametrized learning. *arXiv preprint arXiv:1811.02564*, 2018.

560 Anna Sergeevna Bosman, Andries Engelbrecht, and Mardé Helbig. Visualising basins of attraction
561 for the cross-entropy and the squared error neural network loss functions. *Neurocomputing*, 400:
562 113–136, 2020.

563 Zhenkun Cai, Xiao Yan, Yidi Wu, Kaihao Ma, James Cheng, and Fan Yu. Dgcl: An efficient
564 communication library for distributed gnn training. In *Proceedings of the Sixteenth European
565 Conference on Computer Systems*, pp. 130–144, 2021.

567 Jianfei Chen, Jun Zhu, and Le Song. Stochastic training of graph convolutional networks with
568 variance reduction. *arXiv preprint arXiv:1710.10568*, 2017.

570 Jie Chen, Tengfei Ma, and Cao Xiao. Fastgcn: fast learning with graph convolutional networks via
571 importance sampling. *arXiv preprint arXiv:1801.10247*, 2018.

572 Wei-Lin Chiang, Xuanqing Liu, Si Si, Yang Li, Samy Bengio, and Cho-Jui Hsieh. Cluster-gcn: An
573 efficient algorithm for training deep and large graph convolutional networks. In *Proceedings of the
574 25th ACM SIGKDD international conference on knowledge discovery & data mining*, pp. 257–266,
575 2019.

577 Weilin Cong, Morteza Ramezani, and Mehrdad Mahdavi. On the importance of sampling in training
578 gcns: Tighter analysis and variance reduction. *arXiv preprint arXiv:2103.02696*, 2021a.

580 Weilin Cong, Morteza Ramezani, and Mehrdad Mahdavi. On provable benefits of depth in training
581 graph convolutional networks. *Advances in Neural Information Processing Systems*, 34:9936–9949,
582 2021b.

583 Amit Daniely, Roy Frostig, and Yoram Singer. Toward deeper understanding of neural networks: The
584 power of initialization and a dual view on expressivity. *Advances in neural information processing
585 systems*, 29, 2016.

587 Simon S Du, Xiyu Zhai, Barnabas Poczos, and Aarti Singh. Gradient descent provably optimizes
588 over-parameterized neural networks. *arXiv preprint arXiv:1810.02054*, 2018.

589 Simon S Du, Kangcheng Hou, Russ R Salakhutdinov, Barnabas Poczos, Ruosong Wang, and Keyulu
590 Xu. Graph neural tangent kernel: Fusing graph neural networks with graph kernels. *Advances in
591 neural information processing systems*, 32, 2019.

593 Ran El-Yaniv and Dmitry Pechyony. Transductive rademacher complexity and its applications.
Journal of Artificial Intelligence Research, 35:193–234, 2009.

594 Matthias Fey, Jan E Lenssen, Frank Weichert, and Jure Leskovec. Gnnautoscale: Scalable and
 595 expressive graph neural networks via historical embeddings. In *International conference on*
 596 *machine learning*, pp. 3294–3304. PMLR, 2021.

597

598 Vikas Garg, Stefanie Jegelka, and Tommi Jaakkola. Generalization and representational limits of
 599 graph neural networks. In *International Conference on Machine Learning*, pp. 3419–3430, 2020.

600

601 Justin Gilmer, Samuel S Schoenholz, Patrick F Riley, Oriol Vinyals, and George E Dahl. Neural
 602 message passing for quantum chemistry. In *International conference on machine learning*, pp.
 603 1263–1272, 2017.

604

605 Noah Golmant, Nikita Vemuri, Zhewei Yao, Vladimir Feinberg, Amir Gholami, Kai Rothauge,
 606 Michael W Mahoney, and Joseph Gonzalez. On the computational inefficiency of large batch sizes
 607 for stochastic gradient descent. *arXiv preprint arXiv:1811.12941*, 2018.

608

609 Will Hamilton, Zhitao Ying, and Jure Leskovec. Inductive representation learning on large graphs.
 610 *Advances in neural information processing systems*, 30, 2017.

611

612 Johann Hauswald, Yiping Kang, Michael A Laurenzano, Quan Chen, Cheng Li, Trevor Mudge,
 613 Ronald G Dreslinski, Jason Mars, and Lingjia Tang. Djinn and tonic: Dnn as a service and its
 614 implications for future warehouse scale computers. *ACM SIGARCH Computer Architecture News*,
 615 43(3S):27–40, 2015.

616

617 Weihua Hu, Matthias Fey, Marinka Zitnik, Yuxiao Dong, Hongyu Ren, Bowen Liu, Michele Catasta,
 618 and Jure Leskovec. Open graph benchmark: Datasets for machine learning on graphs. *Advances in*
 619 *neural information processing systems*, 33:22118–22133, 2020.

620

621 Yaochen Hu, Amit Levi, Ishaan Kumar, Yingxue Zhang, and Mark Coates. On batch-size selection
 622 for stochastic training for graph neural networks. 2021.

623

624 Tim Kaler, Nickolas Stathas, Anne Ouyang, Alexandros-Stavros Iliopoulos, Tao Schardl, Charles E
 625 Leiserson, and Jie Chen. Accelerating training and inference of graph neural networks with fast
 626 sampling and pipelining. *Proceedings of Machine Learning and Systems*, 4:172–189, 2022.

627

628 Leonid V Kantorovich. Mathematical methods of organizing and planning production. *Management*
 629 *science*, 6(4):366–422, 1960.

630

631 Nitish Shirish Keskar, Dheevatsa Mudigere, Jorge Nocedal, Mikhail Smelyanskiy, and Ping Tak Peter
 632 Tang. On large-batch training for deep learning: Generalization gap and sharp minima. *arXiv*
 633 *preprint arXiv:1609.04836*, 2016.

634

635 Vladimir Koltchinskii. Rademacher penalties and structural risk minimization. *IEEE Transactions*
 636 *on Information Theory*, 47(5):1902–1914, 2001.

637

638 Shen Li, Yanli Zhao, Rohan Varma, Omkar Salpekar, Pieter Noordhuis, Teng Li, Adam Paszke, Jeff
 639 Smith, Brian Vaughan, Pritam Damania, et al. Pytorch distributed: Experiences on accelerating
 640 data parallel training. *arXiv preprint arXiv:2006.15704*, 2020.

641

642 Yanzhi Li and Yingyu Liang. Learning overparameterized neural networks via stochastic gradient
 643 descent on structured data. *Advances in neural information processing systems*, 31, 2018.

644

645 Renjie Liao, Raquel Urtasun, and Richard Zemel. A pac-bayesian approach to generalization bounds
 646 for graph neural networks. *arXiv preprint arXiv:2012.07690*, 2020.

647

648 Yucong Lin, Silu Li, Jiaxing Xu, Jiawei Xu, Dong Huang, Wendi Zheng, Yuan Cao, and Junwei
 649 Lu. Graph over-parameterization: Why the graph helps the training of deep graph convolutional
 650 network. *Neurocomputing*, 534:77–85, 2023.

651

652 Chaoyue Liu, Dmitriy Drusvyatskiy, Misha Belkin, Damek Davis, and Yian Ma. Aiming towards
 653 the minimizers: fast convergence of sgd for overparametrized problems. *Advances in neural*
 654 *information processing systems*, 36, 2024.

648 Tianfeng Liu, Yangrui Chen, Dan Li, Chuan Wu, Yibo Zhu, Jun He, Yanghua Peng, Hongzheng Chen,
 649 Hongzhi Chen, and Chuanxiong Guo. Bgl:gpu-efficient gnn training by optimizing graph data i/o
 650 and preprocessing. In *20th USENIX Symposium on Networked Systems Design and Implementation*
 651 (*NSDI 23*), pp. 103–118, 2023.

652 Shaogao Lv. Generalization bounds for graph convolutional neural networks via rademacher com-
 653 plexity. *arXiv preprint arXiv:2102.10234*, 2021.

654 Jiaqi Ma, Junwei Deng, and Qiaozhu Mei. Subgroup generalization and fairness of graph neural
 655 networks. *Advances in Neural Information Processing Systems*, 34:1048–1061, 2021.

656 David McAllester. Simplified pac-bayesian margin bounds. In *Learning Theory and Kernel Machines:*
 657 *16th Annual Conference on Learning Theory and 7th Kernel Workshop, COLT/Kernel 2003,*
 658 *Washington, DC, USA, August 24-27, 2003. Proceedings*, pp. 203–215, 2003.

659 Vasimuddin Md, Sanchit Misra, Guixiang Ma, Ramanarayanan Mohanty, Evangelos Georganas, Alexan-
 660 der Heinecke, Dhiraj Kalamkar, Nesreen K Ahmed, and Sasikanth Avancha. Distgnn: Scalable
 661 distributed training for large-scale graph neural networks. In *Proceedings of the International*
 662 *Conference for High Performance Computing, Networking, Storage and Analysis*, pp. 1–14, 2021.

663 Hesham Mostafa. Sequential aggregation and rematerialization: Distributed full-batch training of
 664 graph neural networks on large graphs. *MLSys*, 2022.

665 Seyed Morteza Nabavinejad, Sherief Reda, and Masoumeh Ebrahimi. Batchsizer: Power-performance
 666 trade-off for dnn inference. In *Proceedings of the 26th Asia and South Pacific Design Automation*
 667 *Conference*, pp. 819–824, 2021.

668 Pranjal Naman and Yogesh Simmhan. Performance trade-offs in gnn inference: An early study on
 669 hardware and sampling configurations. In *2024 IEEE 31st International Conference on High*
 670 *Performance Computing, Data and Analytics Workshop (HiPCW)*, pp. 173–174. IEEE, 2024.

671 Kenta Oono and Taiji Suzuki. Optimization and generalization analysis of transduction through
 672 gradient boosting and application to multi-scale graph neural networks. *Advances in Neural*
 673 *Information Processing Systems*, 33:18917–18930, 2020.

674 Jingshu Peng, Zhao Chen, Yingxia Shao, Yanyan Shen, Lei Chen, and Jiannong Cao. Sancus: sta le n
 675 ess-aware c omm u nication-avoiding full-graph decentralized training in large-scale graph neural
 676 networks. *Proceedings of the VLDB Endowment*, 15(9):1937–1950, 2022.

677 Boris Teodorovich Polyak. Gradient methods for minimizing functionals. *Zhurnal vychislitel'noi*
 678 *matematiki i matematicheskoi fiziki*, 3(4):643–653, 1963.

679 Franco Scarselli, Ah Chung Tsoi, and Markus Hagenbuchner. The vapnik–chervonenkis dimension
 680 of graph and recursive neural networks. *Neural Networks*, 108:248–259, 2018.

681 Zhihao Shi, Xize Liang, and Jie Wang. Lmc: Fast training of gnns via subgraph sampling with
 682 provable convergence. *arXiv preprint arXiv:2302.00924*, 2023.

683 Zhihao Shi, Jie Wang, Zhiwei Zhuang, Xize Liang, Bin Li, and Feng Wu. Accurate and scalable
 684 graph neural networks via message invariance. *arXiv preprint arXiv:2502.19693*, 2025.

685 SL Smith. Don't decay the learning rate, increase the batch size. *arXiv preprint arXiv:1711.00489*,
 686 2017.

687 Junwei Su and Chuan Wu. On the interplay between graph structure and learning algorithms in graph
 688 neural networks. In *Forty-second International Conference on Machine Learning*, 2025.

689 Huayi Tang and Yong Liu. Towards understanding generalization of graph neural networks. In
 690 *International Conference on Machine Learning*, pp. 33674–33719, 2023.

691 Vladimir N Vapnik and A Ya Chervonenkis. On the uniform convergence of relative frequencies of
 692 events to their probabilities. In *Measures of complexity: festschrift for alexey chervonenkis*, pp.
 693 11–30. 2015.

702 Petar Veličković, Guillem Cucurull, Arantxa Casanova, Adriana Romero, Pietro Lio, and Yoshua
 703 Bengio. Graph attention networks. *arXiv preprint arXiv:1710.10903*, 2017.

704

705 Saurabh Verma and Zhi-Li Zhang. Stability and generalization of graph convolutional neural networks.
 706 In *Proceedings of the 25th ACM SIGKDD International Conference on Knowledge Discovery &*
 707 *Data Mining*, pp. 1539–1548, 2019.

708 Cheng Wan, Youjie Li, Ang Li, Nam Sung Kim, and Yingyan Lin. Bns-gcn: Efficient full-graph
 709 training of graph convolutional networks with partition-parallelism and random boundary node
 710 sampling. *Proceedings of Machine Learning and Systems*, 4:673–693, 2022a.

711 Cheng Wan, Youjie Li, Cameron R Wolfe, Anastasios Kyrillidis, Nam Sung Kim, and Yingyan
 712 Lin. Pipegcn: Efficient full-graph training of graph convolutional networks with pipelined feature
 713 communication. *arXiv preprint arXiv:2203.10428*, 2022b.

714

715 Xincheng Wan, Kaiqiang Xu, Xudong Liao, Yilun Jin, Kai Chen, and Xin Jin. Scalable and efficient
 716 full-graph gnn training for large graphs. *Proceedings of the ACM on Management of Data*, 1(2):
 717 1–23, 2023.

718 Keyulu Xu, Weihua Hu, Jure Leskovec, and Stefanie Jegelka. How powerful are graph neural
 719 networks? *arXiv preprint arXiv:1810.00826*, 2018.

720

721 Keyulu Xu, Mozhi Zhang, Stefanie Jegelka, and Kenji Kawaguchi. Optimization of graph neural
 722 networks: Implicit acceleration by skip connections and more depth. In *International Conference*
 723 *on Machine Learning*, pp. 11592–11602, 2021.

724 Naganand Yadati. A convex formulation for graph convolutional training: Two layer case. In *2022*
 725 *IEEE International Conference on Data Mining (ICDM)*, pp. 1281–1286. IEEE, 2022.

726

727 Chenxiao Yang, Qitian Wu, David Wipf, Ruoyu Sun, and Junchi Yan. How graph neural networks
 728 learn: Lessons from training dynamics in function space. *arXiv preprint arXiv:2310.05105*, 2023.

729

730 Yang You, Aydin Buluç, and James Demmel. Scaling deep learning on gpu and knights landing
 731 clusters. In *Proceedings of the International Conference for High Performance Computing,
 Networking, Storage and Analysis*, pp. 1–12, 2017.

732

733 Yang You, Jing Li, Sashank Reddi, Jonathan Hseu, Sanjiv Kumar, Srinadh Bhojanapalli, Xiaodan
 734 Song, James Demmel, Kurt Keutzer, and Cho-Jui Hsieh. Large batch optimization for deep
 735 learning: Training bert in 76 minutes. *arXiv preprint arXiv:1904.00962*, 2019.

736

737 Hao Yuan, Yajiong Liu, Yanfeng Zhang, Xin Ai, Qiange Wang, Chaoyi Chen, Yu Gu, and Ge Yu.
 738 Comprehensive evaluation of gnn training systems: A data management perspective. *arXiv preprint*
arXiv:2311.13279, 2023.

739

740 Hanqing Zeng, Hongkuan Zhou, Ajitesh Srivastava, Rajgopal Kannan, and Viktor Prasanna. Graph-
 741 saint: Graph sampling based inductive learning method. *arXiv preprint arXiv:1907.04931*, 2019.

742

743 Muhan Zhang and Yixin Chen. Link prediction based on graph neural networks. *Advances in neural
 744 information processing systems*, 31, 2018.

745

746 Si Zhang, Hanghang Tong, Jiejun Xu, and Ross Maciejewski. Graph convolutional networks: a
 747 comprehensive review. *Computational Social Networks*, 6(1):1–23, 2019.

748

749 Guoyi Zhao, Tian Zhou, and Lixin Gao. Cm-gcn: A distributed framework for graph convolutional
 750 networks using cohesive mini-batches. In *2021 IEEE International Conference on Big Data (Big
 751 Data)*, pp. 153–163. IEEE, 2021.

752

753 Da Zheng, Xiang Song, Chengru Yang, Dominique LaSalle, and George Karypis. Distributed
 754 hybrid cpu and gpu training for graph neural networks on billion-scale heterogeneous graphs. In
 755 *Proceedings of the 28th ACM SIGKDD Conference on Knowledge Discovery and Data Mining*, pp.
 4582–4591, 2022.

756

757 Rong Zhu, Kun Zhao, Hongxia Yang, Wei Lin, Chang Zhou, Baole Ai, Yong Li, and Jingren Zhou.
 758 Aligraph: A comprehensive graph neural network platform. *arXiv preprint arXiv:1902.08730*,
 759 2019.

756 Difan Zou, Yuan Cao, Dongruo Zhou, and Quanquan Gu. Stochastic gradient descent optimizes
757 over-parameterized deep relu networks. *arXiv preprint arXiv:1811.08888*, 2018.
758

759 Difan Zou, Ziniu Hu, Yewen Wang, Song Jiang, Yizhou Sun, and Quanquan Gu. Layer-dependent
760 importance sampling for training deep and large graph convolutional networks. *Advances in neural*
761 *information processing systems*, 32, 2019.

762 Difan Zou, Yuan Cao, Dongruo Zhou, and Quanquan Gu. Gradient descent optimizes over-
763 parameterized deep relu networks. *Machine learning*, 109:467–492, 2020a.
764

765 Difan Zou, Philip M Long, and Quanquan Gu. On the global convergence of training deep linear
766 resnets. *arXiv preprint arXiv:2003.01094*, 2020b.
767
768
769
770
771
772
773
774
775
776
777
778
779
780
781
782
783
784
785
786
787
788
789
790
791
792
793
794
795
796
797
798
799
800
801
802
803
804
805
806
807
808
809

810 THE USE OF LARGE LANGUAGE MODELS (LLMs)
811812 We used a large language model (LLM) only as a general-purpose writing assistant to aid in grammar
813 checking and polishing the writing. The LLM did not contribute to research ideas, experiment design,
814 theoretical analysis, or result interpretation.
815816 A NOTATIONS
817

818 819 Table 2: Notations

n	Number of nodes of the entire graph
$n_{\text{train}} / n_{\text{test}}$	Number of nodes in the training set / the testing set
n_{\min}	The minimal value between training and testing sets
\mathbf{X}/\mathbf{x}_i	Node feature matrix / i -th row of node feature matrix
y_i	Ground truth label of node i
$\mathbf{y}_i / \hat{\mathbf{y}}_i$	Ground truth label in one-hot form / estimated outcomes of node i
r	feature size
b	Batch size
β	Fan-out size
$\mathbf{A}_{\text{train}}^{\min} / \mathbf{A}_{\text{train}}^{\text{full}}$	Adjacency matrix in each mini-batch / full-graph training iteration
$\mathbf{D}_{\text{train}}^{\text{in},\min} / \mathbf{D}_{\text{train}}^{\text{in},\text{full}}$	Diagonal in-degree matrices in each mini-batch / full-graph training iteration
$\mathbf{D}_{\text{train}}^{\text{out},\min} / \mathbf{D}_{\text{train}}^{\text{out},\text{full}}$	Diagonal out-degree matrices in each mini-batch / full-graph training iteration
$\mathbf{A}_{\text{train}}^{\min} / \mathbf{A}_{\text{train}}^{\text{full}}$	Normalized adjacency matrix in a mini-batch / full-graph training iteration
$\tilde{\mathbf{a}}_{\text{train},i}^{\min} / \tilde{\mathbf{a}}_{\text{train},i}^{\text{full}}$	i -th row of normalized adjacency matrix in a mini-batch / full-graph training iteration
$\mathbf{A}_{\text{test}} / \tilde{\mathbf{a}}_{\text{test},i}$	Normalized adjacency matrix / i -th row of Normalized adjacency matrix in testing set
$\mathbf{W}^{\min} / \mathbf{W}^{\text{full}}$	Learnable parameters of the GNN under mini-batch / full-graph training
$\mathbf{w}_i^{\min} / \mathbf{w}_i^{\text{full}}$	i -th row of parameters of the GNN under mini-batch / full-graph training
$\mathbf{W}^{\min*} / \mathbf{W}^{\text{full}*}$	Ground truth of learnable parameters $\mathbf{W}^{\min} / \mathbf{W}^{\text{full}}$
$\mathbf{w}_i^{\min*} / \mathbf{w}_i^{\text{full}*}$	i -th row of ground truth of learnable parameters $\mathbf{W}^{\min} / \mathbf{W}^{\text{full}}$
h	Hidden size
K	Number of label categories
$\sigma(\cdot)$	ReLU activation function
$\hat{\sigma}(\cdot)$	Dual activation function
$L_{\text{train}}(\cdot) / \hat{L}_{\text{train}}(\cdot)$	Expected / empirical training risk
$L_{\text{train}}^{\min}(\cdot) / \hat{L}_{\text{train}}^{\min}(\cdot)$	Expected / empirical training risk in a mini-batch
$L_{\text{test}}(\cdot) / \hat{L}_{\text{test}}(\cdot)$	Expected / empirical testing risk
$\hat{\mathbf{G}}$	Stochastic gradient in mini-batch training
η	Learning rate
\mathcal{P}/\mathcal{Q}	Prior / Posterior distribution of model parameters
$U(\cdot)$	Expected loss discrepancy between training set \mathcal{C} and testing set \mathcal{Z}
$\delta(\cdot)$	Distance function
θ	Covariance

853
854 To easily distinguish the training risk between full-graph and mini-batch training, we rewrite $L_{\text{train}}(\cdot)$
855 and $\hat{L}_{\text{train}}(\cdot)$ as $L_{\text{train}}^{\text{full}}(\cdot)$ and $\hat{L}_{\text{train}}^{\text{full}}(\cdot)$ under full-graph training. Similarly, we rewrite the gradient
856 $\nabla L_{\text{train}}(\cdot)$ as $\nabla \hat{L}_{\text{train}}^{\text{full}}(\cdot)$ during full-graph training, and the stochastic gradient $\hat{\mathbf{G}}$ as $\nabla \hat{L}_{\text{train}}^{\min}(\cdot)$.
857858 B PROOF OF CONVERGENCE THEOREM IN FULL-GRAFH TRAINING WITH
859 MSE
860862 In this section, we provide the proof of the convergence theorem in full-graph training with MSE. We
863 consider multi-class node classification tasks using a one-round GNN trained with the MSE, defined
as $l(\mathbf{W}, \tilde{\mathbf{a}}_{\text{train},i}^{\text{full}}) = \frac{1}{2} \|\hat{\mathbf{y}}_i - \mathbf{y}_i\|_F^2$. The ground truth label y_i is rewritten as $\mathbf{y}_i \in \mathbb{R}^{1 \times K}$ in the one-hot

864 form, where $K \geq 2$ is the number of label categories. The final output of the GNN model is given
 865 by $\hat{\mathbf{y}}_i = \mathbf{z}_i = \sigma(\tilde{\mathbf{a}}_{\text{train},i}^{\text{full}} \mathbf{X} \mathbf{W}^{\top})$, where the ReLU function is modified as $\sigma(x) = \sqrt{2} \max(x, 0)$.
 866 Note that $1/2$ in the MSE function and $\sqrt{2}$ in the ReLU function are introduced to simplify the proof.
 867 The hidden dimension h becomes K . Note that The rows of \mathbf{W} are initialized independently from a
 868 Gaussian distribution $N(0, \kappa^2 \mathbf{I})$.
 869

870 We decompose the analysis of GNN optimization dynamic into three steps.

871 *Step 1: Reformulating loss and gradient expressions on irregular graphs.* We decouple the activation
 872 function from the aggregated node features. For instance, we extract the aggregation from the ReLU
 873 function by reformulating squared loss terms.

874 *Step 2: Bounding the norm of gradient.* Based on the reformulated loss and gradient expressions, we
 875 aim to quantify the magnitude of optimization updates by bounding the gradient norm, facilitating
 876 convergence analysis. This can be achieved by leveraging the Polyak–Łojasiewicz (PL) inequality
 877 (Polyak, 1963), where the squared norm of the gradient is lower bounded by the loss value scaled by
 878 a factor.

879 *Step 3: Bounding the number of iterations to Convergence.* We first leverage the smoothness of the
 880 loss function to derive a per-iteration inequality relating loss reduction to the gradient norm, and then
 881 accumulate these iteration-wise inequalities over GD updates to obtain an upper bound on the number
 882 of iterations required for convergence.
 883

884 B.1 ASSUMPTIONS

885 **Assumption B.1.** The node feature \mathbf{x}_i is drawn i.i.d from $N(0, \mathbf{I}_{r \times r})$ for all i in the graph, with
 886 $\|\mathbf{X}\|_2^2 \leq C_x$ for a constant $C_x > 0$.
 887

888 **Assumption B.2.** The rows of ground truth parameters satisfy $\|\mathbf{w}_i^*\|_2 = 1$ for all $i \in \{1, \dots, h\}$.
 889

890 Assumption B.1 specifies the distribution of node features and bounds the norm of the feature
 891 matrix, and Assumption B.2 limits the norm of ground truth parameters for the GNN model. These
 892 assumptions are also adopted in the GNN convergence analysis on regular graphs (Awasthi et al.,
 893 2021). We emphasize Assumptions B.1 and B.2 are introduced to simplify the proof. Note that
 894 Assumption B.2 can be relaxed to be that $\|\mathbf{w}_i^*\|_2$ is lower and upper bounded by some constants
 895 instead of fixing $\|\mathbf{w}_i^*\|_2 = 1$.
 896

897 **Definition B.3** (Dual activation (Daniely et al., 2016)) The dual activation of σ is the function
 898 $\hat{\sigma} : [-1, 1] \rightarrow \mathbb{R}$ defined as $\hat{\sigma}(\theta) = \mathbb{E}[\sigma(x)\sigma(y)]$, where x and y are jointly Gaussian random
 899 variables with mean zero, variance one, and covariance θ .

900 Definition B.3 demonstrated that dual activations hold continuity over the interval $[-1, 1]$ and
 901 convexity within the range $[0, 1]$.
 902

903 B.2 EXPRESSIONS FOR LOSS AND GRADIENTS.

904 While our ultimate training objective remains empirical risk minimization, we analyze the optimization
 905 dynamics of MSE using its expected risk formulation on node feature distribution. This is done
 906 to simplify the proof, as expected risk offers a cleaner mathematical structure and does not affect
 907 the graph structure. Although this approximation is more accurate in the large-sample regime, we
 908 adopt it here as a modeling tool to study the impact of batch size and fan-out size in convergence,
 909 even when analyzing small-sample settings.
 910

911 **Expression for MSE loss:** We first begin by writing an equivalent expression of $L_{\text{train}}^{\text{full}}(\mathbf{w}_j^{\text{full}})$ with
 912 $j \in \{1, \dots, h\}$ as:
 913

$$914 L_{\text{train}}^{\text{full}}(\mathbf{w}_j^{\text{full}}) = \frac{1}{2n_{\text{train}}} (\mathbb{E} \left[\sum_{i=1}^{n_{\text{train}}} \sigma \left(\tilde{\mathbf{a}}_{\text{train},i}^{\text{full}} \mathbf{X} (\mathbf{w}_j^{\text{full}})^{\top} \right)^2 \right] + \mathbb{E} \left[\sum_{i=1}^{n_{\text{train}}} \sigma \left(\tilde{\mathbf{a}}_{\text{train},i}^{\text{full}} \mathbf{X} (\mathbf{w}_j^{\text{full}*})^{\top} \right)^2 \right] \\ 915 - 2\mathbb{E} \left[\sum_{i,j=1}^{n_{\text{train}}} \sigma \left(\tilde{\mathbf{a}}_{\text{train},i}^{\text{full}} \mathbf{X} (\mathbf{w}_j^{\text{full}})^{\top} \right) \sigma \left(\tilde{\mathbf{a}}_{\text{train},i}^{\text{full}} \mathbf{X} (\mathbf{w}_j^{\text{full}*})^{\top} \right) \right]) \quad (1)$$

We next compute expressions for each of the three terms above.

$$\begin{aligned}
& \frac{1}{n_{\text{train}}} \mathbb{E} \left[\sum_{i=1}^{n_{\text{train}}} \sigma \left(\tilde{\mathbf{a}}_{\text{train},i}^{\text{full}} \mathbf{X} \left(\mathbf{w}_j^{\text{full}} \right)^{\top} \right)^2 \right] \\
&= \frac{1}{n_{\text{train}}} \mathbb{E} \left[\sum_{i,k=1}^{n_{\text{train}}} p_{ij} \sigma \left(\tilde{\mathbf{a}}_{\text{train},i}^{\text{full}} \mathbf{X} \left(\mathbf{w}_j^{\text{full}} \right)^{\top} \right) \sigma \left(\tilde{\mathbf{a}}_{\text{train},k}^{\text{full}} \mathbf{X} \left(\mathbf{w}_j^{\text{full}} \right)^{\top} \right) \right] \\
&= \frac{1}{n_{\text{train}}} \mathbb{E} \left[\left\| \mathbf{w}_j^{\text{full}} \right\|^2 \sum_{i,k=1}^{n_{\text{train}}} p_{ij} \sqrt{\left(\tilde{\mathbf{A}}_{\text{train}}^{\text{full}} \mathbf{1} \right)_i \left(\tilde{\mathbf{A}}_{\text{train}}^{\text{full}} \mathbf{1} \right)_k} \right. \\
&\quad \left. \cdot \sigma \left(\frac{\tilde{\mathbf{a}}_{\text{train},i}^{\text{full}} \mathbf{X} \left(\mathbf{w}_j^{\text{full}} \right)^{\top}}{\sqrt{\left(\tilde{\mathbf{A}}_{\text{train}}^{\text{full}} \mathbf{1} \right)_i} \left\| \mathbf{w}_j^{\text{full}} \right\|} \right) \sigma \left(\frac{\tilde{\mathbf{a}}_{\text{train},k}^{\text{full}} \mathbf{X} \left(\mathbf{w}_j^{\text{full}} \right)^{\top}}{\sqrt{\left(\tilde{\mathbf{A}}_{\text{train}}^{\text{full}} \mathbf{1} \right)_k} \left\| \mathbf{w}_j^{\text{full}} \right\|} \right) \right] \tag{2} \\
&= \frac{\left\| \mathbf{w}_j^{\text{full}} \right\|^2}{n_{\text{train}}} \sum_{i,k=1}^{n_{\text{train}}} p_{ik} \hat{\sigma} \left(\frac{\varrho_{i,k}^{\text{full}}}{\sqrt{\vartheta_{i,k}^{\text{full}}}} \right) \sqrt{\vartheta_{i,k}^{\text{full}}} \\
&= \left\| \mathbf{w}_j^{\text{full}} \right\|^2 \Gamma^{\text{full}},
\end{aligned}$$

where the penultimate equality follows Definition B.3. We use $p_{ij} = 1$ if $i = j$ and $p_{ij} = 0$ if $i \neq j$, $\varrho_{i,j}^{\text{full}}$ to denote the amount of common messages between node i and node j at a given training iteration, and we define:

$$\Gamma^{\text{full}} = \frac{1}{n_{\text{train}}} \sum_{i,j=1}^{n_{\text{train}}} p_{ij} \hat{\sigma} \left(\frac{\varrho_{i,j}^{\text{full}}}{\sqrt{\vartheta_{i,j}^{\text{full}}}} \right) \sqrt{\vartheta_{i,j}^{\text{full}}}, \quad (3)$$

$$\vartheta_{i,j}^{\text{full}} = \left(\tilde{\mathbf{A}}_{\text{train}}^{\text{full}} \mathbb{1} \right)_i \left(\tilde{\mathbf{A}}_{\text{train}}^{\text{full}} \mathbb{1} \right)_j. \quad (4)$$

Similarly, we get the second term as:

$$\frac{1}{n_{\text{train}}} \mathbb{E} \left[\sum_{i=1}^{n_{\text{train}}} \sigma \left(\tilde{\mathbf{a}}_{\text{train},i}^{\text{full}} \mathbf{X} \left(\mathbf{w}_j^{\text{full}*} \right)^{\top} \right)^2 \right] = \left\| \mathbf{w}_j^{\text{full}*} \right\|^2 \Gamma^{\text{full}}. \quad (5)$$

We simplify the last term as:

$$\begin{aligned}
& \frac{1}{n_{\text{train}}} \mathbb{E} \left[\sum_{i,k=1}^{n_{\text{train}}} p_{ik} \sigma \left(\tilde{\mathbf{a}}_{\text{train},i}^{\text{full}} \mathbf{X} \left(\mathbf{w}_j^{\text{full}} \right)^{\top} \right) \sigma \left(\tilde{\mathbf{a}}_{\text{train},k}^{\text{full}} \mathbf{X} \left(\mathbf{w}_j^{\text{full}*} \right)^{\top} \right) \right] \\
&= \frac{1}{n_{\text{train}}} \mathbb{E} \left[\left\| \mathbf{w}_j^{\text{full}} \right\| \left\| \mathbf{w}_j^{\text{full}*} \right\| \sum_{i,k=1}^{n_{\text{train}}} p_{ik} \sqrt{\left(\tilde{\mathbf{A}}_{\text{train}}^{\text{full}} \mathbf{1} \right)_i \left(\tilde{\mathbf{A}}_{\text{train}}^{\text{full}} \mathbf{1} \right)_k} \right. \\
&\quad \left. \cdot \sigma \left(\frac{\tilde{\mathbf{a}}_{\text{train},i}^{\text{full}} \mathbf{X} \left(\mathbf{w}_j^{\text{full}} \right)^{\top}}{\sqrt{\left(\tilde{\mathbf{A}}_{\text{train}}^{\text{full}} \mathbf{1} \right)_i \left\| \mathbf{w}_j^{\text{full}} \right\|}} \right) \sigma \left(\frac{\tilde{\mathbf{a}}_{\text{train},k}^{\text{full}} \mathbf{X} \left(\mathbf{w}_j^{\text{full}*} \right)^{\top}}{\sqrt{\left(\tilde{\mathbf{A}}_{\text{train}}^{\text{full}} \mathbf{1} \right)_k \left\| \mathbf{w}_j^{\text{full}*} \right\|}} \right) \right] \\
&= \frac{1}{n_{\text{train}}} \left\| \mathbf{w}_j^{\text{full}} \right\| \left\| \mathbf{w}_j^{\text{full}*} \right\| \sum_{i,k=1}^{n_{\text{train}}} p_{ik} \hat{\sigma} \left(\frac{\varrho_{i,k}^{\text{full}} \left(\mathbf{w}_j^{\text{full}} \right)^{\top} \mathbf{w}_j^{\text{full}*}}{\sqrt{\vartheta_{i,k}^{\text{full}}} \left\| \mathbf{w}_j^{\text{full}} \right\| \left\| \mathbf{w}_j^{\text{full}*} \right\|} \right) \sqrt{\vartheta_{i,k}^{\text{full}}}.
\end{aligned} \tag{6}$$

Therefore, we have the expression of $L_{\text{train}}^{\text{full}}(\mathbf{w}_i^{\text{full}})$ as:

$$L_{\text{train}}^{\text{full}} \left(\mathbf{w}_j^{\text{full}} \right) = \frac{1}{2} (\| \mathbf{w}_j^{\text{full}} \|^2 \Gamma^{\text{full}} + \| \mathbf{w}_j^{\text{full}*} \|^2 \Gamma^{\text{full}} \\ - \frac{2}{n_{\text{train}}} \left\| \mathbf{w}_j^{\text{full}} \right\| \left\| \mathbf{w}_j^{\text{full}*} \right\| \sum_{i,k=1}^{n_{\text{train}}} p_{ik} \hat{\sigma} \left(\frac{\varrho_{i,k}^{\text{full}}}{\sqrt{\vartheta_{i,k}^{\text{full}}}} \frac{(\mathbf{w}_j^{\text{full}})^\top \mathbf{w}_j^{\text{full}*}}{\| \mathbf{w}_j^{\text{full}} \| \| \mathbf{w}_j^{\text{full}*} \|} \right) \sqrt{\vartheta_{i,k}^{\text{full}}}). \quad (7)$$

972 It is easy to see that if $\mathbf{w}_{j,0}^{\text{full}}$ is the initial value of $\mathbf{w}_j^{\text{full}}$ with $j \in \{1, \dots, h\}$ then each subsequent
 973 iteration will be a linear combination of $\mathbf{w}_{j,0}^{\text{full}}$ and $\mathbf{w}_j^{\text{full}*}$. Hence we can assume that $\mathbf{w}_j^{\text{full}} =$
 974 $\phi^{\text{full}} \mathbf{w}_j^{\text{full}*} + \psi^{\text{full}} \mathbf{w}_j^{\perp}$, where \mathbf{w}^{\perp} is a fixed unit vector (depending on the initialization) orthogonal
 975 to $\mathbf{w}_j^{\text{full}*}$. Then rewriting the loss in terms of ϕ^{full} , ψ^{full} and recalling that $\|\mathbf{w}_j^{\text{full}*}\| = 1$ we get the
 976 simplified expression of $L_{\text{train}}^{\text{full}}(\mathbf{w}_j^{\text{full}})$:
 977

$$979 \quad L_{\text{train}}^{\text{full}}(\phi^{\text{full}}, \psi^{\text{full}}) = \frac{1}{2} \left((\phi^{\text{full}})^2 + (\psi^{\text{full}})^2 + 1 \right) \Gamma^{\text{full}} - \sqrt{(\phi^{\text{full}})^2 + (\psi^{\text{full}})^2} \Upsilon^{\text{full}}, \quad (8)$$

981 where we define:
 982

$$983 \quad \Upsilon^{\text{full}} = \frac{1}{n_{\text{train}}} \sum_{i,j=1}^{n_{\text{train}}} p_{ij} \hat{\sigma} \left(\frac{\phi^{\text{full}}}{\sqrt{(\phi^{\text{full}})^2 + (\psi^{\text{full}})^2}} \frac{\varrho_{i,j}^{\text{full}}}{\sqrt{\vartheta_{i,j}^{\text{full}}}} \right) \sqrt{\vartheta_{i,j}^{\text{full}}}. \quad (9)$$

986 **Expression for gradient:** We compute the gradient of the objective with respect to \mathbf{w} or equivalently
 987 with respect to ϕ, ψ .
 988

$$\begin{aligned} 989 \quad & \frac{\partial L^{\text{full}}(\phi^{\text{full}}, \psi^{\text{full}})}{\partial \phi^{\text{full}}} \\ 990 \quad &= \phi^{\text{full}} \Gamma^{\text{full}} - \frac{\phi^{\text{full}} \Upsilon^{\text{full}}}{\sqrt{(\phi^{\text{full}})^2 + (\psi^{\text{full}})^2}} \\ 991 \quad &+ \frac{1}{n_{\text{train}}^2} \left(\frac{(\psi^{\text{full}})^2}{(\phi^{\text{full}})^2 + (\psi^{\text{full}})^2} \sum_{i,j=1}^{n_{\text{train}}} p_{ij} \varrho_{i,j}^{\text{full}} \hat{\sigma}' \left(\frac{\phi^{\text{full}}}{\sqrt{(\phi^{\text{full}})^2 + (\psi^{\text{full}})^2}} \frac{\varrho_{i,j}^{\text{full}}}{\sqrt{\vartheta_{i,j}^{\text{full}}}} \right) \right) \\ 992 \quad &= \phi^{\text{full}} \Gamma^{\text{full}} - \frac{\phi^{\text{full}} \Upsilon^{\text{full}}}{\sqrt{(\phi^{\text{full}})^2 + (\psi^{\text{full}})^2}} \\ 993 \quad &+ \frac{1}{n_{\text{train}}^2} \left(\frac{(\psi^{\text{full}})^2}{(\phi^{\text{full}})^2 + (\psi^{\text{full}})^2} \sum_{i,j=1}^{n_{\text{train}}} p_{ij} \varrho_{i,j}^{\text{full}} \hat{\sigma}_{\text{step}} \left(\frac{\phi^{\text{full}}}{\sqrt{(\phi^{\text{full}})^2 + (\psi^{\text{full}})^2}} \frac{\varrho_{i,j}^{\text{full}}}{\sqrt{\vartheta_{i,j}^{\text{full}}}} \right) \right), \\ 994 \quad &= \phi^{\text{full}} \Gamma^{\text{full}} - \frac{\phi^{\text{full}} \Upsilon^{\text{full}}}{\sqrt{(\phi^{\text{full}})^2 + (\psi^{\text{full}})^2}} + \frac{(\psi^{\text{full}})^2 \Xi^{\text{full}}}{(\phi^{\text{full}})^2 + (\psi^{\text{full}})^2}, \end{aligned} \quad (10)$$

1007 where in the second equality we use $\hat{\sigma}' = \hat{\sigma}'$ and $\hat{\sigma}' = \sqrt{2} \mathbb{1}(x \geq 0) = \sigma_{\text{step}}(x)$, σ_{step} is the step
 1008 function, and we define:
 1009

$$1010 \quad \Xi^{\text{full}} = \frac{1}{n_{\text{train}}} \sum_{i,j=1}^{n_{\text{train}}} p_{ij} \varrho_{i,j}^{\text{full}} \hat{\sigma}_{\text{step}} \left(\frac{\phi^{\text{full}}}{\sqrt{(\phi^{\text{full}})^2 + (\psi^{\text{full}})^2}} \frac{\varrho_{i,j}^{\text{full}}}{\sqrt{\vartheta_{i,j}^{\text{full}}}} \right). \quad (11)$$

1013 Similarly, we have:
 1014

$$1015 \quad \frac{\partial L^{\text{full}}(\phi^{\text{full}}, \psi^{\text{full}})}{\partial \psi^{\text{full}}} = \psi^{\text{full}} \Gamma^{\text{full}} - \frac{\psi^{\text{full}} \Upsilon^{\text{full}}}{\sqrt{(\phi^{\text{full}})^2 + (\psi^{\text{full}})^2}} + \frac{\phi^{\text{full}} \psi^{\text{full}} \Xi^{\text{full}}}{(\phi^{\text{full}})^2 + (\psi^{\text{full}})^2}. \quad (12)$$

1018 B.3 THEOREM B.4

1020 **Theorem B.4.** (Convergence of Full-graph Training with MSE) Suppose \mathbf{W}^{full} are generated
 1021 by Gaussian initialization. Under Assumptions B.1 and B.2, if the maximal degree satisfies
 1022 $C_1^{\text{full}} \leq d_{\text{max}} \leq C_2^{\text{full}} n_{\text{train}}^{\frac{3}{4}}$ for some constants $C_1^{\text{full}}, C_2^{\text{full}} \in (0, 1)$, then with high probability,
 1023 the training loss satisfies $L_{\text{train}}(\mathbf{W}_T^{\text{full}}, \mathbf{A}_{\text{train}}^{\text{full}}) \leq \epsilon$, provided that the number of iterations
 1024 $T = O\left(n_{\text{train}}^{\frac{7}{2}} h^2 d_{\text{max}}^{-\frac{1}{2}} \epsilon^{-1} \log(h^2 \epsilon^{-1})\right)$ for any $\epsilon \in (0, 1)$ under the full-graph GNN training.
 1025

1026 B.4 PROOF OF THEOREM B.4
10271028 **Lemma B.5** $\frac{1}{\pi n_{\text{train}}} \|\mathbf{A}_{\text{train}}^{\text{full}} \mathbf{1}\|_1 \leq \Gamma^{\text{full}} \leq \frac{1}{n_{\text{train}}} \|\mathbf{A}_{\text{train}}^{\text{full}} \mathbf{1}\|_1$, and $|\Upsilon_t^{\text{full}}| \leq \Gamma^{\text{full}}$, where $n_{\text{train}}^{\frac{1}{2}} d_{\max}^{-\frac{1}{2}} \leq$
1029 $\|\mathbf{A}_{\text{train},t}^{\text{full}} \mathbf{1}\|_1 \leq n_{\text{train}} d_{\max}$.
10301031 **Lemma B.6** If $\mathbf{w}_{j,0}^{\text{full}} \sim N(0, \kappa^2 \mathbf{I})$ and the learning rate $\eta \in (0, \frac{1}{6\pi\Gamma^{\text{full}}}]$, then with probability at
1032 least $1 - e^{-O(1)}$, it holds that for all $t > 0$, $\sqrt{(\phi_t^{\text{full}})^2 + (\psi_t^{\text{full}})^2} \leq C$, and $\sqrt{(\phi_t^{\text{full}})^2 + (\psi_t^{\text{full}})^2} > 0$
1033 for all $t \geq 1$, where $C = \frac{\pi}{2} + O(\kappa\sqrt{r})$ is a positive constant.
10341035 **Lemma B.7** If $\mathbf{w}_{j,0}^{\text{full}} \sim N(0, \kappa^2 \mathbf{I})$ and the learning rate $\eta \in (0, \frac{1}{6\pi\Gamma^{\text{full}}}]$, then for all $t \geq 1$ and any
1036 $C_1 \in [0, 1]$ such that $(\phi^{\text{full}}, \psi^{\text{full}}) = (1 - C_1)(\phi_t^{\text{full}}, \psi_t^{\text{full}}) + C_1(\phi_{t+1}^{\text{full}}, \psi_{t+1}^{\text{full}})$, we have that,
1037

1038
$$\lambda_{\max}(\nabla^2 L_{\text{train}}^{\text{full}}(\phi^{\text{full}}, \psi^{\text{full}})) \leq C_2 \Gamma^{\text{full}},$$

1039

1040 where λ_{\max} is the maximum eigenvalue of the population Hessian denoted by $\nabla^2 L_{\text{train}}^{\text{full}}(\phi^{\text{full}}, \psi^{\text{full}})$,
1041 and $C_2 = 4 \left(1 + \sqrt{\frac{\pi}{2} + O(\kappa\sqrt{r})} + o(1) \right)$ is a positive constant.
10421043 **Lemma B.8** If $\mathbf{w}_{j,0}^{\text{full}} \sim N(0, \kappa^2 \mathbf{I})$ and the learning rate $\eta \in (0, \frac{1}{6\pi\Gamma^{\text{full}}}]$, then with at least $1 - 1/h^2$,
1044 it holds that for all $t \geq C_3 \log(\log h)$, $\sqrt{(\phi_t^{\text{full}})^2 + (\psi_t^{\text{full}})^2} \geq 1 - o(1)$, where $C_3 > 0$ is an absolute
1045 constant.
10461047 **Lemma B.9** If $\mathbf{w}_{j,0}^{\text{full}} \sim N(0, \kappa^2 \mathbf{I})$ and the learning rate $\eta \in (0, \frac{1}{6\pi\Gamma^{\text{full}}}]$, then there is an absolute con-
1048 stant C_3 , such that for all $t \geq C_3 \log(\log h)$, either $|\psi_t^{\text{full}}| \leq \frac{\epsilon^{\frac{1}{2}}}{2h}$ and $\left\| \sqrt{(\phi_t^{\text{full}})^2 + (\psi_t^{\text{full}})^2} - 1 \right\| \leq$
1049 $\frac{\epsilon^{\frac{1}{2}}}{2h}$ or we have that
1050

1051
$$\left\| \nabla L_{\text{train}}^{\text{full}}(\phi_t^{\text{full}}, \psi_t^{\text{full}}) \right\|^2 \geq \mu^{\text{full}} L_{\text{train}}^{\text{full}}(\phi_t^{\text{full}}, \psi_t^{\text{full}}),$$

1052

1053 where $\mu^{\text{full}} \geq C_4 \epsilon h^{-2} d_{\max}^{-2} \Gamma^{\text{full}}$, and C_4 is a positive constant.
10541055 **Proof of Theorem B.4:** We analyze an arbitrary $j \in \{1, \dots, h\}$ and the iterates of the corresponding
1056 $\mathbf{w}_j^{\text{full}}$ vector. Setting $\kappa = 1$, we have from Lemma B.7 that the smoothness parameter C^{full} of the loss
1057 function is
1058

1059
$$C^{\text{full}} \leq C_2 = 4 \left(1 + \sqrt{2 + \frac{\pi}{2}} + o(1) \right) \quad (13)$$

1060

1061 Hence, for any $t > 0$,
1062

1063
$$\begin{aligned} L_{\text{train}}^{\text{full}}(\mathbf{w}_{j,t+1}^{\text{full}}) &\leq L_{\text{train}}^{\text{full}}(\mathbf{w}_{j,t}^{\text{full}}) + \nabla L_{\text{train}}^{\text{full}}(\mathbf{w}_{j,t}^{\text{full}}) (\mathbf{w}_{j,t+1}^{\text{full}} - \mathbf{w}_{j,t}^{\text{full}}) \\ &\quad + \frac{C^{\text{full}}}{2} \left\| \mathbf{w}_{j,t+1}^{\text{full}} - \mathbf{w}_{j,t}^{\text{full}} \right\|^2 \\ &\leq L_{\text{train}}^{\text{full}}(\mathbf{w}_{j,t}^{\text{full}}) - \eta \left\| \nabla L_{\text{train}}^{\text{full}}(\mathbf{w}_{j,t}^{\text{full}}) \right\|^2 + \frac{\eta^2 C^{\text{full}}}{2} \left\| \nabla L_{\text{train}}^{\text{full}}(\mathbf{w}_{j,t}^{\text{full}}) \right\|^2 \\ &= L_{\text{train}}^{\text{full}}(\mathbf{w}_{j,t}^{\text{full}}) - \eta \left\| \nabla L_{\text{train}}^{\text{full}}(\mathbf{w}_{j,t}^{\text{full}}) \right\|^2 \left(1 - \frac{\eta C^{\text{full}}}{2} \right). \end{aligned} \quad (14)$$

1064

1065 By Lemma B.6, we know that $\eta \in (0, \frac{1}{6\pi\Gamma^{\text{full}}}]$. Using Lemma B.5, we first assume that $\frac{C^{\text{full}}}{6\pi} \leq d_{\max} \leq$
1066 $\left(\frac{1}{6C_6} \right)^{\frac{1}{4}} n_{\text{train}}^{\frac{3}{4}}$ where $C_6 < \frac{1}{6}$ is a positive constant. Then, we set $\eta \in \left[\frac{C_6 d_{\max}^3}{\pi n_{\text{train}}^3}, \frac{1}{6\pi d_{\max}} \right]$. We are going
1067 to prove $\eta \in \left[\frac{C_6 d_{\max}^3}{\pi n_{\text{train}}^3}, \frac{1}{6\pi d_{\max}} \right]$ is still within the range $(0, \frac{1}{6\pi\Gamma^{\text{full}}}]$ and $\frac{C_6 d_{\max}^3}{\pi n_{\text{train}}^3} \leq \frac{1}{6\pi d_{\max}}$.
1068

1080 For the right side of the range, we have $\frac{1}{6\pi d_{\max}} \leq \frac{1}{6\pi \Gamma^{\text{full}}}$ due to $\Gamma^{\text{full}} \leq d_{\max}$. For the left side of the
 1081 range, $\frac{C_6 d_{\max}^3}{\pi n_{\text{train}}^3} > 0$ with the positive constant C_6 . Moreover, we have:
 1082

$$\begin{aligned} \frac{1}{6\pi d_{\max}} - \frac{C_6 d_{\max}^3}{\pi n_{\text{train}}^3} &= \frac{1}{\pi} \left(\frac{1}{6d_{\max}} - \frac{C_6 d_{\max}^3}{n_{\text{train}}^3} \right) \\ &\geq \frac{1}{\pi} \left(\frac{1}{6d_{\max}} - \frac{1}{6d_{\max}} \right) = 0. \end{aligned} \quad (15)$$

1088
 1089 With $\eta \in \left[\frac{C_6 d_{\max}^3}{\pi n_{\text{train}}^3}, \frac{1}{6\pi d_{\max}} \right]$, we have:
 1090

$$\eta \Gamma^{\text{full}} \leq \frac{C^{\text{full}}}{6\pi d_{\max}} \leq 1. \quad (16)$$

1094 Furthermore, using Lemma B.9, we have
 1095

$$L_{\text{train}}^{\text{full}}(\mathbf{w}_{j,t+1}^{\text{full}}) < L_{\text{train}}^{\text{full}}(\mathbf{w}_{j,t}^{\text{full}})(1 - \eta \mu^{\text{full}}) \leq L_{\text{train},0}^{\text{full}}(\mathbf{w}_{j,0}^{\text{full}})(1 - \eta \mu^{\text{full}})^t. \quad (17)$$

1099 Then we have:
 1100

$$T \leq C_7 \log \left(\frac{h^2}{\epsilon} \right) \frac{1}{\eta \mu^{\text{full}}}, \quad (18)$$

1102 where C_7 is a positive constant.
 1103

1104 Moreover, we have:
 1105

$$\eta \mu^{\text{full}} \geq \frac{C_4 C_6 d_{\max} \epsilon \Gamma^{\text{full}}}{\pi n_{\text{train}}^3 h^2} \geq \frac{C_4 C_6 d_{\max}^{\frac{1}{2}} \epsilon}{\pi^2 n_{\text{train}}^{\frac{7}{2}} h^2} \quad (19)$$

1108
 1109 Hence, we have $T = O \left(\frac{n_{\text{train}}^{\frac{7}{2}} h^2}{\epsilon d_{\max}^{\frac{1}{2}}} \log \frac{h^2}{\epsilon} \right)$.
 1110

1111 After T time steps, we either have $L_{\text{train}}^{\text{full}}(\mathbf{w}_{j,t}^{\text{full}}) \leq \frac{\epsilon}{h}$, or that $\psi_t^{\text{full}} \leq \frac{\epsilon^{\frac{1}{2}}}{2h}$ and $(\phi_t^{\text{full}})^2 + (\psi_t^{\text{full}})^2 - 1 \leq \frac{\epsilon^{\frac{1}{2}}}{2h}$. The latter implies that $\|\mathbf{w}_{j,t}^{\text{full}} - \mathbf{w}_{j,t}^{\text{full}*}\|^2 \leq \frac{\epsilon}{h}$. In addition, it is easy to see that $L_{\text{train}}^{\text{full}}(\mathbf{w}_{j,t}^{\text{full}}) \leq \|\mathbf{w}_{j,t}^{\text{full}} - \mathbf{w}_{j,t}^{\text{full}*}\|^2$. Hence, if the latter happens, then $L_{\text{train}}^{\text{full}}(\mathbf{w}_{j,t}^{\text{full}}) \leq \frac{\epsilon}{h}$. Hence $L_{\text{train}}^{\text{full}}(\mathbf{W}_T^{\text{full}}) \leq \epsilon$.
 1112

1113 This completes the proof.
 1114

1118 C PROOF OF CONVERGENCE THEOREM IN MINI-BATCH TRAINING WITH 1119 MSE

1121 In this section, we provide the proof of the convergence theorem in mini-batch training with MSE
 1122 of Section 3. We consider multi-class node classification tasks using a one-round GNN trained
 1123 with the MSE, defined as $l(\mathbf{W}, \hat{\mathbf{a}}_{\text{train},i}^{\text{mini}}) = \frac{1}{2} \|\hat{\mathbf{y}}_i - \mathbf{y}_i\|_F^2$. The ground truth label y_i is rewritten as
 1124 $\mathbf{y}_i \in \mathbb{R}^{1 \times K}$ in the one-hot form, where $K \geq 2$ is the number of label categories. The final output
 1125 of the GNN model is given by $\hat{\mathbf{y}}_i = \mathbf{z}_i = \sigma(\hat{\mathbf{a}}_{\text{train},i}^{\text{mini}} \mathbf{X} \mathbf{W}^\top)$, where the ReLU function is modified
 1126 as $\sigma(x) = \sqrt{2} \max(x, 0)$. Note that 1/2 in the MSE function and $\sqrt{2}$ in the ReLU function are
 1127 introduced to simplify the proof. The hidden dimension h becomes K . The rows of \mathbf{W} are initialized
 1128 independently from a Gaussian distribution $N(0, \kappa^2 \mathbf{I})$.
 1129

1130 We decompose the analysis of GNN optimization dynamic into three steps, similar to Appendix B.
 1131

1132 C.1 ASSUMPTION

1133 We still use Assumptions B.1 and B.2 in mini-batch settings for training data and the ground truth.

1134 C.2 EXPRESSIONS FOR LOSS AND GRADIENTS.
1135

1136 While our ultimate training objective remains empirical risk minimization, we analyze the optimization
1137 dynamics of MSE using its expected risk formulation on node feature distribution. This is done
1138 to simplify the proof, as expected risk offers a cleaner mathematical structure and does not affect
1139 the graph structure. Although this approximation is more accurate in the large-sample regime, we
1140 adopt it here as a modeling tool to study the impact of batch size and fan-out size in convergence,
1141 even when analyzing small-sample settings.

1142 **Expression for MSE loss:** We first begin by writing an equivalent expression of $L_{\text{train}}^{\text{mini}}(\mathbf{w}_j^{\text{mini}})$ with
1143 $j \in \{1, \dots, h\}$. We can assume that $\mathbf{w}_j^{\text{mini}} = \phi^{\text{mini}} \mathbf{w}_j^{\text{mini}*} + \psi^{\text{mini}} \mathbf{w}_j^{\text{mini}\perp}$, where \mathbf{w}^{\perp} is a fixed unit
1144 vector (depending on the initialization) orthogonal to $\mathbf{w}_j^{\text{mini}*}$. Then rewriting the loss in terms of
1145 ϕ^{mini} , ψ^{mini} and recalling that $\|\mathbf{w}_j^{\text{mini}*}\| = 1$ we get the simplified expressions of $L_{\text{train}}^{\text{mini}}(\mathbf{w}_j^{\text{mini}})$ and
1146 $L_{\text{train}}^{\text{full}}(\mathbf{w}_j^{\text{mini}})$:

$$1150 L_{\text{train}}^{\text{mini}}(\phi^{\text{mini}}, \psi^{\text{mini}}) = \frac{1}{2} \left((\phi^{\text{mini}})^2 + (\psi^{\text{mini}})^2 + 1 \right) \Gamma^{\text{mini}} - \sqrt{(\phi^{\text{mini}})^2 + (\psi^{\text{mini}})^2} \Upsilon^{\text{mini}}, \quad (20)$$

1152 and

$$1153 L_{\text{train}}^{\text{full}}(\phi^{\text{mini}}, \psi^{\text{mini}}, \tilde{\mathbf{A}}_{\text{train}}^{\text{mini}}) = \frac{1}{2} \left((\phi^{\text{mini}})^2 + (\psi^{\text{mini}})^2 + 1 \right) \Gamma^{\text{full}}(\phi^{\text{mini}}, \psi^{\text{mini}}, \tilde{\mathbf{A}}_{\text{train}}^{\text{mini}}) \\ 1154 - \sqrt{(\phi^{\text{mini}})^2 + (\psi^{\text{mini}})^2} \Upsilon^{\text{full}}(\phi^{\text{mini}}, \psi^{\text{mini}}, \tilde{\mathbf{A}}_{\text{train}}^{\text{mini}}), \quad (21)$$

1155 where we simplify $\Gamma^{\text{full}}(\phi^{\text{mini}}, \psi^{\text{mini}}, \tilde{\mathbf{A}}_{\text{train}}^{\text{mini}})$ and $\Upsilon^{\text{full}}(\phi^{\text{mini}}, \psi^{\text{mini}}, \tilde{\mathbf{A}}_{\text{train}}^{\text{mini}})$ as $\Gamma^{\text{full-mini}}$ and $\Upsilon^{\text{full-mini}}$,
1156 respectively, and we define:

$$1160 \Gamma^{\text{mini}} = \frac{1}{b} \sum_{i,j=1}^b p_{ij} \hat{\sigma} \left(\frac{\varrho_{i,j}^{\text{mini}}}{\sqrt{\vartheta_{i,j}^{\text{mini}}}} \right) \sqrt{\vartheta_{i,j}^{\text{mini}}}, \quad (22)$$

$$1163 \Gamma^{\text{full-mini}} = \Gamma^{\text{full}}(\phi^{\text{mini}}, \psi^{\text{mini}}, \tilde{\mathbf{A}}_{\text{train}}^{\text{mini}}) = \frac{1}{n_{\text{train}}} \sum_{i,j=1}^{n_{\text{train}}} p_{ij} \hat{\sigma} \left(\frac{\varrho_{i,j}^{\text{mini}}}{\sqrt{\vartheta_{i,j}^{\text{mini}}}} \right) \sqrt{\vartheta_{i,j}^{\text{mini}}}, \quad (23)$$

$$1166 \Upsilon^{\text{mini}} = \frac{1}{b} \sum_{i,j=1}^b p_{ij} \hat{\sigma} \left(\frac{\phi^{\text{mini}}}{\sqrt{(\phi^{\text{mini}})^2 + (\psi^{\text{mini}})^2}} \frac{\varrho_{i,j}^{\text{mini}}}{\sqrt{\vartheta_{i,j}^{\text{mini}}}} \right) \sqrt{\vartheta_{i,j}^{\text{mini}}}, \quad (24)$$

$$1169 \Upsilon^{\text{full-mini}} = \Upsilon^{\text{full}}(\phi^{\text{mini}}, \psi^{\text{mini}}, \tilde{\mathbf{A}}_{\text{train}}^{\text{mini}}) \\ 1171 = \frac{1}{n_{\text{train}}} \sum_{i,j=1}^{n_{\text{train}}} p_{ij} \hat{\sigma} \left(\frac{\phi^{\text{mini}}}{\sqrt{(\phi^{\text{mini}})^2 + (\psi^{\text{mini}})^2}} \frac{\varrho_{i,j}^{\text{mini}}}{\sqrt{\vartheta_{i,j}^{\text{mini}}}} \right) \sqrt{\vartheta_{i,j}^{\text{mini}}}, \quad (25)$$

$$1174 \vartheta_{i,j}^{\text{mini}} = (\tilde{\mathbf{A}}_{\text{train}}^{\text{mini}} \mathbf{1})_i (\tilde{\mathbf{A}}_{\text{train}}^{\text{mini}} \mathbf{1})_j, \quad (26)$$

1176 where we use $p_{ij} = 1$ if $i = j$ and $p_{ij} = 0$ if $i \neq j$, $\varrho_{i,j}^{\text{mini}}$ to denote the amount of common messages
1177 between node i and node j at a given training iteration

1178 **Expression for gradient:** We compute the gradient of the objective with respect to \mathbf{w} or equivalently
1179 with respect to ϕ, ψ .

$$1181 \frac{\partial L^{\text{mini}}(\phi^{\text{mini}}, \psi^{\text{mini}})}{\partial \phi^{\text{mini}}} = \phi^{\text{mini}} \Gamma^{\text{mini}} - \frac{\phi^{\text{mini}} \Upsilon^{\text{mini}}}{\sqrt{(\phi^{\text{mini}})^2 + (\psi^{\text{mini}})^2}} + \frac{(\psi^{\text{mini}})^2 \Xi^{\text{mini}}}{(\phi^{\text{mini}})^2 + (\psi^{\text{mini}})^2}, \quad (27)$$

1184 and

$$1186 \frac{\partial L^{\text{full}}(\phi^{\text{mini}}, \psi^{\text{mini}}, \tilde{\mathbf{A}}_{\text{train}}^{\text{mini}})}{\partial \phi^{\text{mini}}} = \phi^{\text{mini}} \Gamma^{\text{full-mini}} - \frac{\phi^{\text{mini}} \Upsilon^{\text{full-mini}}}{\sqrt{(\phi^{\text{mini}})^2 + (\psi^{\text{mini}})^2}} + \frac{(\psi^{\text{mini}})^2 \Xi^{\text{full-mini}}}{(\phi^{\text{mini}})^2 + (\psi^{\text{mini}})^2}, \quad (28)$$

1188 where we define:

1189

$$1190 \Xi^{\text{mini}} = \frac{1}{b} \sum_{i,j=1}^b p_{ij} \varrho_{i,j}^{\text{mini}} \hat{\sigma}_{\text{step}} \left(\frac{\phi^{\text{mini}}}{\sqrt{(\phi^{\text{mini}})^2 + (\psi^{\text{mini}})^2}} \frac{\varrho_{i,j}^{\text{mini}}}{\sqrt{\vartheta_{i,j}^{\text{mini}}}} \right), \quad (29)$$

1191

1192

$$1193 \Xi^{\text{full-mini}} = \Xi^{\text{full}} \left(\phi^{\text{mini}}, \psi^{\text{mini}}, \tilde{\mathbf{A}}_{\text{train}}^{\text{mini}} \right) \\ 1194 = \frac{1}{n_{\text{train}}} \sum_{i,j=1}^{n_{\text{train}}} p_{ij} \varrho_{i,j}^{\text{mini}} \hat{\sigma}_{\text{step}} \left(\frac{\phi^{\text{mini}}}{\sqrt{(\phi^{\text{mini}})^2 + (\psi^{\text{mini}})^2}} \frac{\varrho_{i,j}^{\text{mini}}}{\sqrt{\vartheta_{i,j}^{\text{mini}}}} \right). \quad (30)$$

1195

1196

1197

1198 Similarly, we have:

1199

$$1200 \frac{\partial L^{\text{mini}} \left(\phi^{\text{mini}}, \psi^{\text{mini}} \right)}{\partial \psi^{\text{mini}}} = \psi^{\text{mini}} \Gamma^{\text{mini}} - \frac{\psi^{\text{mini}} \Upsilon^{\text{mini}}}{\sqrt{(\phi^{\text{mini}})^2 + (\psi^{\text{mini}})^2}} + \frac{\phi^{\text{mini}} \psi^{\text{mini}} \Xi^{\text{mini}}}{(\phi^{\text{mini}})^2 + (\psi^{\text{mini}})^2}, \quad (31)$$

1201

1202

1203

1204 and

1205

$$1206 \frac{\partial L^{\text{full}} \left(\phi^{\text{mini}}, \psi^{\text{mini}}, \tilde{\mathbf{A}}_{\text{train}}^{\text{mini}} \right)}{\partial \psi^{\text{mini}}} = \psi^{\text{mini}} \Gamma^{\text{full-mini}} - \frac{\psi^{\text{mini}} \Upsilon^{\text{full-mini}}}{\sqrt{(\phi^{\text{mini}})^2 + (\psi^{\text{mini}})^2}} + \frac{\phi^{\text{mini}} \psi^{\text{mini}} \Xi^{\text{full-mini}}}{(\phi^{\text{mini}})^2 + (\psi^{\text{mini}})^2}. \quad (32)$$

1207

1208

1209 C.3 PROOF OF THEOREM 1

1210

1211 **Lemma C.1** $\frac{1}{\pi b} \|\mathbf{A}_{\text{train},t}^{\text{mini}} \mathbf{1}\|_1 \leq \Gamma_t^{\text{mini}}, \Gamma_t^{\text{full-mini}} \leq \frac{1}{b} \|\tilde{\mathbf{A}}_{\text{train}}^{\text{mini}} \mathbf{1}\|_1, |\Upsilon_t^{\text{mini}}| \leq \Gamma_t^{\text{mini}}$ and $|\Upsilon_t^{\text{full-mini}}| \leq \Gamma_t^{\text{full-mini}}$, where $b^{\frac{1}{2}} \beta^{-\frac{1}{2}} \leq \|\mathbf{A}_{\text{train},t}^{\text{mini}} \mathbf{1}\|_1 \leq b\beta$.

1212

1213

1214

1215 **Lemma C.2** If $\mathbf{w}_{j,0}^{\text{mini}} \sim N(0, \kappa^2 \mathbf{I})$ and the learning rate $\eta_t \in (0, \frac{1}{6\pi\Gamma_t^{\text{mini}}}]$, then with probability at least $1 - e^{-O(1)}$, it holds that for all $t > 0$, $\sqrt{(\phi_t^{\text{mini}})^2 + (\psi_t^{\text{mini}})^2} \leq C$, and $\sqrt{(\phi_t^{\text{mini}})^2 + (\psi_t^{\text{mini}})^2} > 0$ for all $t \geq 1$, where $C = \frac{\pi}{2} + O(\kappa\sqrt{r})$ is a positive constant.

1216

1217

1218

1219

1220 **Lemma C.3** If $\mathbf{w}_{j,0}^{\text{mini}} \sim N(0, \kappa^2 \mathbf{I})$ and the learning rate $\eta_t \in (0, \frac{1}{6\pi\Gamma_t^{\text{mini}}}]$, then for all $t \geq 1$ and any $C_1 \in [0, 1]$ such that $(\phi^{\text{mini}}, \psi^{\text{mini}}) = (1 - C_1)(\phi_t^{\text{mini}}, \psi_t^{\text{mini}}) + C_1(\phi_{t+1}^{\text{mini}}, \psi_{t+1}^{\text{mini}})$, we have that,

1221

1222

$$1223 \lambda_{\max}(\nabla^2 L_{\text{train}}^{\text{full}}(\phi^{\text{mini}}, \psi^{\text{mini}}, \tilde{\mathbf{A}}_{\text{train}}^{\text{mini}})) \leq C_2 \Gamma_t^{\text{full-mini}},$$

1224

1225 where λ_{\max} is the maximum eigenvalue of the population Hessian denoted by $\nabla^2 L_{\text{train}}^{\text{full}}(\phi^{\text{mini}}, \psi^{\text{mini}}, \tilde{\mathbf{A}}_{\text{train}}^{\text{mini}})$, and $C_2 = 4 \left(1 + \sqrt{\frac{\pi}{2} + O(\kappa\sqrt{r})} + o(1) \right)$ is a positive constant.

1226

1227

1228

1229 **Lemma C.4** If $\mathbf{w}_{j,0}^{\text{mini}} \sim N(0, \kappa^2 \mathbf{I})$ and the learning rate $\eta_t \in (0, \frac{1}{6\pi\Gamma_t^{\text{mini}}}]$, then with at least $1 - 1/h^2$, it holds that for all $t \geq C_3 \log(\log h)$, $\sqrt{(\phi_t^{\text{mini}})^2 + (\psi_t^{\text{mini}})^2} \geq 1 - o(1)$, where $C_3 > 0$ is an absolute constant.

1230

1231

1232

1233

1234 **Lemma C.5** If $\mathbf{w}_{j,0}^{\text{mini}} \sim N(0, \kappa^2 \mathbf{I})$ and the learning rate $\eta \in (0, \frac{1}{6\pi\Gamma_t^{\text{mini}}}]$, then there is 1235 an absolute constant C_3 , such that for all $t \geq C_3 \log(\log h)$, either $|\psi_t^{\text{mini}}| \leq \frac{\epsilon^{\frac{1}{2}}}{2h}$ and 1236 1237 1238 1239 1240 1241 1242 1243 1244 1245 1246 1247 1248 1249 1250 1251 1252 1253 1254 1255 1256 1257 1258 1259 1260 1261 1262 1263 1264 1265 1266 1267 1268 1269 1270 1271 1272 1273 1274 1275 1276 1277 1278 1279 1280 1281 1282 1283 1284 1285 1286 1287 1288 1289 1290 1291 1292 1293 1294 1295 1296 1297 1298 1299 1300 1301 1302 1303 1304 1305 1306 1307 1308 1309 1310 1311 1312 1313 1314 1315 1316 1317 1318 1319 1320 1321 1322 1323 1324 1325 1326 1327 1328 1329 1330 1331 1332 1333 1334 1335 1336 1337 1338 1339 1340 1341 1342 1343 1344 1345 1346 1347 1348 1349 1350 1351 1352 1353 1354 1355 1356 1357 1358 1359 1360 1361 1362 1363 1364 1365 1366 1367 1368 1369 1370 1371 1372 1373 1374 1375 1376 1377 1378 1379 1380 1381 1382 1383 1384 1385 1386 1387 1388 1389 1390 1391 1392 1393 1394 1395 1396 1397 1398 1399 1400 1401 1402 1403 1404 1405 1406 1407 1408 1409 1410 1411 1412 1413 1414 1415 1416 1417 1418 1419 1420 1421 1422 1423 1424 1425 1426 1427 1428 1429 1430 1431 1432 1433 1434 1435 1436 1437 1438 1439 1440 1441 1442 1443 1444 1445 1446 1447 1448 1449 1450 1451 1452 1453 1454 1455 1456 1457 1458 1459 1460 1461 1462 1463 1464 1465 1466 1467 1468 1469 1470 1471 1472 1473 1474 1475 1476 1477 1478 1479 1480 1481 1482 1483 1484 1485 1486 1487 1488 1489 1490 1491 1492 1493 1494 1495 1496 1497 1498 1499 1500 1501 1502 1503 1504 1505 1506 1507 1508 1509 1510 1511 1512 1513 1514 1515 1516 1517 1518 1519 1520 1521 1522 1523 1524 1525 1526 1527 1528 1529 1530 1531 1532 1533 1534 1535 1536 1537 1538 1539 1540 1541 1542 1543 1544 1545 1546 1547 1548 1549 1550 1551 1552 1553 1554 1555 1556 1557 1558 1559 1560 1561 1562 1563 1564 1565 1566 1567 1568 1569 1570 1571 1572 1573 1574 1575 1576 1577 1578 1579 1580 1581 1582 1583 1584 1585 1586 1587 1588 1589 1590 1591 1592 1593 1594 1595 1596 1597 1598 1599 1600 1601 1602 1603 1604 1605 1606 1607 1608 1609 1610 1611 1612 1613 1614 1615 1616 1617 1618 1619 1620 1621 1622 1623 1624 1625 1626 1627 1628 1629 1630 1631 1632 1633 1634 1635 1636 1637 1638 1639 1640 1641 1642 1643 1644 1645 1646 1647 1648 1649 1650 1651 1652 1653 1654 1655 1656 1657 1658 1659 1660 1661 1662 1663 1664 1665 1666 1667 1668 1669 1670 1671 1672 1673 1674 1675 1676 1677 1678 1679 1680 1681 1682 1683 1684 1685 1686 1687 1688 1689 1690 1691 1692 1693 1694 1695 1696 1697 1698 1699 1700 1701 1702 1703 1704 1705 1706 1707 1708 1709 1710 1711 1712 1713 1714 1715 1716 1717 1718 1719 1720 1721 1722 1723 1724 1725 1726 1727 1728 1729 1730 1731 1732 1733 1734 1735 1736 1737 1738 1739 1740 1741 1742 1743 1744 1745 1746 1747 1748 1749 1750 1751 1752 1753 1754 1755 1756 1757 1758 1759 1760 1761 1762 1763 1764 1765 1766 1767 1768 1769 1770 1771 1772 1773 1774 1775 1776 1777 1778 1779 1780 1781 1782 1783 1784 1785 1786 1787 1788 1789 1790 1791 1792 1793 1794 1795 1796 1797 1798 1799 1800 1801 1802 1803 1804 1805 1806 1807 1808 1809 1810 1811 1812 1813 1814 1815 1816 1817 1818 1819 1820 1821 1822 1823 1824 1825 1826 1827 1828 1829 1830 1831 1832 1833 1834 1835 1836 1837 1838 1839 1840 1841 1842 1843 1844 1845 1846 1847 1848 1849 1850 1851 1852 1853 1854 1855 1856 1857 1858 1859 1860 1861 1862 1863 1864 1865 1866 1867 1868 1869 1870 1871 1872 1873 1874 1875 1876 1877 1878 1879 1880 1881 1882 1883 1884 1885 1886 1887 1888 1889 1890 1891 1892 1893 1894 1895 1896 1897 1898 1899 1900 1901 1902 1903 1904 1905 1906 1907 1908 1909 1910 1911 1912 1913 1914 1915 1916 1917 1918 1919 1920 1921 1922 1923 1924 1925 1926 1927 1928 1929 1930 1931 1932 1933 1934 1935 1936 1937 1938 1939 1940 1941 1942 1943 1944 1945 1946 1947 1948 1949 1950 1951 1952 1953 1954 1955 1956 1957 1958 1959 1960 1961 1962 1963 1964 1965 1966 1967 1968 1969 1970 1971 1972 1973 1974 1975 1976 1977 1978 1979 1980 1981 1982 1983 1984 1985 1986 1987 1988 1989 1990 1991 1992 1993 1994 1995 1996 1997 1998 1999 2000 2001 2002 2003 2004 2005 2006 2007 2008 2009 2010 2011 2012 2013 2014 2015 2016 2017 2018 2019 2020 2021 2022 2023 2024 2025 2026 2027 2028 2029 2030 2031 2032 2033 2034 2035 2036 2037 2038 2039 2040 2041 2042 2043 2044 2045 2046 2047 2048 2049 2050 2051 2052 2053 2054 2055 2056 2057 2058 2059 2060 2061 2062 2063 2064 2065 2066 2067 2068 2069 2070 2071 2072 2073 2074 2075 2076 2077 2078 2079 2080 2081 2082 2083 2084 2085 2086 2087 2088 2089 $$

1242 **Lemma C.6** [Lemma G.2 in (Du et al., 2018)] Regarding n random variables u_1, \dots, u_n satisfying
1243 $\sum_{i=1}^n u_i = 0$. Let $\mathcal{B} \in [n]$ denote a subset of $[n]$ and $|\mathcal{B}| = b \leq n$, the following holds,
1244

$$1245 \quad 1246 \quad 1247 \quad \mathbb{E} \left[\left(\frac{1}{b} \sum_{i \in \mathcal{B}} u_i \right)^2 \right] \leq \frac{1}{b} \mathbb{E} [u_i^2].$$

1248 **Proof of Theorem 1:** For any $t > 0$, taking expectation conditioning on $\mathbf{w}_{j,t+1}^{\text{mini}}$ gives:
1249

$$1250 \quad \mathbb{E} \left[L_{\text{train}}^{\text{full}}(\mathbf{w}_{j,t+1}^{\text{mini}}, \tilde{\mathbf{A}}_{\text{train}}^{\text{mini}}) | \mathbf{w}_{j,t}^{\text{mini}} \right] \\ 1251 \quad \leq L_{\text{train}}^{\text{full}} \left(\mathbf{w}_{j,t}^{\text{mini}}, \tilde{\mathbf{A}}_{\text{train}}^{\text{mini}} \right) + \nabla L_{\text{train}}^{\text{full}} \left(\mathbf{w}_{j,t}^{\text{mini}}, \tilde{\mathbf{A}}_{\text{train}}^{\text{mini}} \right) \mathbb{E} \left[\left(\mathbf{w}_{j,t+1}^{\text{mini}} - \mathbf{w}_{j,t}^{\text{mini}} \right) | \mathbf{w}_{j,t}^{\text{mini}} \right] \\ 1252 \quad + \frac{C^{\text{mini}}}{2} \mathbb{E} \left[\left\| \mathbf{w}_{j,t+1}^{\text{mini}} - \mathbf{w}_{j,t}^{\text{mini}} \right\|^2 | \mathbf{w}_{j,t}^{\text{mini}} \right] \\ 1253 \quad 1254 \quad 1255 \quad 1256 \quad 1257 \quad 1258 \quad 1259 \quad 1260 \quad 1261 \quad 1262 \quad 1263 \quad 1264 \quad 1265 \quad 1266 \quad 1267 \quad 1268 \quad 1269 \quad 1270 \quad 1271 \quad 1272 \quad 1273 \quad 1274 \quad 1275 \quad 1276 \quad 1277 \quad 1278 \quad 1279 \quad 1280 \quad 1281 \quad 1282 \quad 1283 \quad 1284 \quad 1285 \quad 1286 \quad 1287 \quad 1288 \quad 1289 \quad 1290 \quad 1291 \quad 1292 \quad 1293 \quad 1294 \quad 1295$$

Furthermore, using Lemma C.6, we have:

$$\mathbb{E} \left[\left\| \mathbf{w}_{j,t+1}^{\text{mini}} - \mathbf{w}_{j,t}^{\text{mini}} \right\|^2 | \mathbf{w}_{j,t}^{\text{mini}} \right] \\ = \eta_t^2 \mathbb{E} \left[\left\| \nabla L_{\text{train}}^{\text{mini}} \left(\mathbf{w}_{j,t}^{\text{mini}}, \tilde{\mathbf{A}}_{\text{train}}^{\text{mini}} \right) \right\|_F^2 | \mathbf{w}_{j,t}^{\text{mini}} \right] \\ \leq \eta_t^2 \left(\mathbb{E} \left[\left\| \nabla L_{\text{train}}^{\text{mini}} \left(\mathbf{w}_{j,t}^{\text{mini}}, \tilde{\mathbf{A}}_{\text{train}}^{\text{mini}} \right) - \nabla L_{\text{train}}^{\text{full}} \left(\mathbf{w}_{j,t}^{\text{mini}}, \tilde{\mathbf{A}}_{\text{train}}^{\text{mini}} \right) \right\|^2 | \mathbf{w}_{j,t}^{\text{mini}} \right] \right. \\ \left. + \left\| \nabla L_{\text{train}}^{\text{full}} \left(\mathbf{w}_{j,t}^{\text{mini}}, \tilde{\mathbf{A}}_{\text{train}}^{\text{mini}} \right) \right\|^2 \right) \\ \leq \eta_t^2 \left(\frac{n_{\text{train}}^2}{n_{\text{train}} b} \left\| \nabla L_{\text{train}}^{\text{full}} \left(\mathbf{w}_{j,t}^{\text{mini}}, \tilde{\mathbf{A}}_{\text{train}}^{\text{mini}} \right) \right\|^2 + \left\| \nabla L_{\text{train}}^{\text{full}} \left(\mathbf{w}_{j,t}^{\text{mini}}, \tilde{\mathbf{A}}_{\text{train}}^{\text{mini}} \right) \right\|^2 \right) \\ \leq \eta_t^2 \left(\frac{2n_{\text{train}}}{b} \left\| \nabla L_{\text{train}}^{\text{full}} \left(\mathbf{w}_{j,t}^{\text{mini}}, \tilde{\mathbf{A}}_{\text{train}}^{\text{mini}} \right) \right\|^2 \right).$$

Moreover, we have:

$$\nabla L_{\text{train}}^{\text{full}} \left(\mathbf{w}_{j,t}^{\text{mini}}, \tilde{\mathbf{A}}_{\text{train}}^{\text{mini}} \right) \mathbb{E} \left[\left(\mathbf{w}_{j,t+1}^{\text{mini}} - \mathbf{w}_{j,t}^{\text{mini}} \right) | \mathbf{w}_{j,t+1}^{\text{mini}} \right] \\ = -\eta_t \nabla L_{\text{train}}^{\text{full}} \left(\mathbf{w}_{j,t}^{\text{mini}}, \tilde{\mathbf{A}}_{\text{train}}^{\text{mini}} \right) \mathbb{E} \left[\nabla L_{\text{train},t}^{\text{mini}} \left(\mathbf{w}_{j,t}^{\text{mini}} \right) | \mathbf{w}_{j,t+1}^{\text{mini}} \right] \\ = -\eta_t \left\| \nabla L_{\text{train}}^{\text{full}} \left(\mathbf{w}_{j,t}^{\text{mini}}, \tilde{\mathbf{A}}_{\text{train}}^{\text{mini}} \right) \right\|^2$$

Hence, we have:

$$\mathbb{E} \left[L_{\text{train}}^{\text{full}}(\mathbf{w}_{j,t+1}^{\text{mini}}, \tilde{\mathbf{A}}_{\text{train}}^{\text{mini}}) | \mathbf{w}_{j,t}^{\text{mini}} \right] \\ \leq L_{\text{train}}^{\text{full}} \left(\mathbf{w}_{j,t}^{\text{mini}}, \tilde{\mathbf{A}}_{\text{train}}^{\text{mini}} \right) - \eta_t \left\| \nabla L_{\text{train}}^{\text{full}} \left(\mathbf{w}_{j,t}^{\text{mini}}, \tilde{\mathbf{A}}_{\text{train}}^{\text{mini}} \right) \right\|^2 \\ + \frac{C^{\text{mini}} n_{\text{train}} \eta_t^2}{b} \left\| \nabla L_{\text{train}}^{\text{full}} \left(\mathbf{w}_{j,t}^{\text{mini}}, \tilde{\mathbf{A}}_{\text{train}}^{\text{mini}} \right) \right\|^2 \\ \leq L_{\text{train}}^{\text{full}} \left(\mathbf{w}_{j,t}^{\text{mini}}, \tilde{\mathbf{A}}_{\text{train}}^{\text{mini}} \right) - \eta_t \left\| \nabla L_{\text{train}}^{\text{full}} \left(\mathbf{w}_{j,t}^{\text{mini}}, \tilde{\mathbf{A}}_{\text{train}}^{\text{mini}} \right) \right\|^2 \left(1 - \frac{C^{\text{mini}} n_{\text{train}}}{b} \eta_t \right)$$

By Lemma C.2, we know that $\eta_t \in (0, \frac{1}{6\pi\Gamma_t^{\text{mini}}}]$. Using Lemma C.1, we first assume that $\frac{C^{\text{mini}}}{6\pi} \leq \beta \leq \left(\frac{1}{6C_6} \right)^{\frac{1}{4}} b^{\frac{3}{4}}$ where $C_6 < \frac{1}{6}$ is a positive constant. Then, we set $\eta_t \in \left[\frac{C_6\beta^3}{\pi n_{\text{train}} b^2}, \frac{b}{6\pi\beta n_{\text{train}}} \right]$. We are going to prove $\eta_t \in \left[\frac{C_6\beta^3}{\pi n_{\text{train}} b^2}, \frac{b}{6\pi\beta n_{\text{train}}} \right]$ is still within the range $(0, \frac{1}{6\pi\Gamma^{\text{mini}}}]$ and $\frac{C_6\beta^3}{\pi n_{\text{train}} b^2} \leq \frac{b}{6\pi\beta n_{\text{train}}}$.

1296 For the right side of the range, we have $\frac{b}{6\pi\beta n_{\text{train}}} \leq \frac{b}{6\pi\Gamma_t^{\text{mini}} n_{\text{train}}} \leq \frac{1}{6\pi\Gamma_t^{\text{mini}}}$ due to $\Gamma_t^{\text{mini}} \leq \beta$ and
 1297 $b \leq n_{\text{train}}$. For the left side of the range, $\frac{C_6\beta^3}{\pi n_{\text{train}} b^2}$ with the positive constant C_6 . Moreover, we have:
 1298

$$\begin{aligned} \frac{b}{6\pi\beta n_{\text{train}}} - \frac{C_6\beta^3}{\pi n_{\text{train}} b^2} &= \frac{b}{\pi n_{\text{train}}} \left(\frac{1}{6\beta} - \frac{C_6\beta^3}{b^3} \right) \\ 1302 &\geq \frac{1}{\pi} \left(\frac{1}{6\beta} - \frac{1}{6\beta} \right) = 0. \end{aligned} \quad (37)$$

1304 With $\eta_t \in \left[\frac{C_6\beta^3}{\pi n_{\text{train}} b^2}, \frac{b}{6\pi\beta n_{\text{train}}} \right]$, we have:
 1305

$$\frac{C^{\text{mini}} n_{\text{train}}}{b} \eta_t \leq \frac{C^{\text{mini}}}{6\pi\beta} \leq 1. \quad (38)$$

1309 Furthermore, using Lemma C.5, we have

$$\begin{aligned} 1311 L_{\text{train}}^{\text{full}}(\mathbf{w}_{j,t+1}^{\text{mini}}, \tilde{\mathbf{A}}_{\text{train}}^{\text{mini}}) &\leq L_{\text{train}}^{\text{full}}(\mathbf{w}_{j,t}^{\text{mini}}, \tilde{\mathbf{A}}_{\text{train}}^{\text{mini}})(1 - \eta_t \mu_t^{\text{mini}}) \\ 1313 &\leq L_{\text{train}}^{\text{mini}}(\mathbf{w}_{j,0}^{\text{mini}}, \tilde{\mathbf{A}}_{\text{train}}^{\text{mini}}) \prod_{\tau=1}^t (1 - \eta_\tau \mu_\tau^{\text{mini}}) \\ 1316 &\leq L_{\text{train}}^{\text{mini}}(\mathbf{w}_{j,0}^{\text{mini}}, \tilde{\mathbf{A}}_{\text{train}}^{\text{mini}})(1 - \frac{1}{t} \sum_{\tau=1}^t \eta_\tau \mu_\tau^{\text{mini}})^t, \end{aligned} \quad (39)$$

1318 where the last inequality can be proved: $f(x) = \log(1 - x)$ is a concave function on $0 < x < 1$,
 1319 then, for $0 < x_i < 1$ with $i = \{1, \dots, n\}$, we have $f(\frac{1}{n} \sum_{i=1}^n x_i) \geq \frac{1}{n} \sum_{i=1}^n f(x_i)$, which can be
 1320 written as $\log(1 - \frac{1}{n} \sum_{i=1}^n x_i) \geq \frac{1}{n} \sum_{i=1}^n \log(1 - x_i)$. Therefore, we have $(1 - \frac{1}{n} \sum_{i=1}^n x_i)^n \geq$
 1321 $\prod_{i=1}^n (1 - x_i)$.

1322 Then we have:

$$T \leq C_7 \log\left(\frac{h^2}{\epsilon}\right) \frac{1}{\frac{1}{T} \sum_{\tau=1}^T \eta_\tau \mu_\tau^{\text{mini}}}, \quad (40)$$

1325 where C_7 is a positive constant.

1326 Moreover, we have:

$$\begin{aligned} 1328 \frac{1}{T} \sum_{\tau=1}^T \eta_\tau \mu_\tau^{\text{mini}} &\geq \frac{1}{T} \sum_{\tau=1}^T \frac{C_4 C_6 \beta \epsilon \Gamma_\tau^{\text{full-mini}}}{\pi n_{\text{train}} b^2 h^2} \\ 1331 &\geq \frac{1}{T} \sum_{\tau=1}^T \frac{C_4 C_6 \beta^{\frac{1}{2}} \epsilon}{\pi^2 n_{\text{train}} b^{\frac{5}{2}} h^2} \\ 1334 &= \frac{C_4 C_6 \beta^{\frac{1}{2}} \epsilon}{\pi^2 n_{\text{train}} b^{\frac{5}{2}} h^2} \end{aligned} \quad (41)$$

1336 Hence, we have $T = O\left(\frac{n_{\text{train}} b^{\frac{5}{2}} h^2}{\epsilon \beta^{\frac{1}{2}}} \log \frac{h^2}{\epsilon}\right)$.

1338 After T time steps, we either have $L_{\text{train}}^{\text{full}}(\mathbf{w}_{j,t}^{\text{mini}}, \tilde{\mathbf{A}}_{\text{train}}^{\text{mini}}) \leq \frac{\epsilon}{h}$, or that $\psi_t^{\text{mini}} \leq \frac{\epsilon^{\frac{1}{2}}}{2h}$ and $(\phi_t^{\text{mini}})^2 +$
 1339 $(\psi_t^{\text{mini}})^2 - 1 \leq \frac{\epsilon^{\frac{1}{2}}}{2h}$. The latter implies that $\|\mathbf{w}_{j,t}^{\text{mini}} - \mathbf{w}_{j,t}^{\text{mini}*}\|^2 \leq \frac{\epsilon}{h}$. In addition, it is easy to see that
 1340 $L_{\text{train}}^{\text{full}}(\mathbf{w}_{j,t}^{\text{mini}}, \tilde{\mathbf{A}}_{\text{train}}^{\text{mini}}) \leq \|\mathbf{w}_{j,t}^{\text{mini}} - \mathbf{w}_{j,t}^{\text{mini}*}\|^2$. Hence, if the latter happens, then $L_{\text{train}}^{\text{full}}(\mathbf{w}_{j,t}^{\text{mini}}, \tilde{\mathbf{A}}_{\text{train}}^{\text{mini}}) \leq$
 1343 $\frac{\epsilon}{h}$. Hence $L_{\text{train}}^{\text{full}}(\mathbf{W}_T^{\text{mini}}) \leq \epsilon$.

1344 This completes the proof.

1346 D PROOF OF CONVERGENCE THEOREM IN FULL-GRAF TRAINING WITH CE

1347 In this section, we provide the proof of the convergence theorem in full-graph training with CE. To
 1348 simplify the analysis, we focus on binary node classification using a one-round GNN trained with the

1350 CE, defined as $l(\mathbf{W}, \tilde{\mathbf{a}}_{\text{train},i}^{\text{full}}) = \log(1 + \exp(-y_i \hat{y}_i))$. The final output of the GNN model is given
 1351 by $\hat{y}_i = \mathbf{z}_i \mathbf{v}^\top = \sigma(\tilde{\mathbf{a}}_{\text{train},i}^{\text{full}} \mathbf{X} \mathbf{W}^\top) \mathbf{v}^\top, \forall i \in \text{training set}$, where $\mathbf{v} \in \{-1, +1\} \in \mathbb{R}^{1 \times h}$ is the fixed
 1352 output layer vector with half 1 and half -1 . The rows of \mathbf{W} are initialized independently from a
 1353 Gaussian distribution $N(0, \kappa^2 \mathbf{I})$.
 1354

1355 We decompose the analysis of GNN optimization dynamic into three steps.

1356 *Step 1: Reformulating loss and gradient expressions on irregular graphs.* We represent the ReLU
 1357 function implicitly using a position-wise 0/1 indicator matrix that can directly multiply the aggregated
 1358 node features.
 1359

1360 *Step 2: Bounding the norm of gradient.* Based on the reformulated loss and gradient expressions, we
 1361 aim to quantify the magnitude of optimization updates by bounding the gradient norm, facilitating
 1362 convergence analysis. We can bound the Frobenius norm of the gradient by the average of individual
 1363 node-level gradients.
 1364

1365 *Step 3: Bounding the number of iterations to Convergence.* We first leverage the smoothness of the
 1366 loss function to derive a per-iteration inequality relating loss reduction to the gradient norm, and then
 1367 accumulate these iteration-wise inequalities over GD updates to obtain an upper bound on the number
 1368 of iterations required for convergence.
 1369

1370 D.1 ASSUMPTION

1371 We still use Assumptions D.3 on the training data.

1372 **Assumption D.1.** $\forall i, i' \in \text{training set}$, if $y_i \neq y_{i'}$, then $\|\tilde{\mathbf{a}}_{\text{train},i}^{\text{full}} \mathbf{X} - \tilde{\mathbf{a}}_{\text{train},i'}^{\text{full}} \mathbf{X}\|_2 \geq \alpha$ for some
 1373 $\alpha > 0$.
 1374

1375 Assumption D.1 requires that aggregated node features with different labels in the training data are
 1376 separated by at least a constant, which is often satisfied in practice and can be easily verified based on
 1377 the training data. A similar assumption on the non-aggregated features $\|\mathbf{x}_i - \mathbf{x}_{i'}\|_2$ has been adopted
 1378 in prior analyses of the DNN optimization dynamics without message passing (Zou et al., 2020a;
 1379 2018).
 1380

1381 D.2 EXPRESSIONS FOR GRADIENTS FOR CE LOSS.

1382 We first provide some basic expressions regarding the gradients for the CE loss in the GNN under our
 1383 setting. Note that the node classification task in this case is binary, denoted as $K = 2$.
 1384

1385 **Output after the 1-st layer:** Given an input \mathbf{X} , the i -th column of output after the first layer of the
 1386 GNN under the full-graph training is
 1387

$$1388 \mathbf{z}_i^{\text{full}} = \sigma \left(\tilde{\mathbf{a}}_{\text{train},i}^{\text{full}} \mathbf{X} \left(\mathbf{W}^{\text{full}} \right)^\top \right) = \tilde{\mathbf{a}}_{\text{train},i}^{\text{full}} \mathbf{X} (\Sigma_i^{\text{full}} \mathbf{W}^{\text{full}})^\top, \quad (42)$$

1389 where $\Sigma_i^{\text{full}} = \text{Diag} \left(\mathbf{1} \left\{ \tilde{\mathbf{a}}_{\text{train},i}^{\text{full}} \mathbf{X} \left(\mathbf{W}^{\text{full}} \right)^\top > 0 \right\} \right) \in \mathbb{R}^{h \times h}$ represents whether the j -th element
 1390 $\left\{ \tilde{\mathbf{a}}_{\text{train},i}^{\text{full}} \mathbf{X} \left(\mathbf{W}^{\text{full}} \right)^\top \right\}_j$ is more than zero (1) or is zeroed out (0). Here we slightly abuse the notation
 1391 and denote $\mathbf{1} \{ \mathbf{x} > 0 \} = (\mathbf{1} \{ \mathbf{x}_1 > 0 \}, \dots, \mathbf{1} \{ \mathbf{x}_m > 0 \})^\top$ for a vector $\mathbf{x} \in \mathbb{R}^m$.
 1392

1393 **Output of one-round GNN for the CE loss:** The output of the one-round GNN for the CE loss
 1394 with input \mathbf{X} under the full-graph training can be expressed as:
 1395

$$1396 \hat{y}_i^{\text{full}} = \sigma \left(\tilde{\mathbf{a}}_{\text{train},i}^{\text{full}} \mathbf{X} \left(\mathbf{W}^{\text{full}} \right)^\top \right) \mathbf{v}^\top = \tilde{\mathbf{a}}_{\text{train},i}^{\text{full}} \mathbf{X} (\Sigma_i^{\text{full}} \mathbf{W}^{\text{full}})^\top \mathbf{v}^\top, \quad (43)$$

1397 where $\mathbf{v} \in \{-1, +1\} \in \mathbb{R}^{1 \times h}$ is the fixed output layer weight vector with half 1 and half -1 ,
 1398 corresponding to the binary classification task setting in this case.
 1399

1404 **Gradient for CE loss in GNN:** The partial gradient of the training loss $\hat{L}_{\text{train}}^{\text{full}}(\mathbf{W}^{\text{full}})$ with respect
 1405 to \mathbf{W}^{full} under full-graph training can be expressed as:
 1406

$$1407 \quad \nabla_{\mathbf{W}^{\text{full}}} \hat{L}_{\text{train}}^{\text{full}}(\mathbf{W}^{\text{full}}) = \frac{1}{n_{\text{train}}} \sum_{i=0}^{n_{\text{train}}} l' \left(y_i \hat{y}_i^{\text{full}} \right) \cdot y_i \cdot \nabla_{\mathbf{W}^{\text{full}}} \left[\hat{y}_i^{\text{full}} \right], \quad (44)$$

1410 where the gradient of the GNN is defined as $\nabla_{\mathbf{W}^{\text{full}}} \left[\hat{y}_i^{\text{full}} \right] = (\mathbf{v} \Sigma_i^{\text{full}})^{\top} \tilde{\mathbf{a}}_{\text{train},i}^{\text{full}} \mathbf{X}$.
 1411

1412 D.3 THEOREM D.2.

1414 **Theorem D.2.** (Convergence of Full-graph Training with CE) Suppose \mathbf{W}^{full} are generated by
 1415 Gaussian initialization. Under Assumptions D.3 and D.1, if the hidden dimension of a one-
 1416 round GNN satisfies $h = \Omega(\log(n_{\text{train}}) d_{\text{max}}^{-1} (n_{\text{train}}^2 + \epsilon^{-1}))$, then with high probability, the
 1417 training loss satisfies $\hat{L}_{\text{train}}^{\text{full}}(\mathbf{W}_T^{\text{full}}, \mathbf{A}_{\text{train}}^{\text{full}}) \leq \epsilon$, provided that the number of iterations $T =$
 1418 $O(n_{\text{train}} (\log(n_{\text{train}}))^{\frac{1}{2}} \alpha^{-2} d_{\text{max}}^{-\frac{5}{2}} (n_{\text{train}}^2 + \epsilon^{-1}))$ for any $\epsilon \geq 0$ under the full-graph training.
 1419

1421 D.4 PROOF OF THEOREM D.2.

1423 We first provide the following lemmas.

1425 **Lemma D.3** (Bounded initial training loss) Under Assumptions D.3 and D.1, with the probability
 1426 at least $1 - \delta$, at the initialization the training loss satisfies $\hat{L}_{\text{train}}^{\text{full}}(\mathbf{W}_0^{\text{full}}) \leq C \sqrt{d_{\text{max}} \log(n_{\text{train}}/\delta)}$,
 1427 where C is an absolute constant.

1429 **Lemma D.4** (Gradient lower and upper bound) Under Assumptions D.3 and D.1, with the probability
 1430 at least $1 - \exp(-C_1 h \alpha^2 / n_{\text{train}}^2)$, there exist positive constants C_1, C_2 and C_3 , such that

$$1432 \quad \left\| \nabla_{\mathbf{W}^{\text{full}}} \hat{L}_{\text{train}}^{\text{full}}(\mathbf{W}^{\text{full}}) \right\|_F^2 \geq \frac{C_2 h \alpha^2 d_{\text{max}}^3}{n_{\text{train}}^3} \left(\sum_{i=1}^{n_{\text{train}}} l' \left(y_i \hat{y}_i^{\text{full}} \right) \right)^2,$$

$$1435 \quad \left\| \nabla_{\mathbf{W}^{\text{full}}} \hat{L}_{\text{train}}^{\text{full}}(\mathbf{W}^{\text{full}}) \right\|_F \leq -\frac{C_3 h^{\frac{1}{2}} d_{\text{max}}^{\frac{1}{2}}}{n_{\text{train}}} \sum_{i=1}^{n_{\text{train}}} l' \left(y_i \hat{y}_i^{\text{full}} \right).$$

1439 **Lemma D.4** (Sufficient descent) Let $\mathbf{W}_0^{\text{full}}$ be generated via Gaussian random initialization. Let
 1440 $\mathbf{W}_t^{\text{full}}$ be the t -th iterate in the gradient descent. If $\mathbf{W}_t^{\text{full}}, \mathbf{W}_{t+1}^{\text{full}} \in \mathcal{B}(\mathbf{W}_0^{\text{full}}, \tau)$ and $\tau \leq C_6 / (\alpha d_{\text{max}}^{\frac{1}{2}})$,
 1441 then there exist constants C_4, C_5 and C_6 such that, with probability at least $1 - \exp(-O(1))$, the
 1442 following holds:

$$1444 \quad \hat{L}_{\text{train}}^{\text{full}}(\mathbf{W}_{t+1}^{\text{full}}) - \hat{L}_{\text{train}}^{\text{full}}(\mathbf{W}_t^{\text{full}}) \leq -(\eta - C_4 d_{\text{max}} h \eta^2) \left\| \nabla_{\mathbf{W}^{\text{full}}} \hat{L}_{\text{train}}^{\text{full}}(\mathbf{W}_t^{\text{full}}) \right\|_F^2$$

$$1445 \quad - \frac{C_5 \eta d_{\text{max}}^{\frac{1}{2}} h^{\frac{1}{2}} \left\| \nabla_{\mathbf{W}^{\text{full}}} \hat{L}_{\text{train}}^{\text{full}}(\mathbf{W}_t^{\text{full}}) \right\|_F}{n_{\text{train}} \tau} \sum_{i=1}^{n_{\text{train}}} l' \left(y_i \hat{y}_{i,t}^{\text{full}} \right).$$

1449 **Proof of Theorem D.2:** We first prove that gradient descent can achieve the training loss at the
 1450 value of ϵ under the condition that all iterates are staying inside the perturbation region $\mathcal{B}(\mathbf{W}_0^{\text{full}}, \tau) =$
 1451 $\{\mathbf{W} : \|\mathbf{W} - \mathbf{W}_0^{\text{full}}\|_2 \leq \tau\}$.

1453 Using Lemma D.4, there exists a constant C_2 such that

$$1454 \quad \left\| \nabla_{\mathbf{W}^{\text{full}}} \hat{L}_{\text{train}}^{\text{full}}(\mathbf{W}_t^{\text{full}}) \right\|_F^2 \geq \frac{C_2 h \alpha^2 d_{\text{max}}^3}{n_{\text{train}}^3} \left(\sum_{i=1}^{n_{\text{train}}} l' \left(y_i \hat{y}_{i,t}^{\text{full}} \right) \right)^2 \quad (45)$$

1457 We then set the step size η and the radius τ as follows:

1458

$$1459 \quad \eta = \frac{1}{4C_4 d_{\max} h} = O(d_{\max}^{-1} h^{-1}), \quad (46)$$

$$1460 \quad \tau = \frac{4C_5 n_{\text{train}}^{\frac{1}{2}}}{C_2 \alpha d_{\max}} = O\left(n_{\text{train}}^{\frac{1}{2}} d_{\max}^{-1} \alpha^{-1}\right). \quad (47)$$

1463
1464 Then we have

$$\begin{aligned} 1465 \quad & \hat{L}_{\text{train}}^{\text{full}}(\mathbf{W}_{t+1}^{\text{full}}) - \hat{L}_{\text{train}}^{\text{full}}(\mathbf{W}_t^{\text{full}}) \\ 1466 \quad & \leq -\frac{3}{4}\eta \left\| \nabla_{\mathbf{W}^{\text{full}}} \hat{L}_{\text{train}}^{\text{full}}(\mathbf{W}_t^{\text{full}}) \right\|_F^2 - \frac{C_2 \eta h^{\frac{1}{2}} \alpha d_{\max}^{\frac{3}{2}}}{4n_{\text{train}}^{\frac{3}{2}}} \left\| \nabla_{\mathbf{W}^{\text{full}}} \hat{L}_{\text{train}}^{\text{full}}(\mathbf{W}_t^{\text{full}}) \right\|_F \sum_{i=1}^{n_{\text{train}}} l'(y_i \hat{y}_{i,t}^{\text{full}}) \\ 1467 \quad & \leq -\frac{3}{4}\eta \left\| \nabla_{\mathbf{W}^{\text{full}}} \hat{L}_{\text{train}}^{\text{full}}(\mathbf{W}_t^{\text{full}}) \right\|_F^2 + \frac{\eta}{4} \left\| \nabla_{\mathbf{W}^{\text{full}}} \hat{L}_{\text{train}}^{\text{full}}(\mathbf{W}_t^{\text{full}}) \right\|_F^2 \\ 1468 \quad & = -\frac{1}{2}\eta \left\| \nabla_{\mathbf{W}^{\text{full}}} \hat{L}_{\text{train}}^{\text{full}}(\mathbf{W}_t^{\text{full}}) \right\|_F^2 \\ 1469 \quad & \leq -\eta \frac{C_2 h \alpha^2 d_{\max}^3}{2n_{\text{train}}^3} \left(\sum_{i=0}^{n_{\text{train}}} l'(y_i \hat{y}_{i,t}^{\text{full}}) \right)^2, \end{aligned} \quad (48)$$

1470
1471
1472
1473
1474
1475
1476
1477
1478
1479 where the first inequality is derived from Lemma D.4 and the settings of η and τ , the second inequality
is derived from Lemma D.4, as well as the last inequality follows the gradient lower bound in Lemma
D.4.

1480 We note that $l(x) = \log(1 + \exp(-x))$ satisfies $-l'(x) = 1/(1 + \exp(x)) \geq \min\{u_0, u_1 l(x)\}$,
1481 where $u_0 = 1/2$, $u_1 = 1/(2 \log(2))$. This implies that:

$$\begin{aligned} 1482 \quad & -\sum_{i=0}^{n_{\text{train}}} l'(y_i \hat{y}_{i,t}^{\text{full}}) \geq \min \left\{ u_0, \sum_{i=0}^{n_{\text{train}}} u_1 l'(y_i \hat{y}_{i,t}^{\text{full}}) \right\} \\ 1483 \quad & \geq \min \left\{ u_0, n_{\text{train}} u_0 \hat{L}_{\text{train}}^{\text{full}}(\mathbf{W}_t^{\text{full}}) \right\}. \end{aligned} \quad (49)$$

1487 Since $\min\{a, b\} \geq 1/(1/a + 1/b)$, we have:

$$\begin{aligned} 1488 \quad & \hat{L}_{\text{train}}^{\text{full}}(\mathbf{W}_{t+1}^{\text{full}}) - \hat{L}_{\text{train}}^{\text{full}}(\mathbf{W}_t^{\text{full}}) \\ 1489 \quad & \leq -\eta \min \left\{ \frac{C_2 h \alpha^2 d_{\max}^3}{2n_{\text{train}}^3} u_0^2, \frac{C_2 h \alpha^2 d_{\max}^3}{2n_{\text{train}}} u_1^2 \left(\hat{L}_{\text{train}}^{\text{full}}(\mathbf{W}_t^{\text{full}}) \right)^2 \right\} \\ 1490 \quad & \leq -\eta \left(\frac{2n_{\text{train}}^3}{C_2 h \alpha^2 d_{\max}^3 u_0^2} + \frac{2n_{\text{train}}}{C_2 h \alpha^2 d_{\max}^3 u_1^2 \left(\hat{L}_{\text{train}}^{\text{full}}(\mathbf{W}_t^{\text{full}}) \right)^2} \right)^{-1}. \end{aligned} \quad (50)$$

1493
1494
1495
1496 Rearranging terms, we have:

$$1497 \quad \frac{2n_{\text{train}}^2}{C_2 h \alpha^2 d_{\max}^2 u_0^2} \left(\hat{L}_{\text{train}}^{\text{full}}(\mathbf{W}_{t+1}^{\text{full}}) - \hat{L}_{\text{train}}^{\text{full}}(\mathbf{W}_t^{\text{full}}) \right) + \frac{2 \left(\hat{L}_{\text{train}}^{\text{full}}(\mathbf{W}_{t+1}^{\text{full}}) - \hat{L}_{\text{train}}^{\text{full}}(\mathbf{W}_t^{\text{full}}) \right)}{C_2 h \alpha^2 d_{\max}^2 u_1^2 \left(\hat{L}_{\text{train}}^{\text{full}}(\mathbf{W}_t^{\text{full}}) \right)^2} \leq -\eta. \quad (51)$$

1502
1503 Using $(x - y)/y^2 \geq y^{-1} - x^{-1}$ and taking telescope sum over t , we have:

$$\begin{aligned} 1504 \quad & t\eta \leq \frac{2n_{\text{train}}^3}{C_2 h \alpha^2 d_{\max}^3 u_0^2} \left(\hat{L}_{\text{train}}^{\text{full}}(\mathbf{W}_0^{\text{full}}) - \hat{L}_{\text{train}}^{\text{full}}(\mathbf{W}_t^{\text{full}}) \right) + \frac{2n_{\text{train}} \left(\left(\hat{L}_{\text{train}}^{\text{full}}(\mathbf{W}_t^{\text{full}}) \right)^{-1} - \left(\hat{L}_{\text{train}}^{\text{full}}(\mathbf{W}_0^{\text{full}}) \right)^{-1} \right)}{C_2 h \alpha^2 d_{\max}^3 u_1^2} \\ 1505 \quad & \leq \frac{2n_{\text{train}}^3}{C_2 h \alpha^2 d_{\max}^3 u_0^2} \hat{L}_{\text{train}}^{\text{full}}(\mathbf{W}_0^{\text{full}}) + \frac{2n_{\text{train}} \left(\left(\hat{L}_{\text{train}}^{\text{full}}(\mathbf{W}_t^{\text{full}}) \right)^{-1} - \left(\hat{L}_{\text{train}}^{\text{full}}(\mathbf{W}_0^{\text{full}}) \right)^{-1} \right)}{C_2 h \alpha^2 d_{\max}^3 u_1^2}. \end{aligned} \quad (52)$$

1507
1508
1509
1510
1511 Next, we guarantee that, after T gradient steps, the loss function $\hat{L}_{\text{train}}^{\text{full}}(\mathbf{W}_T^{\text{full}})$ is smaller than ϵ .

1512 Using Lemma D.3, we have $\hat{L}_{\text{train}}^{\text{full}}(\mathbf{W}_0^{\text{full}}) = O\left(d_{\max}^{\frac{1}{2}}(\log(n_{\text{train}}))^{\frac{1}{2}}\right)$.
 1513

1514 Therefore, T satisfies:
 1515

1516
$$T = O\left(n_{\text{train}}^3(\log(n_{\text{train}}))^{\frac{1}{2}} / \left(\alpha^2 d_{\max}^{\frac{5}{2}}\right) + n_{\text{train}}(\log(n_{\text{train}}))^{\frac{1}{2}} / \left(\epsilon \alpha^2 d_{\max}^{\frac{5}{2}}\right)\right). \quad (53)$$

 1517

1518
 1519 Then we are going to verify the condition that all iterates stay inside the perturbation region
 1520 $\mathcal{B}(\mathbf{W}_0^{\text{full}}, \tau)$. Obviously, we have $\mathbf{W}_0^{\text{full}} \in \mathcal{B}(\mathbf{W}_0^{\text{full}}, \tau)$. Hence, we need to prove $\mathbf{W}_{t+1}^{\text{full}} \in$
 1521 $\mathcal{B}(\mathbf{W}_0^{\text{full}}, \tau)$ under the induction hypothesis that $\mathbf{W}_t^{\text{full}} \in \mathcal{B}(\mathbf{W}_0^{\text{full}}, \tau)$ holds for all $t \leq T$.
 1522

1523 Since we have $\hat{L}_{\text{train}}^{\text{full}}(\mathbf{W}_{t+1}^{\text{full}}) - \hat{L}_{\text{train}}^{\text{full}}(\mathbf{W}_t^{\text{full}}) \leq -\frac{1}{2}\eta \left\| \nabla_{\mathbf{W}^{\text{full}}} \hat{L}_{\text{train}}^{\text{full}}(\mathbf{W}_t^{\text{full}}) \right\|_F^2$ for any $t \leq T$, using
 1524 triangle inequality, we have:
 1525

1526
$$\begin{aligned} \left\| \mathbf{W}_t^{\text{full}} - \mathbf{W}_0^{\text{full}} \right\|_2 &\leq \eta \sum_{k=0}^{t-1} \left\| \nabla_{\mathbf{W}_k^{\text{full}}} \hat{L}_{\text{train}}^{\text{full}}(\mathbf{W}_k^{\text{full}}) \right\|_F^2 \\ 1527 &\leq \eta \sqrt{\sum_{k=0}^{t-1} \left\| \nabla_{\mathbf{W}_k^{\text{full}}} \hat{L}_{\text{train}}^{\text{full}}(\mathbf{W}_k^{\text{full}}) \right\|_F^2} \\ 1528 &\leq \sqrt{2t\eta \sum_{k=0}^{t-1} [\hat{L}_{\text{train}}^{\text{full}}(\mathbf{W}_k^{\text{full}}) - \hat{L}_{\text{train}}^{\text{full}}(\mathbf{W}_{k+1}^{\text{full}})]} \\ 1529 &\leq \sqrt{2t\eta \hat{L}_{\text{train}}^{\text{full}}(\mathbf{W}_0^{\text{full}})}. \end{aligned} \quad (54)$$

 1530
 1531

1532
 1533 Using $\hat{L}_{\text{train}}^{\text{full}}(\mathbf{W}_0^{\text{full}}) = O\left(d_{\max}^{\frac{1}{2}}(\log(n_{\text{train}}))^{\frac{1}{2}}\right)$ in Lemma D.3 and our settings of η , we have:
 1534

1535
$$\begin{aligned} \left\| \mathbf{W}_t^{\text{full}} - \mathbf{W}_0^{\text{full}} \right\|_2 &\leq \sqrt{2t\eta \hat{L}_{\text{train}}^{\text{full}}(\mathbf{W}_0^{\text{full}})} \\ 1536 &= O\left(n_{\text{train}}^{\frac{3}{2}}(\log(n_{\text{train}}))^{\frac{1}{2}} \alpha^{-1} d_{\max}^{-\frac{3}{2}} h^{-\frac{1}{2}} + n_{\text{train}}^{\frac{1}{2}}(\log(n_{\text{train}}))^{\frac{1}{2}} \epsilon^{-\frac{1}{2}} \alpha^{-1} d_{\max}^{-\frac{3}{2}} h^{-\frac{1}{2}}\right). \end{aligned} \quad (55)$$

 1537

1538 In addition, by Lemma D.4 and our choice of η , we have
 1539

1540
$$\begin{aligned} \eta \left\| \nabla_{\mathbf{W}^{\text{full}}} \hat{L}_{\text{train}}^{\text{full}}(\mathbf{W}^{\text{full}}) \right\|_2 &\leq -\frac{\eta C_3 h^{\frac{1}{2}} d_{\max}^{\frac{1}{2}}}{n_{\text{train}}} \sum_{i=0}^{n_{\text{train}}} l'(y_i \hat{y}_i^{\text{full}}) \\ 1541 &\leq O\left((\log(n_{\text{train}}))^{\frac{1}{2}} h^{-\frac{1}{2}} d_{\max}^{-\frac{1}{2}}\right), \end{aligned} \quad (56)$$

 1542
 1543

1544 where the second inequality is derived from the fact that $-1 \leq l'(\cdot) \leq 0$.
 1545

1546 Therefore, by triangle inequality, we assume that $h = \Omega\left(n_{\text{train}}^2 \log(n_{\text{train}}) d_{\max}^{-1} + \log(n_{\text{train}}) \epsilon^{-1} d_{\max}^{-1}\right)$
 1547 and we have:
 1548

1549
$$\begin{aligned} \left\| \mathbf{W}_{t+1}^{\text{full}} - \mathbf{W}_t^{\text{full}} \right\|_2 &\leq \eta \left\| \nabla_{\mathbf{W}^{\text{full}}} \hat{L}_{\text{train}}^{\text{full}}(\mathbf{W}_t^{\text{full}}) \right\|_2 + \left\| \mathbf{W}_t^{\text{full}} - \mathbf{W}_0^{\text{full}} \right\|_2 \\ 1550 &= O\left(n_{\text{train}}^{\frac{3}{2}}(\log(n_{\text{train}}))^{\frac{1}{2}} \alpha^{-1} d_{\max}^{-\frac{3}{2}} h^{-\frac{1}{2}} + n_{\text{train}}^{\frac{1}{2}}(\log(n_{\text{train}}))^{\frac{1}{2}} \epsilon^{-\frac{1}{2}} \alpha^{-1} d_{\max}^{-\frac{3}{2}} h^{-\frac{1}{2}}\right) \\ 1551 &= O\left(n_{\text{train}}^{\frac{1}{2}} d_{\max}^{-1} \alpha^{-1}\right), \end{aligned} \quad (57)$$

 1552
 1553

1554 which is exactly the same order of τ in our settings.
 1555

1556 This verifies $\mathbf{W}_{t+1}^{\text{full}} \in \mathcal{B}(\mathbf{W}_0^{\text{full}}, \tau)$.
 1557

1558 Proved.
 1559

1566 **E PROOF OF CONVERGENCE THEOREM IN MINI-BATCH TRAINING WITH CE**
 1567 **AND INTERPRETATION OF THE OBS.1**

1569 In this section, we provide the proof of the convergence theorem in mini-batch training with CE. To
 1570 simplify the analysis, we focus on binary node classification using a one-round GNN trained with the
 1571 CE, defined as $l(\mathbf{W}, \tilde{\mathbf{a}}_{\text{train},i}^{\text{mini}}) = \log(1 + \exp(-y_i \hat{y}_i))$. The final output of the GNN model is given
 1572 by $\hat{y}_i = \mathbf{z}_i \mathbf{v}^\top = \sigma(\tilde{\mathbf{a}}_{\text{train},i}^{\text{mini}} \mathbf{X} \mathbf{W}^\top) \mathbf{v}^\top, \forall i \in \text{training set}$, where $\mathbf{v} \in \{-1, +1\} \in \mathbb{R}^{1 \times h}$ is the fixed
 1573 output layer vector with half 1 and half -1. The rows of \mathbf{W} are initialized independently from a
 1574 Gaussian distribution $N(0, \kappa^2 \mathbf{I})$.
 1575

1576 We decompose the analysis of GNN optimization dynamic into three steps, similar to Appendix D.

1577 **E.1 ASSUMPTION**

1580 We still use Assumptions B.1 on the training data.

1582 **Assumption E.1.** $\forall i, i' \in \text{training set}$, if $y_i \neq y_{i'}$, then $\|\tilde{\mathbf{a}}_{\text{train},i}^{\text{mini}} \mathbf{X} - \tilde{\mathbf{a}}_{\text{train},i'}^{\text{mini}} \mathbf{X}\|_2 \geq \alpha$ for some
 1583 $\alpha > 0$.

1584 Assumption E.1 requires that aggregated node features with different labels in the training data are
 1585 separated by at least a constant.

1587 **E.2 EXPRESSIONS FOR GRADIENTS FOR CE LOSS.**

1589 We first provide some basic expressions regarding the gradients for the CE loss in the GNN under our
 1590 setting. Note that the node classification task in this case is binary, denoted as $K = 2$.

1591 The i -th column of the output $\mathbf{z}_i^{\text{mini}}$ after the first layer, as well as the output \hat{y}_i^{mini} of the one-round
 1592 GNN for the CE loss under mini-batch training, are similar to those in full-graph training in Sec. D,
 1593 with \mathbf{W}^{full} and $\tilde{\mathbf{a}}_{\text{train},i}^{\text{full}}$ replaced by \mathbf{W}^{mini} and $\tilde{\mathbf{a}}_{\text{train},i}^{\text{mini}}$, respectively.
 1594

1595 **Gradient for CE loss in GNN:** The partial gradients of the training losses $\hat{L}_{\text{train}}^{\text{mini}}(\mathbf{W}^{\text{mini}}, \tilde{\mathbf{A}}_{\text{train}}^{\text{mini}})$
 1596 and $\hat{L}_{\text{train}}^{\text{full}}(\mathbf{W}^{\text{mini}}, \tilde{\mathbf{A}}_{\text{train}}^{\text{mini}})$ with respect to \mathbf{W}^{mini} under full-graph training can be expressed as:

$$\nabla \hat{L}_{\text{train}}^{\text{mini}}(\mathbf{W}^{\text{mini}}, \tilde{\mathbf{A}}_{\text{train}}^{\text{mini}}) = \frac{1}{b} \sum_{i=0}^b l' \left(y_i \hat{y}_i^{\text{mini}} \right) \cdot y_i \cdot \nabla_{\mathbf{W}^{\text{mini}}} \left[\hat{y}_i^{\text{mini}} \right], \quad (58)$$

$$\nabla \hat{L}_{\text{train}}^{\text{full}}(\mathbf{W}^{\text{mini}}, \tilde{\mathbf{A}}_{\text{train}}^{\text{mini}}) = \frac{1}{n_{\text{train}}} \sum_{i=0}^{n_{\text{train}}} l' \left(y_i \hat{y}_i^{\text{mini}} \right) \cdot y_i \cdot \nabla_{\mathbf{W}^{\text{mini}}} \left[\hat{y}_i^{\text{mini}} \right], \quad (59)$$

1606 where the gradient of the GNN is defined as $\nabla_{\mathbf{W}^{\text{mini}}} \left[\hat{y}_i^{\text{mini}} \right] = (\mathbf{v} \Sigma_i^{\text{mini}})^\top \tilde{\mathbf{a}}_{\text{train},i}^{\text{mini}} \mathbf{X}$.

1608 **E.3 THEOREM E.2.**

1610 **Theorem E.2.** (Convergence of Mini-batch Training with CE) *Suppose \mathbf{W}^{mini} are generated
 1611 by Gaussian initialization. Under Assumptions B.1 and E.1, if the hidden dimension of a one-
 1612 round GNN satisfies $h = \Omega(n_{\text{train}}^2 \log(n_{\text{train}}) \beta^{-1} + \log(n_{\text{train}}) \beta^{-1} \epsilon^{-1})$, then with high probabili-
 1613 ty, the training loss satisfies $\hat{L}_{\text{train}}(\mathbf{W}_T^{\text{mini}}, \mathbf{A}_{\text{train}}^{\text{mini}}) \leq \epsilon$, provided that the number of iterations
 1614 $T = \tilde{O} \left(n_{\text{train}}^4 (\log(n_{\text{train}}))^{\frac{1}{2}} \alpha^{-2} \beta^{-\frac{5}{2}} b^{-1} + n_{\text{train}}^2 (\log(n_{\text{train}}))^{\frac{1}{2}} \alpha^{-2} \beta^{-\frac{5}{2}} b^{-1} \epsilon^{-1} \right)$ for any $\epsilon \geq 0$
 1615 under the mini-batch GNN training.*

1617 Our bound on the hidden dimension h reveals an over-parameterization setting in this case, where the
 1618 number of trainable parameters exceeds the number of training samples. Since the hidden dimension
 1619 h remains finite, our analysis is conducted in the finite-width setting, in contrast to the infinite-width
 Neural Tangent Kernel (NTK) framework (Yang et al., 2023; Lin et al., 2023).

1620 E.4 PROOF OF E.2.
 1621

1622 We first provide the following lemmas.
 1623

1624 **Lemma E.3** (Bounded initial training loss) Under Assumptions B.1-E.1, with the probability
 1625 at least $1 - \delta$, at the initialization the training loss satisfies $\hat{L}_{\text{train}}^{\text{full}}(\mathbf{W}_0^{\text{mini}}), \hat{L}_{\text{train}}^{\text{mini}}(\mathbf{W}_0^{\text{mini}}) \leq$
 1626 $C\sqrt{\beta \log(n_{\text{train}}/\delta)}$, where C is an absolute constant.
 1627

1628 **Lemma E.4** (Gradient lower and upper bound) Under Assumptions B.1-E.1, with the probability at
 1629 least $1 - \exp(-C_1 h \alpha^2 / (n\beta))$, there exist positive constants C_1, C_2 and C_3 , such that
 1630

$$\begin{aligned} \|\nabla_{\mathbf{W}^{\text{mini}}} \hat{L}_{\text{train}}^{\text{full}}(\mathbf{W}^{\text{mini}}, \tilde{\mathbf{A}}_{\text{train}}^{\text{mini}})\|_F^2 &\geq \frac{C_2 h \alpha^2 \beta^3}{n_{\text{train}}^3} \left(\sum_{i=1}^{n_{\text{train}}} l'(y_i \hat{y}_i^{\text{mini}}) \right)^2, \\ \|\nabla_{\mathbf{W}^{\text{mini}}} \hat{L}_{\text{train}}^{\text{mini}}(\mathbf{W}^{\text{mini}}, \tilde{\mathbf{A}}_{\text{train}}^{\text{mini}})\|_F &\leq -\frac{C_3 h^{\frac{1}{2}} \beta^{\frac{1}{2}}}{b} \sum_{i=1}^b l'(y_i \hat{y}_i^{\text{mini}}). \end{aligned}$$

1631 **Lemma E.5** (Sufficient descent) Let $\mathbf{W}_0^{\text{mini}}$ be generated via Gaussian random initialization. Let
 1632 $\mathbf{W}_t^{\text{mini}}$ be the t -th iterate in the stochastic gradient descent. If $\mathbf{W}_t^{\text{mini}}, \mathbf{W}_{t+1}^{\text{mini}} \in \mathcal{B}(\mathbf{W}_0^{\text{mini}}, \tau)$ and
 1633 $\tau \leq C_6 n^{\frac{1}{2}} / (\alpha \beta)$, then there exist constants C_4, C_5 and C_6 such that, with probability at least
 1634 $1 - \exp(-O(1))$, the following holds:
 1635

$$\begin{aligned} &\mathbb{E} \left[\hat{L}_{\text{train}}^{\text{full}}(\mathbf{W}_{t+1}^{\text{mini}}, \tilde{\mathbf{A}}_{\text{train}}^{\text{mini}}) \mid \mathbf{W}_t^{\text{mini}} \right] - \hat{L}_{\text{train}}^{\text{full}}(\mathbf{W}_t^{\text{mini}}, \tilde{\mathbf{A}}_{\text{train}}^{\text{mini}}) \\ &\leq - \left(\eta - \frac{C_4 \beta h n^2 n_{\text{train}}}{b} \right) \|\nabla_{\mathbf{W}_t^{\text{mini}}} \hat{L}_{\text{train}}^{\text{full}}(\mathbf{W}_t^{\text{mini}}, \tilde{\mathbf{A}}_{\text{train}}^{\text{mini}})\|_F^2 \\ &\quad - \frac{C_5 \eta \beta^{\frac{1}{2}} h^{\frac{1}{2}}}{n_{\text{train}} \tau} \left\| \nabla_{\mathbf{W}_t^{\text{mini}}} \hat{L}_{\text{train}}^{\text{full}}(\mathbf{W}_t^{\text{mini}}, \tilde{\mathbf{A}}_{\text{train}}^{\text{mini}}) \right\|_F \sum_{i=1}^{n_{\text{train}}} l'(y_i \hat{y}_{i,t+1}^{\text{mini}}). \end{aligned}$$

1636 **Proof of E.2:** We first prove that stochastic gradient descent can achieve the training loss at the value
 1637 of ϵ under the condition that all iterates are staying inside the perturbation region $\mathcal{B}(\mathbf{W}_0^{\text{mini}}, \tau) =$
 1638 $\{\mathbf{W} : \|\mathbf{W} - \mathbf{W}_0^{\text{mini}}\|_2 \leq \tau\}$.
 1639

1640 Using Lemma E.4, there exists a constant C_2 such that
 1641

$$\|\nabla_{\mathbf{W}^{\text{full}}} \hat{L}_{\text{train}}^{\text{mini}}(\mathbf{W}_t^{\text{mini}}, \tilde{\mathbf{A}}_{\text{train}}^{\text{mini}})\|_F^2 \geq \frac{C_2 h \alpha^2 \beta^3}{n_{\text{train}}^3} \left(\sum_{i=1}^{n_{\text{train}}} l'(y_i \hat{y}_{i,t}^{\text{mini}}) \right)^2 \quad (60)$$

1642 We then set the step size η and the radius τ as follows:
 1643

$$\eta = \frac{b}{4C_4 \beta h n_{\text{train}}} = O(b \beta^{-1} h^{-1} n_{\text{train}}^{-1}), \quad (61)$$

$$\tau = \frac{4C_5 n_{\text{train}}^{\frac{1}{2}}}{C_2 \alpha \beta} = O\left(n_{\text{train}}^{\frac{1}{2}} \alpha^{-1} \beta^{-1}\right). \quad (62)$$

1644 Then we have:
 1645

$$\begin{aligned} &\mathbb{E} \left[\hat{L}_{\text{train}}^{\text{full}}(\mathbf{W}_{t+1}^{\text{mini}}, \tilde{\mathbf{A}}_{\text{train}}^{\text{mini}}) \mid \mathbf{W}_t^{\text{mini}} \right] - \hat{L}_{\text{train}}^{\text{full}}(\mathbf{W}_t^{\text{mini}}, \tilde{\mathbf{A}}_{\text{train}}^{\text{mini}}) \\ &\leq -\eta \left(\frac{2n_{\text{train}}^3}{C_2 h \alpha^2 \beta^3 u_0^2} + \frac{2n_{\text{train}}}{C_2 h \alpha^2 \beta^3 u_1^2 (\hat{L}_{\text{train}}^{\text{full}}(\mathbf{W}_t^{\text{mini}}, \tilde{\mathbf{A}}_{\text{train}}^{\text{mini}}))^2} \right)^{-1}, \end{aligned} \quad (63)$$

1646 where $u_0 = 1/2, u_1 = 1/(2 \log(2))$.
 1647

1674 Rearranging terms, we have:
1675

$$\begin{aligned} 1676 & \frac{2n_{\text{train}}^3}{C_2 h \alpha^2 \beta^3 u_0^2} \left(\mathbb{E} \left[\hat{L}_{\text{train}}^{\text{full}} \left(\mathbf{W}_{t+1}^{\text{mini}}, \tilde{\mathbf{A}}_{\text{train}}^{\text{mini}} \right) \mid \mathbf{W}_t^{\text{mini}} \right] - \hat{L}_{\text{train}}^{\text{full}} \left(\mathbf{W}_t^{\text{mini}}, \tilde{\mathbf{A}}_{\text{train}}^{\text{mini}} \right) \right) \\ 1677 & + \frac{2n_{\text{train}} \left(\mathbb{E} \left[\hat{L}_{\text{train}}^{\text{full}} \left(\mathbf{W}_{t+1}^{\text{mini}}, \tilde{\mathbf{A}}_{\text{train}}^{\text{mini}} \right) \mid \mathbf{W}_t^{\text{mini}} \right] - \hat{L}_{\text{train}}^{\text{full}} \left(\mathbf{W}_t^{\text{mini}}, \tilde{\mathbf{A}}_{\text{train}}^{\text{mini}} \right) \right)}{C_2 h \alpha^2 \beta^3 u_1^2 \left(\hat{L}_{\text{train}}^{\text{full}} \left(\mathbf{W}_t^{\text{mini}}, \tilde{\mathbf{A}}_{\text{train}}^{\text{mini}} \right) \right)^2} \leq -\eta. \end{aligned} \quad (64)$$

1682 Using $(x - y)/y^2 \geq y^{-1} - x^{-1}$ and taking telescope sum over t , we have:
1683

$$\begin{aligned} 1684 & t\eta \leq \frac{2n_{\text{train}}^3}{C_2 h \alpha^2 \beta^3 u_0^2} \hat{L}_{\text{train}}^{\text{full}} \left(\mathbf{W}_0^{\text{mini}}, \tilde{\mathbf{A}}_{\text{train}}^{\text{mini}} \right) \\ 1685 & + \frac{2n_{\text{train}} \left(\left(\mathbb{E} \left[\hat{L}_{\text{train}}^{\text{full}} \left(\mathbf{W}_t^{\text{mini}}, \tilde{\mathbf{A}}_{\text{train}}^{\text{mini}} \right) \right] \right)^{-1} - \left(\hat{L}_{\text{train}}^{\text{full}} \left(\mathbf{W}_0^{\text{mini}}, \tilde{\mathbf{A}}_{\text{train}}^{\text{mini}} \right) \right)^{-1} \right)}{C_2 h \alpha^2 \beta^3 u_1^2}. \end{aligned} \quad (65)$$

1689 Next, we guarantee that, after T gradient steps, the loss function $\hat{L}_{\text{train}}^{\text{full}} \left(\mathbf{W}_T^{\text{mini}}, \tilde{\mathbf{A}}_{\text{train}}^{\text{mini}} \right)$ is smaller than
1690 ϵ .
1691

1692 Using Lemma E.3, we have $\hat{L}_{\text{train}}^{\text{full}} \left(\mathbf{W}_0^{\text{mini}}, \tilde{\mathbf{A}}_{\text{train}}^{\text{mini}} \right) = O \left(\beta^{\frac{1}{2}} (\log(n_{\text{train}}))^{\frac{1}{2}} \right)$.
1693

1694 Therefore, T satisfies:

$$1695 T = \tilde{O} \left(n_{\text{train}}^4 (\log(n_{\text{train}}))^{\frac{1}{2}} / \left(\alpha^2 \beta^{\frac{5}{2}} b \right) + n_{\text{train}}^2 (\log(n_{\text{train}}))^{\frac{1}{2}} / \left(\epsilon \alpha^2 \beta^{\frac{5}{2}} b \right) \right). \quad (66)$$

1697 Then we are going to verify the condition that all iterates stay inside the perturbation region
1698 $\mathcal{B} \left(\mathbf{W}_0^{\text{mini}}, \tau \right)$. Obviously, we have $\mathbf{W}_0^{\text{mini}} \in \mathcal{B} \left(\mathbf{W}_0^{\text{mini}}, \tau \right)$. Hence, we need to prove $\mathbf{W}_{t+1} \in$
1699 $\mathcal{B} \left(\mathbf{W}_0^{\text{mini}}, \tau \right)$ under the induction hypothesis that $\mathbf{W}_t \in \mathcal{B} \left(\mathbf{W}_0^{\text{mini}}, \tau \right)$ holds for all $t \leq T$.
1700

1701 Since we have $\hat{L}_{\text{train}}^{\text{mini}} \left(\mathbf{W}_{t+1}^{\text{mini}} \right) - \hat{L}_{\text{train}}^{\text{mini}} \left(\mathbf{W}_t^{\text{mini}} \right) \leq -\frac{1}{2}\eta \left\| \nabla_{\mathbf{W}^{\text{mini}}} \hat{L}_{\text{train}}^{\text{mini}} \left(\mathbf{W}_t^{\text{mini}}, \tilde{\mathbf{A}}_{\text{train}}^{\text{mini}} \right) \right\|_F^2$ for any
1702 $t \leq T$, using triangle inequality, we have:

$$1704 \left\| \mathbf{W}_t^{\text{mini}} - \mathbf{W}_0^{\text{mini}} \right\|_2 \leq \sqrt{2t\eta \hat{L}_{\text{train}}^{\text{mini}} \left(\mathbf{W}_0^{\text{mini}}, \tilde{\mathbf{A}}_{\text{train}}^{\text{mini}} \right)}. \quad (67)$$

1707 Using $\hat{L}_{\text{train}}^{\text{mini}} \left(\mathbf{W}_0^{\text{mini}}, \tilde{\mathbf{A}}_{\text{train}}^{\text{mini}} \right) = O \left(\beta^{\frac{1}{2}} (\log(n_{\text{train}}))^{\frac{1}{2}} \right)$ in Lemma E.3 and our settings of η , we have:
1708

$$\begin{aligned} 1709 & \left\| \mathbf{W}_t^{\text{mini}} - \mathbf{W}_0^{\text{mini}} \right\|_2 \\ 1710 & \leq \sqrt{2t\eta \hat{L}_{\text{train}}^{\text{mini}} \left(\mathbf{W}_0^{\text{mini}}, \tilde{\mathbf{A}}_{\text{train}}^{\text{mini}} \right)} \\ 1711 & = O \left(n_{\text{train}}^{\frac{3}{2}} (\log(n_{\text{train}}))^{\frac{1}{2}} b^{\frac{1}{2}} \alpha^{-1} \beta^{-\frac{3}{2}} h^{-\frac{1}{2}} + n_{\text{train}}^{\frac{1}{2}} (\log(n_{\text{train}}))^{\frac{1}{2}} b^{\frac{1}{2}} \epsilon^{-\frac{1}{2}} \alpha^{-1} \beta^{-\frac{3}{2}} h^{-\frac{1}{2}} \right). \end{aligned} \quad (68)$$

1715 In addition, by Lemma E.4 and our choice of η , we have

$$\begin{aligned} 1717 & \eta \left\| \nabla_{\mathbf{W}^{\text{mini}}} \hat{L}_{\text{train}}^{\text{mini}} \left(\mathbf{W}_t^{\text{mini}}, \tilde{\mathbf{A}}_{\text{train}}^{\text{mini}} \right) \right\|_2 \leq -\frac{\eta C_3 h^{\frac{1}{2}} \beta^{\frac{1}{2}}}{b} \sum_{i=0}^b l' \left(y_i \hat{y}_i^{\text{mini}} \right) \\ 1718 & \leq O \left((\log(n_{\text{train}}))^{\frac{1}{2}} h^{-\frac{1}{2}} b^{-\frac{1}{2}} \right), \end{aligned} \quad (69)$$

1721 where the second inequality is derived from the fact that $-1 \leq l'(\cdot) \leq 0$.
1722

1723 Therefore, by triangle inequality, we assume that $h = \Omega \left(n_{\text{train}}^2 \log(n_{\text{train}}) \beta^{-1} + \log(n_{\text{train}}) \epsilon^{-1} \beta^{-1} \right)$
1724 and we have:

$$\begin{aligned} 1725 & \left\| \mathbf{W}_{t+1}^{\text{mini}} - \mathbf{W}_t^{\text{mini}} \right\|_2 \leq \eta \left\| \nabla_{\mathbf{W}^{\text{mini}}} \hat{L}_{\text{train}}^{\text{mini}} \left(\mathbf{W}_t^{\text{mini}}, \tilde{\mathbf{A}}_{\text{train}}^{\text{mini}} \right) \right\|_2 + \left\| \mathbf{W}_t^{\text{mini}} - \mathbf{W}_0^{\text{mini}} \right\|_2 \\ 1726 & = O \left(n_{\text{train}}^{\frac{1}{2}} \alpha^{-1} \beta^{-1} \right), \end{aligned} \quad (70)$$

1728 which is exactly the same order of τ in our settings.
 1729

1730 This verifies $\mathbf{W}_{t+1}^{\text{mini}} \in \mathcal{B}(\mathbf{W}_0^{\text{mini}}, \tau)$.
 1731

1732 Proved.
 1733

1734 F INTERPRETATION OF THE OBS.1 FROM CONVERGENCE THEOREMS

1736 **Understanding the impact of batch size on GNN convergence.** The popular explanation posits
 1737 that increasing batch size reduces gradient variance, resulting in fewer iterations to converge (Cong
 1738 et al., 2021a; Zou et al., 2020b; Liu et al., 2024; Li & Liang, 2018; Hu et al., 2021). This explanation
 1739 does not fully account for the impact of batch size on GNN convergence, necessitating additional
 1740 consideration of the impact of message passing on the loss and gradient.

1741 **MSE:** Taking the MSE as an example, the impact of batch size on GNN convergence is explained in
 1742 three steps: (1). Activation similarity: Larger batch place more sampled nodes and their neighbors
 1743 into the same graph subset in a single iteration, where message passing enables direct or indirect
 1744 information exchange, resulting in similar activations processed by the same GNN parameters. In
 1745 contrast, smaller batches spread nodes across iterations with varying graph subsets and updated
 1746 parameters, reducing such similarity. (2). Gradient similarity: As MSE penalizes the numerical
 1747 difference between predicted and target activations, the nodes with similar activations produce similar
 1748 gradients. The GNN with larger batch sizes yields more coherent update directions after gradient
 1749 averaging, capturing dominant structural patterns among nodes. (3). Bias: These updates may
 1750 reduce node representational distinctiveness and overlook graph structural diversity, introducing
 1751 bias and steering optimization toward suboptimal local minima. As batch size grows, convergence
 1752 requires more iterations to escape these biased regions. DNNs typically assume i.i.d. training
 1753 samples, enabling large batches to retain diversity and reduce gradient bias. This explains why GNN
 1754 findings on MSE differ from expectations based on gradient variance alone, highlighting how the
 1755 interplay between message passing and the loss function affects the impact of batch sizes on the GNN
 1756 optimization dynamic, diverging from DNN behavior.

1757 **CE:CE** focuses on optimizing the predicted probability of the true class, rather than minimizing the
 1758 numerical differences between activations. Thus, the activation similarity does not necessarily lead to
 1759 similar gradient directions under CE. This allows larger batch sizes to benefit from reduced gradient
 1760 variance without introducing significant bias under CE, leading to fewer iterations to converge.

1761 **Understanding the impact of fan-out size on convergence.** A larger fan-out size allows each node
 1762 to aggregate more neighbors, enriching the node’s embedding and enhancing the effective gradient
 1763 even when using MSE. This leads to the reduced gradient variance, thereby more stable updates and
 1764 fewer iterations for GNN convergence.

1766 G PROOF OF GENERALIZATION THEOREM IN MINI-BATCH TRAINING

1768 In this section, we provide the proof of Theorem 3 in Section 4.

1770 We can characterize the GNN generalization under mini-batch training via the PAC-Bayesian frame-
 1771 work (McAllester, 2003). This framework decomposes the generalization gap into two components:
 1772 (1) the divergence between the prior distribution \mathcal{P} and the posterior distribution \mathcal{Q} over the hypothe-
 1773 sis space that includes all possible models that a learning algorithm can select, and (2) the discrepancy
 1774 between expected training and testing losses over \mathcal{P} . The first component is easily re-derived follow-
 1775 ing the PAC-Bayesian framework. We mainly focus on bounding the second component, namely the
 1776 discrepancy U between expected training and testing losses over \mathcal{P} .

1777 As the training and testing datasets are split before training, analyzing this loss discrepancy U reflects
 1778 the structural difference between training and testing graphs. To isolate the impact of this structural
 1779 difference on generalization, we demonstrate that the discrepancy U is bounded by the Wasserstein
 1780 distance $\Delta(\beta, b)$ from the training graph to the testing graph, such that $U \leq C_u \Delta(\beta, b)$ for a
 1781 constant $C_u > 0$. This bound suggests that the more similar the training and testing graph structures
 are, the smaller the expected loss discrepancy is.

1782 G.1 ASSUMPTIONS
17831784 We introduce assumptions on graph data and model parameters.
17851786 **Assumption G.1.** There exists a constant $C_F > 0$ such that $\|\mathbf{X}\|_F^2 \leq C_F$.
17871788 **Assumption G.2.** There exists a constant $C_w > 0$ such that $\|\mathbf{w}_i\|_2^2 \leq C_w$ for all i .
17891790 Assumption G.1 bounds the Frobenius norm of the feature matrix, and Assumption G.2 requires the
1791 norm of parameters to be upper-bounded during mini-batch training. These assumptions are also
1792 employed in the analyses of GNN generalization (Tang & Liu, 2023; Garg et al., 2020; Liao et al.,
1793 2020), which are introduced to simplify the proof.
17941795 The rows of \mathbf{W} are initialized independently from a Gaussian distribution $N(0, \kappa^2 \mathbf{I})$.
17961797 G.2 PROOF OF THEOREM 3
17981799 **Definition G.3.** (Expected Loss Discrepancy (Ma et al., 2021)). For a constant $C_u > 0$, define the
1800 expected loss discrepancy between training and testing datasets before GNN training as:
1801

1802
$$U = \ln \mathbb{E}_{\mathbf{W}^{\text{mini}} \sim \mathcal{P}} \left[e^{C_u (L_{\text{test}}(\mathbf{W}^{\text{mini}}, \mathbf{A}_{\text{test}}^{\text{full}}) - L_{\text{train}}(\mathbf{W}^{\text{mini}}, \mathbf{A}_{\text{train}}^{\text{mini}}))} \right],$$

1803

1804 where \mathcal{P} represents the prior distribution over hypothesis space that includes all possible models that
1805 a learning algorithm can select.
18061807 Definition G.3 captures the difference between training and testing datasets.
18081809 **Definition G.4.** (Distance between Training Set and Testing Set). Define the distance from the
1810 training set to the testing set as the Wasserstein distance given by:
1811

1812
$$\begin{aligned} \Delta(\beta, b) &= \left\{ \inf_{\theta \in \Theta[\rho_{\text{train}}, \rho_{\text{test}}]} \sum_{i \in \text{train set}} \sum_{j \in \text{test set}} \theta_{i,j} \delta(y_i, y_j, \beta, b) \right\} \\ &= \left\{ \sup_{f(\cdot), g(\cdot)} \sum_{i \in \text{train set}} f(y_i) \rho_{\text{train}}(y_i) + \sum_{j \in \text{test set}} g(y_j) \rho_{\text{test}}(y_j) \right\}, \end{aligned} \quad (71)$$

1813

1814 where $\rho_{\text{train}}(y_i)$ and $\rho_{\text{test}}(y_i)$ denote the probability of y_i appearing in training and testing sets,
1815 respectively. $\Theta[\rho_{\text{train}}, \rho_{\text{test}}]$ is the joint probability of ρ_{train} and ρ_{test} , and $f(y_i)$ and $g(y_i)$ are
1816 functions of y_i with $i \in \mathcal{V}$. The infimum in the first equality is conditioned on $\sum_{j \in \text{test set}} \theta_{i,j} =$
1817 $\rho_{\text{train}}(y_i)$, $\sum_{i \in \text{training set}} \theta_{i,j} = \rho_{\text{test}}(y_j)$, $\theta_{i,j} \geq 0$, and the supremum in the second equality is condi-
1818 tioned on $f(y_i) + g(y_j) \leq \delta(y_i, y_j, \beta, b)$. $\delta(y_i, y_j, \beta, b)$ is the distance function of any two points
1819 from training and testing sets, respectively.
18201821 The Wasserstein distance effectively measures differences in non-i.i.d. data, particularly regarding
1822 geometric variations. A dual representation is provided in Eq (71).
18231824 **Theorem G.5.** (PAC-Bayesian Generalization Theorem). For any $C_u > 0$, for any "prior" distribution
1825 \mathcal{P} of the output hypothesis function of a GNN that is independent of node labels from training
1826 dataset, with probability at least $1 - C_G$, for the distribution \mathcal{Q} of the output hypothesis function of a
1827 GNN, we have:
1828

1829
$$L_{\text{test}}(\mathbf{W}^{\text{mini}}, \tilde{\mathbf{A}}_{\text{test}}^{\text{full}}, \mathcal{Q}) \leq \hat{L}_{\text{train}}^{\text{full}}(\mathbf{W}^{\text{mini}}, \tilde{\mathbf{A}}_{\text{train}}^{\text{mini}}, \mathcal{Q}) + \frac{1}{C_u} (D_{KL}(\mathcal{Q} \parallel \mathcal{P}) + \ln \frac{1}{C_G} + \frac{C_u^2}{4n_{\text{train}}} + U).$$

1830

1831 **Lemma G.6** For any $C_u > 0$, assume the "prior" \mathcal{P} on hypothesis space is defined by sampling the
1832 model parameters. If the in-degree of each node is $O(\beta)$ and the out-degree of each node is $O(b)$, we
1833 have:
1834

1835
$$U \leq C_u \Delta(\beta, b),$$

1836 and,
1837

1838
$$\Delta(\beta, b) \propto \sum_{i \in \text{train set}} \sum_{j \in \text{test set}} \theta_{i,j} \delta_i^{\text{full-mini}} = \sum_{i \in \text{train set}} \sum_{j \in \text{test set}} \theta_{i,j} \left\| \tilde{\mathbf{a}}_{\text{train},i}^{\text{full}} - \tilde{\mathbf{a}}_{\text{train},i}^{\text{mini}} \right\|_F^2. \quad (72)$$

1839

1840
$$\Delta(\beta, b_1) \leq \Delta(\beta, b_2) \text{ with } b_1 \geq b_2$$

1841

1836 where $\delta_i^{\text{full-mini}}$ has a overall non-increasing trend when the fan-out size β increases but small non-
 1837 monotonic fluctuations can exist. Note that fan-out size β plays a more dominant role than batch size
 1838 b in influencing generalization.
 1839

1840 **Proof of Theorem 3:** Using Theorem G.5, we have

$$\begin{aligned} 1841 \quad L_{\text{test}}\left(\mathbf{W}^{\text{mini}}, \tilde{\mathbf{A}}_{\text{train}}^{\text{full}}; \mathcal{Q}\right) &\leq \hat{L}_{\text{train}}^{\text{full}}\left(\mathbf{W}^{\text{mini}}, \tilde{\mathbf{A}}_{\text{train}}^{\text{mini}}; \mathcal{Q}\right) \\ 1842 \quad &+ \frac{1}{C_u}(D_{KL}(\mathcal{Q}||\mathcal{P}) + \ln \frac{1}{C_G} + \frac{C_u^2}{4n_{\text{train}}} + U). \end{aligned} \quad (73)$$

1845 Since both \mathcal{P} and \mathcal{Q} are normal distributions (Ma et al., 2021), assuming that $\|\mathbf{w}_{j,T}^{\text{mini}}\|_F^2 \leq C_w$, we
 1846 know that
 1847

$$D_{KL}(\mathcal{Q}||\mathcal{P}) \leq \frac{\|\mathbf{W}_T^{\text{mini}}\|_F^2}{2h\kappa^2} = \frac{\sum_j^h \|\mathbf{w}_{j,T}^{\text{mini}}\|_F^2}{2h\kappa^2} \leq \frac{C_w}{2\kappa^2}, \quad (74)$$

1850 where C_T is a positive constant.
 1851

Hence,

$$\begin{aligned} 1852 \quad L_{\text{test}}\left(\mathbf{W}^{\text{mini}}, \tilde{\mathbf{A}}_{\text{train}}^{\text{full}}; \mathcal{Q}\right) \\ 1853 \quad &\leq \hat{L}_{\text{train}}^{\text{full}}\left(\mathbf{W}^{\text{mini}}, \tilde{\mathbf{A}}_{\text{train}}^{\text{mini}}; \mathcal{Q}\right) + \frac{1}{C_u}(D_{KL}(\mathcal{Q}||\mathcal{P}) + \ln \frac{1}{C_G} + \frac{C_u^2}{4n_{\text{train}}} + U) \\ 1854 \quad &\leq \hat{L}_{\text{train}}^{\text{full}}\left(\mathbf{W}^{\text{mini}}, \tilde{\mathbf{A}}_{\text{train}}^{\text{mini}}; \mathcal{Q}\right) + \frac{1}{C_u}\left(\frac{C_w}{2\kappa^2} + \ln \frac{1}{C_G} + \frac{C_u^2}{4n_{\text{train}}} + C_u\Delta(\beta, b)\right). \end{aligned} \quad (75)$$

H EXTENSION TO MULTI-LAYER GNNs

1861 Our theoretical analysis readily extends to multi-layer GNNs, as long as each layer introduces only
 1862 one non-linearity (e.g., ReLU activation). In such settings, the key difference is that the output of
 1863 each layer is recursively defined based on the previous layer.

1864 This recursive definition preserves the same message-passing structure at each layer. In convergence
 1865 analysis, we bound the gradient norms layer by layer; in generalization analysis, the pre-training
 1866 loss discrepancy propagates across layers. These recursive structures allow our convergence and
 1867 generalization bounds to translate naturally to multi-layer GNNs.

1868 Our key theoretical insights (from the view of batch size and fan-out size) are generalizable to
 1869 multi-layer GNNs. This is because adding more layers simply nests the same operations, without
 1870 changing the qualitative roles of batch size and fan-out size. Hence, the analytical trends observed in
 1871 the one-layer case remain consistent.

1872 Therefore, our theoretical analyses support the multi-layer GNN settings.
 1873

I PROOF OF THE MAIN LEMMAS OF CONVERGENCE THEOREMS WITH MSE

I.1 PROOF OF LEMMA B.5 AND C.1

1878 We first focus on the mini-batch training. Note that $\hat{\sigma}(x) \geq \frac{1}{\pi}$ whenever $x \geq 0$ (Daniely et al., 2016).
 1879 Then, the bound on Γ^{mini} follows as:

$$\begin{aligned} 1880 \quad \Gamma^{\text{mini}} &= \frac{1}{b} \sum_{i,j=1}^b p_{ij} \hat{\sigma}\left(\frac{\varrho_{i,j}^{\text{mini}}}{\sqrt{\vartheta_{i,j}^{\text{mini}}}}\right) \sqrt{\vartheta_{i,j}^{\text{mini}}} \\ 1881 \quad &\geq \frac{1}{\pi b} \sum_{i,j=1}^b p_{ij} \sqrt{\vartheta_{i,j}^{\text{mini}}} = \frac{1}{\pi b} \sum_{i,j=1}^b p_{ij} \sqrt{\left(\tilde{\mathbf{A}}_{\text{train}}^{\text{mini}} \mathbf{1}\right)_i \left(\tilde{\mathbf{A}}_{\text{train}}^{\text{mini}} \mathbf{1}\right)_j} \\ 1882 \quad &= \frac{1}{\pi b} \sum_{i=1}^b \left(\tilde{\mathbf{A}}_{\text{train}}^{\text{mini}} \mathbf{1}\right)_i, \\ 1883 \quad &= \frac{1}{\pi b} \left\| \tilde{\mathbf{A}}_{\text{train}}^{\text{mini}} \mathbf{1} \right\|_1. \end{aligned} \quad (76)$$

To bound Υ_t^{mini} , we notice that $|\hat{\sigma}(x)| \leq \hat{\sigma}(|x|)$, and $\hat{\sigma}(\cdot)$ is a non-decreasing function in $[0, 1]$. Hence, we get $|\Upsilon_t^{\text{mini}}| \leq \Gamma^{\text{mini}}$.

we have the normalized adjacency matrix of a graph with b nodes as:

$$\begin{aligned} \tilde{\mathbf{A}}_{\text{train}}^{\text{mini}} &= \begin{bmatrix} \frac{1}{\sqrt{d_1^{\text{in}}}} & & & \\ & \ddots & & \\ & & \frac{1}{\sqrt{d_b^{\text{in}}}} & \\ & & & \end{bmatrix} \begin{bmatrix} a_{11} & \cdots & a_{1n} \\ \vdots & \ddots & \vdots \\ a_{b1} & \cdots & a_{bn} \end{bmatrix} \begin{bmatrix} \frac{1}{\sqrt{d_1^{\text{out}}}} & & & \\ & \ddots & & \\ & & \frac{1}{\sqrt{d_n^{\text{out}}}} & \\ & & & \end{bmatrix} \\ &= \begin{bmatrix} \frac{1}{\sqrt{d_1^{\text{in}}}} \frac{1}{\sqrt{d_1^{\text{out}}}} a_{11} & \cdots & \frac{1}{\sqrt{d_1^{\text{in}}}} \frac{1}{\sqrt{d_n^{\text{out}}}} a_{1n} \\ \vdots & \ddots & \vdots \\ \frac{1}{\sqrt{d_b^{\text{in}}}} \frac{1}{\sqrt{d_b^{\text{out}}}} a_{b1} & \cdots & \frac{1}{\sqrt{d_b^{\text{in}}}} \frac{1}{\sqrt{d_n^{\text{out}}}} a_{bn} \end{bmatrix}, \end{aligned} \quad (77)$$

where $a_{ij} \in \{0, 1\}$ represents whether node i connects with node j (1) or not (0).

Since $d_i^{\text{in}} \leq \beta$ and $d^{\text{out}} \leq b$, we have:

$$\begin{aligned} \|\tilde{\mathbf{A}}_{\text{train}}^{\text{mini}} \mathbf{1}\|_1 &= \sum_{i=1}^b \frac{1}{\sqrt{d_i^{\text{in}}} \sqrt{d_1^{\text{out}}}} a_{i1} + \cdots + \frac{1}{\sqrt{d_i^{\text{in}}} \sqrt{d_n^{\text{out}}}} a_{in} \\ &\geq \sum_{i=1}^b \frac{1}{\beta^{\frac{1}{2}} b^{\frac{1}{2}}} (a_{i1} + \cdots + a_{in}) \\ &\geq \frac{b^{\frac{1}{2}}}{\beta^{\frac{1}{2}}} \min_i (a_{i1} + \cdots + a_{in}) \\ &\geq \frac{b^{\frac{1}{2}}}{\beta^{\frac{1}{2}}}. \end{aligned} \quad (78)$$

Moreover, since $\varrho_{i,j}^{\text{mini}}$ denotes the amount of common messages between node i and node j at a given training iteration, we know that $\frac{\varrho_{i,j}^{\text{mini}}}{\sqrt{\vartheta_{i,j}^{\text{mini}}}} \leq 1$. Then we have:

$$\begin{aligned} \Gamma^{\text{mini}} &= \frac{1}{b} \sum_{i,j=1}^b p_{ij} \hat{\sigma} \left(\frac{\varrho_{i,j}^{\text{mini}}}{\sqrt{\vartheta_{i,j}^{\text{mini}}}} \right) \sqrt{\vartheta_{i,j}^{\text{full}}} \\ &\leq \frac{1}{b} \left\| \tilde{\mathbf{A}}_{\text{train}}^{\text{mini}} \mathbf{1} \right\|_1 \end{aligned} \quad (79)$$

Moreover, since $1 / \left(\sqrt{d_i^{\text{in}}} \sqrt{d_1^{\text{out}}} \right) \leq 1$, we have:

$$\begin{aligned} \|\tilde{\mathbf{A}}_{\text{train}}^{\text{mini}} \mathbf{1}\|_1 &= \sum_{i=1}^b \frac{1}{\sqrt{d_i^{\text{in}}} \sqrt{d_1^{\text{out}}}} a_{i1} + \cdots + \frac{1}{\sqrt{d_i^{\text{in}}} \sqrt{d_n^{\text{out}}}} a_{in} \\ &\leq \sum_{i=1}^b (a_{i1} + \cdots + a_{in}) \\ &\leq \beta b, \end{aligned} \quad (80)$$

where the last inequality holds because there exist at most β terms that are not equal to 0.

Similarly, for $\Gamma^{\text{full-mini}}$, we have:

$$\begin{aligned} \Gamma^{\text{full-mini}} &\geq \frac{1}{\pi n_{\text{train}}} \sum_{i=1}^{n_{\text{train}}} \left(\tilde{\mathbf{A}}_{\text{train}}^{\text{mini}} \mathbf{1} \right)_i, \\ &= \frac{1}{\pi n_{\text{train}}} \frac{n_{\text{train}}}{b} \sum_{i=1}^b \left(\tilde{\mathbf{A}}_{\text{train}}^{\text{mini}} \mathbf{1} \right)_i, \\ &= \frac{1}{\pi b} \left\| \tilde{\mathbf{A}}_{\text{train}}^{\text{mini}} \mathbf{1} \right\|_1, \end{aligned} \quad (81)$$

1944 and

$$1945 \quad \Gamma^{\text{full-mini}} \leq \frac{1}{b} \left\| \tilde{\mathbf{A}}_{\text{train}}^{\text{mini}} \mathbf{1} \right\|_1. \quad (82)$$

1947

1948 Moreover, $|\Upsilon^{\text{full-mini}}| \leq \Gamma^{\text{full-mini}}$ holds.

1949

1950 Similarly, in the full-graph training, we can replace b and β by n_{train} and d_{max} , respectively. Therefore,
1951 we have:

1952

$$\frac{1}{\pi n_{\text{train}}} \left\| \tilde{\mathbf{A}}_{\text{train}}^{\text{full}} \mathbf{1} \right\|_1 \leq \Gamma^{\text{full}} \leq \frac{1}{n_{\text{train}}} \left\| \tilde{\mathbf{A}}_{\text{train}}^{\text{full}} \mathbf{1} \right\|_1. \quad (83)$$

1953

$$1954 \quad \frac{n_{\text{train}}^{\frac{1}{2}}}{d_{\text{max}}^{\frac{1}{2}}} \leq \left\| \tilde{\mathbf{A}}_{\text{train}}^{\text{full}} \mathbf{1} \right\|_1 \leq n_{\text{train}} d_{\text{max}}. \quad (84)$$

1955

$$1956 \quad |\Upsilon^{\text{full}}| \leq \Gamma^{\text{full}} \quad (85)$$

1957

1958 This complete the proof.

1959

1960 I.2 PROOF OF LEMMA B.6 AND C.2

1961

1962 **Lemma I.1** In the mini-batch training, $|\Xi_t^{\text{mini}}| = o(\Gamma_t^{\text{mini}})$, $|\Xi_t^{\text{full-mini}}| = o(\Gamma_t^{\text{full-mini}})$, and, when
1963 $\phi_t^{\text{mini}} \geq -\frac{1}{100}$ and $\sqrt{(\phi_t^{\text{mini}})^2 + (\psi_t^{\text{mini}})^2} \geq 1 - o(1)$, then $\Xi_t^{\text{mini}} \geq \frac{\Gamma_t^{\text{mini}}}{2\beta}$ and $\Xi_t^{\text{full-mini}} \geq \frac{\Gamma_t^{\text{full-mini}}}{2\beta}$. In the
1964 full-graph training, $|\Xi_t^{\text{full}}| = o(\Gamma_t^{\text{full}})$, and, when $\phi_t^{\text{full}} \geq -\frac{1}{100}$ and $\sqrt{(\phi_t^{\text{full}})^2 + (\psi_t^{\text{full}})^2} \geq 1 - o(1)$,
1965 then $\Xi_t^{\text{full}} \geq \frac{\Gamma_t^{\text{full}}}{2d_{\text{max}}}$.

1966

1967 **Proof of Lemma B.6 and C.2:** We first focus on the mini-batch training. Considering the gradient,
1968 we are going to analyze $(\phi_{t+1}^{\text{mini}})^2 + (\psi_{t+1}^{\text{mini}})^2$:

1969

$$1970 \quad \begin{aligned} & (\phi_{t+1}^{\text{mini}})^2 + (\psi_{t+1}^{\text{mini}})^2 \\ 1971 &= \left(\phi_t^{\text{mini}} - \eta_t \frac{\partial L_{\text{train},t}^{\text{mini}}(\phi_t^{\text{mini}}, \psi_t^{\text{mini}})}{\partial \phi_t^{\text{mini}}} \right)^2 + \left(\psi_t^{\text{mini}} - \eta_t \frac{\partial L_{\text{train},t}^{\text{mini}}(\phi_t^{\text{mini}}, \psi_t^{\text{mini}})}{\partial \psi_t^{\text{mini}}} \right)^2 \\ 1972 &= \left(\phi_t^{\text{mini}} - \eta_t \phi_t^{\text{mini}} \Gamma_t^{\text{mini}} + \eta_t \frac{\phi_t^{\text{mini}}}{\sqrt{(\phi_t^{\text{mini}})^2 + (\psi_t^{\text{mini}})^2}} \Upsilon_t^{\text{mini}} + \eta_t \frac{(\psi_t^{\text{mini}})^2}{(\phi_t^{\text{mini}})^2 + (\psi_t^{\text{mini}})^2} \Xi_t^{\text{mini}} \right)^2 \\ 1973 &+ \left(\psi_t^{\text{mini}} - \eta_t \psi_t^{\text{mini}} \Gamma_t^{\text{mini}} + \eta_t \frac{\psi_t^{\text{mini}}}{\sqrt{(\phi_t^{\text{mini}})^2 + (\psi_t^{\text{mini}})^2}} \Upsilon_t^{\text{mini}} + \eta_t \frac{\phi_t^{\text{mini}} \psi_t^{\text{mini}}}{(\phi_t^{\text{mini}})^2 + (\psi_t^{\text{mini}})^2} \Xi_t^{\text{mini}} \right)^2 \quad (86) \\ 1974 &= (\phi_t^{\text{mini}})^2 + (\psi_t^{\text{mini}})^2 + \eta_t^2 \Gamma_t^{\text{mini}}^2 \left((\phi_t^{\text{mini}})^2 + (\psi_t^{\text{mini}})^2 \right) + \eta_t^2 \Upsilon_t^{\text{mini}}^2 \\ 1975 &+ \eta_t^2 \frac{(\psi_t^{\text{mini}})^2}{(\phi_t^{\text{mini}})^2 + (\psi_t^{\text{mini}})^2} \left(\Xi_t^{\text{mini}} \right)^2 - 2\eta_t \Gamma_t^{\text{mini}} \left((\phi_t^{\text{mini}})^2 + (\psi_t^{\text{mini}})^2 \right) \\ 1976 &+ 2\eta_t \sqrt{(\phi_t^{\text{mini}})^2 + (\psi_t^{\text{mini}})^2} \Upsilon_t^{\text{mini}} - 2\eta_t^2 \Gamma_t^{\text{mini}} \Upsilon_t^{\text{mini}} \sqrt{(\phi_t^{\text{mini}})^2 + (\psi_t^{\text{mini}})^2} \end{aligned}$$

1977

1978 Hence, By Lemma C.1 and Lemma I.1, we have:

1979

1980

1981

1982

1983

1984

1985

1986

1987

1988

1989

1990

1991

1992

1993

1994

1995

1996

1997

$$\left(\phi_{t+1}^{\text{mini}} \right)^2 + \left(\psi_{t+1}^{\text{mini}} \right)^2 \leq \left(\sqrt{(\phi_t^{\text{mini}})^2 + (\psi_t^{\text{mini}})^2} \left(1 - \frac{C}{\pi} \right) \right)^2 + C, \quad (87)$$

when the learning rate $\eta_t \in \left[\frac{C}{\pi \Gamma_t^{\text{mini}}}, \frac{1}{6\pi \Gamma_t^{\text{mini}}} \right]$ (Awasthi et al., 2021), where $C \leq \frac{1}{16}$ is a small enough
and positive constant. Hence, we can rewrite the range of η as $\eta_t \in (0, \frac{1}{6\pi \Gamma_t^{\text{mini}}}]$

Then, for all $t \geq 1$, we have:

$$\begin{aligned}
\sqrt{(\phi_t^{\text{mini}})^2 + (\psi_t^{\text{mini}})^2} &\leq \left(1 - \frac{C}{\pi}\right)^t \sqrt{(\phi_0^{\text{mini}})^2 + (\psi_0^{\text{mini}})^2} + \frac{C}{1 - \left(1 - \frac{C}{\pi}\right)^2} \\
&< \sqrt{(\phi_0^{\text{mini}})^2 + (\psi_0^{\text{mini}})^2} + \frac{\pi}{2 - C} \\
&< \sqrt{(\phi_0^{\text{mini}})^2 + (\psi_0^{\text{mini}})^2} + \frac{\pi}{2}
\end{aligned} \tag{88}$$

Moreover, with probability at least $1 - e^{-O(r)}$, we will have $\sqrt{\left(\phi_0^{\text{mini}}\right)^2 + \left(\psi_0^{\text{mini}}\right)^2} = O(\kappa\sqrt{r})$.

Hence, we have $\sqrt{(\phi_t^{\text{mini}})^2 + (\psi_t^{\text{mini}})^2} \leq C_1$.

We also have that if $\Upsilon_t^{\min} > 0$, then

$$\begin{aligned}
\left(\phi_{t+1}^{\text{mini}}\right)^2 + \left(\psi_{t+1}^{\text{mini}}\right)^2 &\geq \left(\left(\phi_t^{\text{mini}}\right)^2 + \left(\psi_t^{\text{mini}}\right)^2\right)(1 - \eta_t \Gamma_t^{\text{mini}})^2 \\
&\quad + 2\eta_t \Gamma_t^{\text{mini}} \sqrt{\left(\phi_t^{\text{mini}}\right)^2 + \left(\psi_t^{\text{mini}}\right)^2} (1 - \eta_t \Gamma_t^{\text{mini}}) + \eta_t^2 \Gamma_t^{\text{mini}^2} \\
&> \eta_t^2 \Gamma_t^{\text{mini}^2} > 0
\end{aligned} \tag{89}$$

Similarly, in the full-graph training, we can replace b and β by n_{train} and d_{max} , respectively.

This completes the proof.

I.3 PROOF OF LEMMA B.7 AND C.3

We first focus on the mini-batch training. From Lemma C.2, we immediately have $\sqrt{(\phi^{\text{mini}})^2 + (\psi^{\text{mini}})^2} \leq C$, where C is a positive constant.

Next, we analyze the upper bound of $\lambda_{\max}(\nabla^2 L_{\text{train}}^{\text{full}}(\phi^{\text{mini}}, \psi^{\text{mini}}, \tilde{\mathbf{A}}_{\text{train}}^{\text{mini}}))$. We have:

$$\begin{aligned}
& \lambda_{\max}(\nabla^2 L_{\text{train}}^{\text{full}}(\phi_t^{\text{mini}}, \psi_t^{\text{mini}}, \tilde{\mathbf{A}}_{\text{train}}^{\text{mini}})) \\
& \leq \left| \frac{\partial^2 L_{\text{train}}^{\text{full}}(\phi_t^{\text{mini}}, \psi_t^{\text{mini}}, \tilde{\mathbf{A}}_{\text{train}}^{\text{mini}})}{\partial (\phi_t^{\text{mini}})^2} \right| + \left| \frac{\partial^2 L_{\text{train}}^{\text{full}}(\phi_t^{\text{mini}}, \psi_t^{\text{mini}}, \tilde{\mathbf{A}}_{\text{train}}^{\text{mini}})}{\partial (\psi_t^{\text{mini}})^2} \right| \\
& \quad + \left| \frac{\partial^2 L_{\text{train}}^{\text{full}}(\phi_t^{\text{mini}}, \psi_t^{\text{mini}}, \tilde{\mathbf{A}}_{\text{train}}^{\text{mini}})}{\partial \phi_t^{\text{mini}} \partial \psi_t^{\text{mini}}} \right| + \left| \frac{\partial^2 L_{\text{train}}^{\text{full}}(\phi_t^{\text{mini}}, \psi_t^{\text{mini}}, \tilde{\mathbf{A}}_{\text{train}}^{\text{mini}})}{\partial \psi_t^{\text{mini}} \partial \phi_t^{\text{mini}}} \right|. \tag{90}
\end{aligned}$$

Taking the second derivatives, we get:

$$\left| \frac{\partial^2 L_{\text{train}}^{\text{full}}(\phi_t^{\text{mini}}, \psi_t^{\text{mini}}, \tilde{\mathbf{A}}_{\text{train}}^{\text{mini}})}{\partial (\phi_t^{\text{mini}})^2} \right| = \Gamma_t^{\text{full-mini}} - \frac{\phi_t^{\text{mini}}}{\|\mathbf{w}_{j,t}^{\text{mini}}\|} \frac{\partial \Upsilon_t^{\text{full-mini}}}{\partial \phi_t^{\text{mini}}} - \frac{(\psi_t^{\text{mini}})^2}{\|\mathbf{w}_{j,t}^{\text{mini}}\|^{\frac{3}{2}}} \Upsilon_t^{\text{full-mini}} \\ - \frac{(\psi_t^{\text{mini}})^2}{\|\mathbf{w}_{j,t}^{\text{mini}}\|^2} \frac{\partial \Xi_t^{\text{full-mini}}}{\partial \phi_t^{\text{mini}}} + \frac{2\phi_t^{\text{mini}} (\psi_t^{\text{mini}})^2}{\|\mathbf{w}_{j,t}^{\text{mini}}\|^4} \Xi_t^{\text{full-mini}}, \quad (91)$$

$$\begin{aligned}
& \left| \frac{\partial^2 L_{\text{train}}^{\text{full}}(\phi_t^{\text{mini}}, \psi_t^{\text{mini}}, \tilde{\mathbf{A}}_{\text{train}}^{\text{mini}})}{\partial (\psi_t^{\text{mini}})^2} \right| \\
&= \Gamma_t^{\text{full-mini}} - \frac{\psi_t^{\text{mini}}}{\|\mathbf{w}_{j,t}^{\text{mini}}\|} \frac{\partial \Upsilon_t^{\text{full-mini}}}{\partial \psi_t^{\text{mini}}} + \frac{\phi_t^{\text{mini}} \psi_t^{\text{mini}}}{\|\mathbf{w}_{j,t}^{\text{mini}}\|^{\frac{3}{2}}} \Upsilon_t^{\text{full-mini}} \\
&+ \frac{\phi_t^{\text{mini}} \psi_t^{\text{mini}}}{\|\mathbf{w}_{j,t}^{\text{mini}}\|^2} \frac{\partial \Xi_t^{\text{full-mini}}}{\partial \phi_t^{\text{mini}}} + \frac{\phi_t^{\text{mini}} ((\phi_t^{\text{mini}})^2 - (\psi_t^{\text{mini}})^2)}{\|\mathbf{w}_{j,t}^{\text{mini}}\|^4} \Xi_t^{\text{full-mini}}, \tag{92}
\end{aligned}$$

$$\begin{aligned}
 \frac{\partial^2 L_{\text{train}}^{\text{full}}(\phi_t^{\text{mini}}, \psi_t^{\text{mini}}, \tilde{\mathbf{A}}_{\text{train}}^{\text{mini}})}{\partial \phi_t^{\text{mini}} \partial \psi_t^{\text{mini}}} &= -\frac{\psi_t^{\text{mini}}}{\|\mathbf{w}_{j,t}^{\text{mini}}\|} \frac{\partial \Upsilon_t^{\text{full-mini}}}{\partial \phi_t^{\text{mini}}} + \frac{\phi_t^{\text{mini}} \psi_t^{\text{mini}}}{\|\mathbf{w}_{j,t}^{\text{mini}}\|^{\frac{3}{2}}} \Upsilon_t^{\text{full-mini}} \\
 &\quad + \frac{\phi_t^{\text{mini}} \psi_t^{\text{mini}}}{\|\mathbf{w}_{j,t}^{\text{mini}}\|^2} \frac{\partial \Xi_t^{\text{full-mini}}}{\partial \phi_t^{\text{mini}}} + \frac{\phi_t^{\text{mini}} \psi_t^{\text{mini}}}{\|\mathbf{w}_{j,t}^{\text{mini}}\|^2} \frac{\partial \Xi_t^{\text{full-mini}}}{\partial \phi_t^{\text{mini}}} \\
 &\quad + \frac{\psi_t^{\text{mini}} \left((\psi_t^{\text{mini}})^2 - (\phi_t^{\text{mini}})^2 \right)}{\|\mathbf{w}_{j,t}^{\text{mini}}\|^4} \Xi_t^{\text{full-mini}}, \tag{93}
 \end{aligned}$$

$$\begin{aligned}
 \frac{\partial^2 L_{\text{train}}^{\text{full}}(\phi_t^{\text{mini}}, \psi_t^{\text{mini}}, \tilde{\mathbf{A}}_{\text{train}}^{\text{mini}})}{\partial \psi_t^{\text{mini}} \partial \phi_t^{\text{mini}}} &= -\frac{\phi_t^{\text{mini}}}{\|\mathbf{w}_{j,t}^{\text{mini}}\|} \frac{\partial \Upsilon_t^{\text{full-mini}}}{\partial \psi_t^{\text{mini}}} + \frac{\phi_t^{\text{mini}} \psi_t^{\text{mini}}}{\|\mathbf{w}_{j,t}^{\text{mini}}\|^{\frac{3}{2}}} \Upsilon_t^{\text{full-mini}} \\
 &\quad + \frac{\phi_t^{\text{mini}} \psi_t^{\text{mini}}}{\|\mathbf{w}_{j,t}^{\text{mini}}\|^2} \frac{\partial \Xi_t^{\text{full-mini}}}{\partial \phi_t^{\text{mini}}} - 2 \frac{\phi_t^{\text{mini}} (\psi_t^{\text{mini}})^2}{\|\mathbf{w}_{j,t}^{\text{mini}}\|^4} \Xi_t^{\text{full-mini}}. \tag{94}
 \end{aligned}$$

Next we have

$$\begin{aligned}
 \left| \frac{\partial \Upsilon_t^{\text{full-mini}}}{\partial \phi_t^{\text{mini}}} \right| &= \left| \frac{1}{n_{\text{train}}} \sum_{i,k=1}^{n_{\text{train}}} p_{ik} \varrho_{i,k}^{\text{mini}} \hat{\sigma}_{\text{step}} \left(\frac{\varrho_{i,k}^{\text{mini}}}{\sqrt{\vartheta_{i,k}^{\text{mini}}}} \frac{\phi_t^{\text{mini}}}{\sqrt{(\phi_t^{\text{mini}})^2 + (\psi_t^{\text{mini}})^2}} \right) \cdot \frac{(\psi_t^{\text{mini}})^2}{\|\mathbf{w}_{j,t}^{\text{mini}}\|^{\frac{3}{2}}} \right| \\
 &\leq \left((\phi_t^{\text{mini}})^2 + (\psi_t^{\text{mini}})^2 \right)^{\frac{1}{4}} \left| \Xi_t^{\text{full-mini}} \right| = o(\Gamma_t^{\text{full-mini}}) \tag{95}
 \end{aligned}$$

$$\begin{aligned}
 \left| \frac{\partial \Upsilon_t^{\text{full-mini}}}{\partial \psi_t^{\text{mini}}} \right| &= \left| \frac{1}{n_{\text{train}}} \sum_{i,k=1}^{n_{\text{train}}} p_{ik} \varrho_{i,k}^{\text{mini}} \hat{\sigma}_{\text{step}} \left(\frac{\varrho_{i,k}^{\text{mini}}}{\sqrt{\vartheta_{i,k}^{\text{mini}}}} \frac{\phi_t^{\text{mini}}}{\sqrt{(\phi_t^{\text{mini}})^2 + (\psi_t^{\text{mini}})^2}} \right) \cdot \frac{\phi_t^{\text{mini}} \psi_t^{\text{mini}}}{\|\mathbf{w}_{j,t}^{\text{mini}}\|^{\frac{3}{2}}} \right| \\
 &\leq \left((\phi_t^{\text{mini}})^2 + (\psi_t^{\text{mini}})^2 \right)^{\frac{1}{4}} \left| \Xi_t^{\text{full-mini}} \right| = o(\Gamma_t^{\text{full-mini}}), \tag{96}
 \end{aligned}$$

where we use $|\Xi_t^{\text{full-mini}}| = o(\Gamma_t^{\text{full-mini}})$ in the Lemma I.1.

To differentiate $\Xi_t^{\text{full-mini}}$, we employ $\hat{\sigma}(\theta) = 1 - \frac{\arccos(\theta)}{\pi}$ (Daniely et al., 2016) and $\arccos'(\theta) = -\frac{1}{\sqrt{1-\theta^2}}$ to get:

$$\begin{aligned}
 \left| \frac{\partial \Xi_t^{\text{full-mini}}}{\partial \phi_t^{\text{mini}}} \right| &= \left| \frac{1}{n_{\text{train}}} \sum_{i,k=1}^{n_{\text{train}}} p_{ik} \frac{(\varrho_{i,k}^{\text{mini}})^2}{\vartheta_{i,k}^{\text{mini}}} \frac{\|\mathbf{w}_{j,t}^{\text{mini}}\|}{\psi_t^{\text{mini}}} \frac{(\psi_t^{\text{mini}})^2}{\|\mathbf{w}_{j,t}^{\text{mini}}\|^{\frac{3}{2}}} \right| \\
 &\leq \frac{1}{n_{\text{train}}} \sum_{i,k=1}^{n_{\text{train}}} \left((\phi_t^{\text{mini}})^2 + (\psi_t^{\text{mini}})^2 \right)^{\frac{1}{4}} \frac{(\varrho_{i,k}^{\text{mini}})^2}{\vartheta_{i,k}^{\text{mini}}} = o(\Gamma_t^{\text{full-mini}}), \tag{97}
 \end{aligned}$$

$$\begin{aligned}
 \left| \frac{\partial \Xi_t^{\text{full-mini}}}{\partial \psi_t^{\text{mini}}} \right| &= \left| \frac{1}{n_{\text{train}}} \sum_{i,k=1}^{n_{\text{train}}} p_{ik} \frac{(\varrho_{i,k}^{\text{mini}})^2}{\vartheta_{i,k}^{\text{mini}}} \frac{\|\mathbf{w}_{j,t}^{\text{mini}}\|}{\psi_t^{\text{mini}}} \frac{\phi_t^{\text{mini}} \psi_t^{\text{mini}}}{\|\mathbf{w}_{j,t}^{\text{mini}}\|^{\frac{3}{2}}} \right| \\
 &\leq \frac{1}{n_{\text{train}}} \sum_{i,k=1}^{n_{\text{train}}} \left((\phi_t^{\text{mini}})^2 + (\psi_t^{\text{mini}})^2 \right)^{\frac{1}{4}} \frac{(\varrho_{i,k}^{\text{mini}})^2}{\vartheta_{i,k}^{\text{mini}}} = o(\Gamma_t^{\text{full-mini}}). \tag{98}
 \end{aligned}$$

Therefore, we have:

$$\begin{aligned}
 \left| \frac{\partial^2 L_{\text{train}}^{\text{full}}(\phi_t^{\text{mini}}, \psi_t^{\text{mini}}, \tilde{\mathbf{A}}_{\text{train}}^{\text{mini}})}{\partial (\phi_t^{\text{mini}})^2} \right| &\leq \Gamma_t^{\text{full-mini}} + \left((\phi_t^{\text{mini}})^2 + (\psi_t^{\text{mini}})^2 \right)^{\frac{1}{4}} \Gamma_t^{\text{full-mini}} + o(\Gamma_t^{\text{full-mini}}) \\
 &\leq \Gamma_t^{\text{full-mini}} (1 + \sqrt{C} + o(1)) = C_1 \Gamma_t^{\text{full-mini}} \tag{99}
 \end{aligned}$$

$$\begin{aligned}
 \left| \frac{\partial^2 L_{\text{train}}^{\text{full}}(\phi_t^{\text{mini}}, \psi_t^{\text{mini}}, \tilde{\mathbf{A}}_{\text{train}}^{\text{mini}})}{\partial (\psi_t^{\text{mini}})^2} \right| &\leq \Gamma_t^{\text{full-mini}} + \left((\phi_t^{\text{mini}})^2 + (\psi_t^{\text{mini}})^2 \right)^{\frac{1}{4}} \Gamma_t^{\text{full-mini}} + o(\Gamma_t^{\text{full-mini}}) \\
 &\leq \Gamma_t^{\text{full-mini}} (1 + \sqrt{C} + o(1)) = C_1 \Gamma_t^{\text{full-mini}} \tag{100}
 \end{aligned}$$

$$\begin{aligned}
\left| \frac{\partial^2 L_{\text{train}}^{\text{full}}(\phi_t^{\text{mini}}, \psi_t^{\text{mini}}, \tilde{\mathbf{A}}_{\text{train}}^{\text{mini}})}{\partial \phi_t^{\text{mini}} \partial \psi_t^{\text{mini}}} \right| &\leq \left((\phi_t^{\text{mini}})^2 + (\psi_t^{\text{mini}})^2 \right)^{\frac{1}{4}} \Gamma_t^{\text{full-mini}} + o(\Gamma_t^{\text{full-mini}}) \\
&\leq \Gamma_t^{\text{full-mini}} (\sqrt{C} + o(1)) = C_2 \Gamma_t^{\text{full-mini}}
\end{aligned} \tag{101}$$

$$\begin{aligned}
\left| \frac{\partial^2 L_{\text{train}}^{\text{full}}(\phi_t^{\text{mini}}, \psi_t^{\text{mini}}, \tilde{\mathbf{A}}_{\text{train}}^{\text{mini}})}{\partial \psi_t^{\text{mini}} \partial \phi_t^{\text{mini}}} \right| &\leq \left((\phi_t^{\text{mini}})^2 + (\psi_t^{\text{mini}})^2 \right)^{\frac{1}{4}} \Gamma_t^{\text{full-mini}} + o(\Gamma_t^{\text{full-mini}}) \\
&\leq \Gamma_t^{\text{full-mini}} (\sqrt{C} + o(1)) = C_2 \Gamma_t^{\text{full-mini}},
\end{aligned} \tag{102}$$

where C_1 and C_2 are absolute constants.

Hence, we have:

$$\lambda_{\max}(\nabla^2 L_{\text{train}}^{\text{full}}(\phi^{\text{mini}}, \psi^{\text{mini}}, \tilde{\mathbf{A}}_{\text{train}}^{\text{mini}})) \leq C_3 \Gamma_t^{\text{full-mini}}, \tag{103}$$

where $C_3 = 4 \left(1 + \sqrt{\frac{\pi}{2} + O(\kappa \sqrt{r})} + o(1) \right)$ is an absolute constant.

Similarly, in the full-graph training, we have:

$$\lambda_{\max}(\nabla^2 L_{\text{train}}^{\text{full}}(\phi^{\text{full}}, \psi^{\text{full}})) \leq C_4 \Gamma^{\text{full}}, \tag{104}$$

where $C_4 = 4 \left(1 + \sqrt{\frac{\pi}{2} + O(\kappa \sqrt{r})} + o(1) \right)$ is an absolute constant.

I.4 PROOF OF LEMMA B.8 AND C.4

We first focus on the mini-batch training. Due to random initialization, with probability at least $1 - \frac{1}{h^2}$, we have that $\sqrt{(\phi_0^{\text{mini}})^2 + (\psi_0^{\text{mini}})^2} = o(\kappa \sqrt{r})$ and $\phi_0^{\text{mini}} \geq -C \kappa \sqrt{\log h}$ with a constant $C > 0$. Furthermore, we have the following updates:

$$\begin{aligned}
&(\phi_{t+1}^{\text{mini}})^2 + (\psi_{t+1}^{\text{mini}})^2 \\
&= \left(\sqrt{(\phi_t^{\text{mini}})^2 + (\psi_t^{\text{mini}})^2} \left(1 - \eta_t \Gamma_t^{\text{mini}} + \eta_t \Upsilon_t^{\text{mini}} \right) \right)^2 + \eta_t^2 \frac{(\psi_t^{\text{mini}})^2}{(\phi_t^{\text{mini}})^2 + (\psi_t^{\text{mini}})^2} (\Xi_t^{\text{mini}})^2,
\end{aligned} \tag{105}$$

$$\phi_{t+1}^{\text{mini}} = \phi_t^{\text{mini}} \left(1 - \eta_t \Gamma_t^{\text{mini}} \right) + \eta_t \frac{\phi_t^{\text{mini}}}{\sqrt{(\phi_t^{\text{mini}})^2 + (\psi_t^{\text{mini}})^2}} \Upsilon_t^{\text{mini}} + \eta_t \frac{(\psi_t^{\text{mini}})^2}{(\phi_t^{\text{mini}})^2 + (\psi_t^{\text{mini}})^2} \Xi_t^{\text{mini}}. \tag{106}$$

Since $\Upsilon_t^{\text{mini}} > 0$ and is bounded by Γ_t^{mini} and $\Xi_t^{\text{mini}} = o(\Gamma_t^{\text{mini}})$, if $\phi_t^{\text{mini}} < 0$ and $\sqrt{(\phi_t^{\text{mini}})^2 + (\psi_t^{\text{mini}})^2} \geq 2$, we have:

$$\sqrt{(\phi_{t+1}^{\text{mini}})^2 + (\psi_{t+1}^{\text{mini}})^2} \geq \sqrt{(\phi_t^{\text{mini}})^2 + (\psi_t^{\text{mini}})^2} \left(1 - \eta_t \Gamma_t^{\text{mini}} \right), \tag{107}$$

$$\phi_{t+1}^{\text{mini}} \geq \phi_t^{\text{mini}} \left(1 - \frac{\eta_t}{2} \Gamma_t^{\text{mini}} - \eta_t o(\Gamma_t^{\text{mini}}) \right). \tag{108}$$

Hence, after $t \geq C_1 \log(\kappa \log h)$ steps, we have that $\phi_t^{\text{mini}} \geq -\frac{1}{100}$ and $\sqrt{(\phi_t^{\text{mini}})^2 + (\psi_t^{\text{mini}})^2} \geq 2$.

Next we show that from this point on ϕ_t^{mini} and $\sqrt{(\phi_t^{\text{mini}})^2 + (\psi_t^{\text{mini}})^2}$, the conditions in this Lemma continue to be satisfied. We have:

$$\begin{aligned}
&\sqrt{(\phi_{t+1}^{\text{mini}})^2 + (\psi_{t+1}^{\text{mini}})^2} \\
&\geq \sqrt{(\phi_t^{\text{mini}})^2 + (\psi_t^{\text{mini}})^2} - \eta_t \Gamma_t^{\text{mini}} \left(\sqrt{(\phi_t^{\text{mini}})^2 + (\psi_t^{\text{mini}})^2} - 1 \right) + \eta_t \left(\Upsilon_t^{\text{mini}} - \Gamma_t^{\text{mini}} \right),
\end{aligned} \tag{109}$$

where

$$\begin{aligned}
&\Upsilon_t^{\text{mini}} - \Gamma_t^{\text{mini}} \\
&= \frac{1}{b} \sum_{i,j: \varrho_{i,j}^{\text{mini}} \neq 0}^b p_{ij} \sqrt{\vartheta_{i,j}^{\text{mini}}} \left(\hat{\sigma} \left(\frac{\varrho_{i,j}^{\text{mini}}}{\sqrt{\vartheta_{i,j}^{\text{mini}}}} \frac{\phi_t^{\text{mini}}}{\sqrt{(\phi_t^{\text{mini}})^2 + (\psi_t^{\text{mini}})^2}} \right) - \hat{\sigma} \left(\frac{\varrho_{i,j}^{\text{mini}}}{\sqrt{\vartheta_{i,j}^{\text{mini}}}} \right) \right).
\end{aligned} \tag{110}$$

2160 Once $\phi_t^{\text{mini}} \geq -\frac{1}{100}$, we have:

$$2162 \quad \left| \hat{\sigma} \left(\frac{\varrho_{i,j}^{\text{mini}}}{\sqrt{\vartheta_{i,j}^{\text{mini}}}} \frac{\phi_t^{\text{mini}}}{\sqrt{(\phi_t^{\text{mini}})^2 + (\psi_t^{\text{mini}})^2}} \right) - \hat{\sigma} \left(\frac{\varrho_{i,j}^{\text{mini}}}{\sqrt{\vartheta_{i,j}^{\text{mini}}}} \right) \right| \leq 2 \frac{\varrho_{i,j}^{\text{mini}}}{\sqrt{\vartheta_{i,j}^{\text{mini}}}}. \quad (111)$$

2166 Hence, we have that if $\phi_t^{\text{mini}} \geq -\frac{1}{100}$, then $\sqrt{(\phi_t^{\text{mini}})^2 + (\psi_t^{\text{mini}})^2} \geq 1 - o(1)$.

2168 Next we discuss that ϕ_t^{mini} continues to be larger than $-\frac{1}{100}$. First, if $\phi_t^{\text{mini}} > 0$, then
2169 $\sqrt{(\phi_t^{\text{mini}})^2 + (\psi_t^{\text{mini}})^2} \geq 1 - o(1)$ remains. Furthermore, if $\phi_t^{\text{mini}} \in [-\frac{1}{100}, 0)$, then Ξ_t^{mini} is non
2170 negative and is at least $\frac{1}{4b} \sum_{i,j, \varrho_{i,j}^{\text{mini}} \neq 0}^b p_{ij} \frac{\varrho_{i,j}^{\text{mini}}}{\sqrt{\vartheta_{i,j}^{\text{mini}}}}$. Hence, we have:

$$2174 \quad \phi_{t+1}^{\text{mini}} \geq \phi_t^{\text{mini}} - \eta_t \Gamma_t^{\text{mini}} \phi_t^{\text{mini}} \left(1 - \frac{1}{\sqrt{(\phi_t^{\text{mini}})^2 + (\psi_t^{\text{mini}})^2}} \right) \\ 2175 \quad + \eta_t \frac{\phi_t^{\text{mini}}}{\sqrt{(\phi_t^{\text{mini}})^2 + (\psi_t^{\text{mini}})^2}} (\Upsilon_t^{\text{mini}} - \Gamma_t^{\text{mini}}) \\ 2176 \quad + \eta_t \frac{(\psi_t^{\text{mini}})^2}{(\phi_t^{\text{mini}})^2 + (\psi_t^{\text{mini}})^2} \frac{\sum_{i,j, \varrho_{i,j}^{\text{mini}} \neq 0}^b p_{ij} \frac{\varrho_{i,j}^{\text{mini}}}{\sqrt{\vartheta_{i,j}^{\text{mini}}}}}{4b}. \quad (112)$$

2180 Using $\left| \sqrt{(\phi_t^{\text{mini}})^2 + (\psi_t^{\text{mini}})^2} - 1 \right| = O(1)$ and the fact that if $\phi_t^{\text{mini}} \in [-\frac{1}{100}, 0)$ and
2181 $\sqrt{(\phi_t^{\text{mini}})^2 + (\psi_t^{\text{mini}})^2} \geq 1 - o(1)$, then $\left| \frac{\psi_t^{\text{mini}}}{\sqrt{(\phi_t^{\text{mini}})^2 + (\psi_t^{\text{mini}})^2}} \right| \geq \frac{1}{2}$, we have that $\phi_{t+1}^{\text{mini}} \geq \phi_t^{\text{mini}}$.

2183 Similarly, under the full-graph training, we can replace b by n_{train} .

2191 I.5 PROOF OF LEMMA B.9 AND E.5

2193 We first focus on the full-graph training. We have

$$2195 \quad \left\| \nabla L_{\text{train},t}^{\text{full}} (\phi_t^{\text{full}}, \psi_t^{\text{full}}) \right\|^2 \\ 2196 \quad = \left(\phi_t^{\text{full}} \Gamma^{\text{full}} - \frac{\phi_t^{\text{full}}}{\sqrt{(\phi_t^{\text{full}})^2 + (\psi_t^{\text{full}})^2}} \Upsilon_t^{\text{full}} - \frac{(\psi_t^{\text{full}})^2}{(\phi_t^{\text{full}})^2 + (\psi_t^{\text{full}})^2} \Xi_t^{\text{full}} \right)^2 \\ 2197 \quad + \left(\psi_t^{\text{full}} \Gamma^{\text{full}} - \frac{\psi_t^{\text{full}}}{\sqrt{(\phi_t^{\text{full}})^2 + (\psi_t^{\text{full}})^2}} \Upsilon_t^{\text{full}} - \frac{\phi_t^{\text{full}} \psi_t^{\text{full}}}{(\phi_t^{\text{full}})^2 + (\psi_t^{\text{full}})^2} \Xi_t^{\text{full}} \right)^2 \\ 2198 \quad = \left(\sqrt{(\phi_t^{\text{full}})^2 + (\psi_t^{\text{full}})^2} \Gamma^{\text{full}} - \Upsilon_t^{\text{full}} \right)^2 + \frac{(\psi_t^{\text{full}})^2}{(\phi_t^{\text{full}})^2 + (\psi_t^{\text{full}})^2} \left(\Xi_t^{\text{full}} \right)^2. \quad (113)$$

2200 On the other hand, the loss $L_{\text{train},t}^{\text{full}} (\phi_t^{\text{full}}, \psi_t^{\text{full}})$ can be written as :

$$2209 \quad L_{\text{train},t}^{\text{full}} (\phi_t^{\text{full}}, \psi_t^{\text{full}}) \\ 2210 \quad = \frac{1}{2} \left(\left(\phi_t^{\text{full}} \right)^2 + \left(\psi_t^{\text{full}} \right)^2 + 1 \right) \Gamma^{\text{full}} - \sqrt{(\phi_t^{\text{full}})^2 + (\psi_t^{\text{full}})^2} \Upsilon_t^{\text{full}} \\ 2211 \quad \leq \frac{1}{2} \left(\left(\phi_t^{\text{full}} \right)^2 + \left(\psi_t^{\text{full}} \right)^2 + 1 \right) \Gamma^{\text{full}}. \quad (114)$$

2214 Hence, we have:
 2215

$$\begin{aligned} \frac{\|\nabla L_{\text{train},t}^{\text{full}}(\phi_t^{\text{full}}, \psi_t^{\text{full}})\|^2}{L_{\text{train},t}^{\text{full}}(\phi_t^{\text{full}}, \psi_t^{\text{full}})} &\geq \frac{\left(\sqrt{(\phi_t^{\text{full}})^2 + (\psi_t^{\text{full}})^2} \Gamma^{\text{full}} - \Upsilon_t^{\text{full}}\right)^2}{\Gamma^{\text{full}}} \\ &\quad + 2 \frac{(\psi_t^{\text{full}})^2 (\Xi_t^{\text{full}})^2}{\left((\phi_t^{\text{full}})^2 + (\psi_t^{\text{full}})^2\right) \left((\phi_t^{\text{full}})^2 + (\psi_t^{\text{full}})^2 + 1\right) \Gamma^{\text{full}}}. \end{aligned} \quad (115)$$

2219
 2220 If $\sqrt{(\phi_t^{\text{full}})^2 + (\psi_t^{\text{full}})^2} - 1 > \frac{\epsilon^{\frac{1}{2}}}{2h}$, then the first term above combined with $\Upsilon_t^{\text{full}} \leq \Gamma^{\text{full}}$ leads to
 2221

$$\frac{\|\nabla L_{\text{train},t}^{\text{full}}(\phi_t^{\text{full}}, \psi_t^{\text{full}})\|^2}{L_{\text{train},t}^{\text{full}}(\phi_t^{\text{full}}, \psi_t^{\text{full}})} \geq \frac{\epsilon \Gamma^{\text{full}}}{4h^2 \Gamma^{\text{full}}} = \frac{\epsilon \Gamma^{\text{full}}}{4h^2}. \quad (116)$$

2222
 2223 If $\left|\sqrt{(\phi_t^{\text{full}})^2 + (\psi_t^{\text{full}})^2} - 1\right| \leq \frac{\epsilon^{\frac{1}{2}}}{2h} \leq 2$ and $|\psi_t^{\text{full}}| > \frac{\epsilon^{\frac{1}{2}}}{2h}$, then the second term leads to
 2224

$$\begin{aligned} \frac{\|\nabla L_{\text{train},t}^{\text{full}}(\phi_t^{\text{full}}, \psi_t^{\text{full}})\|^2}{L_{\text{train},t}^{\text{full}}(\phi_t^{\text{full}}, \psi_t^{\text{full}})} &\geq 2 \frac{(\psi_t^{\text{full}})^2 (\Xi_t^{\text{full}})^2}{\left((\phi_t^{\text{full}})^2 + (\psi_t^{\text{full}})^2\right) \left((\phi_t^{\text{full}})^2 + (\psi_t^{\text{full}})^2 + 1\right) \Gamma^{\text{full}}} \\ &\geq 2 \frac{(\psi_t^{\text{full}})^2 (\Xi_t^{\text{full}})^2}{9(9+1) \Gamma^{\text{full}}} \\ &\geq 2 \frac{(\Xi_t^{\text{full}})^2}{90 \Gamma^{\text{full}}} \frac{\epsilon}{4h^2} \\ &\geq 2 \frac{\Gamma^{\text{full}}}{360 d_{\text{max}}^2} \frac{\epsilon}{4h^2} \end{aligned} \quad (117)$$

2241 Hence, we have:
 2242

$$\|\nabla L_{\text{train},t}^{\text{full}}(\phi_t^{\text{full}}, \psi_t^{\text{full}})\|^2 \geq \mu^{\text{full}} L_{\text{train},t}^{\text{full}}(\phi_t^{\text{full}}, \psi_t^{\text{full}}), \quad (118)$$

2243 where $\mu^{\text{full}} \geq C_1 \epsilon h^{-2} d_{\text{max}}^{-2} \Gamma^{\text{full}}$, and C_1 is a positive constant.
 2244

2245 Similarly, in the mini-batch training, we can replace d_{max} by β , we have:
 2246

$$\|\nabla L_{\text{train},t}^{\text{full}}(\phi_t^{\text{mini}}, \psi_t^{\text{mini}}, \tilde{\mathbf{A}}_{\text{train}}^{\text{mini}})\|^2 \geq \mu_t^{\text{mini}} L_{\text{train},t}^{\text{full}}(\phi_t^{\text{mini}}, \psi_t^{\text{mini}}, \tilde{\mathbf{A}}_{\text{train}}^{\text{mini}}), \quad (119)$$

2247 where $\mu_t^{\text{mini}} \geq C_2 \epsilon h^{-2} \beta^{-2} \Gamma^{\text{full-mini}}$, and C_2 is a positive constant.
 2248

2249 Finally, we are going to consider the case in the full-graph training when $\sqrt{(\phi_t^{\text{full}})^2 + (\psi_t^{\text{full}})^2} \leq$
 2250 $1 - \frac{\epsilon^{\frac{1}{2}}}{2h}$. We can assume that $\left|\Upsilon_t^{\text{full}} - \sqrt{(\phi_t^{\text{full}})^2 + (\psi_t^{\text{full}})^2} \Gamma^{\text{full}}\right| \leq \frac{\epsilon^{\frac{1}{2}}}{2h} \Gamma^{\text{full}}$ since otherwise we get the
 2251 same bound as in (116). In this case, we show that $\|\psi_t^{\text{full}}\|$ must be at least $\frac{\epsilon^{\frac{1}{2}}}{2h}$ and hence the bound
 2252 of (117) can be applicable. Using $\hat{\sigma}(\cdot)$ is convex in $[0, 1]$, we can get
 2253

$$\begin{aligned} n_{\text{train}} p_{ij} &\left(\sqrt{\vartheta_{i,j}^{\text{full}}} \left(\hat{\sigma} \left(\frac{\varrho_{i,j}^{\text{full}}}{\sqrt{\vartheta_{i,j}^{\text{full}}}} \frac{\phi_t^{\text{full}}}{\sqrt{(\phi_t^{\text{full}})^2 + (\psi_t^{\text{full}})^2}} \right) - \hat{\sigma} \left(\frac{\varrho_{i,j}^{\text{full}}}{\sqrt{\vartheta_{i,j}^{\text{full}}}} \right) \right) \right) \\ &\geq p_{ij} \varrho_{i,j}^{\text{full}} \frac{\phi_t^{\text{full}} - \sqrt{(\phi_t^{\text{full}})^2 + (\psi_t^{\text{full}})^2}}{\sqrt{(\phi_t^{\text{full}})^2 + (\psi_t^{\text{full}})^2}} \hat{\sigma}_{\text{step}} \left(\frac{\varrho_{i,j}^{\text{full}}}{\sqrt{\vartheta_{i,j}^{\text{full}}}} \right). \end{aligned} \quad (120)$$

2264 Summing over i, j , we have
 2265

$$n_{\text{train}} (\Upsilon_t^{\text{full}} - \Gamma^{\text{full}}) \geq \frac{\phi_t^{\text{full}} - \sqrt{(\phi_t^{\text{full}})^2 + (\psi_t^{\text{full}})^2}}{\sqrt{(\phi_t^{\text{full}})^2 + (\psi_t^{\text{full}})^2}} \sum_{i,j} p_{ij} \varrho_{i,j}^{\text{full}} \hat{\sigma}_{\text{step}} \left(\frac{\varrho_{i,j}^{\text{full}}}{\sqrt{\vartheta_{i,j}^{\text{full}}}} \right). \quad (121)$$

Substituting $\Upsilon_t^{\text{full}} = \sqrt{(\phi_t^{\text{full}})^2 + (\psi_t^{\text{full}})^2} \Gamma^{\text{full}} \pm \frac{\epsilon^{\frac{1}{2}} \Gamma^{\text{full}}}{2h}$, we have

$$n_{\text{train}} \left(\left(\sqrt{(\phi_t^{\text{full}})^2 + (\psi_t^{\text{full}})^2} - 1 \right) \Gamma^{\text{full}} \pm \frac{\epsilon^{\frac{1}{2}} \Gamma^{\text{full}}}{2h} \right) \\ \geq \frac{\phi_t^{\text{full}} - \sqrt{(\phi_t^{\text{full}})^2 + (\psi_t^{\text{full}})^2}}{\sqrt{(\phi_t^{\text{full}})^2 + (\psi_t^{\text{full}})^2}} \sum_{i,j} p_{ij} \varrho_{i,j}^{\text{full}} \hat{\sigma}_{\text{step}}\left(\frac{\varrho_{i,j}^{\text{full}}}{\sqrt{\vartheta_{i,j}^{\text{full}}}}\right). \quad (122)$$

Using the bound on $\sqrt{(\phi_t^{\text{full}})^2 + (\psi_t^{\text{full}})^2}$, the above implies that

$$\frac{\epsilon^{\frac{1}{2}} n_{\text{train}} \Gamma^{\text{full}}}{2h} \leq \frac{\sqrt{(\phi_t^{\text{full}})^2 + (\psi_t^{\text{full}})^2} - \phi_t^{\text{full}}}{\sqrt{(\phi_t^{\text{full}})^2 + (\psi_t^{\text{full}})^2}} \sum_{i,j} p_{ij} \varrho_{i,j}^{\text{full}} \hat{\sigma}_{\text{step}}\left(\frac{\varrho_{i,j}^{\text{full}}}{\sqrt{\vartheta_{i,j}^{\text{full}}}}\right) \quad (123)$$

Noticing that $\Gamma^{\text{full}} \geq \frac{1}{\pi n_{\text{train}}} \|\tilde{\mathbf{A}}_{\text{train},t}^{\text{full}} \mathbf{1}\|_1$ by Lemma C.1, we have

$$\frac{\sqrt{(\phi_t^{\text{full}})^2 + (\psi_t^{\text{full}})^2} - \phi_t^{\text{full}}}{\sqrt{(\phi_t^{\text{full}})^2 + (\psi_t^{\text{full}})^2}} \geq \frac{\epsilon^{\frac{1}{2}} \|\tilde{\mathbf{A}}_{\text{train},t}^{\text{full}} \mathbf{1}\|_1}{2\pi h \sum_{i,j} p_{ij} \varrho_{i,j}^{\text{full}} \hat{\sigma}_{\text{step}}\left(\frac{\varrho_{i,j}^{\text{full}}}{\sqrt{\vartheta_{i,j}^{\text{full}}}}\right)} \quad (124)$$

Therefore, we have

$$\begin{aligned}
\psi_t^{\text{full}} &\geq \sqrt{(\phi_t^{\text{full}})^2 + (\psi_t^{\text{full}})^2} - \phi_t^{\text{full}} \\
&\geq \frac{\epsilon^{\frac{1}{2}} \|\tilde{\mathbf{A}}_{\text{train},t}^{\text{full}} \mathbf{1}\|_1}{2\pi h \sum_{i,j} p_{ij} \varrho_{i,j}^{\text{full}} \hat{\sigma}_{\text{step}}\left(\frac{\varrho_{i,j}^{\text{full}}}{\sqrt{v_{i,j}^{\text{full}}}}\right)} \sqrt{(\phi_t^{\text{full}})^2 + (\psi_t^{\text{full}})^2} \\
&\geq \frac{\epsilon^{\frac{1}{2}} \|\tilde{\mathbf{A}}_{\text{train},t}^{\text{full}} \mathbf{1}\|_1}{2\pi h \sum_{i,j} p_{ij} \varrho_{i,j}^{\text{full}} \hat{\sigma}_{\text{step}}\left(\frac{\varrho_{i,j}^{\text{full}}}{\sqrt{v_{i,j}^{\text{full}}}}\right)} \\
&> \frac{\epsilon^{\frac{1}{2}} \|\tilde{\mathbf{A}}_{\text{train},t}^{\text{full}} \mathbf{1}\|_1}{2h n_{\text{train}}} \\
&\geq \frac{\epsilon^{\frac{1}{2}}}{2h n_{\text{train}}^{\frac{1}{2}} d_{\text{max}}^{\frac{1}{2}}} > \frac{\epsilon^{\frac{1}{2}}}{2h}
\end{aligned} \tag{125}$$

where the second last inequality uses $\sum_{i,j} p_{ij} \varrho_{i,j}^{\text{full}} \hat{\sigma}_{\text{step}}\left(\frac{\varrho_{i,j}^{\text{full}}}{\sqrt{\vartheta_{i,j}^{\text{full}}}}\right) \leq n_{\text{train}}$ because there exist n_{train} nodes that have the common messages.

Similarly, in the mini-batch training, we can replace n_{train} and d_{max} by b and β , respectively.

J PROOF OF AUXILIARY LEMMAS OF CONVERGENCE THEOREMS WITH MSE

1.1 PROOF OF LEMMA 1.1:

We first focus on the mini-batch training. We are going to analyze the upper bound of Ξ^{mini} :

$$\Xi^{\text{mini}} = \frac{1}{b} \sum_{i,j=1}^b p_{ij} \varrho_{i,j}^{\text{mini}} \hat{\sigma}_{\text{step}} \left(\frac{\phi^{\text{mini}}}{\sqrt{(\phi^{\text{mini}})^2 + (\psi^{\text{mini}})^2}} \frac{\varrho_{i,j}^{\text{mini}}}{\sqrt{\vartheta_{i,j}^{\text{mini}}}} \right), \quad (126)$$

where each term in summation is non-zero only when $\rho_i^{\min} \neq 0$ if $i \in \mathcal{I}$.

Hence, there are at most b non-zero terms in the summation, and Ξ_t^{\min} is upper bounded by Γ_t^{\min} , namely $\Xi_t^{\min} = o(\Gamma_t^{\min})$.

2322 Note that $\hat{\sigma}_{\text{step}}(x) \geq \frac{1}{2}$ whenever $|x| \leq \frac{1}{50}$ (Daniely et al., 2016), which is ensured by $\phi_t \geq -\frac{1}{100}$ and
 2323 $\sqrt{(\phi_t^{\text{mini}})^2 + (\psi_t^{\text{mini}})^2} \geq 1 - o(1)$. Hence, in this case, each term in the summation in the expression
 2324 of Ξ_t^{mini} will be non-negative. Then, for $i = j$, each of the b terms in the summation will contributed
 2325 at least $\frac{1}{200}$ (Awasthi et al., 2021). Therefore, in this case $\Xi_t^{\text{mini}} \geq \frac{1}{2} \geq \frac{\Gamma_t^{\text{mini}}}{2\beta}$ with $\Gamma_t^{\text{mini}} \leq \beta$.
 2326

2327 Similarly, we have $\Xi_t^{\text{full-mini}} = o(\Gamma_t^{\text{full-mini}})$, and, when $\phi_t^{\text{mini}} \geq -\frac{1}{100}$ and $\sqrt{(\phi_t^{\text{mini}})^2 + (\psi_t^{\text{mini}})^2} \geq$
 2328 $1 - o(1)$, $\Xi_t^{\text{full-mini}} \geq \frac{\Gamma_t^{\text{full-mini}}}{2\beta}$.
 2329

2330 Similarly, under the full-graph training, we place b and β by n_{train} and d_{max} , respectively.
 2331

K PROOF OF THE MAIN LEMMAS OF CONVERGENCE THEOREMS WITH CE

K.1 PROOF OF LEMMA D.3 AND E.3

2337 **Lemma K.1** Let $\tilde{\mathbf{A}}$ be the normalized adjacency matrix with self-loops. Given a mini-batch of size
 2338 b and fan-out size β , the following inequalities hold:
 2339

$$\|\tilde{\mathbf{a}}_{\text{train},i}^{\text{mini}}\|_2^2 \leq \beta,$$

2340 and
 2341

$$\|\tilde{\mathbf{a}}_{\text{train},i}^{\text{full}}\|_2^2 \leq d_{\text{max}},$$

2342 for any i in the training set.
 2343

2344 **Lemma K.2** With Gaussian random initialization, for any $\delta \in (0, 1)$, if $h \geq C \log(n/\delta)$ for some
 2345 large enough constant C , then with probability at least $1 - \delta$, the following inequalities hold:
 2346

$$\left| \|\mathbf{z}_i^{\text{mini}}\|_2 - C_x^{\frac{1}{2}} \beta^{\frac{1}{2}} \right| \leq C_1 \sqrt{\beta \frac{\log(n_{\text{train}}/\delta)}{h}},$$

2347 and
 2348

$$\left| \|\mathbf{z}_i^{\text{full}}\|_2 - C_x^{\frac{1}{2}} d_{\text{max}}^{\frac{1}{2}} \right| \leq C_2 \sqrt{d_{\text{max}} \frac{\log(n_{\text{train}}/\delta)}{h}},$$

2349 for any i in the training set, where C_1 and C_2 are absolute constants.
 2350

2351 **Proof of Lemma D.3 and E.3:** Since half of the elements of \mathbf{v} are 1's and the other half of the
 2352 elements are -1 's, without loss of generality, we can assume that $\mathbf{v}_1 = \dots = \mathbf{v}_{h/2} = 1$ and
 2353 $\mathbf{v}_{h/2+1} = \dots = \mathbf{v}_h = -1$.
 2354

2355 Obviously, we have $\mathbb{E}(\hat{y}_i^{\text{mini}}) = \mathbb{E}(\hat{y}_i^{\text{full}}) = 0$ for any i in the training set.
 2356

2357 We first focus on the mini-batch training. Using the value of \mathbf{v} , we have:
 2358

$$\hat{y}_i^{\text{mini}} = \sum_{i=1}^{h/2} \left[\sigma \left(\tilde{\mathbf{a}}_{\text{train},i}^{\text{mini}} \mathbf{X} \left(\mathbf{w}_j^{\text{mini}} \right)^{\top} \right) - \sigma \left(\tilde{\mathbf{a}}_{\text{train},i}^{\text{mini}} \mathbf{X} \left(\mathbf{w}_{j+h/2}^{\text{mini}} \right)^{\top} \right) \right] \quad (127)$$

2359 With the Lipschitz property of ReLU function, we have:
 2360

$$\begin{aligned} & \left\| \sigma \left(\tilde{\mathbf{a}}_{\text{train},i}^{\text{mini}} \mathbf{X} \left(\mathbf{w}_j^{\text{mini}} \right)^{\top} \right) - \sigma \left(\tilde{\mathbf{a}}_{\text{train},i}^{\text{mini}} \mathbf{X} \left(\mathbf{w}_{j+h/2}^{\text{mini}} \right)^{\top} \right) \right\|_2 \\ & \leq \left\| \tilde{\mathbf{a}}_{\text{train},i}^{\text{mini}} \mathbf{X} \left(\mathbf{w}_j^{\text{mini}} \right)^{\top} - \tilde{\mathbf{a}}_{\text{train},i}^{\text{mini}} \mathbf{X} \left(\mathbf{w}_{j+h/2}^{\text{mini}} \right)^{\top} \right\|_2 \\ & = \left\| \tilde{\mathbf{a}}_{\text{train},i}^{\text{mini}} \mathbf{X} \left(\mathbf{w}_j^{\text{mini}} - \mathbf{w}_{j+h/2}^{\text{mini}} \right)^{\top} \right\|_2 \\ & \leq \left\| \tilde{\mathbf{a}}_{\text{train},i}^{\text{mini}} \right\|_2 \left\| \mathbf{X} \right\|_2 \left\| \mathbf{w}_j^{\text{mini}} - \mathbf{w}_{j+h/2}^{\text{mini}} \right\|_2 \\ & \leq C_3 h^{-\frac{1}{2}} \beta^{\frac{1}{2}}, \end{aligned} \quad (128)$$

2376 for some absolute constant C_3 . Here the last inequality follows Lemma K.1.
 2377

2378 Therefore, by Hoeffding's inequality and Lemma K.2, we have:
 2379

$$\begin{aligned} 2380 \mathbb{P} \left(\left| \hat{y}_i^{\text{mini}} \right| > u \right) &\leq 2 \exp \left(- \frac{u^2}{\sum_{j=0}^{h/2} \left(C_3 h^{-\frac{1}{2}} \beta^{\frac{1}{2}} \right)^2} \right) \\ 2383 \mathbb{P} \left(\left| \hat{y}_i^{\text{mini}} \right| > u \right) &\leq 2 \exp \left(- \frac{2u^2}{C_3^2 \beta} \right) \end{aligned} \quad (129)$$

2385 Taking union bound over i , we have
 2386

$$\mathbb{P} \left(\left| \hat{y}_i^{\text{mini}} \right| > u, i = 1, \dots, n_{\text{train}} \right) \leq 2n_{\text{train}} \exp \left(- \frac{2u^2}{C_3^2 \beta} \right). \quad (130)$$

2390 Let $2n \exp \left(- \frac{2u^2}{C_3^2 \beta} \right) = \delta$, we have:
 2391

$$\begin{aligned} 2393 \exp \left(- \frac{2u^2}{C_3^2 \beta} \right) &= \frac{\delta}{2n_{\text{train}}}, \\ 2394 - \frac{2u^2}{C_3^2 \beta} &= \log \left(\frac{\delta}{2n_{\text{train}}} \right), \\ 2395 u^2 &= \frac{C_3^2 \beta}{2} \log \left(\frac{\delta}{2n_{\text{train}}} \right) > 0, \\ 2396 u &= C_4 \sqrt{\beta \log \left(\frac{\delta}{2n_{\text{train}}} \right)}. \end{aligned} \quad (131)$$

2403 Then $\mathbb{P} \left(\left| \hat{y}_i^{\text{mini}} \right| > C_4 \sqrt{\beta \log \left(\frac{\delta}{2n_{\text{train}}} \right)}, i = 1, \dots, n_{\text{train}} \right) \leq \delta$.
 2404

2405 Therefore, with the probability at least $1 - \delta$, it holds that
 2406

$$\left| \hat{y}_i^{\text{mini}} \right| \leq C_4 \sqrt{\beta \log \left(\frac{\delta}{2n_{\text{train}}} \right)}, \quad (132)$$

2410 for any i in the training set.
 2411

2412 Then substituting the above bound into the formula of loss function $l(y_i \hat{y}_i^{\text{mini}})$, we complete the proof
 2413 of Lemma E.3. Further, substituting the β with d_{max} , we complete the proof of Lemma D.3 for the
 2414 full-graph training.
 2415

K.2 PROOF OF LEMMA D.4 AND E.4

2417 **Lemma K.3** There exist absolute constants $C, C_1, C_2 > 0$ such that, with the probability at
 2418 least $1 - \exp(-Ch\alpha^2 / (n_{\text{train}}d_{\text{max}}))$, for any $\mathbf{m} = (\mathbf{m}_1, \dots, \mathbf{m}_{n_{\text{train}}}) \in \mathbb{R}_+^{n_{\text{train}}}$, there exist at least
 2419 $C_1 h \alpha^2 / (n_{\text{train}}d_{\text{max}})$ GNN nodes in $\{1, \dots, j, \dots, h\}$ that satisfy:
 2420

$$\left\| \frac{1}{n_{\text{train}}} \sum_{i=1}^{n_{\text{train}}} m_i y_i \sigma' \left(\tilde{\mathbf{a}}_{\text{train},i}^{\text{full}} \mathbf{X} (\mathbf{w}_j^{\text{mini}})^\top \right) \tilde{\mathbf{a}}_{\text{train},i}^{\text{full}} \mathbf{X} \right\|_2 \geq C_2 \|\mathbf{m}\|_\infty d_{\text{max}}^2.$$

2424 **Lemma K.4** There exist absolute constants $C_3, C_4, C_5 > 0$ such that, with the probability at
 2425 least $1 - \exp(-C_3 h \alpha^2 / (n_{\text{train}}\beta))$, for any $\mathbf{m} = (\mathbf{m}_1, \dots, \mathbf{m}_{n_{\text{train}}}) \in \mathbb{R}_+^{n_{\text{train}}}$, there exist at least
 2426 $C_4 h \alpha^2 / (n_{\text{train}}\beta)$ GNN nodes in $\{1, \dots, j, \dots, h\}$ that satisfy:
 2427

$$\left\| \frac{1}{n_{\text{train}}} \sum_{i=1}^{n_{\text{train}}} m_i y_i \sigma' \left(\tilde{\mathbf{a}}_{\text{train},i}^{\text{mini}} \mathbf{X} (\mathbf{w}_j^{\text{mini}})^\top \right) \tilde{\mathbf{a}}_{\text{train},i}^{\text{mini}} \mathbf{X} \right\|_2 \geq C_5 \|\mathbf{m}\|_\infty \beta^2.$$

2430 **Proof of Lemma D.4 and E.4:** We first focus on the mini-batch training. We are going to prove the
 2431 gradient upper bound. The gradient $\nabla_{\mathbf{W}^{\text{mini}}} l(y_i \hat{y}_i^{\text{mini}})$ can be written as:
 2432

$$\begin{aligned} \nabla_{\mathbf{W}^{\text{mini}}} l(y_i \hat{y}_i^{\text{mini}}) &= l'(y_i \hat{y}_i^{\text{mini}}) \cdot y_i \cdot \nabla_{\mathbf{W}^{\text{mini}}} \hat{y}_i^{\text{mini}} \\ &= l'(y_i \hat{y}_i^{\text{mini}}) \cdot y_i \cdot (\mathbf{v} \boldsymbol{\Sigma}_i^{\text{mini}})^{\top} \tilde{\mathbf{a}}_{\text{train},i}^{\text{mini}} \mathbf{X}. \end{aligned} \quad (133)$$

2437 Since $\boldsymbol{\Sigma}_i^{\text{mini}}$ is a diagonal matrix with $(\boldsymbol{\Sigma}_i^{\text{mini}})_{jj} \in \{0, 1\}$ for any $j \in \{1, \dots, h\}$, we have $\|\boldsymbol{\Sigma}_i^{\text{mini}}\|_2 =$
 2438 1 for any i in the training set.
 2439

2440 Hence, we have the following upper bound on $\|\nabla_{\mathbf{W}^{\text{mini}}} l(y_i \hat{y}_i^{\text{mini}})\|_F$:

$$\begin{aligned} \|\nabla_{\mathbf{W}^{\text{mini}}} l(y_i \hat{y}_i^{\text{mini}})\|_F &= \|\nabla_{\mathbf{W}^{\text{mini}}} l(y_i \hat{y}_i^{\text{mini}})\|_2 \\ &\leq -l'(y_i \hat{y}_i^{\text{mini}}) \|\boldsymbol{\Sigma}_i^{\text{mini}}\|_2 \|\mathbf{v}\|_2 \|\tilde{\mathbf{a}}_{\text{train},i}^{\text{mini}}\|_2 \|\mathbf{X}\|_2 \\ &\leq -l'(y_i \hat{y}_i^{\text{mini}}) C_x^{\frac{1}{2}} h^{\frac{1}{2}} \beta^{\frac{1}{2}}, \end{aligned} \quad (134)$$

2447 where the first equality holds due to the fact that $\nabla_{\mathbf{W}^{\text{mini}}} l(y_i \hat{y}_i^{\text{mini}})$ is a rank-one matrix, and the last
 2448 inequality follows Lemma K.1 and $\|\mathbf{v}\|_2 = h^{\frac{1}{2}}$.
 2449

2450 Further, we have the following for $\nabla_{\mathbf{W}^{\text{mini}}} \hat{L}_{\text{train}}^{\text{mini}}(\mathbf{W}^{\text{mini}}, \tilde{\mathbf{A}}_{\text{train}}^{\text{mini}})$:

$$\begin{aligned} \|\nabla_{\mathbf{W}^{\text{mini}}} \hat{L}_{\text{train}}^{\text{mini}}(\mathbf{W}^{\text{mini}}, \tilde{\mathbf{A}}_{\text{train}}^{\text{mini}})\|_F &= \left\| \frac{1}{b} \sum_{i=0}^b \nabla_{\mathbf{W}^{\text{mini}}} l(y_i \hat{y}_i^{\text{mini}}) \right\|_F \\ &\leq \frac{1}{b} \sum_{i=0}^b \|\nabla_{\mathbf{W}^{\text{mini}}} l(y_i \hat{y}_i^{\text{mini}})\|_F \\ &\leq -\frac{C_6 h^{\frac{1}{2}} \beta^{\frac{1}{2}}}{b} \sum_{i=0}^b l'(y_i \hat{y}_i^{\text{mini}}), \end{aligned} \quad (135)$$

2460 where C_6 is a positive constant.

2461 Then, replacing b and β by n_{train} and d_{max} respectively, we have:
 2462

$$\|\nabla_{\mathbf{W}^{\text{full}}} \hat{L}_{\text{train}}^{\text{full}}(\mathbf{W}^{\text{full}})\|_F \leq -\frac{C_6 h^{\frac{1}{2}} d_{\text{max}}^{\frac{1}{2}}}{n_{\text{train}}} \sum_{i=1}^{n_{\text{train}}} l'(y_i \hat{y}_i^{\text{full}}), \quad (136)$$

2465 for the full-graph training.
 2466

2467 Next, we still focus on the mini-batch training. We are going to prove the gradient lower bound.
 2468

2469 Given the initialization $\mathbf{W}_0^{\text{mini}}$ and any $\tilde{\mathbf{W}}^{\text{mini}} \in \mathcal{B}(\mathbf{W}_0^{\text{mini}}, \tau)$, where $\mathcal{B}(\mathbf{W}_0^{\text{mini}}, \tau) =$
 2470 $\{\mathbf{W} : \|\mathbf{W} - \mathbf{W}_0^{\text{mini}}\|_2 \leq \tau\}$.
 2471

We define:
 2472

$$\mathbf{g}_j = \frac{1}{n_{\text{train}}} \sum_{i=0}^{n_{\text{train}}} l'(y_i \hat{y}_i^{\text{mini}}) y_i \mathbf{v}_j \sigma'(\tilde{\mathbf{a}}_{\text{train},i}^{\text{mini}} \mathbf{X} (\mathbf{W}_{i,0}^{\text{mini}})^{\top}) \tilde{\mathbf{a}}_{\text{train},i}^{\text{mini}} \mathbf{X}. \quad (137)$$

2474 Then, since \mathbf{W}_0 is generated via Gaussian random initialization, by Lemma K.4, we have the
 2475 following inequality holds for at least $C_4 h \alpha^2 / (n_{\text{train}} \beta)$ GNN nodes:
 2476

$$\|\mathbf{g}_j\|_2 \geq C_5 \max_i |l'(y_i \hat{y}_i^{\text{mini}})| \beta^2, \quad (138)$$

2479 where C_4 and C_5 are positive absolute constants.
 2480

2481 Further, we can rewrite $\nabla_{\mathbf{W}_j^{\text{mini}}} \hat{L}_{\text{train}}^{\text{full}}(\mathbf{w}_j^{\text{mini}}, \tilde{\mathbf{A}}_{\text{train}}^{\text{mini}})$ as follows:
 2482

$$\nabla_{\tilde{\mathbf{w}}_j^{\text{mini}}} \hat{L}_{\text{train}}^{\text{full}}(\tilde{\mathbf{w}}_j^{\text{mini}}, \tilde{\mathbf{A}}_{\text{train}}^{\text{mini}}) = \frac{1}{n_{\text{train}}} \sum_{i=1}^{n_{\text{train}}} l'(y_i \hat{y}_i^{\text{mini}}) y_i \mathbf{v}_j \sigma'(\tilde{\mathbf{a}}_{\text{train},i}^{\text{mini}} \mathbf{X} (\tilde{\mathbf{w}}_j^{\text{mini}})^{\top}) \tilde{\mathbf{a}}_{\text{train},i}^{\text{mini}} \mathbf{X}. \quad (139)$$

Let $\mathbf{z}_{i,j} = l' (y_i \hat{y}_i^{\text{mini}}) y_i \mathbf{v}_j$, we have:

$$\begin{aligned}
& \|\mathbf{g}_j\|_2 - \left\| \nabla_{\tilde{\mathbf{w}}_j^{\text{mini}}} \hat{L}_{\text{train}}^{\text{full}} \left(\tilde{\mathbf{w}}_j^{\text{mini}}, \tilde{\mathbf{A}}_{\text{train}}^{\text{mini}} \right) \right\|_2 \\
&= \left\| \frac{1}{n_{\text{train}}} \sum_{i=1}^{n_{\text{train}}} \mathbf{z}_{i,j} \sigma' \left(\tilde{\mathbf{a}}_{\text{train},i}^{\text{mini}} \mathbf{X} \left(\mathbf{w}_{j,0}^{\text{mini}} \right)^{\top} \right) \tilde{\mathbf{a}}_{\text{train},i}^{\text{mini}} \mathbf{X} \right\|_2 \\
&\quad - \left\| \frac{1}{n_{\text{train}}} \sum_{i=1}^{n_{\text{train}}} \mathbf{z}_{i,j} \sigma' \left(\tilde{\mathbf{a}}_{\text{train},i}^{\text{mini}} \mathbf{X} \left(\tilde{\mathbf{w}}_j^{\text{mini}} \right)^{\top} \right) \tilde{\mathbf{a}}_{\text{train},i}^{\text{mini}} \mathbf{X} \right\|_2 \\
&\leq \left\| \frac{1}{n_{\text{train}}} \sum_{i=1}^{n_{\text{train}}} \mathbf{z}_{i,j} \left(\sigma' \left(\tilde{\mathbf{a}}_{\text{train},i}^{\text{mini}} \mathbf{X} \left(\mathbf{w}_{j,0}^{\text{mini}} \right)^{\top} \right) - \sigma' \left(\tilde{\mathbf{a}}_{\text{train},i}^{\text{mini}} \mathbf{X} \left(\tilde{\mathbf{w}}_j^{\text{mini}} \right)^{\top} \right) \right) \tilde{\mathbf{a}}_{\text{train},i}^{\text{mini}} \mathbf{X} \right\|_2 \\
&\leq \frac{1}{n_{\text{train}}} \sum_{i=1}^{n_{\text{train}}} C_x^{\frac{1}{2}} \beta^{\frac{1}{2}} \max_i \left| l' \left(y_i \hat{y}_i^{\text{mini}} \right) \right| \\
&= C_7 \beta^{\frac{1}{2}} \max_i \left| l' \left(y_i \hat{y}_i^{\text{mini}} \right) \right|,
\end{aligned} \tag{140}$$

where C_7 is an absolute constant.

Therefore, there are at least $C_4 h \alpha^2 / (n_{\text{train}} \beta)$ GNN nodes, satisfying

$$\begin{aligned}
& \left\| \nabla_{\tilde{\mathbf{w}}_j^{\text{mini}}} \hat{L}_{\text{train}}^{\text{full}} \left(\tilde{\mathbf{w}}_j^{\text{mini}}, \tilde{\mathbf{A}}_{\text{train}}^{\text{mini}} \right) \right\|_2 \\
& \geq C_5 \max_i \left| l' \left(y_i \hat{y}_i^{\text{mini}} \right) \right| \beta^2 - C_7 \beta^{\frac{1}{2}} \max_i \left| l' \left(y_i \hat{y}_i^{\text{mini}} \right) \right| \\
& \geq C_8 \max_i \left| l' \left(y_i \hat{y}_i^{\text{mini}} \right) \right| \beta^2.
\end{aligned} \tag{141}$$

Therefore, we have:

$$\begin{aligned}
& \left\| \nabla_{\tilde{\mathbf{W}}^{\text{mini}}} \hat{L}_{\text{train}}^{\text{full}} \left(\tilde{\mathbf{W}}^{\text{mini}}, \tilde{\mathbf{A}}_{\text{train}}^{\text{mini}} \right) \right\|_2 \\
&= \sum_{j=1}^h \left\| \nabla_{\tilde{\mathbf{w}}_j^{\text{mini}}} \hat{L}_{\text{train}}^{\text{full}} \left(\tilde{\mathbf{w}}_j^{\text{mini}}, \tilde{\mathbf{A}}_{\text{train}}^{\text{mini}} \right) \right\|_2 \\
&\geq \frac{C_4 h \alpha^2}{n_{\text{train}} \beta} \left(C_8 \max_i \left| l' \left(y_i \hat{y}_i^{\text{mini}} \right) \right| \beta^2 \right)^2 \\
&\geq \frac{C_9 h \alpha^2 \beta^3}{n_{\text{train}}^3} \left(\sum_{i=1}^{n_{\text{train}}} l' \left(y_i \hat{y}_i^{\text{mini}} \right) \right)^2. \tag{142}
\end{aligned}$$

Then, replacing β by d_{\max} , we have:

$$\left\| \nabla_{\tilde{\mathbf{W}}^{\text{full}}} \hat{L}_{\text{train}}^{\text{full}} \left(\tilde{\mathbf{W}}^{\text{full}} \right) \right\|_2 \geq \frac{C_9 h \alpha^2 d_{\max}^3}{n_{\text{train}}^3} \left(\sum_{i=1}^{n_{\text{train}}} l' \left(y_i, \hat{y}_i^{\text{full}} \right) \right)^2, \quad (143)$$

for the full-graph training.

Proved.

K.3 PROOF OF LEMMA D.5

Lemma K.5 For any $\delta > 0$, with probability at least $1 - e^{-O(1)}$, if $\mathbf{W}_t^{\text{full}} \in \mathcal{B}(\mathbf{W}_0^{\text{full}}, \tau)$, it holds that:

$$\|\mathbf{w}_{i,t}^{\text{full}}\|_2 \leq C + \tau,$$

and

$$\|\mathbf{w}_{i,0}^{\text{full}}\| \leq C,$$

for $j \in \{1, \dots, h\}$, where $C = \kappa(\sqrt{r} + \delta)$ is positive constant.

2538 **Proof of Lemma D.5:** Since $l(x)$ is $1/4$ -smooth, the following holds for any Δ and x :

$$2540 \quad l(x + \Delta) \leq l(x) + l'(x)\Delta + \frac{1}{8}\Delta^2. \quad (144)$$

2543 Then we have the following upper bound on $\hat{L}_{\text{train}}^{\text{full}}(\mathbf{W}_{t+1}^{\text{full}}) - \hat{L}_{\text{train}}^{\text{full}}(\mathbf{W}_t^{\text{full}})$:

$$2545 \quad \hat{L}_{\text{train}}^{\text{full}}(\mathbf{W}_{t+1}^{\text{full}}) - \hat{L}_{\text{train}}^{\text{full}}(\mathbf{W}_t^{\text{full}}) = \frac{1}{n_{\text{train}}} \sum_{i=1}^{n_{\text{train}}} \left[l\left(y_i \hat{y}_{i,t+1}^{\text{full}}\right) - l\left(y_i \hat{y}_{i,t}^{\text{full}}\right) \right] \\ 2546 \\ 2547 \quad = \frac{1}{n_{\text{train}}} \sum_{i=1}^{n_{\text{train}}} \left[l'\left(y_i \hat{y}_{i,t+1}^{\text{full}}\right) \Delta_{i,t+1}^{\text{full}} + \frac{1}{8} \left(\Delta_{i,t+1}^{\text{full}}\right)^2 \right], \quad (145)$$

2550 where $\Delta_{i,t+1}^{\text{full}} = y_i (\hat{y}_{i,t+1}^{\text{full}} - \hat{y}_{i,t}^{\text{full}})$.

2552 Therefore, we are going to bound $\Delta_{i,t}^{\text{full}}$. The upper bound of $|\Delta_{i,t}^{\text{full}}|$ can be derived as:

$$2554 \quad \left| \Delta_{i,t}^{\text{full}} \right| = \left| y_i \tilde{\mathbf{a}}_{\text{train},i}^{\text{full}} \mathbf{X} \left(\Sigma_{i,t+1}^{\text{full}} \mathbf{W}_{t+1}^{\text{full}} \right)^{\top} \mathbf{v}^{\top} - y_i \tilde{\mathbf{a}}_{\text{train},i}^{\text{full}} \mathbf{X} \left(\Sigma_{i,t}^{\text{full}} \mathbf{W}_t^{\text{full}} \right)^{\top} \mathbf{v}^{\top} \right| \\ 2555 \\ 2556 \quad = \left| y_i \tilde{\mathbf{a}}_{\text{train},i}^{\text{full}} \mathbf{X} \left(\Sigma_{i,t+1}^{\text{full}} \mathbf{W}_{t+1}^{\text{full}} - \Sigma_{i,t}^{\text{full}} \mathbf{W}_t^{\text{full}} \right)^{\top} \mathbf{v}^{\top} \right| \\ 2557 \\ 2558 \quad \leq C_x^{\frac{1}{2}} d_{\max}^{\frac{1}{2}} h^{\frac{1}{2}} \left\| \Sigma_{i,t+1}^{\text{full}} \mathbf{W}_{t+1}^{\text{full}} - \Sigma_{i,t}^{\text{full}} \mathbf{W}_t^{\text{full}} \right\|_2, \quad (146)$$

2560 where the last inequality follows Lemma K.1.

2561 Hence, we have:

$$2563 \quad \left| \Delta_{i,t}^{\text{full}} \right| \leq C_x^{\frac{1}{2}} d_{\max}^{\frac{1}{2}} h^{\frac{1}{2}} \left\| \left(\mathbf{W}_{t+1}^{\text{full}} - \mathbf{W}_t^{\text{full}} \right) \Sigma_{i,t+1}^{\text{full}} \right\|_2 + \left\| \mathbf{W}_t^{\text{full}} \left(\Sigma_{i,t+1}^{\text{full}} - \Sigma_{i,t}^{\text{full}} \right) \right\|_2 \\ 2564 \\ 2565 \leq 2C_x^{\frac{1}{2}} d_{\max}^{\frac{1}{2}} h^{\frac{1}{2}} \left(\left\| \mathbf{W}_{t+1}^{\text{full}} - \mathbf{W}_t^{\text{full}} \right\|_2 + \left\| \mathbf{W}_t^{\text{full}} \right\|_2 \right) \\ 2566 \\ 2567 \leq C_1 d_{\max}^{\frac{1}{2}} h^{\frac{1}{2}} \eta \left(\left\| \nabla_{\mathbf{W}_t^{\text{full}}} \hat{L}_{\text{train}}^{\text{full}}(\mathbf{W}_t^{\text{full}}) \right\|_2 + C + \tau \right) \\ 2568 \\ 2569 = C_1 d_{\max}^{\frac{1}{2}} h^{\frac{1}{2}} \eta \left(\left\| \nabla_{\mathbf{W}_t^{\text{full}}} \hat{L}_{\text{train}}^{\text{full}}(\mathbf{W}_t^{\text{full}}) \right\|_F + C + \tau \right). \quad (147)$$

2570 Note that τ has an upper bound, the third term in the brackets on the right-hand side of the above
2571 inequality is dominated by the first one. Then we have:
2572

$$2573 \quad \left| \Delta_{i,t}^{\text{full}} \right| \leq C_1 d_{\max}^{\frac{1}{2}} h^{\frac{1}{2}} \eta \left\| \nabla_{\mathbf{W}_t^{\text{full}}} \hat{L}_{\text{train}}^{\text{full}}(\mathbf{W}_t^{\text{full}}) \right\|_F. \quad (148)$$

2575 Then we are going to prove the lower bound of $\Delta_{i,t}^{\text{full}}$.

2577 Since $\Delta_{i,t}^{\text{full}} = y_i \tilde{\mathbf{a}}_{\text{train},i}^{\text{full}} \mathbf{X} \left(\Sigma_{i,t+1}^{\text{full}} \mathbf{W}_{t+1}^{\text{full}} - \Sigma_{i,t}^{\text{full}} \mathbf{W}_t^{\text{full}} \right)^{\top} \mathbf{v}^{\top} = y_i (\mathbf{z}_{i,t+1}^{\text{full}} - \mathbf{z}_{i,t}^{\text{full}}) \mathbf{v}^{\top}$, thus we mainly
2578 focus on bounding the term $\mathbf{z}_{i,t+1}^{\text{full}} - \mathbf{z}_{i,t}^{\text{full}}$.

2580 We define the diagonal matrix $\tilde{\Sigma}_{i,t}^{\text{full}}$ as:

$$2582 \quad \left(\tilde{\Sigma}_{i,t}^{\text{full}} \right)_{jj} = \left(\Sigma_{i,t+1}^{\text{full}} - \Sigma_{i,t}^{\text{full}} \right)_{jj} \frac{\left(\mathbf{w}_{j,t+1}^{\text{full}} \right)^{\top}}{\left(\mathbf{w}_{j,t+1}^{\text{full}} - \mathbf{w}_{j,t}^{\text{full}} \right)^{\top}}, \quad (149)$$

2586 for any $j \in \{1, \dots, h\}$.

2587 Then we have:

$$2588 \quad \mathbf{z}_{i,t+1}^{\text{full}} - \mathbf{z}_{i,t}^{\text{full}} \\ 2589 \\ 2590 = \tilde{\mathbf{a}}_{\text{train},i}^{\text{full}} \mathbf{X} \left(\mathbf{W}_{t+1}^{\text{full}} - \mathbf{W}_t^{\text{full}} \right)^{\top} \left(\Sigma_{i,t}^{\text{full}} + \tilde{\Sigma}_{i,t}^{\text{full}} \right)^{\top} \\ 2591 \\ = -\eta \tilde{\mathbf{a}}_{\text{train},i}^{\text{full}} \mathbf{X} \nabla_{\mathbf{W}_t^{\text{full}}} \hat{L}_{\text{train}}^{\text{full}}(\mathbf{W}_t^{\text{full}}) \left(\Sigma_{i,t}^{\text{full}} + \tilde{\Sigma}_{i,t}^{\text{full}} \right)^{\top}. \quad (150)$$

2592 Thus, the following holds:
 2593

$$\begin{aligned}
 \Delta_{i,t}^{\text{full}} &= y_i \left(\mathbf{z}_{i,t+1}^{\text{full}} - \mathbf{z}_{i,t}^{\text{full}} \right) \mathbf{v}^{\top} \\
 &= -\eta y_i \tilde{\mathbf{a}}_{\text{train},i}^{\text{full}} \mathbf{X} \nabla_{\mathbf{W}_t^{\text{full}}} \hat{L}_{\text{train}}^{\text{full}} \left(\mathbf{W}_t^{\text{full}} \right) \left(\mathbf{v} \left(\Sigma_{i,t}^{\text{full}} + \tilde{\Sigma}_{i,t}^{\text{full}} \right) \right)^{\top} \\
 &= -\eta y_i \tilde{\mathbf{a}}_{\text{train},i}^{\text{full}} \mathbf{X} \nabla_{\mathbf{W}_t^{\text{full}}} \hat{L}_{\text{train}}^{\text{full}} \left(\mathbf{W}_t^{\text{full}} \right) \left(\mathbf{v} \tilde{\Sigma}_{i,t}^{\text{full}} \right)^{\top} \\
 &\quad - \eta y_i \tilde{\mathbf{a}}_{\text{train},i}^{\text{full}} \mathbf{X} \nabla_{\mathbf{W}_t^{\text{full}}} \hat{L}_{\text{train}}^{\text{full}} \left(\mathbf{W}_t^{\text{full}} \right) \left(\mathbf{v} \Sigma_{i,t}^{\text{full}} \right)^{\top} \\
 &= \mathbf{U}_{i,t}^{(1)} + \mathbf{U}_{i,t}^{(2)},
 \end{aligned} \tag{151}$$

2602 where we define:
 2603

$$\mathbf{U}_{i,t}^{(1)} = -\eta y_i \tilde{\mathbf{a}}_{\text{train},i}^{\text{full}} \mathbf{X} \nabla_{\mathbf{W}_t^{\text{full}}} \hat{L}_{\text{train}}^{\text{full}} \left(\mathbf{W}_t^{\text{full}} \right) \left(\mathbf{v} \tilde{\Sigma}_{i,t}^{\text{full}} \right)^{\top}, \tag{152}$$

2604 and
 2605

$$\mathbf{U}_{i,t}^{(2)} = -\eta y_i \tilde{\mathbf{a}}_{\text{train},i}^{\text{full}} \mathbf{X} \nabla_{\mathbf{W}_t^{\text{full}}} \hat{L}_{\text{train}}^{\text{full}} \left(\mathbf{W}_t^{\text{full}} \right) \left(\mathbf{v} \Sigma_{i,t}^{\text{full}} \right)^{\top}. \tag{153}$$

2606 For $\mathbf{U}_{i,t}^{(1)}$, we notice that:
 2607

$$\begin{aligned}
 \left\| \mathbf{v} \tilde{\Sigma}_{i,t}^{\text{full}} \right\|_2 &\leq \left\| \mathbf{v} \right\|_2 \left\| \tilde{\Sigma}_{i,t}^{\text{full}} \right\|_2 \\
 &\leq h^{\frac{1}{2}} \max_j \left| \left(\Sigma_{i,t+1}^{\text{full}} - \Sigma_{i,t}^{\text{full}} \right)_{jj} \frac{(\mathbf{w}_{j,t+1}^{\text{full}})^{\top}}{(\mathbf{w}_{j,t+1}^{\text{full}} - \mathbf{w}_{j,t}^{\text{full}})^{\top}} \right| \\
 &\leq h^{\frac{1}{2}} \max_j \left| \frac{(\mathbf{w}_{j,t+1}^{\text{full}})^{\top}}{(\mathbf{w}_{j,t+1}^{\text{full}} - \mathbf{w}_{j,t}^{\text{full}})^{\top}} \right|.
 \end{aligned} \tag{154}$$

2608 Using Lemma K.5 and noticing that τ has a upper bound, we have:
 2609

$$\left| \frac{(\mathbf{w}_{j,t+1}^{\text{full}})^{\top}}{(\mathbf{w}_{j,t+1}^{\text{full}} - \mathbf{w}_{j,t}^{\text{full}})^{\top}} \right| \leq \frac{\left\| \mathbf{w}_{j,t+1}^{\text{full}} \right\|_2}{\left\| \mathbf{w}_{j,t+1}^{\text{full}} \right\|_2 - \left\| \mathbf{w}_{j,t}^{\text{full}} \right\|_2} \leq \frac{\left\| \mathbf{w}_{j,0}^{\text{full}} \right\|_2 + \tau}{\varepsilon \tau} \leq C_2 \tau^{-1}, \tag{155}$$

2610 where ε represents a positive small enough constant and C_2 is a positive constant.
 2611

2612 Then we have $\left\| \mathbf{v} \tilde{\Sigma}_{i,t}^{\text{full}} \right\|_2 \leq C_2 h^{\frac{1}{2}} \tau^{-1}$, thereby we know that $\left\| \mathbf{U}_{i,t}^{(1)} \right\| \leq$
 2613 $C_3 \eta d_{\max}^{\frac{1}{2}} h^{\frac{1}{2}} \tau^{-1} \left\| \nabla_{\mathbf{W}_t^{\text{full}}} \hat{L}_{\text{train}}^{\text{full}} \left(\mathbf{W}_t^{\text{full}} \right) \right\|_F$.
 2614

2615 Moreover, we have:
 2616

$$\begin{aligned}
 &\frac{1}{n_{\text{train}}} \sum_{i=1}^{n_{\text{train}}} l' \left(y_i \hat{y}_{i,t}^{\text{full}} \right) \mathbf{U}_{i,t}^{(2)} \\
 &= -\frac{\eta}{n_{\text{train}}} \sum_{i=1}^{n_{\text{train}}} l' \left(y_i \hat{y}_{i,t}^{\text{full}} \right) y_i \tilde{\mathbf{a}}_{\text{train},i}^{\text{full}} \mathbf{X} \nabla_{\mathbf{W}_t^{\text{full}}} \hat{L}_{\text{train}}^{\text{full}} \left(\mathbf{W}_t^{\text{full}} \right) \left(\mathbf{v} \Sigma_{i,t}^{\text{full}} \right)^{\top} \\
 &= -\eta \left\| \nabla_{\mathbf{W}_t^{\text{full}}} \hat{L}_{\text{train}}^{\text{full}} \left(\mathbf{W}_t^{\text{full}} \right) \right\|_F^2.
 \end{aligned} \tag{156}$$

2617 Therefore, putting everything together, we have:
 2618

$$\begin{aligned}
 &\hat{L}_{\text{train}}^{\text{full}} \left(\mathbf{W}_{t+1}^{\text{full}} \right) - \hat{L}_{\text{train}}^{\text{full}} \left(\mathbf{W}_t^{\text{full}} \right) \\
 &= \frac{1}{n_{\text{train}}} \sum_{i=1}^{n_{\text{train}}} \left[l' \left(y_i \hat{y}_{i,t+1}^{\text{full}} \right) \Delta_{i,t+1}^{\text{full}} + \frac{1}{8} \left(\Delta_{i,t+1}^{\text{full}} \right)^2 \right] \\
 &\leq \frac{1}{n_{\text{train}}} l' \left(y_i \hat{y}_{i,t+1}^{\text{full}} \right) \left(\mathbf{U}_{i,t}^{(1)} + \mathbf{U}_{i,t}^{(2)} \right) + C_4 d_{\max} h \eta^2 \left\| \nabla_{\mathbf{W}_t^{\text{full}}} \hat{L}_{\text{train}}^{\text{full}} \left(\mathbf{W}_t^{\text{full}} \right) \right\|_F^2 \\
 &\leq -(\eta - C_4 d_{\max} h \eta^2) \left\| \nabla_{\mathbf{W}_t^{\text{full}}} \hat{L}_{\text{train}}^{\text{full}} \left(\mathbf{W}_t^{\text{full}} \right) \right\|_F^2 \\
 &\quad - \frac{C_3 \eta d_{\max}^{\frac{1}{2}} h^{\frac{1}{2}} \left\| \nabla_{\mathbf{W}_t^{\text{full}}} \hat{L}_{\text{train}}^{\text{full}} \left(\mathbf{W}_t^{\text{full}} \right) \right\|_F}{n_{\text{train}} \tau} \sum_{i=1}^{n_{\text{train}}} l' \left(y_i \hat{y}_{i,t+1}^{\text{full}} \right).
 \end{aligned} \tag{157}$$

2646 Since we both have the condition "with the probability at least $1 - \exp(-O(h\alpha^2/(n_{\text{train}}d_{\text{max}})))$ " and
 2647 "with the probability at least $1 - \exp(-O(1))$ ", we can write the condition as "with the probability
 2648 at least $1 - \exp(-O(1))$ ".
 2649

2650 Proved.
 2651

2652 K.4 PROOF OF LEMMA E.5

2654 **Lemma K.6** For any $\delta > 0$, with probability at least $1 - e^{-O(1)}$, if $\mathbf{W}_t^{\text{mini}} \in \mathcal{B}(\mathbf{W}_0^{\text{mini}}, \tau)$, it holds
 2655 that:

$$2656 \|\mathbf{w}_{j,t}^{\text{mini}}\|_2 \leq C + \tau, \\ 2657$$

2658 and

$$2659 \|\mathbf{w}_{j,0}^{\text{mini}}\|_2 \leq C, \\ 2660$$

2661 for $j \in \{1, \dots, h\}$, where $C = \kappa(\sqrt{r} + \delta)$ is positive constant.
 2662

2663 **Proof of Lemma E.5:** Since $l(x)$ is $1/4$ -smooth, the following holds for any Δ and x :
 2664

$$2665 l(x + \Delta) \leq l(x) + l'(x)\Delta + \frac{1}{8}\Delta^2. \quad (158) \\ 2666$$

2668 Then we have the following upper bound on $\hat{L}_{\text{train}}^{\text{full}}(\mathbf{W}_{t+1}^{\text{mini}}) - \hat{L}_{\text{train}}^{\text{full}}(\mathbf{W}_t^{\text{mini}})$:
 2669

$$2670 \hat{L}_{\text{train}}^{\text{full}}(\mathbf{W}_{t+1}^{\text{mini}}, \tilde{\mathbf{A}}_{\text{train}}^{\text{mini}}) - \hat{L}_{\text{train}}^{\text{full}}(\mathbf{W}_t^{\text{mini}}, \tilde{\mathbf{A}}_{\text{train}}^{\text{mini}}) \\ 2671 = \frac{1}{n_{\text{train}}} \sum_{i=1}^{n_{\text{train}}} \left[l(y_i \hat{y}_{i,t+1}^{\text{mini}}) - l(y_i \hat{y}_{i,t}^{\text{mini}}) \right] \\ 2672 = \frac{1}{n_{\text{train}}} \sum_{i=1}^{n_{\text{train}}} \left[l'(y_i \hat{y}_{i,t+1}^{\text{mini}}) \Delta_{i,t+1}^{\text{mini}} + \frac{1}{8} (\Delta_{i,t+1}^{\text{mini}})^2 \right], \\ 2673 \quad (159) \\ 2674 \\ 2675 \\ 2676$$

2677 where $\Delta_{i,t+1}^{\text{mini}} = y_i (\hat{y}_{i,t+1}^{\text{mini}} - \hat{y}_{i,t}^{\text{mini}})$.
 2678

2679 Then, taking expectation conditioning $\mathbf{W}_t^{\text{mini}}$ gives:
 2680

$$2681 \mathbb{E} \left[\hat{L}_{\text{train}}^{\text{full}}(\mathbf{W}_{t+1}^{\text{mini}}, \tilde{\mathbf{A}}_{\text{train}}^{\text{mini}}) \mid \mathbf{W}_t^{\text{mini}} \right] - \hat{L}_{\text{train}}^{\text{full}}(\mathbf{W}_t^{\text{mini}}, \tilde{\mathbf{A}}_{\text{train}}^{\text{mini}}) \\ 2682 = \frac{1}{n_{\text{train}}} \sum_{i=1}^{n_{\text{train}}} \left[l'(y_i \hat{y}_{i,t+1}^{\text{mini}}) \mathbb{E} [\Delta_{i,t+1}^{\text{mini}} \mid \mathbf{W}_t^{\text{mini}}] + \frac{1}{8} \mathbb{E} [(\Delta_{i,t+1}^{\text{mini}})^2 \mid \mathbf{W}_t^{\text{mini}}] \right]. \\ 2683 \quad (160) \\ 2684$$

2686 Similar to the proof of Lemma D.5, we have:
 2687

$$2688 \frac{1}{n_{\text{train}}} \sum_{i=1}^{n_{\text{train}}} l'(y_i \hat{y}_{i,t+1}^{\text{mini}}) \mathbb{E} [\Delta_{i,t+1}^{\text{mini}} \mid \mathbf{W}_t^{\text{mini}}] \\ 2689 \leq -\eta \left\| \nabla_{\mathbf{W}_t^{\text{mini}}} \hat{L}_{\text{train}}^{\text{full}}(\mathbf{W}_t^{\text{mini}}, \tilde{\mathbf{A}}_{\text{train}}^{\text{mini}}) \right\|_F^2 \\ 2690 \leq -\eta \left\| \nabla_{\mathbf{W}_t^{\text{mini}}} \hat{L}_{\text{train}}^{\text{full}}(\mathbf{W}_t^{\text{mini}}, \tilde{\mathbf{A}}_{\text{train}}^{\text{mini}}) \right\|_F^2 \\ 2691 - \frac{C_1 \eta \beta^{\frac{1}{2}} h^{\frac{1}{2}} \left\| \nabla_{\mathbf{W}_t^{\text{mini}}} \hat{L}_{\text{train}}^{\text{full}}(\mathbf{W}_t^{\text{mini}}, \tilde{\mathbf{A}}_{\text{train}}^{\text{mini}}) \right\|_F}{n_{\text{train}} \tau} \sum_{i=1}^{n_{\text{train}}} l'(y_i \hat{y}_{i,t+1}^{\text{mini}}). \\ 2692 \quad (161) \\ 2693 \\ 2694 \\ 2695$$

2696 In terms of $\mathbb{E} [(\Delta_{i,t+1}^{\text{mini}})^2 \mid \mathbf{W}_t^{\text{mini}}]$, similar to the proof of Lemma D.5, we have:
 2697

$$2698 \mathbb{E} [(\Delta_{i,t+1}^{\text{mini}})^2 \mid \mathbf{W}_t^{\text{mini}}] \leq C_2 \beta h \eta^2 \mathbb{E} \left[\left\| \nabla_{\mathbf{W}_t^{\text{mini}}} \hat{L}_{\text{train}}^{\text{mini}}(\mathbf{W}_t^{\text{mini}}, \tilde{\mathbf{A}}_{\text{train}}^{\text{mini}}) \right\|_F^2 \mid \mathbf{W}_t^{\text{mini}} \right]. \\ 2699 \quad (162)$$

Furthermore, using Lemma E.6, we have:

$$\begin{aligned}
 & \mathbb{E} \left[\left\| \nabla_{\mathbf{W}_t^{\text{mini}}} \hat{L}_{\text{train}}^{\text{mini}} \left(\mathbf{W}_t^{\text{mini}}, \tilde{\mathbf{A}}_{\text{train}}^{\text{mini}} \right) \right\|_F^2 | \mathbf{W}_t^{\text{mini}} \right] \\
 & \leq \mathbb{E} \left[\left\| \nabla_{\mathbf{W}_t^{\text{mini}}} \hat{L}_{\text{train}}^{\text{mini}} \left(\mathbf{W}_t^{\text{mini}}, \tilde{\mathbf{A}}_{\text{train}}^{\text{mini}} \right) - \nabla_{\mathbf{W}_t^{\text{mini}}} \hat{L}_{\text{train}}^{\text{full}} \left(\mathbf{W}_t^{\text{mini}}, \tilde{\mathbf{A}}_{\text{train}}^{\text{mini}} \right) \right\|_F^2 | \mathbf{W}_t^{\text{mini}} \right] \\
 & \quad + \left\| \nabla_{\mathbf{W}_t^{\text{mini}}} \hat{L}_{\text{train}}^{\text{full}} \left(\mathbf{W}_t^{\text{mini}}, \tilde{\mathbf{A}}_{\text{train}}^{\text{mini}} \right) \right\|_F^2 \\
 & \leq \frac{n_{\text{train}}^2}{n_{\text{train}} b} \left\| \nabla_{\mathbf{W}_t^{\text{mini}}} \hat{L}_{\text{train}}^{\text{full}} \left(\mathbf{W}_t^{\text{mini}}, \tilde{\mathbf{A}}_{\text{train}}^{\text{mini}} \right) \right\|_F^2 + \left\| \nabla_{\mathbf{W}_t^{\text{mini}}} \hat{L}_{\text{train}}^{\text{full}} \left(\mathbf{W}_t^{\text{mini}}, \tilde{\mathbf{A}}_{\text{train}}^{\text{mini}} \right) \right\|_F^2 \\
 & \leq \frac{2n_{\text{train}}}{b} \left\| \nabla_{\mathbf{W}_t^{\text{mini}}} \hat{L}_{\text{train}}^{\text{full}} \left(\mathbf{W}_t^{\text{mini}}, \tilde{\mathbf{A}}_{\text{train}}^{\text{mini}} \right) \right\|_F^2.
 \end{aligned} \tag{163}$$

Hence, the following holds:

$$\mathbb{E} \left[\left(\Delta_{i,t+1}^{\text{mini}} \right)^2 | \mathbf{W}_t^{\text{mini}} \right] \leq \frac{C_3 \beta h n_{\text{train}} \eta^2}{b} \left\| \nabla_{\mathbf{W}_t^{\text{mini}}} \hat{L}_{\text{train}}^{\text{full}} \left(\mathbf{W}_t^{\text{mini}}, \tilde{\mathbf{A}}_{\text{train}}^{\text{mini}} \right) \right\|_F^2 \tag{164}$$

Therefore, we have:

$$\begin{aligned}
 & \mathbb{E} \left[\hat{L}_{\text{train}}^{\text{full}} \left(\mathbf{W}_{t+1}^{\text{mini}}, \tilde{\mathbf{A}}_{\text{train}}^{\text{mini}} \right) | \mathbf{W}_t^{\text{mini}} \right] - \hat{L}_{\text{train}}^{\text{full}} \left(\mathbf{W}_t^{\text{mini}}, \tilde{\mathbf{A}}_{\text{train}}^{\text{mini}} \right) \\
 & \leq - \left(\eta - \frac{C_3 n_{\text{train}} \beta h \eta^2}{b} \right) \left\| \nabla_{\mathbf{W}_t^{\text{mini}}} \hat{L}_{\text{train}}^{\text{full}} \left(\mathbf{W}_t^{\text{mini}}, \tilde{\mathbf{A}}_{\text{train}}^{\text{mini}} \right) \right\|_F^2 \\
 & \quad - \frac{C_1 \eta \beta^{\frac{1}{2}} h^{\frac{1}{2}} \left\| \nabla_{\mathbf{W}_t^{\text{mini}}} \hat{L}_{\text{train}}^{\text{full}} \left(\mathbf{W}_t^{\text{mini}}, \tilde{\mathbf{A}}_{\text{train}}^{\text{mini}} \right) \right\|_F}{n_{\text{train}} \tau} \sum_{i=1}^{n_{\text{train}}} l' \left(y_i \hat{y}_{i,t+1}^{\text{mini}} \right)
 \end{aligned} \tag{165}$$

Since we both have the condition "with the probability at least $1 - \exp(-O(h\alpha^2/(n_{\text{train}}\beta)))$ " and "with the probability at least $1 - \exp(-O(1))$ ", we can write the condition as "with the probability at least $1 - \exp(-O(1))$ ".

Proved.

L PROOF OF AUXILIARY LEMMAS OF CONVERGENCE THEOREMS WITH CE

L.1 PROOF OF LEMMA K.1:

We first focus on the mini-batch training. The normalized adjacency matrix can be expressed as:

$$\begin{aligned}
 \tilde{\mathbf{A}}_{\text{train}}^{\text{mini}} &= \begin{bmatrix} \frac{1}{\sqrt{d_1^{\text{in}}}} & & & \\ & \ddots & & \\ & & \frac{1}{\sqrt{d_b^{\text{in}}}} & \\ & & & \ddots & \end{bmatrix} \begin{bmatrix} a_{11} & \cdots & a_{1n} \\ \vdots & \ddots & \vdots \\ a_{b1} & \cdots & a_{bn} \end{bmatrix} \begin{bmatrix} \frac{1}{\sqrt{d_1^{\text{out}}}} & & & \\ & \ddots & & \\ & & \ddots & \\ & & & \frac{1}{\sqrt{d_n^{\text{out}}}} \end{bmatrix} \\
 &= \begin{bmatrix} \frac{1}{\sqrt{d_1^{\text{in}}}} \frac{1}{\sqrt{d_1^{\text{out}}}} a_{11} & \cdots & \frac{1}{\sqrt{d_1^{\text{in}}}} \frac{1}{\sqrt{d_n^{\text{out}}}} a_{1n} \\ \vdots & \ddots & \vdots \\ \frac{1}{\sqrt{d_b^{\text{in}}}} \frac{1}{\sqrt{d_b^{\text{out}}}} a_{b1} & \cdots & \frac{1}{\sqrt{d_b^{\text{in}}}} \frac{1}{\sqrt{d_n^{\text{out}}}} a_{bn} \end{bmatrix},
 \end{aligned} \tag{166}$$

where $a_{ij} \in \{0, 1\}$ for any node i in the mini batch and $j \in \{1, \dots, n\}$.

Then, the following inequality holds on the l_2 -norm of $\tilde{\mathbf{a}}_{\text{train},i}^{\text{mini}}$:

$$\left\| \tilde{\mathbf{a}}_{\text{train},i}^{\text{mini}} \right\|_2^2 \leq \frac{1}{d_i^{\text{in}} d_1^{\text{out}}} + \cdots + \frac{1}{d_i^{\text{in}} d_n^{\text{out}}} \leq \beta, \tag{167}$$

where the first inequality has at most β terms because there exist at most β terms with $a_{ij} = 1$, and the last inequality follows $\frac{1}{d_i^{\text{in}} d_j^{\text{out}}} \leq 1$.

Similarly, under the full-graph training, we have:

$$\left\| \tilde{\mathbf{a}}_{\text{train},i}^{\text{full}} \right\|_2^2 \leq \frac{1}{d_i^{\text{in}} d_1^{\text{out}}} + \cdots + \frac{1}{d_i^{\text{in}} d_n^{\text{out}}} \leq d_{\max}. \tag{168}$$

This completes the proof.

2754 L.2 PROOF OF LEMMA K.2:
27552756 We first focus on the mini-batch training.
27572758 For any fixed $i \in \{1, \dots, n_{\text{train}}\}$ and $j \in \{1, \dots, h\}$, conditioned on $\tilde{\mathbf{a}}_{\text{train},i}^{\text{mini}} \mathbf{X}$, we have:
2759

2760
$$\mathbb{E} \left[\sigma^2 \left(\tilde{\mathbf{a}}_{\text{train},i}^{\text{mini}} \mathbf{X} \left(\mathbf{w}_j^{\text{mini}} \right)^\top \right) \middle| \tilde{\mathbf{a}}_{\text{train},i}^{\text{mini}} \mathbf{X} \right] = \frac{1}{2} \mathbb{E} \left[\left(\tilde{\mathbf{a}}_{\text{train},i}^{\text{mini}} \mathbf{X} \left(\mathbf{w}_j^{\text{mini}} \right)^\top \right)^2 \middle| \tilde{\mathbf{a}}_{\text{train},i}^{\text{mini}} \mathbf{X} \right] \\ 2761 = \left\| \tilde{\mathbf{a}}_{\text{train},i}^{\text{mini}} \mathbf{X} \right\|_2^2 \kappa^2, \\ 2762$$
 (169)

2763 where the last inequality is due to $\tilde{\mathbf{a}}_{\text{train},i}^{\text{mini}} \mathbf{X} \left(\mathbf{w}_j^{\text{mini}} \right)^\top \sim \mathcal{N} \left(0, \left\| \tilde{\mathbf{a}}_{\text{train},i}^{\text{mini}} \mathbf{X} \right\|_2^2 \kappa^2 \mathbf{I} \right)$ conditioned on
2764 $\tilde{\mathbf{a}}_{\text{train},i}^{\text{mini}} \mathbf{X}$.
27652766 Then, since $\mathbf{z}_i^{\text{mini}} = \tilde{\mathbf{a}}_{\text{train},i}^{\text{mini}} \mathbf{X} (\Sigma_i^{\text{mini}} \mathbf{W}^{\text{mini}})^\top$, by Bernstein inequality, for any $\xi \geq 0$, we have:
2767

2768
$$\mathbb{P} \left(\left| \left\| \mathbf{z}_i^{\text{mini}} \right\|_2^2 - \left\| \tilde{\mathbf{a}}_{\text{train},i}^{\text{mini}} \mathbf{X} \right\|_2^2 \right| \geq \left\| \tilde{\mathbf{a}}_{\text{train},i}^{\text{mini}} \mathbf{X} \right\|_2^2 \xi \middle| \tilde{\mathbf{a}}_{\text{train},i}^{\text{mini}} \mathbf{X} \right) \\ 2769 \leq 2 \exp \left(-Ch \min \{ \xi^2, \xi \} \right). \\ 2770$$
 (170)

2771 Taking union bound over i , we have:
2772

2773
$$\mathbb{P} \left(\left| \left\| \mathbf{z}_i^{\text{mini}} \right\|_2^2 - \left\| \tilde{\mathbf{a}}_{\text{train},i}^{\text{mini}} \mathbf{X} \right\|_2^2 \right| \leq \left\| \tilde{\mathbf{a}}_{\text{train},i}^{\text{mini}} \mathbf{X} \right\|_2^2 \xi, i = 1, \dots, n_{\text{train}} \right) \\ 2774 \leq 1 - 2n_{\text{train}} \exp \left(-Ch \min \{ \xi^2, \xi \} \right), \\ 2775$$
 (171)

2776 which further implies that, if $h \geq C_1^2 \log(n_{\text{train}}/\delta)$, then with probability at least $1 - \delta$, we have:
2777

2778
$$\left| \left\| \mathbf{z}_i^{\text{mini}} \right\|_2^2 - \left\| \tilde{\mathbf{a}}_{\text{train},i}^{\text{mini}} \mathbf{X} \right\|_2^2 \right| \leq C_1 \left\| \tilde{\mathbf{a}}_{\text{train},i}^{\text{mini}} \mathbf{X} \right\|_2^2 \sqrt{\frac{\log(n_{\text{train}}/\delta)}{h}}, \\ 2779$$
 (172)

2780 for any $i = 1, \dots, n_{\text{train}}$, where C_1 is an absolute constant.
27812782 This inequality implies that:
2783

2784
$$\left\| \mathbf{z}_i^{\text{mini}} \right\|_2^2 \leq \left[1 + C_1 \sqrt{\frac{\log(n_{\text{train}}/\delta)}{h}} \right]^{\frac{1}{2}} \left\| \tilde{\mathbf{a}}_{\text{train},i}^{\text{mini}} \mathbf{X} \right\|_2^2 \\ 2785 \leq \left[1 + C_1 \sqrt{\frac{\log(n_{\text{train}}/\delta)}{h}} \right]^{\frac{1}{2}} \left\| \tilde{\mathbf{a}}_{\text{train},i}^{\text{mini}} \right\|_2^2 \left\| \mathbf{X} \right\|_2^2 \\ 2786 \leq C_x^{\frac{1}{2}} \beta^{\frac{1}{2}} \left(1 + C_1 \sqrt{\frac{\log(n_{\text{train}}/\delta)}{h}} \right), \\ 2787$$
 (173)

2788 where the last inequality follows by the fact that $(1+x)^{\frac{1}{2}} \leq 1+x$ for $x > 0$, which is applicable
2789 here.
27902791 Similarly, we can also prove that:
2792

2793
$$\left\| \mathbf{z}_i^{\text{mini}} \right\|_2^2 \geq C_x^{\frac{1}{2}} \beta^{\frac{1}{2}} \left(1 - C_2 \sqrt{\frac{\log(n_{\text{train}}/\delta)}{h}} \right), \\ 2794$$
 (174)

2795 for some absolute constant C_2 . Hence, we have:
2796

2797
$$\left| \left\| \mathbf{z}_i^{\text{mini}} \right\|_2^2 - C_x^{\frac{1}{2}} \beta^{\frac{1}{2}} \right| \leq C_3 \sqrt{\beta \frac{\log(n_{\text{train}}/\delta)}{h}}, \\ 2798$$
 (175)

2799 where C_3 is an absolute constant.
28002801 For the full-graph training, we can replace β by d_{max} as:
2802

2803
$$\left| \left\| \mathbf{z}_i^{\text{mini}} \right\|_2^2 - C_x^{\frac{1}{2}} d_{\text{max}}^{\frac{1}{2}} \right| \leq C_4 \sqrt{d_{\text{max}} \frac{\log(n_{\text{train}}/\delta)}{h}}, \\ 2804$$
 (176)

2805 where C_4 is an absolute constant.
28062807 This completes the proof.
2808

2808 L.3 PROOF OF LEMMA K.3 AND K.4
2809

2810 **Lemma L.1** Assume that for $i \neq j$ such that $y_i \neq y_j$, $\|\tilde{\mathbf{a}}_{\text{train},i}^{\text{full}} \mathbf{X} - \tilde{\mathbf{a}}_{\text{train},j}^{\text{full}} \mathbf{X}\|_2 \geq \alpha$
2811 and $\|\tilde{\mathbf{a}}_{\text{train},i}^{\text{mini}} \mathbf{X} - \tilde{\mathbf{a}}_{\text{train},j}^{\text{mini}} \mathbf{X}\|_2 \geq \alpha$. For any $\mathbf{m} = (\mathbf{m}_1, \dots, \mathbf{m}_{n_{\text{train}}}) \in \mathbb{R}_+^{n_{\text{train}}}$,
2812 we define $h(\mathbf{w}_j^{\text{full}}) = \sum_{i=1}^{n_{\text{train}}} \mathbf{m}_i y_i \sigma'(\tilde{\mathbf{a}}_{\text{train},i}^{\text{full}} \mathbf{X} (\mathbf{w}_j^{\text{full}})^\top) \tilde{\mathbf{a}}_{\text{train},i}^{\text{full}} \mathbf{X}$ and $h(\mathbf{w}_j^{\text{mini}}) =$
2813 $\sum_{i=1}^{n_{\text{train}}} \mathbf{m}_i y_i \sigma'(\tilde{\mathbf{a}}_{\text{train},i}^{\text{mini}} \mathbf{X} (\mathbf{w}_j^{\text{mini}})^\top) \tilde{\mathbf{a}}_{\text{train},i}^{\text{mini}} \mathbf{X}$, where \mathbf{w}_j is a Gaussian random vector for any
2814 $j = 1, \dots, h$. There exist absolute constant $C, C_1, C_2, C_3 > 0$ such that:
2815

$$2817 \mathbb{P} \left[\|h(\mathbf{w}_j^{\text{full}})\|_2 \geq C \|\mathbf{m}\|_\infty \right] \geq C_1 \frac{\alpha^2}{n_{\text{train}} d_{\max}}.$$

2819 and

$$2820 \mathbb{P} \left[\|h(\mathbf{w}_j^{\text{mini}})\|_2 \geq C_2 \|\mathbf{m}\|_\infty \right] \geq C_3 \frac{\alpha^2}{n_{\text{train}} \beta}.$$

2823 **Proof of Lemma K.3 and K.4:** We first focus on the mini-batch training. Under the assumption,
2824 we know that for $i \neq j$ and $y_i \neq y_j$, $\|\tilde{\mathbf{a}}_{\text{train},i}^{\text{mini}} \mathbf{X} - \tilde{\mathbf{a}}_{\text{train},j}^{\text{mini}} \mathbf{X}\|_2 \geq \alpha$. For any given $j = \{1, \dots, h\}$ and
2825 $\hat{\mathbf{m}}$ with $\|\hat{\mathbf{m}}\|_\infty = 1$, by Lemma L.1, we have:

$$2827 \mathbb{P} \left[\left\| \frac{1}{n_{\text{train}}} \sum_{i=1}^{n_{\text{train}}} \hat{\mathbf{m}}_i y_i \sigma'(\tilde{\mathbf{a}}_{\text{train},i}^{\text{mini}} \mathbf{X} (\mathbf{w}_j^{\text{mini}})^\top) \tilde{\mathbf{a}}_{\text{train},i}^{\text{mini}} \mathbf{X} \right\|_2 \geq \frac{C_2}{n_{\text{train}}} \right] \geq \frac{C_3 \alpha^2}{n_{\text{train}} \beta}. \quad (177)$$

2830 Let $\mathcal{S}_{\infty,+}^{n_{\text{train}}-1} = \{\mathbf{m} \in \mathbb{R}_+^{n_{\text{train}} : \|\mathbf{m}\|_\infty = 1}\}$, and $\mathcal{U} = \mathcal{U}[\mathcal{S}_{\infty,+}^{n_{\text{train}}-1}, C_2/(4n_{\text{train}})]$ be a $C_2/(4n_{\text{train}})$ -
2831 net covering $\mathcal{S}_{\infty,+}^{n_{\text{train}}-1}$ in l_∞ -norm. Then we have:

$$2832 |\mathcal{U}| \leq (4n_{\text{train}}/C_2)^{n_{\text{train}}}. \quad (178)$$

2834 For $j = 1, \dots, h$, we define:

$$2836 \mathbf{Z}_{ij} = \mathbf{1} \left[\left\| \frac{1}{n_{\text{train}}} \sum_{i=1}^{n_{\text{train}}} \hat{\mathbf{m}}_i y_i \sigma'(\tilde{\mathbf{a}}_{\text{train},i}^{\text{mini}} \mathbf{X} (\mathbf{w}_j^{\text{mini}})^\top) \tilde{\mathbf{a}}_{\text{train},i}^{\text{mini}} \mathbf{X} \right\|_2 \geq \frac{C_2}{n_{\text{train}}} \right]. \quad (179)$$

2839 Let $p_\alpha = \frac{C_3 \alpha^2}{n_{\text{train}} \beta}$, by Bernstein inequality and union bound, with probability at least $1 - \exp(-C_4 h p_\alpha + n_{\text{train}} \log(4n_{\text{train}}/C_2)) \geq 1 - \exp(-C_5 h \alpha^2 / (n_{\text{train}} \beta))$, we have:

$$2842 \frac{1}{h} \sum_{j=1}^h \mathbf{Z}_{ij} \geq \frac{p_\alpha}{2}, \quad (180)$$

2845 where C_4 and C_5 are absolute constants.

2846 For any $\mathbf{m} \in \mathcal{S}_{\infty,+}^{n_{\text{train}}-1}$, there exists $\hat{\mathbf{m}} \in \mathcal{U}$ such that:

$$2848 \|\mathbf{m} - \hat{\mathbf{m}}\|_\infty \leq C_2/(4n_{\text{train}}). \quad (181)$$

2849 Therefore, we have:

$$2851 \left| \left\| \frac{1}{n_{\text{train}}} \sum_{i=1}^{n_{\text{train}}} \mathbf{m}_i y_i \sigma'(\tilde{\mathbf{a}}_{\text{train},i}^{\text{mini}} \mathbf{X} (\mathbf{w}_j^{\text{mini}})^\top) \tilde{\mathbf{a}}_{\text{train},i}^{\text{mini}} \mathbf{X} \right\|_2 \right. \\ 2852 \left. - \left\| \frac{1}{n_{\text{train}}} \sum_{i=1}^{n_{\text{train}}} \hat{\mathbf{m}}_i y_i \sigma'(\tilde{\mathbf{a}}_{\text{train},i}^{\text{mini}} \mathbf{X} (\mathbf{w}_j^{\text{mini}})^\top) \tilde{\mathbf{a}}_{\text{train},i}^{\text{mini}} \mathbf{X} \right\|_2 \right| \leq C_6 \beta^2. \quad (182)$$

2856 where C_6 is an absolute constant.

2858 It is clear that with probability $1 - \exp(-C_5 h \alpha^2 / (n_{\text{train}} \beta))$, for any $\mathbf{m} \in \mathcal{S}_{\infty,+}^{n_{\text{train}}-1}$, there exist at
2859 least $C_3 h \alpha^2 / (n_{\text{train}} \beta)$ GNN nodes that satisfy:

$$2861 \left\| \frac{1}{n_{\text{train}}} \sum_{i=1}^{n_{\text{train}}} \hat{\mathbf{m}}_i y_i \sigma'(\tilde{\mathbf{a}}_{\text{train},i}^{\text{mini}} \mathbf{X} (\mathbf{w}_j^{\text{mini}})^\top) \tilde{\mathbf{a}}_{\text{train},i}^{\text{mini}} \mathbf{X} \right\|_2 \geq C_6 \beta^2 = C_6 \beta^2 \|\mathbf{m}\|_\infty. \quad (183)$$

2862 Similarly, for the full-graph training, we replace β by d_{\max} . It is clear that with probability $1 - \exp(-C_7 h \alpha^2 / (n_{\text{train}} d_{\max}))$, for any $\mathbf{m} \in \mathcal{S}_{\infty,+}^{n_{\text{train}}-1}$, there exist at least $C_8 h \alpha^2 / (n_{\text{train}} d_{\max})$ GNN
2863 nodes that satisfy:
2864

$$2866 \left\| \frac{1}{n_{\text{train}}} \sum_{i=1}^{n_{\text{train}}} \hat{\mathbf{m}}_i y_i \sigma' \left(\tilde{\mathbf{a}}_{\text{train},i}^{\text{full}} \mathbf{X} \left(\mathbf{w}_j^{\text{full}} \right)^{\top} \right) \tilde{\mathbf{a}}_{\text{train},i}^{\text{full}} \mathbf{X} \right\|_2 \geq C_9 d_{\max}^2 = C_9 d_{\max}^2 \|\mathbf{m}\|_{\infty}. \quad (184)$$

2868 where C_7, C_8 and C_9 are absolute constants.
2869

2870 This completes the proof.
2871

2872 L.4 PROOF OF LEMMA K.5 AND K.6:

2873 We first focus on the mini-batch training. Under the assumption, we know that each row of $\mathbf{W}_0^{\text{mini}}$
2874 follows $\mathcal{N}(0, \kappa^2 \mathbf{I})$. We define:
2875

$$2876 \mathbf{W}_0^{\text{mini}} = \kappa \mathbf{Z}, \quad (185)$$

2877 where $\mathbf{Z} \in \mathbb{R}^{h \times r}$ with $\mathbf{Z}_j \in \mathbb{R}^{1 \times r} \sim \mathcal{N}(0, \mathbf{I})$.
2878

2879 Using Vershynin's result, we have:
2880

$$2881 \mathbb{P} \left(\|\mathbf{Z}\|_2 \leq \sqrt{r} + \sqrt{h} + \delta \right) \geq 1 - e^{-\frac{\delta^2}{2}}, \quad (186)$$

2882 and
2883

$$2884 \mathbb{P} \left(\|\mathbf{Z}_j\|_2 \leq \sqrt{r} + \delta \right) \geq 1 - e^{-\frac{\delta^2}{2}}. \quad (187)$$

2885 Therefore, with probability at least $1 - e^{-\frac{\delta^2}{2}}$, we have:
2886

$$2887 \left\| \mathbf{w}_{j,0}^{\text{mini}} \right\|_2 \leq \kappa (\sqrt{r} + \delta) \quad (188)$$

2888 Since $\mathbf{W}_t^{\text{mini}} \in \mathcal{B}(\mathbf{W}_0^{\text{mini}}, \tau)$, we have:
2889

$$2890 \left\| \mathbf{w}_{j,t}^{\text{mini}} \right\|_2 \leq \kappa (\sqrt{r} + \delta) + \tau \quad (189)$$

2891 Similarly, under the full-graph training, we have:
2892

$$2893 \left\| \mathbf{w}_{j,0}^{\text{full}} \right\|_2 \leq \kappa (\sqrt{r} + \delta) \quad (190)$$

2894 and
2895

$$2896 \left\| \mathbf{w}_{j,t}^{\text{full}} \right\|_2 \leq \kappa (\sqrt{r} + \delta) + \tau \quad (191)$$

2900 L.5 PROOF OF LEMMA L.1:

2901 We first focus on the mini-batch training. Without loss of generality, we assume that $\mathbf{m}_1 = \|\mathbf{m}\|_{\infty}$.
2902 Let $\tilde{\mathbf{z}}_1 = \tilde{\mathbf{a}}_{\text{train},1}^{\text{mini}} \mathbf{X} / \left\| \tilde{\mathbf{a}}_{\text{train},1}^{\text{mini}} \mathbf{X} \right\|_2$, we can construct an orthonormal matrix $\mathbf{Q} = [\tilde{\mathbf{z}}_1, \mathbf{Q}'] \in \mathbb{R}^{r \times r}$.
2903

2904 Let $\mathbf{u} = \mathbf{Q}^{\top} \mathbf{w}_j^{\text{mini}} \sim \mathcal{N}(0, \kappa^2 \mathbf{I})$ be a Gaussian random vector with $0 < \kappa \leq 1$. Then we have:
2905

$$2906 \mathbf{w}_j^{\text{mini}} = \left\| \tilde{\mathbf{a}}_{\text{train},1}^{\text{mini}} \mathbf{X} \right\|_2 \mathbf{Q} \mathbf{u} = \mathbf{u}_1 \tilde{\mathbf{a}}_{\text{train},1}^{\text{mini}} \mathbf{X} + \left\| \tilde{\mathbf{a}}_{\text{train},1}^{\text{mini}} \mathbf{X} \right\|_2 \mathbf{Q}' \mathbf{u}', \quad (192)$$

2907 where $\mathbf{u}' = (\mathbf{u}_2, \dots, \mathbf{u}_r)^{\top}$.
2908

2909 We define the following two events based on a parameter $\gamma \in (0, 1]$:
2910

$$2911 \mathcal{E}_1(\gamma) = \{ C_x \beta | \mathbf{u}_1 | \leq \gamma \}, \quad (193)$$

2912 and
2913

$$2914 \mathcal{E}_2(\gamma) = \{ \left| \left\langle \tilde{\mathbf{a}}_{\text{train},1}^{\text{mini}} \mathbf{X} \right\|_2 \mathbf{Q}' \mathbf{u}', \tilde{\mathbf{a}}_{\text{train},i}^{\text{mini}} \mathbf{X} \right\rangle \leq \gamma \quad (194)$$

$$2915 \text{ for all } \tilde{\mathbf{a}}_{\text{train},i}^{\text{mini}} \mathbf{X} \text{ such that } \left\| \tilde{\mathbf{a}}_{\text{train},i}^{\text{mini}} \mathbf{X} - \tilde{\mathbf{a}}_{\text{train},1}^{\text{mini}} \mathbf{X} \right\|_2 \geq \alpha \}.$$

Let $\mathcal{E}(\gamma) = \mathcal{E}_1(\gamma) \cap \mathcal{E}_2(\gamma)$. We first give lower bound for $\mathbb{P}(\mathcal{E}) = \mathbb{P}(\mathcal{E}_1) \mathbb{P}(\mathcal{E}_2)$.

Since $\mathbf{u}_1 \sim \mathcal{N}(0, \kappa^2)$, we have:

$$\begin{aligned} \mathbb{P}(\mathcal{E}_1) &\geq \mathbb{P}(\{C_x \beta |\mathbf{u}_1| \leq \kappa^2 \gamma\}) \\ &= \frac{1}{\sqrt{2\pi}} \int_{-\frac{\gamma \kappa^2}{C_x \beta}}^{\frac{\gamma \kappa^2}{C_x \beta}} \exp\left(-\frac{1}{2}x^2\right) dx \\ &\geq \sqrt{\frac{2}{\pi e}} \frac{\gamma \kappa^2}{C_x \beta}. \end{aligned} \quad (195)$$

Moreover, by definition, for any $i = 1, \dots, n_{\text{train}}$, we have:

$$\begin{aligned} &< \left\| \tilde{\mathbf{a}}_{\text{train},1}^{\text{mini}} \mathbf{X} \right\|_2 \mathbf{Q}' \mathbf{u}', \tilde{\mathbf{a}}_{\text{train},i}^{\text{mini}} \mathbf{X} > \\ &\sim \mathcal{N}\left[0, \left\| \tilde{\mathbf{a}}_{\text{train},1}^{\text{mini}} \mathbf{X} \right\|_2^2 \left\| \tilde{\mathbf{a}}_{\text{train},i}^{\text{mini}} \mathbf{X} \right\|_2^2 - \left(\left(\tilde{\mathbf{a}}_{\text{train},1}^{\text{mini}} \mathbf{X} \right)^\top \tilde{\mathbf{a}}_{\text{train},i}^{\text{mini}} \mathbf{X} \right)^2 \right]. \end{aligned} \quad (196)$$

Let $\mathcal{I} = \{i : \left\| \tilde{\mathbf{a}}_{\text{train},i}^{\text{mini}} \mathbf{X} - \tilde{\mathbf{a}}_{\text{train},1}^{\text{mini}} \mathbf{X} \right\|_2 \geq \alpha\}$. For any $i \in \mathcal{I}$, we have:

$$\begin{aligned} &\left\| \tilde{\mathbf{a}}_{\text{train},i}^{\text{mini}} \mathbf{X} - \tilde{\mathbf{a}}_{\text{train},1}^{\text{mini}} \mathbf{X} \right\|_2 \\ &= \left\| \tilde{\mathbf{a}}_{\text{train},i}^{\text{mini}} \mathbf{X} \right\|_2 + \left\| \tilde{\mathbf{a}}_{\text{train},1}^{\text{mini}} \mathbf{X} \right\|_2 - 2 < \tilde{\mathbf{a}}_{\text{train},i}^{\text{mini}} \mathbf{X}, \tilde{\mathbf{a}}_{\text{train},1}^{\text{mini}} \mathbf{X} >. \end{aligned} \quad (197)$$

Then we have:

$$-C_x \beta + \frac{\alpha^2}{2} \leq < \tilde{\mathbf{a}}_{\text{train},i}^{\text{mini}} \mathbf{X}, \tilde{\mathbf{a}}_{\text{train},1}^{\text{mini}} \mathbf{X} > \leq C_x \beta - \frac{\alpha^2}{2}, \quad (198)$$

and if $\alpha^2 \leq 2C_x \beta$, then:

$$\begin{aligned} &C_x^2 \beta^2 - \left(\left(\tilde{\mathbf{a}}_{\text{train},1}^{\text{mini}} \mathbf{X} \right)^\top \tilde{\mathbf{a}}_{\text{train},i}^{\text{mini}} \mathbf{X} \right)^2 \\ &\geq C_x^2 \beta^2 - \left(C_x^2 \beta^2 - \frac{\alpha^2}{2} \right)^2 \\ &\geq C_x^2 \beta^2 \geq \frac{\alpha^2}{4} \end{aligned} \quad (199)$$

Therefore, for any $i \in \mathcal{I}$, we have:

$$\begin{aligned} &\mathbb{P}\left[\left| < \left\| \tilde{\mathbf{a}}_{\text{train},1}^{\text{mini}} \mathbf{X} \right\|_2 \mathbf{Q}' \mathbf{u}', \tilde{\mathbf{a}}_{\text{train},i}^{\text{mini}} \mathbf{X} > \right| \leq \gamma \right] \\ &= \frac{1}{\sqrt{2\pi}} \int_{-\left[\left\| \tilde{\mathbf{a}}_{\text{train},1}^{\text{mini}} \mathbf{X} \right\|_2^2 \left\| \tilde{\mathbf{a}}_{\text{train},i}^{\text{mini}} \mathbf{X} \right\|_2^2 - \left(\left(\tilde{\mathbf{a}}_{\text{train},1}^{\text{mini}} \mathbf{X} \right)^\top \tilde{\mathbf{a}}_{\text{train},i}^{\text{mini}} \mathbf{X} \right)^2 \right]^{\frac{1}{2}} \gamma}^{\left[\left\| \tilde{\mathbf{a}}_{\text{train},1}^{\text{mini}} \mathbf{X} \right\|_2^2 \left\| \tilde{\mathbf{a}}_{\text{train},i}^{\text{mini}} \mathbf{X} \right\|_2^2 - \left(\left(\tilde{\mathbf{a}}_{\text{train},1}^{\text{mini}} \mathbf{X} \right)^\top \tilde{\mathbf{a}}_{\text{train},i}^{\text{mini}} \mathbf{X} \right)^2 \right]^{\frac{1}{2}} \gamma} \exp\left(-\frac{1}{2}x^2\right) dx \\ &\leq \frac{1}{\sqrt{2\pi}} \int_{-\left[C_x^2 \beta^2 - \left(\left(\tilde{\mathbf{a}}_{\text{train},1}^{\text{mini}} \mathbf{X} \right)^\top \tilde{\mathbf{a}}_{\text{train},i}^{\text{mini}} \mathbf{X} \right)^2 \right]^{\frac{1}{2}} \gamma}^{\left[C_x^2 \beta^2 - \left(\left(\tilde{\mathbf{a}}_{\text{train},1}^{\text{mini}} \mathbf{X} \right)^\top \tilde{\mathbf{a}}_{\text{train},i}^{\text{mini}} \mathbf{X} \right)^2 \right]^{\frac{1}{2}} \gamma} \exp\left(-\frac{1}{2}x^2\right) dx \\ &\leq \sqrt{\frac{2}{\pi}} \frac{\gamma}{\left[C_x^2 \beta^2 - \left(\left(\tilde{\mathbf{a}}_{\text{train},1}^{\text{mini}} \mathbf{X} \right)^\top \tilde{\mathbf{a}}_{\text{train},i}^{\text{mini}} \mathbf{X} \right)^2 \right]^{\frac{1}{2}}} \\ &\leq \sqrt{\frac{2}{\pi}} \frac{\gamma}{\alpha^2/2} \end{aligned} \quad (200)$$

Taking union bound over \mathcal{I} , we have:

$$\mathbb{P}(\mathcal{E}_2) \geq 1 - \frac{2\sqrt{2}}{\sqrt{\pi}} n_{\text{train}} \gamma \alpha^{-2}. \quad (201)$$

2970 Therefore, we have:

$$2971 \mathbb{P}(\mathcal{E}) \geq \sqrt{\frac{2}{\pi e}} \frac{\gamma \kappa^2}{C_x \beta} \left(1 - \frac{2\sqrt{2}}{\sqrt{\pi}} n_{\text{train}} \gamma \alpha^{-2}\right). \quad (202)$$

2974 Setting $\gamma = \frac{\sqrt{\pi} \alpha^2}{4\sqrt{2}n_{\text{train}}}$, we obtain:

$$2976 \mathbb{P}(\mathcal{E}) \geq \sqrt{\frac{2}{\pi e}} \frac{\kappa^2}{C_x \beta} \frac{\sqrt{\pi} \alpha^2}{4\sqrt{2}n_{\text{train}}} \left(1 - \frac{2\sqrt{2}}{\sqrt{\pi}} n_{\text{train}} \frac{\sqrt{\pi} \alpha^2}{4\sqrt{2}n_{\text{train}}} \alpha^{-2}\right) \\ 2977 = \frac{\kappa^2 \alpha^2}{8\sqrt{e} C_x n_{\text{train}} \beta}. \quad (203)$$

2981 Let $\mathcal{I}' = [n_{\text{train}}] \setminus (\mathcal{I} \cup \{1\})$. Conditioning on event \mathcal{E} , we have:

$$2983 h\left(\mathbf{w}_j^{\text{mini}}\right) \\ 2984 = \sum_{i=1}^{n_{\text{train}}} \mathbf{m}_i y_i \sigma' \left(\tilde{\mathbf{a}}_{\text{train},i}^{\text{mini}} \mathbf{X} \left(\mathbf{w}_j^{\text{mini}} \right)^{\top} \right) \tilde{\mathbf{a}}_{\text{train},i}^{\text{mini}} \mathbf{X} \\ 2985 = \mathbf{m}_1 y_1 \sigma' \left(\mathbf{u}_1 \right) \tilde{\mathbf{a}}_{\text{train},1}^{\text{mini}} \mathbf{X} \\ 2986 + \sum_{i \in \mathcal{I}} \mathbf{m}_i y_i \sigma' \left(\mathbf{u}_1 < \tilde{\mathbf{a}}_{\text{train},1}^{\text{mini}} \mathbf{X}, \tilde{\mathbf{a}}_{\text{train},i}^{\text{mini}} \mathbf{X} >, < \left\| \tilde{\mathbf{a}}_{\text{train},1}^{\text{mini}} \mathbf{X} \right\|_2 \mathbf{Q}' \mathbf{u}', \tilde{\mathbf{a}}_{\text{train},i}^{\text{mini}} \mathbf{X} > \right) \tilde{\mathbf{a}}_{\text{train},i}^{\text{mini}} \mathbf{X} \\ 2987 + \sum_{i \in \mathcal{I}'} \mathbf{m}_i y_i \sigma' \left(\mathbf{u}_1 < \tilde{\mathbf{a}}_{\text{train},1}^{\text{mini}} \mathbf{X}, \tilde{\mathbf{a}}_{\text{train},i}^{\text{mini}} \mathbf{X} >, < \left\| \tilde{\mathbf{a}}_{\text{train},1}^{\text{mini}} \mathbf{X} \right\|_2 \mathbf{Q}' \mathbf{u}', \tilde{\mathbf{a}}_{\text{train},i}^{\text{mini}} \mathbf{X} > \right) \tilde{\mathbf{a}}_{\text{train},i}^{\text{mini}} \mathbf{X} \\ 2988 = \mathbf{m}_1 y_1 \sigma' \left(\mathbf{u}_1 \right) \tilde{\mathbf{a}}_{\text{train},1}^{\text{mini}} \mathbf{X} + \sum_{i \in \mathcal{I}} \mathbf{m}_i y_i \sigma' \left(< \left\| \tilde{\mathbf{a}}_{\text{train},1}^{\text{mini}} \mathbf{X} \right\|_2 \mathbf{Q}' \mathbf{u}', \tilde{\mathbf{a}}_{\text{train},i}^{\text{mini}} \mathbf{X} > \right) \tilde{\mathbf{a}}_{\text{train},i}^{\text{mini}} \mathbf{X} \\ 2989 + \sum_{i \in \mathcal{I}'} \mathbf{m}_i y_i \sigma' \left(\mathbf{u}_1 < \tilde{\mathbf{a}}_{\text{train},1}^{\text{mini}} \mathbf{X}, \tilde{\mathbf{a}}_{\text{train},i}^{\text{mini}} \mathbf{X} >, < \left\| \tilde{\mathbf{a}}_{\text{train},1}^{\text{mini}} \mathbf{X} \right\|_2 \mathbf{Q}' \mathbf{u}', \tilde{\mathbf{a}}_{\text{train},i}^{\text{mini}} \mathbf{X} > \right) \tilde{\mathbf{a}}_{\text{train},i}^{\text{mini}} \mathbf{X}, \quad (204)$$

2991 where the last equality follows from the fact that conditioning on event \mathcal{E} , for all $i \in \mathcal{I}$, it hold that:

$$2999 \left| < \left\| \tilde{\mathbf{a}}_{\text{train},1}^{\text{mini}} \mathbf{X} \right\|_2 \mathbf{Q}' \mathbf{u}', \tilde{\mathbf{a}}_{\text{train},i}^{\text{mini}} \mathbf{X} > \right| \geq |\mathbf{u}_1 C_x \beta| \geq \left| \mathbf{u}_1 < \tilde{\mathbf{a}}_{\text{train},1}^{\text{mini}} \mathbf{X}, \tilde{\mathbf{a}}_{\text{train},i}^{\text{mini}} \mathbf{X} > \right|. \quad (205)$$

3002 We then consider two cases: $\mathbf{u}_1 > 0$ and $\mathbf{u}_1 < 0$, which occur equally likely conditioning on \mathcal{E} .

3003 Therefore, we have:

$$3005 \mathbb{P} \left[\left\| h\left(\mathbf{w}_j^{\text{mini}}\right) \right\|_2 \geq \inf_{\mathbf{u}_1^{(1)} > 0, \mathbf{u}_1^{(2)} < 0} \max \left\{ \left\| h\left(\mathbf{w}_j^{\text{mini},(1)}\right) \right\|_2, \left\| h\left(\mathbf{w}_j^{\text{mini},(2)}\right) \right\|_2 \right\} \mid \mathcal{E} \right] \geq \frac{1}{2}, \quad (206)$$

3008 where we define $\mathbf{w}_j^{\text{mini},(1)} = \mathbf{u}_1^{(1)} \tilde{\mathbf{a}}_{\text{train},1}^{\text{mini}} \mathbf{X} + \left\| \tilde{\mathbf{a}}_{\text{train},1}^{\text{mini}} \mathbf{X} \right\|_2 \mathbf{Q}' \mathbf{u}'$ and $\mathbf{w}_j^{\text{mini},(2)} = \mathbf{u}_1^{(2)} \tilde{\mathbf{a}}_{\text{train},1}^{\text{mini}} \mathbf{X} + \left\| \tilde{\mathbf{a}}_{\text{train},1}^{\text{mini}} \mathbf{X} \right\|_2 \mathbf{Q}' \mathbf{u}'$.

3011 By the inequality $\max \{ \|\mathbf{a}\|_2, \|\mathbf{b}\|_2 \} \geq \|\mathbf{a} - \mathbf{b}\|_2 / 2$, we have:

$$3013 \mathbb{P} \left[\left\| h\left(\mathbf{w}_j^{\text{mini}}\right) \right\|_2 \geq \inf_{\mathbf{u}_1^{(1)} > 0, \mathbf{u}_1^{(2)} < 0} \left\| h\left(\mathbf{w}_j^{\text{mini},(1)}\right) - h\left(\mathbf{w}_j^{\text{mini},(2)}\right) \right\|_2 / 2 \mid \mathcal{E} \right] \geq \frac{1}{2}, \quad (207)$$

3016 By Eq 204, we have:

$$3018 h\left(\mathbf{w}_j^{\text{mini},(1)}\right) - h\left(\mathbf{w}_j^{\text{mini},(2)}\right) = \mathbf{m}_1 y_1 \tilde{\mathbf{a}}_{\text{train},1}^{\text{mini}} \mathbf{X} + \sum_{i \in \mathcal{I}'} \mathbf{m}_i' y_i \tilde{\mathbf{a}}_{\text{train},i}^{\text{mini}} \mathbf{X}, \quad (208)$$

3020 where we define:

$$3022 \mathbf{m}_i' = \mathbf{m}_i \left[\sigma' \left(\mathbf{u}_1^{(1)} < \tilde{\mathbf{a}}_{\text{train},1}^{\text{mini}} \mathbf{X}, \tilde{\mathbf{a}}_{\text{train},i}^{\text{mini}} \mathbf{X} >, < \left\| \tilde{\mathbf{a}}_{\text{train},1}^{\text{mini}} \mathbf{X} \right\|_2 \mathbf{Q}' \mathbf{u}', \tilde{\mathbf{a}}_{\text{train},i}^{\text{mini}} \mathbf{X} > \right) \right. \\ 3023 \left. - \sigma' \left(\mathbf{u}_1^{(2)} < \tilde{\mathbf{a}}_{\text{train},1}^{\text{mini}} \mathbf{X}, \tilde{\mathbf{a}}_{\text{train},i}^{\text{mini}} \mathbf{X} >, < \left\| \tilde{\mathbf{a}}_{\text{train},1}^{\text{mini}} \mathbf{X} \right\|_2 \mathbf{Q}' \mathbf{u}', \tilde{\mathbf{a}}_{\text{train},i}^{\text{mini}} \mathbf{X} > \right) \right]. \quad (209)$$

3024 Note that for all $i \in \mathcal{I}'$, we have $y_i = y_1$ and $\langle \tilde{\mathbf{a}}_{\text{train},1}^{\text{mini}} \mathbf{X}, \tilde{\mathbf{a}}_{\text{train},i}^{\text{mini}} \mathbf{X} \rangle \geq C_x \beta - \alpha^2/2 \geq 0$. Therefore,
 3025 since $\mathbf{u}_1^{(1)} > 0 > \mathbf{u}_1^{(2)}$, we have:
 3026

$$\begin{aligned} 3027 \quad & \sigma' \left(\mathbf{u}_1^{(1)} \langle \tilde{\mathbf{a}}_{\text{train},1}^{\text{mini}} \mathbf{X}, \tilde{\mathbf{a}}_{\text{train},i}^{\text{mini}} \mathbf{X} \rangle, \langle \tilde{\mathbf{a}}_{\text{train},1}^{\text{mini}} \mathbf{X} \rangle_2 \mathbf{Q}' \mathbf{u}', \tilde{\mathbf{a}}_{\text{train},i}^{\text{mini}} \mathbf{X} \rangle \right) \\ 3028 \quad & - \sigma' \left(\mathbf{u}_1^{(2)} \langle \tilde{\mathbf{a}}_{\text{train},1}^{\text{mini}} \mathbf{X}, \tilde{\mathbf{a}}_{\text{train},i}^{\text{mini}} \mathbf{X} \rangle, \langle \tilde{\mathbf{a}}_{\text{train},1}^{\text{mini}} \mathbf{X} \rangle_2 \mathbf{Q}' \mathbf{u}', \tilde{\mathbf{a}}_{\text{train},i}^{\text{mini}} \mathbf{X} \rangle \right) \geq 0. \end{aligned} \quad (210)$$

3031 Therefore, $\mathbf{m}'_i \geq 0$ for all $i \in \mathcal{I}'$ and
 3032

$$3033 \quad h \left(\mathbf{w}_j^{\text{mini},(1)} \right) - h \left(\mathbf{w}_j^{\text{mini},(2)} \right) = y_1 \left(\mathbf{m}_1 \tilde{\mathbf{a}}_{\text{train},1}^{\text{mini}} \mathbf{X} + \sum_{i \in \mathcal{I}'} \mathbf{m}'_i \tilde{\mathbf{a}}_{\text{train},i}^{\text{mini}} \mathbf{X} \right). \quad (211)$$

3036 Then we have:
 3037

$$\begin{aligned} 3038 \quad & \left\| h \left(\mathbf{w}_j^{\text{mini},(1)} \right) - h \left(\mathbf{w}_j^{\text{mini},(2)} \right) \right\|_2 \\ 3039 \quad & \geq \left\| y_1 \left(\mathbf{m}_1 \tilde{\mathbf{a}}_{\text{train},1}^{\text{mini}} \mathbf{X} + \sum_{i \in \mathcal{I}'} \mathbf{m}'_i \tilde{\mathbf{a}}_{\text{train},i}^{\text{mini}} \mathbf{X} \right) \right\|_2 \\ 3040 \quad & \geq \langle \mathbf{m}_1 \tilde{\mathbf{a}}_{\text{train},1}^{\text{mini}} \mathbf{X} + \sum_{i \in \mathcal{I}'} \mathbf{m}'_i \tilde{\mathbf{a}}_{\text{train},i}^{\text{mini}} \mathbf{X}, \tilde{\mathbf{a}}_{\text{train},1}^{\text{mini}} \mathbf{X} \rangle / \left\| \tilde{\mathbf{a}}_{\text{train},1}^{\text{mini}} \mathbf{X} \right\|_2 \\ 3041 \quad & \geq \mathbf{m}_1. \end{aligned} \quad (212)$$

3045 Since the inequality above holds for any $\mathbf{u}_1^{(1)} > 0$ and $\mathbf{u}_1^{(2)} < 0$, taking infimum, we have:
 3046

$$3047 \quad \inf_{\mathbf{u}_1^{(1)} > 0, \mathbf{u}_1^{(2)} < 0} \left\| h \left(\mathbf{w}_j^{\text{mini},(1)} \right) - h \left(\mathbf{w}_j^{\text{mini},(2)} \right) \right\|_2 \geq \mathbf{m}_1. \quad (213)$$

3049 Therefore, we have:
 3050

$$3051 \quad \mathbb{P} \left[\left\| h \left(\mathbf{w}_j^{\text{mini}} \right) \right\|_2 \geq \mathbf{m}_1/2 \mid \mathcal{E} \right] \geq \frac{1}{2}. \quad (214)$$

3053 Since $\mathbf{m}_1 = \|\mathbf{m}\|_\infty$ and $\mathbb{P}(\mathcal{E}) \geq \frac{\kappa^2 \alpha^2}{8\sqrt{e} C_x n_{\text{train}} \beta}$, we have:
 3054

$$3055 \quad \mathbb{P} \left[\left\| h \left(\mathbf{w}_j^{\text{mini}} \right) \right\|_2 \geq C \|\mathbf{m}\|_\infty \right] \geq \frac{C_1 \alpha^2}{n_{\text{train}} \beta}, \quad (215)$$

3057 where C and C_1 are absolute constants.
 3058

3059 Similarly, for the full-graph training, we can replace β by d_{max} as:
 3060

$$3061 \quad \mathbb{P} \left[\left\| h \left(\mathbf{w}_j^{\text{full}} \right) \right\|_2 \geq C_2 \|\mathbf{m}\|_\infty \right] \geq \frac{C_3 \alpha^2}{n_{\text{train}} d_{\text{max}}}, \quad (216)$$

3062 where C_2 and C_3 are absolute constants.
 3063

3064 Proved.
 3065

3066 M PROOFS OF THE MAIN THEOREM AND LEMMA OF THEOREM 5

3068 M.1 PROOF OF THEOREM G.5

3070 **Lemma M.1.** (Lemma 4 in (Ma et al., 2021)) For any two distributions \mathcal{P} and \mathcal{Q} defined on the
 3071 hypothesis space, and any function $f(\cdot) \in \mathbb{R}$ with $\text{dom } f$ in this hypothesis space, we have:
 3072

$$3073 \quad \mathbb{E}_{x \sim \mathcal{Q}} \leq D_{KL}(\mathcal{Q} \parallel \mathcal{P}) + \mathbb{E}_{x \sim \mathcal{P}} e^{f(x)}.$$

3074 **Lemma M.2.** (Lemma 2 in (Ma et al., 2021)) Suppose x_1, x_2, \dots, x_n are independent random
 3075 variables with $a_i \leq x_i \leq b_i, \forall i = 1, 2, \dots, n$. Let $\bar{x} = \frac{1}{n} \sum_{i=1}^n x_i$. Then, for any $C > 0$,
 3076

$$3077 \quad \mathbb{P}(|\bar{x} - \mathbb{E}(\bar{x})| > C) \leq 2e^{-\frac{n^2 C^2}{\sum_{i=1}^n (b_i - a_i)^2}}.$$

3078 **Lemma M.3.** (Lemma 3 in (Ma et al., 2021)) If x is a centered random variable, i.e., $\mathbb{E}(x) = 0$,
 3079 and if $\exists C_1 > 0$, for any $C_2 > 0$,

$$3080 \quad \mathbb{P}(|x| > C_2) \leq 2e^{-C_1 C_2^2}.$$

3082 Then, for any $C_u > 0$,

$$3083 \quad \mathbb{E}(e^{C_u x}) \leq e^{\frac{C_u^2}{2C_1}}.$$

3085 **Proof of Theorem G.5:** We are going to prove the result by upper-bounding the quantity
 3086 $C_u(L_{\text{test}}(\mathbf{W}^{\text{mini}}, \tilde{\mathbf{A}}_{\text{test}}; \mathcal{Q}) - \hat{L}_{\text{train}}^{\text{full}}(\mathbf{W}^{\text{mini}}, \tilde{\mathbf{A}}_{\text{train}}^{\text{mini}}; \mathcal{Q}))$. First, we have:

$$\begin{aligned} 3088 \quad & C_u(L_{\text{test}}(\mathbf{W}^{\text{mini}}, \tilde{\mathbf{A}}_{\text{test}}; \mathcal{Q}) - \hat{L}_{\text{train}}^{\text{full}}(\mathbf{W}^{\text{mini}}, \tilde{\mathbf{A}}_{\text{train}}^{\text{mini}}; \mathcal{Q})) \\ 3089 \quad & \leq \mathbb{E}_{\mathbf{W}^{\text{mini}} \sim \mathcal{Q}} [C_u(L_{\text{test}}(\mathbf{W}^{\text{mini}}, \tilde{\mathbf{A}}_{\text{test}}) - \hat{L}_{\text{train}}^{\text{full}}(\mathbf{W}^{\text{mini}}, \tilde{\mathbf{A}}_{\text{train}}^{\text{mini}}))] \\ 3090 \quad & \leq D_{KL}(\mathcal{Q} \parallel \mathcal{P}) + \ln \mathbb{E}_{\mathbf{W}^{\text{mini}} \sim \mathcal{P}} [e^{(L_{\text{test}}(\mathbf{W}^{\text{mini}}, \tilde{\mathbf{A}}_{\text{test}}) - \hat{L}_{\text{train}}^{\text{full}}(\mathbf{W}^{\text{mini}}, \tilde{\mathbf{A}}_{\text{train}}^{\text{mini}}))}], \\ 3091 \quad & \\ 3092 \quad & \end{aligned} \quad (217)$$

3093 where the last inequality uses Lemma M.1.

3094 Next, we upper-bound the second term in the RHS of (217). Here the term $\Lambda =$
 3095 $\mathbb{E}_{\mathbf{W}^{\text{mini}} \sim \mathcal{P}} [e^{(L_{\text{test}}(\mathbf{W}^{\text{mini}}, \tilde{\mathbf{A}}_{\text{test}}) - \hat{L}_{\text{train}}^{\text{full}}(\mathbf{W}^{\text{mini}}, \tilde{\mathbf{A}}_{\text{train}}^{\text{mini}}))}]$ is a random variable with the randomness coming
 3096 from the sample of node labels in training dataset, and \mathcal{P} is independent of node labels \mathbf{y} from training
 3097 dataset. Applying Markov's inequality to the term Λ , we have for any $C_G > 0$, with probability
 3098 at least $1 - C_G$ over \mathbf{y} from training set,

$$3100 \quad \Lambda \leq \frac{1}{C_G} \mathbb{E}_{\mathbf{y} \sim \text{training set}} [\Lambda], \quad (218)$$

3102 and hence,

$$3103 \quad \ln \Lambda \leq \ln \frac{1}{C_G} \mathbb{E}_{\mathbf{y} \sim \text{training set}} [\Lambda] = \ln \frac{1}{C_G} + \ln \mathbb{E}_{\mathbf{y} \sim \text{training set}} [\Lambda]. \quad (219)$$

3105 Then we need to upper-bound $\ln \mathbb{E}_{\mathbf{y} \sim \text{training set}} [\Lambda]$. We can rewrite it as:

$$\begin{aligned} 3107 \quad & \ln \mathbb{E}_{\mathbf{y} \sim \text{training set}} [\Lambda] \\ 3108 \quad & = \ln \mathbb{E}_{\mathbf{y} \sim \text{training set}} \mathbb{E}_{\mathbf{W}^{\text{mini}} \sim \mathcal{P}} [e^{(L_{\text{test}}(\mathbf{W}^{\text{mini}}, \tilde{\mathbf{A}}_{\text{test}}) - \hat{L}_{\text{train}}^{\text{full}}(\mathbf{W}^{\text{mini}}, \tilde{\mathbf{A}}_{\text{train}}^{\text{mini}}))}] \\ 3109 \quad & = \ln \mathbb{E}_{\mathbf{W}^{\text{mini}} \sim \mathcal{P}} \mathbb{E}_{\mathbf{y} \sim \text{training set}} [e^{(L_{\text{test}}(\mathbf{W}^{\text{mini}}, \tilde{\mathbf{A}}_{\text{test}}) - \hat{L}_{\text{train}}^{\text{full}}(\mathbf{W}^{\text{mini}}, \tilde{\mathbf{A}}_{\text{train}}^{\text{mini}}))}]. \\ 3110 \quad & \end{aligned} \quad (220)$$

3111 For a fixed model with model parameters \mathbf{W}^{mini} , we have

$$\begin{aligned} 3113 \quad & \mathbb{E}_{\mathbf{y} \sim \text{training set}} [e^{(L_{\text{test}}(\mathbf{W}^{\text{mini}}, \tilde{\mathbf{A}}_{\text{test}}) - \hat{L}_{\text{train}}^{\text{full}}(\mathbf{W}^{\text{mini}}, \tilde{\mathbf{A}}_{\text{train}}^{\text{mini}}))}] \\ 3114 \quad & = \mathbb{E}_{\mathbf{y} \sim \text{training set}} [e^{(L_{\text{test}}(\mathbf{W}^{\text{mini}}, \tilde{\mathbf{A}}_{\text{test}}) - L_{\text{train}}^{\text{full}}(\mathbf{W}^{\text{mini}}, \tilde{\mathbf{A}}_{\text{train}}^{\text{mini}}) + L_{\text{train}}^{\text{full}}(\mathbf{W}^{\text{mini}}, \tilde{\mathbf{A}}_{\text{train}}^{\text{mini}}) - \hat{L}_{\text{train}}^{\text{full}}(\mathbf{W}^{\text{mini}}, \tilde{\mathbf{A}}_{\text{train}}^{\text{mini}}))}] \\ 3115 \quad & = \mathbb{E}_{\mathbf{y} \sim \text{training set}} [e^{(L_{\text{test}}(\mathbf{W}^{\text{mini}}, \tilde{\mathbf{A}}_{\text{test}}) - L_{\text{train}}^{\text{full}}(\mathbf{W}^{\text{mini}}, \tilde{\mathbf{A}}_{\text{train}}^{\text{mini}}))} e^{(L_{\text{train}}^{\text{full}}(\mathbf{W}^{\text{mini}}, \tilde{\mathbf{A}}_{\text{train}}^{\text{mini}}) - \hat{L}_{\text{train}}^{\text{full}}(\mathbf{W}^{\text{mini}}, \tilde{\mathbf{A}}_{\text{train}}^{\text{mini}}))}] \\ 3116 \quad & = e^{(L_{\text{test}}(\mathbf{W}^{\text{mini}}, \tilde{\mathbf{A}}_{\text{test}}) - L_{\text{train}}^{\text{full}}(\mathbf{W}^{\text{mini}}, \tilde{\mathbf{A}}_{\text{train}}^{\text{mini}}))} \mathbb{E}_{\mathbf{y} \sim \text{training set}} [e^{(L_{\text{train}}^{\text{full}}(\mathbf{W}^{\text{mini}}, \tilde{\mathbf{A}}_{\text{train}}^{\text{mini}}) - \hat{L}_{\text{train}}^{\text{full}}(\mathbf{W}^{\text{mini}}, \tilde{\mathbf{A}}_{\text{train}}^{\text{mini}}))}]. \\ 3117 \quad & \\ 3118 \quad & \end{aligned} \quad (221)$$

3120 In the following, we will give an upper bound on $\mathbb{E}_{\mathbf{y} \sim \text{training set}} [e^{(L_{\text{train}}^{\text{full}}(\mathbf{W}^{\text{mini}}, \tilde{\mathbf{A}}_{\text{train}}^{\text{mini}}) - \hat{L}_{\text{train}}^{\text{full}}(\mathbf{W}^{\text{mini}}, \tilde{\mathbf{A}}_{\text{train}}^{\text{mini}}))}]$
 3121 that is independent of \mathbf{W}^{mini} . For the entire training dataset, $\hat{L}_{\text{train}}^{\text{full}}(\mathbf{W}^{\text{mini}}, \tilde{\mathbf{A}}_{\text{train}}^{\text{mini}})$ can be written as:

$$3124 \quad \hat{L}_{\text{train}}^{\text{full}}(\mathbf{W}^{\text{mini}}, \tilde{\mathbf{A}}_{\text{train}}^{\text{mini}}) = \frac{1}{n_{\text{train}}} \sum_{i \in \text{training set}} \|\hat{\mathbf{y}}_i^{\text{mini}} - \mathbf{y}_i\|_F^2, \quad (222)$$

3126 where the node labels are independently sampled. Hence, $\hat{L}_{\text{train}}^{\text{full}}(\mathbf{W}^{\text{mini}}, \tilde{\mathbf{A}}_{\text{train}}^{\text{mini}})$ is the empirical
 3127 mean of n_{train} independent Bernoulli random variables and $L_{\text{train}}^{\text{full}}(\mathbf{W}^{\text{mini}}, \tilde{\mathbf{A}}_{\text{train}}^{\text{mini}})$ is the expectation
 3128 of $\hat{L}_{\text{train}}^{\text{full}}(\mathbf{W}^{\text{mini}}, \tilde{\mathbf{A}}_{\text{train}}^{\text{mini}})$. By Lemma M.2, for any $C_1 > 0$,

$$3131 \quad \mathbb{P}(|L_{\text{train}}^{\text{full}}(\mathbf{W}^{\text{mini}}, \tilde{\mathbf{A}}_{\text{train}}^{\text{mini}}) - \hat{L}_{\text{train}}^{\text{full}}(\mathbf{W}^{\text{mini}}, \tilde{\mathbf{A}}_{\text{train}}^{\text{mini}})| \geq C_1) \leq 2e^{-2n_{\text{train}}C_1^2}, \quad (223)$$

3132 and hence, by Lemma M.1, we have
3133

$$3134 \mathbb{E}_{\mathbf{y} \sim \text{training set}} \left[e^{C_u (L_{\text{train}}^{\text{full}}(\mathbf{W}^{\text{mini}}, \tilde{\mathbf{A}}_{\text{train}}^{\text{mini}}) - \hat{L}_{\text{train}}^{\text{full}}(\mathbf{W}^{\text{mini}}, \tilde{\mathbf{A}}_{\text{train}}^{\text{mini}}))} \right] \leq e^{\frac{C_u^2}{4n_{\text{train}}}}. \quad (224)$$

3136 Therefore, we have
3137

$$3138 \ln \Lambda \leq \ln \mathbb{E}_{\mathbf{W}^{\text{mini}} \sim \mathcal{P}} \left[e^{(L_{\text{test}}(\mathbf{W}^{\text{mini}}, \tilde{\mathbf{A}}_{\text{test}}^{\text{full}}) - L_{\text{train}}^{\text{full}}(\mathbf{W}^{\text{mini}}, \tilde{\mathbf{A}}_{\text{train}}^{\text{mini}}))} e^{\frac{C_u^2}{4n_{\text{train}}}} \right] \quad (225)$$

$$3141 = U + \frac{C_u^2}{4n_{\text{train}}}.$$

3143 Finally, we get
3144

$$3145 C_u(L_{\text{test}}(\mathbf{W}^{\text{mini}}, \tilde{\mathbf{A}}_{\text{test}}^{\text{full}}; \mathcal{Q}) - \hat{L}_{\text{train}}^{\text{full}}(\mathbf{W}^{\text{mini}}, \tilde{\mathbf{A}}_{\text{train}}^{\text{mini}}; \mathcal{Q})) \\ 3146 \leq D_{KL}(\mathcal{Q} \parallel \mathcal{P}) + \ln \mathbb{E}_{\mathbf{W}^{\text{mini}} \sim \mathcal{P}} \left[e^{(L_{\text{test}}(\mathbf{W}^{\text{mini}}, \tilde{\mathbf{A}}_{\text{test}}^{\text{full}}) - \hat{L}_{\text{train}}^{\text{full}}(\mathbf{W}^{\text{mini}}, \tilde{\mathbf{A}}_{\text{train}}^{\text{mini}}))} \right] \quad (226) \\ 3148 \leq D_{KL}(\mathcal{Q} \parallel \mathcal{P}) + \ln \frac{1}{C_G} + \frac{C_u^2}{4n_{\text{train}}} + U.$$

3151 Hence, we have the final result
3152

$$3153 L_{\text{test}}(\mathbf{W}^{\text{mini}}, \tilde{\mathbf{A}}_{\text{test}}^{\text{full}}; \mathcal{Q}) \\ 3154 \leq \hat{L}_{\text{train}}^{\text{full}}(\mathbf{W}^{\text{mini}}, \tilde{\mathbf{A}}_{\text{train}}^{\text{mini}}; \mathcal{Q}) + \frac{1}{C_u} \left(D_{KL}(\mathcal{Q} \parallel \mathcal{P}) + \ln \frac{1}{C_G} + \frac{C_u^2}{4n_{\text{train}}} + U \right). \quad (227)$$

3157 M.2 PROOF OF LEMMA G.6

3159 Recall that

$$3160 U = \ln \mathbb{E}_{\mathbf{W}^{\text{mini}} \sim \mathcal{P}} \left[e^{C_u (L_{\text{test}}(\mathbf{W}^{\text{mini}}, \tilde{\mathbf{A}}_{\text{test}}^{\text{full}}) - L_{\text{train}}^{\text{full}}(\mathbf{W}^{\text{mini}}, \tilde{\mathbf{A}}_{\text{train}}^{\text{mini}}))} \right]. \quad (228)$$

3162 First, we focus on the term $L_{\text{test}}(\mathbf{W}^{\text{mini}}, \tilde{\mathbf{A}}_{\text{test}}^{\text{full}}) - L_{\text{train}}^{\text{full}}(\mathbf{W}^{\text{mini}}, \tilde{\mathbf{A}}_{\text{train}}^{\text{mini}})$. Set $l_{\text{train}}^{\text{mini}}(\mathbf{y}_i) = \|\hat{\mathbf{y}}_i^{\text{mini}} - \mathbf{y}_i\|_F^2, \forall i \in \text{train set}$ and $l_{\text{test}}^{\text{mini}}(\mathbf{y}_j) = \|\hat{\mathbf{y}}_j^{\text{mini}} - \mathbf{y}_j\|_F^2, \forall j \in \text{test set}$. Then we have

$$3166 L_{\text{test}}(\mathbf{W}^{\text{mini}}, \tilde{\mathbf{A}}_{\text{test}}^{\text{full}}) - L_{\text{train}}^{\text{full}}(\mathbf{W}^{\text{mini}}, \tilde{\mathbf{A}}_{\text{train}}^{\text{mini}}) \\ 3167 = \mathbb{E}_{\mathbf{y} \sim \text{test set}} \left[\frac{1}{n_{\text{test}}} \sum_{j \in \text{test set}} l_{\text{test}}^{\text{mini}}(\mathbf{y}_j) \right] - \mathbb{E}_{\mathbf{y} \sim \text{train set}} \left[\frac{1}{n_{\text{train}}} \sum_{i \in \text{train set}} l_{\text{train}}^{\text{mini}}(\mathbf{y}_i) \right] \quad (229) \\ 3170 = \frac{1}{n_{\text{test}}} \sum_{j \in \text{test set}} l_{\text{test}}^{\text{mini}}(\mathbf{y}_j) \rho_{\text{test}}(\mathbf{y}_j) - \frac{1}{n_{\text{train}}} \sum_{i \in \text{train set}} l_{\text{train}}^{\text{mini}}(\mathbf{y}_i) \rho_{\text{train}}(\mathbf{y}_i)$$

3173 Furthermore, we define $\Sigma_{\text{train},i} = \text{Diag} \left(\mathbb{1} \left\{ \tilde{\mathbf{a}}_{\text{train},i}^{\text{mini}} \mathbf{X} (\mathbf{W}^{\text{mini}})^{\top} > 0 \right\} \right) \in \mathbb{R}^{h \times h}$ to represent
3174 whether the j -th element $\left\{ \tilde{\mathbf{a}}_{\text{train},i}^{\text{mini}} \mathbf{X} (\mathbf{W}^{\text{mini}})^{\top} \right\}_j$ is more than zero (1) or is zeroed out (0). Then we
3175 have:
3176

$$3178 \sigma \left(\tilde{\mathbf{a}}_{\text{train},i}^{\text{mini}} \mathbf{X} (\mathbf{W}^{\text{mini}})^{\top} \right) = \tilde{\mathbf{a}}_{\text{train},i}^{\text{mini}} \mathbf{X} (\Sigma_{\text{train},i} \mathbf{W}^{\text{mini}})^{\top}. \quad (230)$$

3180 Similarly, we have $\sigma \left(\tilde{\mathbf{a}}_{\text{train},i}^{\text{mini}} \mathbf{X} (\mathbf{W}^{\text{mini}})^{\top} \right) = \tilde{\mathbf{a}}_{\text{train},i}^{\text{mini}} \mathbf{X} (\Sigma_{\text{train},i}^* \mathbf{W}^{\text{mini}})^{\top}$,
3181 $\sigma \left(\tilde{\mathbf{a}}_{\text{test},i}^{\text{full}} \mathbf{X} (\mathbf{W}^{\text{mini}})^{\top} \right) = \tilde{\mathbf{a}}_{\text{test},i}^{\text{full}} \mathbf{X} (\Sigma_{\text{test},i} \mathbf{W}^{\text{mini}})^{\top}$, and $\sigma \left(\tilde{\mathbf{a}}_{\text{test},i}^{\text{full}} \mathbf{X} (\mathbf{W}^{\text{mini}})^{\top} \right) =$
3183 $\tilde{\mathbf{a}}_{\text{test},i}^{\text{full}} \mathbf{X} (\Sigma_{\text{test},i}^* \mathbf{W}^{\text{mini}})^{\top}$.

3184 we set $f(\mathbf{y}_i) = -\frac{1}{n_{\text{train}}} l_{\text{train}}^{\text{mini}}(\mathbf{y}_i)$ with $\forall i \in \text{train set}$ and $g(\mathbf{y}_j) = \frac{1}{n_{\text{test}}} l_{\text{test}}^{\text{mini}}(\mathbf{y}_j)$ with $\forall j \in \text{test set}$ and
3185 $n_{\text{min}} = \min\{n_{\text{train}}, n_{\text{test}}\}$.

3186 Hence, we have:

$$\begin{aligned}
 & f(\mathbf{y}_i) + g(\mathbf{y}_j) \\
 &= \frac{1}{n_{\text{test}}} l_{\text{test}}^{\text{mini}}(\mathbf{y}_j) - \frac{1}{n_{\text{train}}} l_{\text{train}}^{\text{mini}}(\mathbf{y}_i) \\
 &\leq \frac{1}{n_{\text{min}}} (l_{\text{test}}^{\text{mini}}(\mathbf{y}_j) - l_{\text{train}}^{\text{mini}}(\mathbf{y}_i)) \\
 &= \frac{1}{n_{\text{min}}} \left\| \sigma \left(\tilde{\mathbf{a}}_{\text{test},j}^{\text{full}} \mathbf{X} \left(\mathbf{W}^{\text{mini}} \right)^{\top} \right) - \sigma \left(\tilde{\mathbf{a}}_{\text{test},j}^{\text{full}} \mathbf{X} \left(\mathbf{W}^{\text{mini}*} \right)^{\top} \right) \right\|_F^2 \\
 &\quad - \frac{1}{n_{\text{min}}} \left\| \sigma \left(\tilde{\mathbf{a}}_{\text{train},i}^{\text{mini}} \mathbf{X} \left(\mathbf{W}^{\text{mini}} \right)^{\top} \right) - \sigma \left(\tilde{\mathbf{a}}_{\text{train},i}^{\text{mini}} \mathbf{X} \left(\mathbf{W}^{\text{mini}*} \right)^{\top} \right) \right\|_F^2 \\
 &\leq \frac{1}{n_{\text{min}}} \left\| \sigma \left(\tilde{\mathbf{a}}_{\text{test},j}^{\text{full}} \mathbf{X} \left(\mathbf{W}^{\text{mini}} \right)^{\top} \right) - \sigma \left(\tilde{\mathbf{a}}_{\text{test},j}^{\text{full}} \mathbf{X} \left(\mathbf{W}^{\text{mini}*} \right)^{\top} \right) \right. \\
 &\quad \left. - \left(\sigma \left(\tilde{\mathbf{a}}_{\text{train},i}^{\text{mini}} \mathbf{X} \left(\mathbf{W}^{\text{mini}} \right)^{\top} \right) - \sigma \left(\tilde{\mathbf{a}}_{\text{train},i}^{\text{mini}} \mathbf{X} \left(\mathbf{W}^{\text{mini}*} \right)^{\top} \right) \right) \right\|_F^2 \\
 &= \frac{1}{n_{\text{min}}} \left\| \tilde{\mathbf{a}}_{\text{test},j}^{\text{full}} \mathbf{X} \left(\mathbf{W}^{\text{mini}} \right)^{\top} \Sigma_{\text{test},j}^{\top} - \tilde{\mathbf{a}}_{\text{test},j}^{\text{full}} \mathbf{X} \left(\mathbf{W}^{\text{mini}*} \right)^{\top} \Sigma_{\text{test},j}^* \right. \\
 &\quad \left. - \left(\tilde{\mathbf{a}}_{\text{train},i}^{\text{mini}} \mathbf{X} \left(\mathbf{W}^{\text{mini}} \right)^{\top} \Sigma_{\text{train},i}^{\top} - \tilde{\mathbf{a}}_{\text{train},i}^{\text{mini}} \mathbf{X} \left(\mathbf{W}^{\text{mini}*} \right)^{\top} \Sigma_{\text{train},i}^* \right) \right\|_F^2 \\
 &\leq \frac{\|\mathbf{X}\|_F^2}{n_{\text{min}}} \left(\left\| \mathbf{W}^{\text{mini}*} \right\|_F^2 \left\| \Sigma_{\text{train},i}^* \right\|_F^2 + \left\| \mathbf{W}^{\text{mini}} \right\|_F^2 \left\| \Sigma_{\text{train},i} \right\|_F^2 \right) \left\| \tilde{\mathbf{a}}_{\text{test},j}^{\text{full}} - \tilde{\mathbf{a}}_{\text{train},i}^{\text{mini}} \right\|_F^2 \\
 &\quad + \left\| \mathbf{W}^{\text{mini}*} \right\|_F^2 \left\| \Sigma_{\text{train},i}^* - \Sigma_{\text{test},j}^* \right\|_F^2 \left\| \tilde{\mathbf{a}}_{\text{test},j}^{\text{full}} \right\|_F^2 \\
 &\quad + \left\| \mathbf{W}^{\text{mini}} \right\|_F^2 \left\| \Sigma_{\text{train},i} - \Sigma_{\text{test},j} \right\|_F^2 \left\| \tilde{\mathbf{a}}_{\text{test},j}^{\text{full}} \right\|_F^2 \\
 &\leq \frac{C_F (C_w + 1) h^2}{n_{\text{min}}} \left(\left\| \tilde{\mathbf{a}}_{\text{test},j}^{\text{full}} - \tilde{\mathbf{a}}_{\text{train},i}^{\text{mini}} \right\|_F^2 + 2 \left\| \tilde{\mathbf{a}}_{\text{test},j}^{\text{full}} \right\|_F^2 \right) \\
 &\leq \frac{C_F (C_w + 1) h^2}{n_{\text{min}}} \left(\left\| \tilde{\mathbf{a}}_{\text{test},j}^{\text{full}} - \tilde{\mathbf{a}}_{\text{train},i}^{\text{full}} \right\|_F^2 + 2 \left\| \tilde{\mathbf{a}}_{\text{test},j}^{\text{full}} \right\|_F^2 + \left\| \tilde{\mathbf{a}}_{\text{train},i}^{\text{full}} - \tilde{\mathbf{a}}_{\text{train},i}^{\text{mini}} \right\|_F^2 \right), \\
 &= \frac{C_F (C_w + 1) h^2}{n_{\text{min}}} \left(\delta_{i,j}^{\text{full}} + \delta_i^{\text{full-mini}} \right) \\
 &= \delta(\mathbf{y}_i, \mathbf{y}_j, \beta, b)
 \end{aligned} \tag{231}$$

3219 where the penultimate inequality follows $\left\| \Sigma_{\text{train},i} \right\|_F^2, \left\| \Sigma_{\text{train},i}^* \right\|_F^2 \leq h$,
3220 $\left\| \Sigma_{\text{train},i}^* - \Sigma_{\text{test},i}^* \right\|_F^2, \left\| \Sigma_{\text{train},i} - \Sigma_{\text{test},i} \right\|_F^2 \leq 2h$ because Σ_i is a diagonal matrix with
3221 $(\Sigma_i)_{jj} \in \{0, 1\}$ for any $j \in \{1, \dots, h\}$. The penultimate expression is exactly the distance function
3222 defined in Definition 1., $\delta_{i,j}^{\text{full-mini}} = \left\| \tilde{\mathbf{a}}_{\text{train},i}^{\text{full}} - \tilde{\mathbf{a}}_{\text{train},i}^{\text{mini}} \right\|_F^2$, and $\delta_{i,j}^{\text{full}} = \left\| \tilde{\mathbf{a}}_{\text{test},j}^{\text{full}} - \tilde{\mathbf{a}}_{\text{train},i}^{\text{full}} \right\|_F^2 + 2 \left\| \tilde{\mathbf{a}}_{\text{test},j}^{\text{full}} \right\|_F^2$
3223 is a constant based on the split of training and testing.

3224 Hence, we have

$$\begin{aligned}
 & L_{\text{test}} \left(\mathbf{W}^{\text{mini}}, \tilde{\mathbf{A}}_{\text{test}}^{\text{full}} \right) - L_{\text{train}} \left(\mathbf{W}^{\text{mini}}, \tilde{\mathbf{A}}_{\text{train}}^{\text{mini}} \right) \\
 &= \frac{1}{2n_{\text{test}}} \sum_{j \in \text{test set}} l_{\text{test}}^{\text{mini}}(\mathbf{y}_j) \rho_{\text{test}}(\mathbf{y}_j) - \frac{1}{2n_{\text{train}}} \sum_{i \in \text{train set}} l_{\text{train}}^{\text{mini}}(\mathbf{y}_i) \rho_{\text{train}}(\mathbf{y}_i) \\
 &\leq \Delta_{\text{train,test}}(\beta, b) = \min \sum_{i \in \text{train set}} \sum_{j \in \text{test set}} \theta_{i,j} \delta(\mathbf{y}_i, \mathbf{y}_j, \beta, b) \\
 &= \min \sum_{i \in \text{train set}} \sum_{j \in \text{test set}} \theta_{i,j} \frac{C_F (C_w + 1) h^2}{n_{\text{min}}} \left(\delta_{i,j}^{\text{full}} + \delta_i^{\text{full-mini}} \right)
 \end{aligned} \tag{232}$$

3236 Then we mainly focus on the elements of $\delta_i^{\text{full-mini}}$.

3237 Recall that $\tilde{\mathbf{a}}_{\text{train},i,j}^{\text{full}} = \frac{1}{\sqrt{d_i^{\text{in,full}}} \sqrt{d_j^{\text{out,full}}} a_{ij}^{\text{full}}$ and $\tilde{\mathbf{a}}_{\text{train},i,j}^{\text{mini}} = \frac{1}{\sqrt{d_i^{\text{in,mini}}} \sqrt{d_j^{\text{out,mini}}} a_{ij}^{\text{mini}}$, where $a_{ij}^{\text{full}}, a_{ij}^{\text{mini}} \in$
3238 $\{0, 1\}$ represents whether node i receives a message from node j (1) or not (0).

3240 Hence, we have:

$$3242 \quad \|\tilde{\mathbf{a}}_{\text{train},i}^{\text{full}} - \tilde{\mathbf{a}}_{\text{train},i}^{\text{mini}}\|_F^2 = \sum_{j=1}^n \left| \frac{1}{\sqrt{d_i^{\text{in},\text{full}}} \sqrt{d_j^{\text{out},\text{full}}}} a_{ij}^{\text{full}} - \frac{1}{\sqrt{d_i^{\text{in},\text{mini}}} \sqrt{d_j^{\text{out},\text{mini}}}} a_{ij}^{\text{mini}} \right|^2, \quad (233)$$

3246 where $\frac{1}{\sqrt{d_i^{\text{in},\text{full}}} \sqrt{d_j^{\text{out},\text{full}}}} \leq \frac{1}{\sqrt{d_i^{\text{in},\text{mini}}} \sqrt{d_j^{\text{out},\text{mini}}}}$.

3248 We fix the batch size b . Notice that when the fan-out size β increases, $d_j^{\text{out},\text{mini}}$ may increase and
3249 we have four cases: (1). a_{ij}^{mini} keeps as 0 given $a_{ij}^{\text{full}} = 0$, (2). a_{ij}^{mini} keeps as 0 given $a_{ij}^{\text{full}} = 1$,
3250 (3). a_{ij}^{mini} keeps as 1 given $a_{ij}^{\text{full}} = 1$, (4). a_{ij}^{mini} becomes 1 from 0 given $a_{ij}^{\text{full}} = 1$. Then
3251

3252 we have $\sum_{j=1}^n \left| \frac{1}{\sqrt{d_i^{\text{in},\text{full}}} \sqrt{d_j^{\text{out},\text{full}}}} a_{ij}^{\text{full}} - \frac{1}{\sqrt{d_i^{\text{in},\text{mini}}} \sqrt{d_j^{\text{out},\text{mini}}}} a_{ij}^{\text{mini}} \right|^2$ are non-increasing when β increases
3253

3254 at the first three cases. However, at the fourth case, we may both have $\left| \frac{1}{\sqrt{d_i^{\text{in},\text{full}}} \sqrt{d_j^{\text{out},\text{full}}}} \right|^2 \leq$
3255 $\left| \frac{1}{\sqrt{d_i^{\text{in},\text{full}}} \sqrt{d_j^{\text{out},\text{full}}}} - \frac{1}{\sqrt{d_i^{\text{in},\text{mini}}} \sqrt{d_j^{\text{out},\text{mini}}}} \right|^2$ and $\left| \frac{1}{\sqrt{d_i^{\text{in},\text{full}}} \sqrt{d_j^{\text{out},\text{full}}}} \right|^2 \geq \left| \frac{1}{\sqrt{d_i^{\text{in},\text{full}}} \sqrt{d_j^{\text{out},\text{full}}}} - \frac{1}{\sqrt{d_i^{\text{in},\text{mini}}} \sqrt{d_j^{\text{out},\text{mini}}}} \right|^2$.
3256

3257 Hence, $\delta_i^{\text{full-mini}}$ has a overall non-increasing trend when β increases but small non-monotonic
3258 fluctuations can exist.

3259 We fix the fan-out size β . Notice that when the batch size b increases, $d_j^{\text{in},\text{mini}}$ may increase and we
3260 have three situations: (1). a_{ij}^{mini} keeps as 0 given $a_{ij}^{\text{full}} = 0$, (2). a_{ij}^{mini} keeps as 0 given $a_{ij}^{\text{full}} = 1$, (3).
3261 a_{ij}^{mini} keeps as 1 given $a_{ij}^{\text{full}} = 1$. Then we have $\delta_i^{\text{full-mini}}$ is non-increasing when b increases.

3262 Note that fan-out size β plays a more dominant role than batch size b in influencing generalization.
3263 This is because the variation in fan-out size β not only increases the number of sampled neighbors
3264 but also potentially alters the structure of the adjacency matrix of node i — by introducing new
3265 connections during mini-batch sampling (i.e., the fourth case). This structural change can lead to more
3266 significant variations in generalization performance. In contrast, changes in batch size b primarily
3267 supplement the number of sampled nodes without modifying the adjacency structure of the node i .

3268 Since $\delta(\mathbf{y}_i, \mathbf{y}_j, \beta, b)$ is proportional to $\delta_{i,j}^{\text{full-mini}} = \|\tilde{\mathbf{a}}_{\text{train},i}^{\text{full}} - \tilde{\mathbf{a}}_{\text{train},i}^{\text{mini}}\|_F^2$ and $\Delta(\beta, b)$ is proportional
3269 to $\delta(\mathbf{y}_i, \mathbf{y}_j, \beta, b)$, we have the upper bound $\Delta(\beta, b)$ of $L_{\text{test}}(\mathbf{W}^{\text{mini}}, \tilde{\mathbf{A}}_{\text{test}}^{\text{full}}) - L_{\text{train}}^{\text{full}}(\mathbf{W}^{\text{mini}}, \tilde{\mathbf{A}}_{\text{train}}^{\text{mini}})$
3270 keeps non-increasing when b increases, and overall have the non-increasing trend when β increases
3271 but small non-monotonic fluctuations exist.

3272 Finally, we have

$$3273 \quad U = \ln \mathbb{E}_{\mathbf{W}^{\text{mini}} \sim \mathcal{P}} \left[e^{C_u (L_{\text{test}}(\mathbf{W}^{\text{mini}}, \tilde{\mathbf{A}}_{\text{test}}^{\text{full}}) - L_{\text{train}}^{\text{full}}(\mathbf{W}^{\text{mini}}, \tilde{\mathbf{A}}_{\text{train}}^{\text{mini}}))} \right] \\ 3274 \leq \ln \mathbb{E}_{\mathbf{W}^{\text{mini}} \sim \mathcal{P}} \left[e^{C_u \Delta(\beta, b)} \right] \\ 3275 = \ln(e^{C_u \Delta(\beta, b)}) \\ 3276 = C_u \Delta(\beta, b). \quad (234)$$

3277 This completes the proof.

3287 N EXPERIMENTS

3289 N.1 TRAINING SETTINGS

3290 **Testbed:** The experiments, except those on the ogbn-papers100M, are conducted on a machine with
3291 512GB of host memory and four NVIDIA A100 GPUs, each with 40GB of memory, inter-connected
3292 via 900GB/s NVLink 4.0. The experiments on ogbn-papers100M are run on two machines without
3293 GPUs, each equipped with 1024GB of host memory and an interconnect bandwidth of 50 Gbps.

3294

3295

3296

3297

3298

3299

3300

3301

3302

3303

3304

3305

3306

3307

3308

3309

Metrics: 1). We evaluate convergence performance using three metrics: iteration-to-loss, iteration-to-accuracy, and time-to-accuracy. These metrics measure training progress towards a target convergence point in terms of training loss or validation accuracy. For all GNN models and datasets except ogbn-papers100M, the target training loss is defined as the maximum loss observed over 100 consecutive iterations at the smallest batch size, provided that the variance of these loss values is below 5×10^{-4} . Similarly, the target validation accuracy is defined as the minimum accuracy over 100 consecutive iterations at the smallest batch size, provided that the variance of these accuracies is below 4×10^{-4} . Note that the defined target training loss and the defined target validation accuracy are applied across all hyperparameter settings for the specific model and dataset. For ogbn-papers100M, training is limited to 200 iterations due to the extremely large graph size and training time constraints. Note that using the smallest batch size as the reference is common in prior works (Bajaj et al., 2024), and serves as a conservative criterion: because fluctuations are most pronounced under the smallest batch size, requiring stability in this setting to prevent mistaking transient variations for convergence and to provide a uniform benchmark across batch sizes. Moreover, by enforcing a variance threshold, this definition remains unbiased toward larger or smaller batch sizes and offers a fair basis for comparing convergence across settings. 2). For generalization, test accuracy is used as the metric in the training iteration. 3). For system efficiency, we measure the training throughput in terms of the number of target nodes processed per second (number of nodes/s). This metric ensures that throughput reflects the rate of training examples processed.

3327

We run all implementations using Python 3.8.10 and dgl>=1.0.0. The uniform neighbor sampling is used for mini-batch training. Due to the massive comparisons, adding error bars to every figure would make them overly cluttered and difficult to interpret. We have repeated all experiments at least three times using different seeds and observed low variance. For example, in Figure 6, the standard deviation of the final accuracy is less than 3.17%. This small variance does not affect the observed convergence trends, which remain consistent across runs.

3333

3334

N.2 METRICS: ITERATION-TO-LOSS

3335

3336

3337

Simple mathematical derivation. In distributed systems with two devices, assuming:

3338

3339

3340

3341

3342

3343

3344

3345

3346

3347

Datasets	#Nodes	#Edges	Avg. Degree	#Classes	#Features
Reddit	232,965	11,606,919	50	41	602
Ogbn-arxiv	169,343	1,166,243	7	40	128
Ogbn-products	2,449,029	61,859,140	25	47	100
Ogbn-papers100M	111,059,956	1,615,685,872	15	172	128

Table 4: Datasets Info2.

Datasets	Train/Val/Test
Reddit	152,410/23,699/55,334
Ogbn-arxiv	90,941/29,799/48,603
Ogbn-products	195,922/48,980/2,204,127
Ogbn-papers100M	1,207,179 / 125,265/214,338

We run all implementations using Python 3.8.10 and dgl>=1.0.0. The uniform neighbor sampling is used for mini-batch training. Due to the massive comparisons, adding error bars to every figure would make them overly cluttered and difficult to interpret. We have repeated all experiments at least three times using different seeds and observed low variance. For example, in Figure 6, the standard deviation of the final accuracy is less than 3.17%. This small variance does not affect the observed convergence trends, which remain consistent across runs.

- Per-iteration calculation time t_{cal} : $t_{cal} = (b * \beta + b) / C$, where b is batch size, β is fan-out size, and C is compute capacity (nodes/s);
- Per-iteration communication time t_{comm} : $t_{comm} = b / H$ for mini-batch training and $t_{comm} = (b * \beta + b) / H$ for full-graph training, where H is the bandwidth.
- time-to-accuracy t : $t = n \times (t_{cal} + t_{comm})$, where n is iteration-to-accuracy.

Consider two training setups:

- Full-graph training: $b_l = 1000$, $\beta_l = 50$, $n_l = 10$ iterations to converge
- Mini-batch training: $b_s = 10$, $\beta_s = 10$, $n_s = 10000$ iterations to converge

3348 Under the same compute power $C = 1$ node/s, but different bandwidths:
 3349

- 3350 • High bandwidth: $H_h = 1000$ nodes/s
- 3351 • Low bandwidth: $H_s = 0.1$ nodes/s

3353 Plugging into the formulas:

- 3354 • High bandwidth: 1). Full-graph: $t = 10 \times \left(\frac{1000 \cdot 50 + 1000}{1} + \frac{1000 \cdot 50 + 1000}{1000} \right) = 5.1051 \times 10^5$ s
 3355 2). Mini-batch: $t = 10000 \times \left(\frac{10 \cdot 10 + 10}{1} + \frac{10}{1000} \right) = 1.1001 \times 10^6$ s
 3356 Therefore, Full-graph training is faster.

- 3357 • Low bandwidth: 1). Full-graph: $t = 10 \times \left(\frac{1000 \cdot 50 + 1000}{1} + \frac{1000 \cdot 50 + 1000}{0.1} \right) = 5.61 \times 10^6$ s
 3358 2). Mini-batch: $t = 10000 \times \left(\frac{10 \cdot 10 + 10}{1} + \frac{10}{0.1} \right) = 2.1 \times 10^6$ s
 3359 Therefore, Mini-batch training is faster.

3360
 3361
 3362 This example shows that time-to-accuracy may flip conclusions depending on hardware, while
 3363 iteration-to-accuracy remains stable.

3364
 3365 **Experiments.** The vanilla distributed system (i.e., the standard implementation without any optimiza-
 3366 tions) is used for full-graph training, and the Distributed Data Parallel (DDP) technique (Li et al.,
 3367 2020) is applied for mini-batch training. We examine a three-layer GraphSAGE model on Reddit
 3368 and a three-layer GCN model on ogbn-products. These models include normalization layers and are
 3369 trained using a cross-entropy loss function and Adam optimizer with a learning rate of 0.01. The
 3370 target validation accuracy is set at 0.9 for ogbn-products and 0.95 for Reddit. The total batch size is
 3371 2000 and the fan-out size is [5,10,15]. To simulate infinite bandwidth (i.e., bw1), we use a single GPU
 3372 or CPU. For limited bandwidth (i.e., bw2), we use two GPUs interconnected via 900GB/s NVLink.

3373 N.3 CONVERGENCE

3374
 3375 For experiments on one-layer GNN models, the basic setups are without drop-out or normalization
 3376 layers and with ReLU activation, and SGD optimizer for both full-graph and mini-batch training. For
 3377 experiments in more general settings, multiple-layer GNNs are adopted without dropout layers and
 3378 with ReLU activation and Adam optimizer for both full-graph and mini-batch training. The SAR
 3379 system (Mostafa, 2022) is used for full-graph and mini-batch training on ogbn-papers100M via the
 3380 *gloo* backend, while other datasets are mainly trained on a single GPU.

3381
 3382 **Convergence of one-round GNN trained with MSE.** To align with theoretical analysis, we use
 3383 iteration-to-loss here. The details are as follows: 1). The target training losses are 0.0226 for
 3384 ogbn-arxiv, 0.0225 for reddit and ogbn-products, and [0.005, 0.0054, 0.0065] for ogbn-papers100M
 3385 on GCN, GraphSAGE, GAT, respectively. 2). When varying the batch sizes, the fan-out size is 5. 3).
 3386 When varying the fan-out sizes, the batch size is 500 for ogbn-arxiv, ogbn-products and reddit, as
 3387 well as is 10000 for ogbn-papers100M.

3388 Figure 7-8 shows the iteration-to-loss for four datasets under GAT, GCN, and GraphSAGE trained
 3389 with MSE across different learning rates and either varying batch sizes or varying fan-out sizes.

3390
 3391 **Convergence of one-round GNN trained with CE.** To align with theoretical analysis, we use
 3392 iteration-to-loss here. We set the original multi-class node classification task as the binary node
 3393 classification task. The details are as follows: 1). The target training losses are 0.51 for ogbn-arxiv,
 3394 [0.325,0.325,0.2] for reddit on GCN, GraphSAGE, GAT, respectively, [0.08,0.051,0.051] for ogbn-
 3395 products on GCN, GraphSAGE, GAT, respectively, and [0.009, 0.0087, 0.0087] for ogbn-papers100M
 3396 on GCN, GraphSAGE, GAT, respectively. 2). When varying the batch sizes, the fan-out size is 5. 3).
 3397 When varying the fan-out sizes, the batch size is 500 for ogbn-arxiv, ogbn-products and reddit, as
 3398 well as is 10000 for ogbn-papers100M.

3399 Figure 9-10 shows the iteration-to-loss for four datasets under GAT, GCN, and GraphSAGE trained
 3400 with MSE across different learning rates and either varying batch sizes or varying fan-out sizes.

3401 **Convergence in more general settings.** For the comparison at the dimension of batch size and fan-
 3402 out size, we use 3-layer GraphSAGE models with hidden dimension of 256 for reddit, ogbn-products,

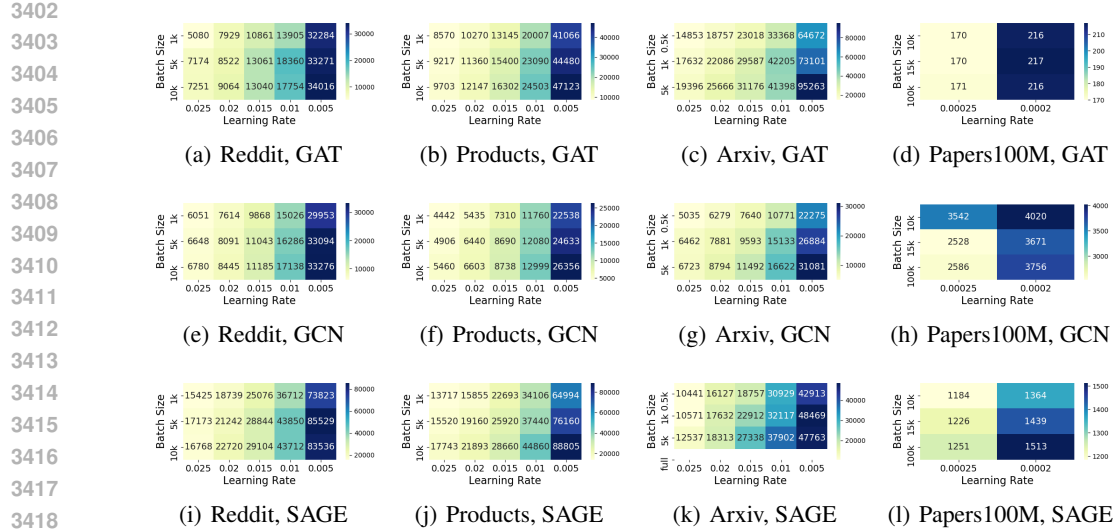


Figure 7: Iteration-to-loss for real-world datasets for one-round GAT, GCN, GraphSAGE across different batch sizes and learning rates under MSE .

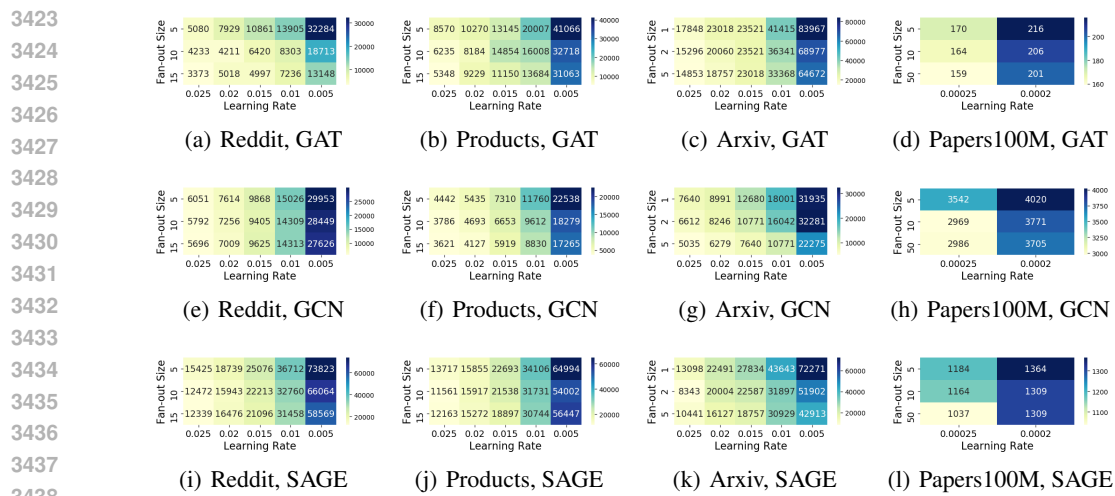


Figure 8: Iteration-to-loss for real-world datasets for one-round GAT, GCN, GraphSAGE across different fan-out sizes and learning rates under MSE .

and ogbn-arxiv, and 2-layer GraphSAGE models with hidden dimension of 128 for ogbn-papers100M. The activation function is ReLU function. The optimizer is Adam with a learning rate of 0.001 and a weight decay of 0. Due to the extremely large graph size of the ogbn-papers100M dataset and limited computational resources, we use separate machines for full-graph and mini-batch training on this dataset, making it infeasible to compare system efficiency between the two methods.

The target losses are $[0.2, 0.1, 0.8, 1.52]$ under CE, and $[0.005, 0.005, 0.013, 0.0055]$ under MSE for the products, reddit, arXiv, and papers100M datasets, respectively. The corresponding target accuracies are $[0.918, 0.962, 0.708, 0.599]$ under CE, and $[0.89, 0.946, 0.676, 0.5]$ under MSE for the same datasets.

Figure 11 (under CE) and 12 (under MSE) illustrate time-to-accuracy on GraphSAGE across varying batch sizes and fan-out sizes for ogbn-products, ogbn-arxiv and ogbn-papers100M.

Figure 14 (under MSE) and 13 (under CE) illustrate time-to-accuracy on GraphSAGE across varying batch sizes and fan-out sizes for ogbn-products, ogbn-arxiv and ogbn-papers100M.

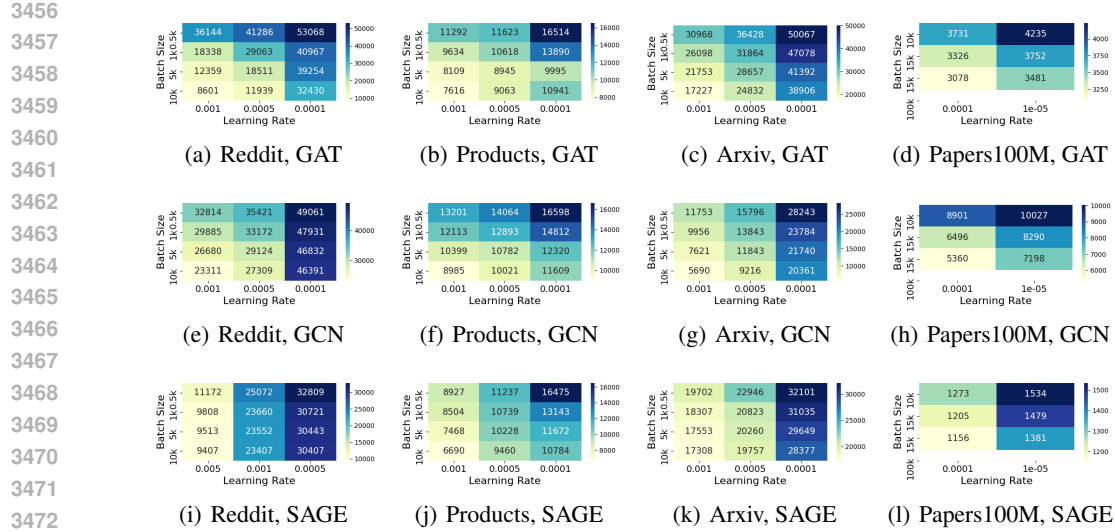


Figure 9: Iteration-to-loss for one-round real-world datasets for GAT, GCN, GraphSAGE across different batch sizes and learning rates under CE .

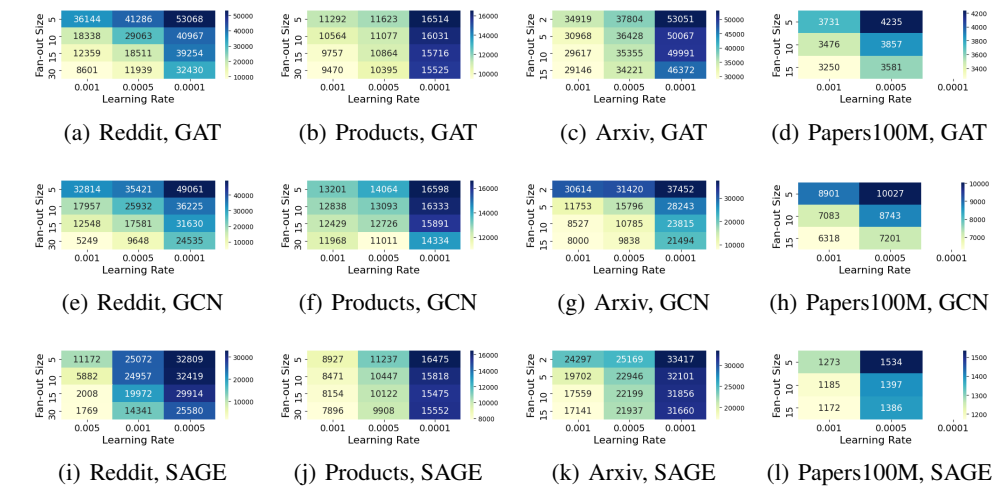


Figure 10: Iteration-to-loss for one-round real-world datasets for GAT, GCN, GraphSAGE across different fan-out sizes and learning rates under CE .

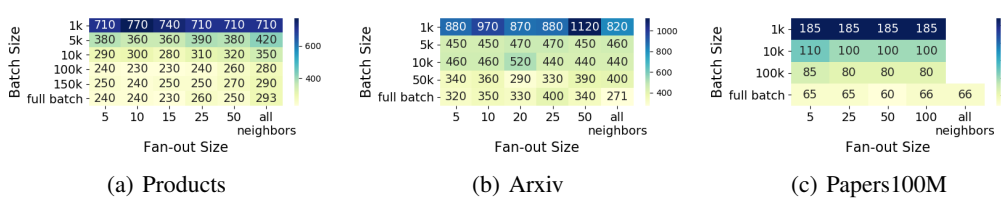


Figure 11: Iteration-to-acc of multi-layer GraphSAGE under CE across varying batch sizes and fan-out sizes.

N.4 GENERALIZATION

Generalization of one-round GNN trained with MSE. For test accuracy, the number of iterations are 5×10^5 for GraphSAGE and GCN, or 1×10^5 for GAT, for ogbn-arxiv, ogbn-products, and reddit.

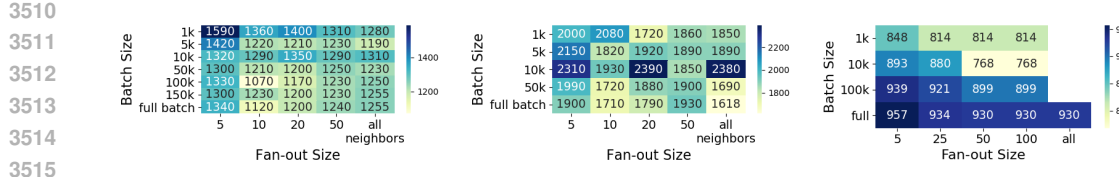


Figure 12: Iteration-to-acc of multi-layer GraphSAGE under MSE across varying batch sizes and fan-out sizes.

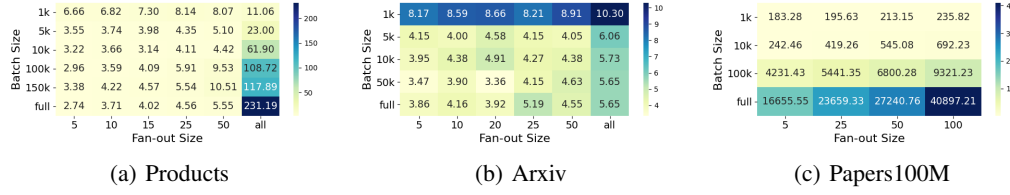


Figure 13: Time-to-accuracy (s) of multi-layer GraphSAGE under CE across varying batch sizes and fan-out sizes.

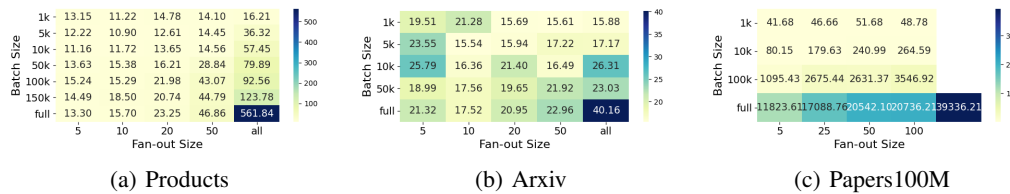


Figure 14: Time-to-accuracy (s) of multi-layer GraphSAGE under MSE across varying batch sizes and fan-out sizes.

And the number of iterations are 1×10^4 for ogbn-papers100M across all GNN models. The *learning rates* are [0.015, 0.02, 0.025] for ogbn-arxiv, ogbn-products, and reddit, and [0.00025, 0.0002] for ogbn-papers100M. The batch sizes and the fan-out sizes are consistent with the settings used in the experiments measuring time-to-accuracy. Other settings are the same as Appendix N.3.

Figure 15-16 shows the test accuracies for four datasets under GAT, GCN, and GraphSAGE trained with MSE across different learning rates and either varying batch sizes or varying fan-out sizes.

Generalization in more general settings. The settings are the same as the general settings in Appendix N.3.

Figure 17 (under CE) and 18 (under MSE) illustrate test accuracies on GraphSAGE across varying batch sizes and fan-out sizes for reddit, ogbn-arxiv and ogbn-papers100M.

N.5 COMPUTATIONAL EFFICIENCY

The settings are the same as the general settings in Appendix N.3.

Figure 17 (under CE) and 18 (under MSE) illustrate training throughput as the number of processed nodes per second on GraphSAGE across varying batch sizes and fan-out sizes for reddit, ogbn-arxiv and ogbn-papers100M.

N.6 FULL-GRAFH VS. MINI-BATCH TRAINING AFTER HYPERPARAMETER TUNING.

The settings are the same as the general settings in Appendix N.3.

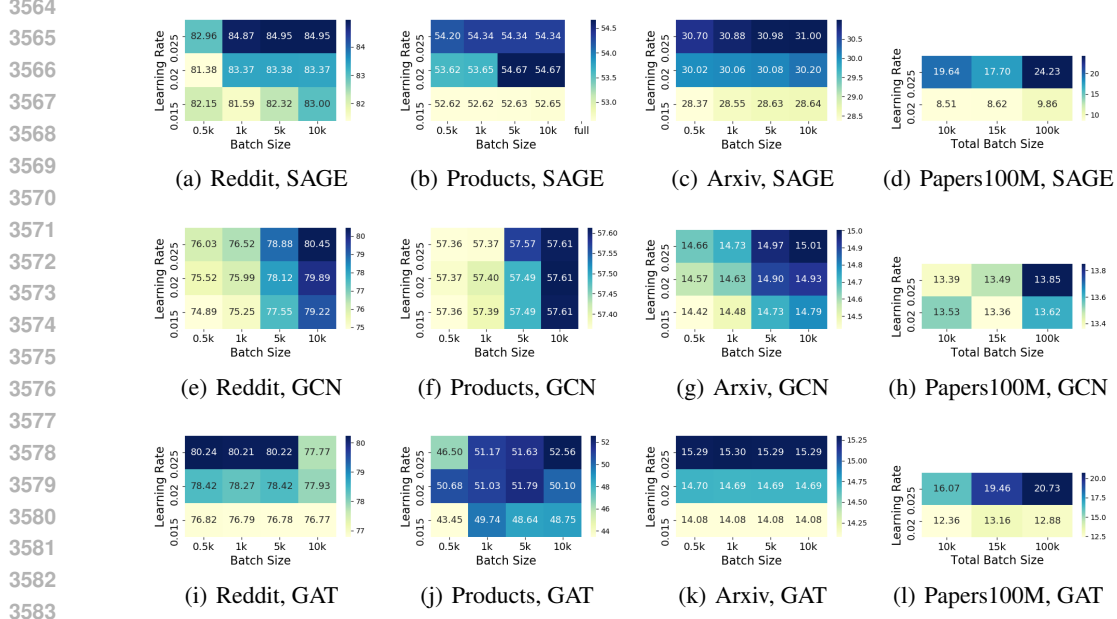


Figure 15: Test accuracy for real-world datasets for one-round GAT, GCN, GraphSAGE across different batch sizes and learning rates under MSE.

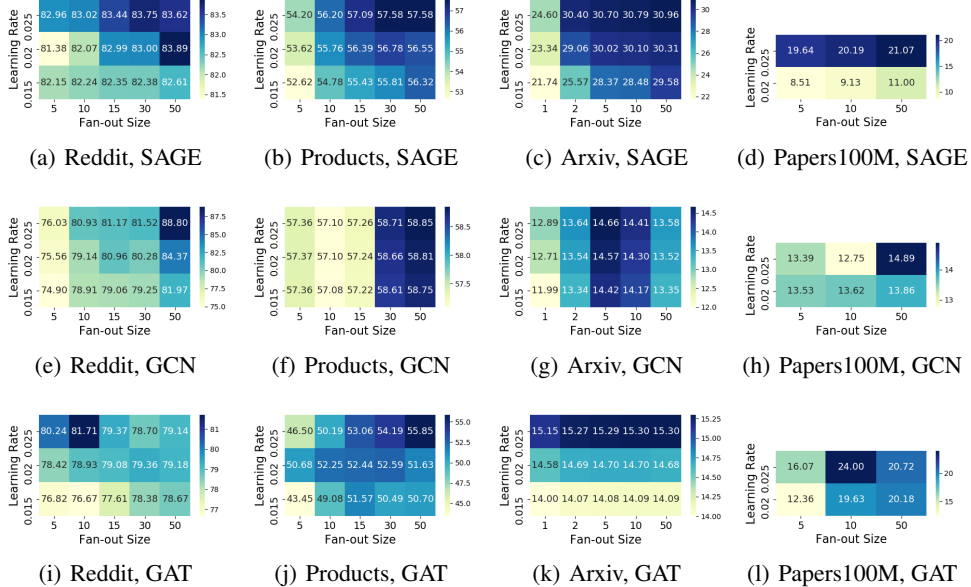


Figure 16: Test accuracy for real-world datasets for one-round GAT, GCN, GraphSAGE across different fan-out sizes and learning rates under MSE.

N.7 ADDITIONAL RUNS FOR KEY EXPERIMENTS

The Tables 5-12 are as follows. We use b as the batch size and β as the fan-out size.

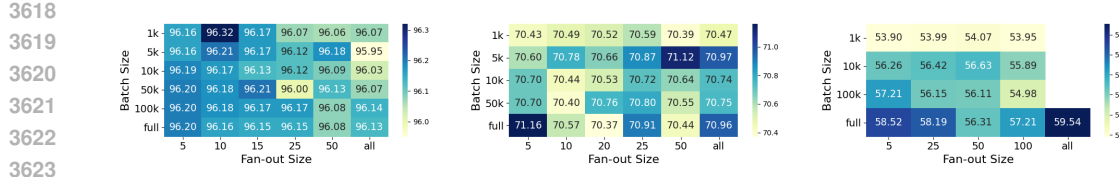


Figure 17: Test accuracies of multi-layer GraphSAGE trained with CE across varying batch sizes and fan-out sizes.

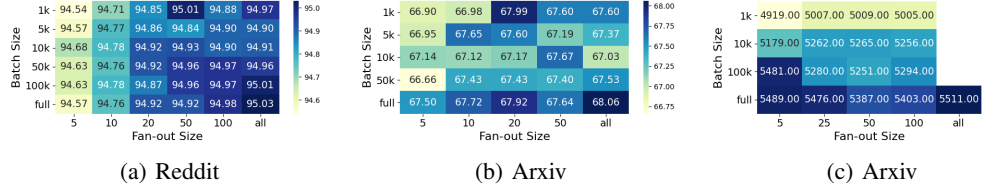


Figure 18: Test accuracies of multi-layer GraphSAGE trained with MSE across varying batch sizes and fan-out sizes.

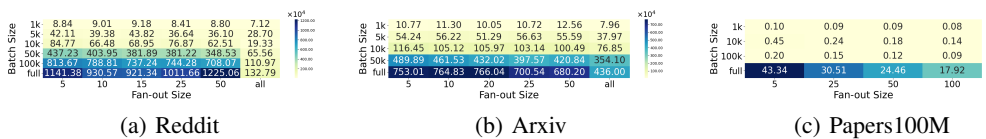


Figure 19: Training throughput (# nodes/s) of multi-layer GraphSAGE trained with CE across varying batch sizes and fan-out sizes.

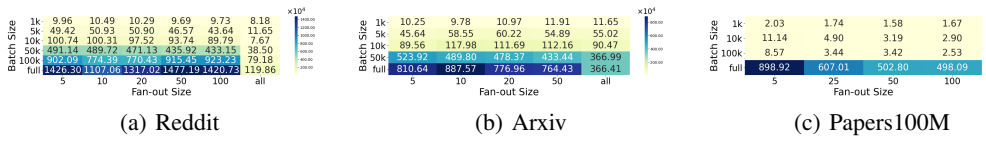


Figure 20: Training throughput (# nodes/s) of multi-layer GraphSAGE trained with MSE across varying batch sizes and fan-out sizes.

O RELATED WORK

For full-graph vs. mini-batch GNN training, the existing literature presents conflicting empirical findings on the GNN performance (i.e., convergence and generalization) and computational efficiency: some studies (Cai et al., 2021; Wan et al., 2022a;b; 2023) argue that full-graph training achieves higher model accuracy and faster convergence than mini-batch training, while others (Kaler et al., 2022; Zheng et al., 2022; Zhao et al., 2021; Bajaj et al., 2024) present contrasting findings. Furthermore, due to the message-passing process, performance insights from DNNs (Keskar et al., 2016; You et al., 2019; Smith, 2017; Golmant et al., 2018; Zou et al., 2020a; Bassily et al., 2018; Nabavinejad et al., 2021; Hauswald et al., 2015) cannot directly transfer to GNNs.

The only existing comparison work (Bajaj et al., 2024) between full-graph and mini-batch GNN training empirically evaluates overall performance but does not investigate the impact of key hyperparameters (e.g., batch size and fan-out size) on model performance and computational efficiency, thereby overlooking the trade-offs achieved by tuning these hyperparameters. Recent efforts (Yuan et al., 2023; Hu et al., 2021) focus on these hyperparameters but remain limited. For instance, Yuan et al. (Yuan et al., 2023) lack theoretical support, consider only limited batch sizes and fan-out values that are far smaller than those of full-graph training, and overlook the interplay of the batch size and

3672

3673

3674

3675

3676

3677

3678

3679

3680

3681

3682

3683

3684

3685

3686

3687

3688

3689

3690

3691

the fan-out size. Hu et al. (Hu et al., 2021) rely on gradient variance to explain the role of batch size but do not consider fan-out size, thus their explanation conflicts with their empirical observations.

Existing theoretical analyses of GNN training typically focus on singular aspects (e.g., convergence, or generalization), overlooking key graph-related factors (e.g., irregular graphs with nodes of varying degrees, the difference between training and testing graphs in mini-batch settings) and the impact of non-linear activation on gradients. For *convergence* analysis, Yang et al. (Yang et al., 2023) and Lin et al. (Lin et al., 2023) apply the NTK framework by assuming infinite-width GNNs. Xu et al. (Xu et al., 2021) analyze multi-layer linear GNNs. Awasthi et al. (Awasthi et al., 2021) employ PL conditions to study one-round GNNs with ReLU activation, simplifying the analysis to regular graphs. All these convergence analyses are solely on full-graph training. For *generalization* analysis, full-graph GNN training has been studied (Scarselli et al., 2018; Vapnik & Chervonenkis, 2015; Garg et al., 2020; Lv, 2021; El-Yaniv & Pechyony, 2009; Ono & Suzuki, 2020; Koltchinskii, 2001; Cong et al., 2021b; Du et al., 2019; Liao et al., 2020) under the well-established frameworks (e.g., PAC-Bayesian framework (McAllester, 2003)), while the previous analyses of mini-batch training impractically assume the same graph structures used in training and testing (Tang & Liu, 2023; Verma & Zhang, 2019). The difference among graph structures in training and testing can result in generalization performance degradation or overfitting to graph structures used in training.

P EXTENSIONS AND FUTURE WORK

P.1 EXTENSIONS

Multi-layer GNN models in theoretical analysis. We focus on a one-layer GNN with ReLU activation in theoretical analysis. We discuss the extension of theoretical results to multi-layer settings in Appendix H, and conduct experiments using multi-layer GNNs in Sec 5 and Appendix N. The results validate that our key insights remain applicable in such settings. Therefore, our theoretical and empirical analyses support the multi-layer GNN settings.

Sampling methods. We focus on uniform neighbor sampling before mini-batch training. There exist many other sampling methods (Hamilton et al., 2017; Chen et al., 2018; Zou et al., 2019; Chiang et al., 2019; Zeng et al., 2019) that have been proposed at the layer- or subgraph-level to enhance performance. Our core insights could extend to more sampling methods.

For example, compared to uniform neighbor sampling, the key difference in some advanced samplers lies in introducing specific constraints on the effective fan-out size by either assigning non-uniform sampling probabilities (Chen et al., 2018), or imposing layer-wise upper bounds on the number of neighbors per node (Zou et al., 2019). These specific constraints preserve the qualitative trend of the amount of aggregated information per node in the message-passing when varying fan-out sizes. In convergence analysis, following our analysis in Appendix G, increasing the effective fan-out size

3726

3727

Table 7: Run 1 for Figure 4(e).

Test acc	$\beta = 5$	$\beta = 10$	$\beta = 20$	$\beta = 50$	all
$b = 1000$	1167	928	854	817	801
$b = 10000$	1232	1028	991	907	861
$b = 100000$	1250	1025	1005	919	902
$b = 150000$	1256	1047	1013	928	909
full batch	1295	1035	1007	945	925

3734

3735

Table 8: Run 2 for Figure 4(e).

Test acc	$\beta = 5$	$\beta = 10$	$\beta = 20$	$\beta = 50$	all
$b = 1000$	1169	943	872	809	787
$b = 10000$	1222	1016	993	923	847
$b = 100000$	1257	943	936	929	886
$b = 150000$	1230	1037	978	923	902
full batch	1279	998	946	938	927

3742

3743

can enrich each target node’s aggregated neighbors, improving embeddings and reducing gradient variance. Therefore, the mechanism “larger fan-out size \rightarrow more iterations to convergence” still holds in GNN training under these samplers. For generalization, a larger fan-out size can reduce the Wasserstein distance $\Delta(\beta, b)$ under these constraints, which leads to improved generalization. While these advanced samplers may lessen the sensitivity of generalization to fan-out size, they cannot completely eliminate the effect of including unsampled but valid edges as fan-out increases (see Obs. 2). Consequently, generalization remains more sensitive to fan-out size than to batch size. Overall, our key insights remain applicable to these sampling methods.

3751

On the other hand, we notice that some advanced works (Chen et al., 2017; Shi et al., 2023; Fey et al., 2021; Shi et al., 2025) use historical embeddings to incorporate nearly full-graph information at each iteration. Therefore, from a model performance perspective, these methods reduce the variance caused by different batch sizes and behave more like full-graph training. From a system design perspective, they also rely on additional memory to store historical embeddings, making them closer to full-graph training systems than typical mini-batch ones. In contrast, we preserve and study the effects of batch size and fan-out, rather than eliminating them. Hence, we adopt the standard neighbor-aggregation scheme that is commonly used in practice and do not consider these sampling methods.

3759

Link prediction tasks. We focus on node classification tasks in GNN training, which can be easily extended to graph classification. Different from node classification, link prediction tasks use node pairs (connected and unconnected) for edge prediction, which can be transformed to node classification tasks using the line graph method in the graph theory. The new line graph $L(G)$ is constructed in the following way: for each edge in the original graph G , make a vertex in $L(G)$; for every two edges in G that have a vertex in common, make an edge between their corresponding vertices in $L(G)$. Hence, our analyses and core insights naturally carry over to link prediction tasks.

3767

Inductive GNN tasks. We focus on transductive GNN tasks. Unlike transductive tasks, inductive tasks apply different graphs between testing and training. For convergence, our analysis can be applied to inductive tasks without considering the testing graphs. For generalization, our analysis can be easily extended to inductive tasks by revising $\delta_{i,j}^{\text{full}}$ in the Wasserstein distance to consider graph structure differences between testing and training graphs.

3772

P.2 FUTURE WORK

3774

3775

Different activations: GeLU and Tanh. Our theoretical analysis readily extends to the GeLU and Tanh functions as the activation under our settings. The key difference lies in how the activation affects the gradient norm bound. GeLU is a smooth approximation of ReLU and shares a similar upper bound, while Tanh is even smoother with bounded high-order derivatives that control the gradient norm. As a result, both our convergence and generalization methodology naturally translate to these activation functions.

3780

3781

Table 9: Run 1 for Figure 6(a).

Test acc	$\beta = 5$	$\beta = 15$	$\beta = 25$	$\beta = 50$	all
$b = 1000$	0.7767	0.7832	0.7821	0.7810	0.7789
$b = 5000$	0.7817	0.7846	0.7825	0.7803	0.7698
$b = 10000$	0.7851	0.7818	0.7812	0.7775	0.7713
$b = 100000$	0.7869	0.7823	0.7818	0.7783	0.7753
$b = 150000$	0.7852	0.7818	0.7809	0.7781	0.7761
full batch	0.7868	0.7810	0.7778	0.7778	0.7803

3788

3789

3790

Table 10: Run 2 for Figure 6(a).

Test acc	$\beta = 5$	$\beta = 15$	$\beta = 25$	$\beta = 50$	all
$b = 1000$	0.7793	0.7840	0.7820	0.7818	0.7792
$b = 5000$	0.7825	0.7842	0.7833	0.7817	0.7702
$b = 10000$	0.7852	0.7821	0.7818	0.7771	0.7713
$b = 100000$	0.7862	0.7825	0.7816	0.7780	0.7762
$b = 150000$	0.7860	0.7818	0.7800	0.7768	0.7760
full batch	0.7864	0.7808	0.7778	0.7775	0.7808

3798

3799

3800 Our core insights are clearly generalizable to GeLU due to its similarity with ReLU. However,
 3801 whether the same insights hold for Tanh is less certain, as its bounded and more intricate derivative
 3802 structure may affect the theoretical bounds in a nontrivial way.

3803

3804

Heterogeneous graphs. Different from homogeneous graphs, heterogeneous graphs require spe-
 3805 cialized handling to address different types of nodes and edges, involving distinct aggregation and
 3806 transformation functions for each type, such as using separate neural networks for different edge
 3807 types. This can be explored.

3808

3809

3810

3811

3812

3813

3814

3815

3816

3817

3818

3819

3820

3821

3822

3823

3824

3825

3826

3827

3828

3829

3830

3831

3832

3833

3834
 3835
 3836
 3837
 3838
 3839
 3840
 3841
 3842
 3843

3844

Table 11: Run 1 for Figure 6(b).

Test acc	$\beta = 5$	$\beta = 10$	$\beta = 20$	$\beta = 50$	all
$b = 1000$	0.6617	0.6891	0.7117	0.7241	0.7242
$b = 5000$	0.7113	0.7207	0.7336	0.7345	0.7369
$b = 10000$	0.7209	0.7292	0.7341	0.7344	0.7362
$b = 100000$	0.7318	0.7348	0.7373	0.7403	0.7415
$b = 150000$	0.7329	0.7357	0.7372	0.7378	0.7401
full batch	0.7345	0.7391	0.7386	0.7384	0.7385

3852
 3853
 3854
 3855
 3856
 3857
 3858
 3859
 3860
 3861
 3862
 3863
 3864
 3865
 3866
 3867
 3868
 3869
 3870

3871

Table 12: Run 2 for Figure 6(b).

Test acc	$\beta = 5$	$\beta = 10$	$\beta = 20$	$\beta = 50$	all
$b = 1000$	0.7295	0.7321	0.7344	0.7345	0.7341
$b = 5000$	0.7307	0.7343	0.7361	0.7364	0.7371
$b = 10000$	0.7326	0.7353	0.7366	0.7365	0.7381
$b = 100000$	0.7342	0.7372	0.7392	0.7400	0.7411
$b = 150000$	0.7343	0.7361	0.7385	0.7393	0.7405
full batch	0.7341	0.7396	0.7391	0.7389	0.7403

3879
 3880
 3881
 3882
 3883
 3884
 3885
 3886
 3887